VOLATILE ORGANIC COMPOUND AND METHANE TRANSPORT THROUGH COMPOSITE BARRIERS WITH CO-EXTRUDED GEOMEMBRANE CONTAINING ETHYLENE VINYL-ALCOHOL

By

Jongwan Eun

A dissertation submitted in partial fulfillment of

the requirements for the degree of

Doctor of Philosophy

(Civil and Environmental Engineering)

at the

UNIVERSITY OF WISCONSIN-MADISON

2014

Date of final oral examination: 01/07/2014

The dissertation is approved by the following members of the Final Oral Committee:

James M. Tinjum, Assistant Professor, Engineering Professional Development
Craig H. Benson, Dist. Professor, Chair, Civil and Environmental Engineering
Tuncer B. Edil, Professor, Geological Engineering
Jim K. Park, Professor, Civil and Environmental Engineering
Samuel K. Kung, Professor, Soil Science

Abstract

VOLATILE ORGANIC COMPOUND AND METHANE TRANSPORT THROUGH COMPOSITE BARRIERS WITH CO-EXTRUDED GEOMEMBRANE CONTAINING ETHYLENE VINYL-ALCOHOL

Jongwan Eun

Under the Supervision of Professor James M. Tinjum and
Professor Craig H. Benson at the University of Wisconsin-Madison

A co-extruded geomembrane (GM) with a layer of ethylene vinyl-alcohol (EVOH) is being introduced in environmental containment applications to take advantage of the hydrophobic properties of polyethylene as a barrier to contaminant flux; specifically, the potential to substantially reduce the diffusion of non-polar volatile organic compounds (VOCs) and methane. This dissertation presents a comprehensive study on the migration of VOC and methane through composite barriers constructed with co-extruded EVOH GM. The specific methods, results, and findings drawn from this study are summarized below.

This research effort involved the experimental measurement of the relative migration of five common VOCs through composite landfill liners constructed with two types of co-extruded EVOH GM overlying either a compacted clay liner (CCL) or a geosynthetic clay liner (GCL). VOC breakthrough in composite liners employing high-density polyethylene (HDPE) GMs occurred within approximately 35 d. This was more than two to four times faster than the composite liners composed of a co-extruded EVOH GM with a linear low density polyethylene (LLDPE) or HDPE outer layer where breakthrough occurred at 70 and 150 d,

respectively, with significantly higher VOC concentrations. Co-extruded EVOH GMs with LLDPE or HDPE as an outer layer had measured diffusion coefficients (0.11-0.57 × 10^{-13} m^2/s and 0.14-0.58 × 10^{-13} m^2/s, respectively) more than 20 times smaller in comparison to conventional HDPE GM (2.86-11.05 × 10^{-13} m^2/s). For the CCL and GCL composite liners, the concentration of VOCs at a depth of 80 mm below the GM layer was much lower in the CCL compared to the GCL. Numerical modeling (i.e., finite difference method) of VOC migration through a composite liner with 0.6-m-thick and 1.2-m-thick CCL with a co-extruded EVOH GM indicated that contaminant transport was approximately 14% and 22% lower at 100 years, respectively, in comparison to the equivalent HDPE composite liner. Thus, co-extruded EVOH GMs can act as an effective barrier to VOC migration in composite liners.

The transport parameters (i.e., partition and diffusion coefficients) of co-extruded GM were evaluated with a series of batch tests. Overall, the LLDPE GM had the highest partition coefficient (1.9-195.8 L/kg) and the pure EVOH laminar had the lowest partition coefficient (0.69-0.94 L/kg). The diffusion coefficient of co-extruded GM (0.14-0.59 × 10^{-13} m^2/s) was approximately 16-29 times smaller than that of HDPE GM (2.86–11.05 × 10^{-13} m^2/s). The chemical characteristics (i.e., octanol-water partition coefficient, aqueous solubility, and molecular diameter) of each material in the co-extruded EVOH GM showed a strong linear relationship with the partition coefficient. The relationship with HDPE, LLDPE, and maleic anhydride was reversed for EVOH due to the polarity of the EVOH. An equivalent diffusion coefficient was derived analytically based on sorptive and

diffusive behavior through the co-extruded GM (i.e., non-homogeneous layers in series). For validation of the proposed equation to estimate the equivalent diffusion coefficient, the transport parameters for a co-extruded GM obtained using batch tests were compared to the transport parameters obtained from a modified double compartment test. The measured and estimated diffusion coefficients were statistically identical, thus the equation to estimate the equivalent diffusion coefficient can provide reliable values. For another validation of the equivalent diffusion coefficient, the flux of VOCs predicted by numerical modeling (i.e., finite difference method) using the equivalent diffusion coefficient was compared to the flux measured in diffusion column testing. For each VOC, the magnitude of the equivalent diffusion coefficient agreed with the VOC migration demonstrated in the diffusion column test.

The relative rates of transport of methane through an interim cover constructed with a co-extruded GM that contains a layer of EVOH were evaluated and compared to conventional GMs including polyethylene (PE), LLDPE, and polyvinyl chloride (PVC). Based on the experimental results from these diffusion column tests employing composite covers, soil type minimally influenced diffusive behavior of methane through the interim cover in comparison to GM type. The LLDPE and PVC GMs produced five times more rapid breakthrough (≈ 20 d) of methane and higher flux in comparison to the EVOH GM (≈ 100 d). Further, the co-extruded EVOH GM had measured diffusion coefficients that were more than 170-250 times smaller compared to conventional single-composition GMs. Analytical modeling of methane migration through a composite cover indicated

that the EVOH GM helped reduce the flux of methane [approximately 0.96 mL(STP) m^{-2} d^{-1}] to levels two orders of magnitude lower than the flux for the conventional GMs. Therefore, co-extruded EVOH GMs can act as an effective barrier to methane migration in interim landfill covers.

Acknolegements

I would like to give my sincere gratitude to Dr. James M. Tinjum and Dr. Craig H. Benson for their patience, guidance, and support during this study. Their encouragement during this study as well as their insightful thoughts during our discussions allowed me to accomplish this dissertation. I would also like to thank Dr. Tuncer B. Edil for giving me constructive guidance and ideas throughout this study. I would like to acknowledge Dr. Jim K. Park and Dr. Samuel K. Kung for serving as committee members and giving their advice. I also thank Mr. Xiadong Wang and Ms. Jackie Cooper, both academic staff, for their assistance with designing and constructing equipment, and for instructing me on laboratory procedures.

Also, I extend my gratitude to Dr. Junhwan Lee and Dr. Sang Seom Jeong, who were advisors when I was at Yonsei University in Korea, for showing consistent interest and encouragement to me.

I also thank all the graduate students in geological engineering at the University of Wisconsin-Madison. They made my experience in Madison during this study enjoyable.

Most importantly, I would like to thank my family for their love, patience, and trust. I would like to give special thanks to my wife, Nami Kim, for her patience, love, positive encouragement, and endless support.

Support for this study was provided by Kuraray Co. Ltd. I appreciate the support of Kuraray CO., Ltd. during this study. The findings, opinions, and conclusions reported in this dissertation are solely those of the author.

Table of Contents

List of Tables

List of Figures

Chapter 1 Introduction

1.1 RESEARCH MOTIVATION

In a municipal solid waste (MSW) landfill, composite liners (e.g., a geomembrane overlying a compacted clay layer, CCL, or geosynthetic clay liner, GCL) are typically required as bottom liners for barrier systems (Subtitle D of the Resource Conservation and Recovery Act). Composite liners effectively contain leachate because the geomembrane component prevents advection of water, while the soil beneath the geomembrane is designed to have low hydraulic conductivity, which limits advection through defects in the geomembrane (Giroud and Bonaparte 1989; Othman et al. 1997). However, certain contaminants can be transported through composite liners via diffusion. In particular, organic compounds can be transported through geomembranes in a short period of time (Britton et al. 1989; Park and Bontoux 1991; Park and Nibras 1993; Buss et al. 1995; Park et al. 1996; Rowe 1998; Aminabhavi and Naik 1999; Xiao et al. 1999; Sangam and Rowe 2001a, b; Joo et al. 2004, 2005). Defects in geomembranes also occur, thus permitting leakage (Giroud and Bonaparte 1989). Consequently, the mechanism of contaminant transport through geomembranes is important when evaluating the effectiveness of a composite liner.

Analyses have shown that transport of volatile organic compounds (VOCs) through landfill liners generally is more critical than transport of inorganic compounds (e.g., toxic heavy metals) even though VOCs are often found at lower concentrations in leachate (Rowe 1998; Park and Nibras 1993; Park et al.

1996; Sangam and Rowe 2001a; Edil 2003, 2007). Foose et al. (2001, 2002) demonstrated that, for a well-constructed composite liner having few defects, the mass flux of VOCs through intact portions of the composite liner can be four to six orders of magnitude greater than that through defects alone. Diffusive transport can thus be the dominant mode of contaminant transport in composite liners.

Enhanced geomembranes are being developed that have higher performance and durability as chemical barriers for use in landfill liner applications. For example, co-extruded geomembranes with ethylene vinyl-alcohol (EVOH) layers are being manufactured that have the dual advantage of polyethylene as a water barrier and the potential to substantially reduce the diffusion of VOC due to the EVOH layer. The EVOH molecule includes electric dipoles, which cause the molecule to be polar and, as a result, EVOH has outstanding barrier properties to non-polar gases such as oxygen, nitrogen, volatile compounds, and helium (Zhang et al. 1999; Zhang et al. 2000; Byun et al. 2007; McWatters and Rowe 2010, 2011).

However, there are few studies that have investigated the relative performance of composite liners that use an EVOH geomembrane as a contaminant barrier for VOCs. Also, the most effective configuration of the liner layers (e.g., GCL underlying a geomembrane) has not been established. Therefore, an experimental study to evaluate VOC transport and identify the situational performance of geomembranes reinforced with EVOH is warranted. Further, a numerical analysis to simulate field conditions against validated

laboratory results is of interest to predict transport behavior through composite layers employing EVOH geomembrane.

A considerable amount of gas is generated in MSW landfills as the organic waste decomposes. Landfill gas (primarily carbon dioxide and methane, but also with small concentrations of hydrogen sulfide) emissions to the atmosphere have become a sensitive issue in recent years because of their contribution to greenhouse gas emissions that induce global warming (Boeckx et al. 1996; Didier et al. 2000; Mackie and Cooper 2009) and the release of nuisance odors. A major portion of landfill gas (LFG) is methane (≈ 50%), which is produced by the anaerobic degradation of organic waste and can occur for more than 30 years. Because methane is more than 20 times more potent than CO_2, methane emissions substantially contribute to global warming (Mackie and Cooper 2009).

There are two primary methods for managing the emission of methane from landfill sites (Aitchison 1993; Boeckx et al. 1996). One method is to undertake LFG recovery and energy production, which is generally regarded as the optimal approach. For reducing emissions in smaller and older landfills with lower amounts of methane generation, another option is to encourage methane-oxidation in the soil covering the landfill. This can be an economical and more effective option compared to gas extraction, which becomes inefficient at low methane contents (Aitchison 1993; Boeckx et al. 1996). However, compacted soil in daily, intermediate, or final covers may become desiccated by the high temperatures typical of a landfill environment and thus may not effectively contain the methane gas (Gebert et al. 2010).

An alternative method to handle methane emission is to incorporate geomembranes that are impermeable to the gas generated within the interim cover layer during operation of the landfill site. A geomembrane is intended to minimize gas emission through the cover; however, a cover may allow for some gas emission via diffusion through the geomembrane. Several researchers (Haxo et al. 1984; Haxo 1990; Haxo and Pierson 1991; Pierson and Barroso 2002) reported the diffusive gas permeability for geomembranes. Haxo et al. (1984) showed that the gas permeability of polymeric materials differs for a given generic polymer type and structure. Polymer crystallinity in a geomembrane represents the degree of structural order specified as a percentage of the volume of the material that is crystalline to that which is amorphous. In general, the greater the polymer crystallinity is, the lower the gas permeability is. Haxo et al. (1984) also showed that gas permeability varies with the type of gas and temperature. Mark and Gaylord (1964) showed that the gas permeability coefficient is independent of geomembrane thickness, assuming no pinholes in the geomembrane, because the gas permeability coefficient is a material property for non-porous media that reflects the permeability of the geomembrane compound. Stark and Choi (2005) investigated the methane gas transmission rate, permeance, and permeability coefficient of polyvinyl chloride (PVC), linear low density polyethylene (LLDPE), and high density polyethylene (HDPE) geomembranes by performing standard gas transport tests (ASTM D1434 2003). The measured permeability of methane through a PVC geomembrane was

slightly less than the gas permeability through an LLDPE geomembrane, but slightly higher than the gas permeability through an HDPE geomembrane.

A thin EVOH film has been developed to enhance the properties of geomembranes used in covers. Co-extruded geomembranes with EVOH layers have the potential to substantially reduce the diffusion of methane. However, there are few studies that have investigated the performance of various geomembrane covers that incorporate EVOH as a contaminant barrier for methane. Moreover, the composite action of the cover, including soil layers, has not been considered in detail. This study experimentally evaluates methane transport through an interim cover and identifies the relative performance of an interim cover that includes EVOH as part of the geomembrane component. Further, a numerical analysis is conducted to extend laboratory work to various configurations of composite covers to support the feasibility of incorporating EVOH geomembrane as a cover material.

1.2 RESEARCH OBJECTIVES

This research effort has three main objectives:

(1) Evaluate and compare the relative rates of migration for common VOCs through composite landfill liners constructed with co-extruded geomembranes that contain EVOH in addition to conventional HDPE.

(2) Compare the relative rates of migration for methane from interim landfill cover profiles constructed with soil alone and soil underlain with a thin EVOH geomembrane.

(3) Measure transport parameters for EVOH geomembrane to estimate the rate of release of VOCs and methane in a realistic manner that simulates practical landfill applications.

The first two objectives were achieved by conducting bench-scale prototype experiments simulating landfill liner and cover profiles using methods previously established and validated at the University of Wisconsin-Madison (Kim et al. 2001; Park et al. 2012). The third objective was achieved by conducting batch tests (i.e., sorption/immersion test) and double-compartment tests (i.e., column-type diffusion test) to obtain transport parameters of VOC and methane (i.e., partition and diffusion coefficient for VOC; diffusion coefficient for methane). Further, numerical simulations of VOC and methane transport were performed for common liners and cover geometries using finite difference method (FDM). Data from the bench-scale experiments was used to validate the numerical model. Also, batch testing was conducted to obtain transport parameters to simulate VOC and methane transport. The intent of the first objective is to illustrate how the lower diffusion coefficient of EVOH reduces the diffusion of VOC compared to composite liners containing HDPE geomembranes. The intent of the second objective is to illustrate how deploying a low-cost EVOH geomembrane in an interim cover can reduce greenhouse gas emissions, which is a major concern of the solid waste industry. The intent of the third objective is to provide examples and illustrations of these concepts that engineers and regulators can readily incorporate into their design scenarios and review processes.

1.3 HYPOTHESES

Associated with the objectives of research, this research has three main hypotheses:

(1) Co-extruded EVOH geomembrane allows less migration of VOCs in comparison to conventional HDPE geomembrane as incorporated into a composite liner system.

(2) The transport of VOCs through a multi-layered composite liner can be simulated and quantified numerically by using measured transport parameters.

(3) Co-extruded EVOH geomembrane allows less migration of methane transport; thus, an interim cover installed with co-extruded EVOH geomembrane will be effective as a barrier.

1.4 DISSERTATION OUTLINE

This dissertation is organized into five chapters. Chapters 2 to 4 are written as independent articles. The research objectives are stated separately in each chapter. Following this introductory chapter, the relative rates of transport of five VOCs through composite landfill liners constructed with two types of co-extruded geomembrane that contains EVOH are evaluated and compared in Chapter 2. To simulate the *in situ* configuration of composite liners in a landfill, a series of diffusion column tests employing different type of geomembranes with CCL and GCL were conducted. Based on experimental results from the column

tests with composite liners, migration of VOCs through a co-extruded EVOH geomembrane are quantified in comparison to those through HDPE geomembranes. The transport characteristics of composite liners employing CCL and GCL are then compared. Additionally, VOC transport is estimated for varying configurations of composite liners. Accordingly, a design recommendation is proposed for the installation of a geomembrane enhanced with EVOH for field conditions.

Based on the review of literature presented in Chapter 2, transport behavior of non-polar organic contaminants (e.g., common VOCs found in landfill leachate) through a co-extruded geomembrane containing EVOH are investigated with a series of batch tests in Chapter 3. To evaluate the equivalency of transport behavior in co-extruded EVOH geomembrane, the transport parameters of each layer for the EVOH geomembrane consisting of the geomembrane were separately measured with batch tests. Sorptive and diffusive behaviors at the layered interfaces of co-extruded geomembranes (i.e., non-homogeneous layers in series) are accounted for with a derived equation that estimates the equivalent diffusion coefficient. For validation of the equation, the transport parameters for a co-extruded geomembrane obtained using batch tests is compared to the transport parameters obtained from modified double-compartment (MDCA) apparatus tests. The relationships between the chemical characteristics (i.e., octanol-water partition coefficient, aqueous solubility and molecular diameter) and transport parameters of each material in a co-extruded EVOH geomembrane are investigated to identify the transport behavior through

the geomembrane and to evaluate the migration of solute through a co-extruded EVOH geomembrane. Finally, the migration of VOCs through composite liners employing the geomembrane is modeled numerically in using equivalent diffusion coefficients, and compared to experimental data from diffusion column tests.

In Chapter 4, methane transport through an interim cover is experimentally evaluated and the performance of an interim cover that includes EVOH as part of the geomembrane component is identified. Based on the results of diffusion testing with composite liners employing a co-extruded EVOH geomembrane, diffusion coefficients are evaluated and quantified as compared to those of thin polyethylene (PE), LLDPE, and PVC geomembrane. Further, a numerical analysis was conducted to extend laboratory work to various configurations of composite covers to support the feasibility of incorporating EVOH geomembrane as a cover material.

Chapter 5 presents conclusions of this study. Based on results of this study, the co-extruded EVOH geomembrane acted as an effective barrier to non-polar organic contaminants. Future research is also suggested.

1.5 REFERENCES

Aitchison, E. (1993). “Options for reducing-methane emission from landfill sites.” In Methane and Nitrous Oxide: Methods in National Emissions Inventories and Options for Control (A. R. van Amstel, Ed.), pp. Z-230. *International IPCC Workshop*, 1993. Amersfoort, the Netherlands.

ASTM (2003). “Standard test method for determining gas permeability characteristics of plastic film and sheeting.” *D1434*. West Conshohocken, PA: American Society for Testing and Materials.

Aminabhavi, T. M., and Naik, H. G. (1999). “Sorption/desorption, diffusion, and swelling characteristics of geomembranes in the presence of halo-organic liquids.” *Journal of Applied Polymer Science,* 72 (3), 349-359.

Boeckx, P., Van Cleemput, O., and Villaralvo, I. (1996). “Methane emission from a landfill and the methane oxidation capacity of its covering soil.” *Soil Biology and Biochemistry*, 28 (10 - 11), 1397-1405.

Britton, L. N., Ashman, R. B., Aminabhavi, T. M., and Cassidy, P. E. (1989). “Permeation and diffusion of environmental pollutants through flexible polymers.” *Journal of Applied Polymer Science*, 38 (2), 227-236.

Buss, S. E., Butler, C. J., Sollars, C. J., and Perry, R. (1995). “Migration of organics through HDPE landfill lining material.” *Proceeding*, Sardinia 95, *5th International Landfill Symposium*, Cagliari, Italy, 377-386.

Byun, Y. J., Hong, S. I., Kim, K. B., Jeon, D. H., Kim, J. M., Whiteside, W. S., and Park, H. J. (2007). “Physical and chemical properties of γ-irradiated EVOH film.” *Radiation Physics and Chemistry*, 76 (6), 974-981.

Didier, G., Bouazza, A., and Cazaus, D. (2000). “Gas permeability of geosynthetic clay liner.” *Geotextiles and Geomembranes*, 18 (2-4), 235-250.

Edil, T. B. (2003). “A review of aqueous-phase VOC transport in modern landfill liners.” *Waste Management*, 23 (7), 561-571.

Edil, T. B. (2007). “Is aqueous-phase VOC transport from modern landfills a potential environmental problem?” *Proceeding,* Sardinia 2007, *11th International Landfill Symposium*, Cagliari, Italy, 461-469.

Foose, G. J., Benson, C. H., and Edil, T. B. (2001). “Analytical equations for predicting concentration and mass flux from composite liners.” *Geosynthetics International*, 8 (6), 551-575.

Foose, G. J., Benson, C. H., and Edil, T. B. (2002). “Comparison of solute transport in three composite liners.” *Journal of Geotechnical and Geoenvironmental Engineering*, 128 (5), 1-13.

Gebert, J., Groengroeft, A., and Pfeiffer, E. (2010). “Relevance of soil physical properties for the microbial oxidation of methane in landfill covers.” *Soil Biology and Biochemistry,* 43 (9), 1759-1767.

Giroud, J. P., and Bonaparte, R. (1989). “Leakage through liners constructed with geomembranes-Parts I and II.” *Geotextiles and Geomembranes*, 8 (27-67), 71-111.

Haxo, H. E. (1990). “Determining the transport through geomembranes of various permeants in different applications.” *In Geosynthetic Testing for Waste*

Containment Applications (ed. R. M. Koerner), *STP 1081*, 75–94. West Conshohocken, PA: American Society for Testing and Materials.

Haxo, H. E. and Pierson, P. (1991). "Permeability testing." *In Geomembranes Identification and Performance Testing* (eds A. Rolling and J-M. Rigo), RILEM Report 4, 219-240. RILEM.

Haxo, H. E., Miedema, J. A., and Nelson, N. A. (1984). "Permeability of polymeric membrane lining materials." *Proceedings of the International Conference on Geomembrane*, Denver, CO, 151-156.

Joo, J. C., Kim, J. Y., and Nam, K. (2004). "Mass transfer of organic compounds in dilute aqueous solutions into high density polyethylene geomembranes." *Journal of Geotechnical and Geoenvironmental Engineering*, 130 (2), 175-183.

Joo, J. C., Nam, K., and Kim, J. Y. (2005). "Estimation of mass transport parameters of organic compounds through high density polyethylene geomembranes using a modified double-compartment apparatus." *Journal of Geotechnical and Geoenvironmental Engineering*, 131 (5), 790-799.

Kim, J. Y., Edil, T. B., and Park, J. K. (2001). "Volatile organic compound (VOC) transport through compacted clay." *Journal of Geotechnical and Geoenvironmental Engineering*, 127 (2), 126-134.

Mackie, K. R. and Cooper, C. D. (2009). "Landfill gas emission prediction using Voronoi diagrams and importance sampling." *Environmental modeling and software*, 24, 1223-1232.

Mark, H. F. and Gaylord, N. G. (1964). Encyclopedia of Polymer and Technology: Plastics, Resins, Rubbers, Fibers. New York: Interscience Publishers.

McWatters, R. S. and Rowe, R. K. (2010). “Diffusive transport of VOCs through LLDPE and Two coextruded geomembrane.” *Journal of Geotechnical and Geoenvironmental Engineering*, 136 (9), 1167-1177.

McWatters, R. S. and Rowe, R. K. (2011). “Sorption and diffusion of BTEX through thin-film EVOH.” *Geo-Frontiers 2011,* ASCE, 2073-2083.

Othman, M. A. Bonaparte, R., and Gross, B. A. (1997). “Preliminary results of composite liner field performance study.” *Geotextiles and Geomembranes*, New York, 289-312.

Park, J. K. and Bontoux, L. (1991). “Effects of temperature, repeated exposure, and aging on polybutylene permeation by organic chemicals” *Journal of Applied Polymer Science*, 42, 2989-2995.

Park, J. K., and Nibras, M. (1993). “Mass flux of organic chemicals through polyethylene geomembranes.” *Water Environment Research*, 65 (3), 227-237.

Park, J. K., Sakti, J. P., Hoopes, J. A. (1996). “Transport of organic compounds in thermoplastic geomembranes, I: Mathematical model.” *Journal of Environmental Engineering*, 122 (9), 800-806.

Park, M. G., Edil T. B. and Benson, C. H. (2012b). “Modeling volatile organic compound transport in composite liners.” *Journal of Geotechnical and Geoenvironmental Engineering*, 138 (6), 641-657.

Pierson, P. and Barroso, M. (2002). “A pouch test for characterizing gas permeability of geomembranes.” *Geosynthetics International*, 9 (4), 345-372.

Rowe, R. K. (1998). “Geosynthetics and the minimization of contaminant migration through barrier systems beneath solid waste.” *Proceedings of the Sixth International Conference on Geosynthetics*, Atlanta, Industrial Fabrics Association International, St. Paul, MN, 22-102.

Sangam, H. P. and Rowe, R. K. (2001a). “Migration of dilute aqueous organic pollutants through HDPE geomembranes.” *Geotextiles and Geomembranes*, 19, 329-357.

Sangam, H. P. and Rowe, R. K. (2001b). “The role of HDPE geomembranes in retarding the diffusive migration of organic contaminants through composite liner systems.” *Proceeding*, Sardinia 2001, *8th International Landfill Symposium*, Thomas Telford, Cagliari, Italy, 245-254.

Stark, T. D. and Choi, H. (2005). “Methane gas migration through geomembranes.” *Geosynthetics International*, 12 (1), 1-6.

Xiao, S., Moresoli, C., Burezyk, A., Pintauro, P., and De Kee, D. (1999). “Transport of organic contaminants in geomembranes under stress.” *Journal of Environmental Engineering*, 125 (7), 647-652.

Zhang, Z., Britt, I. J., and Tung, M. A. (1999). “Water absorption in EVOH films and its influence on glass transition temperature.” *Journal of Polymer Science Part B. Polymer Physics*. 37, 691–699.

Zhang, Q., Lin, W., Chen, Q., and Yang, G. (2000). “Phase structure of EVOH copolymers as revealed by variable temperature solid state high resolution.” 13C NMR spectroscopy. *Macromolecules*. 33, 8904-8906.

Chapter 2 Transport of Volatile Organic Compounds (VOCs) through Composite Liner with Co-Extruded Geomembrane Containing Ethylene Vinyl-Alcohol (EVOH)

2.1 ABSTRACT

A co-extruded geomembrane (GM) with a layer of ethylene vinyl-alcohol (EVOH) has applicability in environmental containment applications as the hydrophobic properties of the polyethylene retards contaminant flux; specifically, the diffusion of non-polar volatile organic compounds (VOCs). This research experimentally measured the relative migration of five common VOCs through composite landfill liners constructed with two types of co-extruded GM containing EVOH. To simulate *in situ* configurations of composite liners, a series of column tests with different types of GMs overlying either a compacted clay liner (CCL) or a geosynthetic clay liner (GCL) were conducted. VOC breakthrough in composite linear employing high-density polyethylene (HDPE) GMs (35 d) occurred more than two and four times faster than employing co-extruded EVOH GMs with LLDPE and HDPE outer layer, respectively (≈ 70 and 150 d) and with significantly higher VOC concentrations. Co-extruded EVOH GMs with LLDPE and HDPE as an outer layer had measured diffusion coefficients (0.11 - 0.57 × 10^{-13} m^2/s and 0.14 - 0.58 × 10^{-13} m^2/s, respectively) more than 20 times smaller in comparison to conventional HDPE GM (2.86 - 11.05 × 10^{-13} m^2/s). For the CCL and GCL composite liners, the concentration of VOCs at 80-mm depth was much lower in the CCL compared to the GCL. Numerical modeling (finite difference

method) of VOC migration through a composite liner with 0.6-m-thick and 1.2-m-thick CCL with a co-extruded EVOH GM indicated that contaminant transport was approximately 14% and 22% lower, respectively in one hundred years. To achieve the same level of protection as provided by the co-extruded GM underlain by 0.6 m and 1.2 m of CCL, an additional 0.1 m and 0.27 m of compacted clay is needed, respectively, in conjunction with a conventional GM. Thus, co-extruded EVOH GMs acted as an effective barrier to VOC migration in composite liners.

Keywords: EVOH (Ethylene-vinyl alcohol); Co-extruded geomembrane; Compacted clay liner (CCL); Geosynthetic clay liner (GCL); Composite liner; Diffusion; Sorption; Volatile organic compounds.

2.2 INTRODUCTION

Co-extruded geomembranes (GM) are a type of GM that may limit contaminant flux (Sangam and Rowe 2005; Edil 2007). One type of co-extruded GM includes polyamide (nylon) as the inner layer (McWatters and Rowe 2010). Polyamides have lower permeability to organic solvents and gases than pure polyethylene resins (Yeh and Fan-Chiang 1996). Co-extruded GMs with an ethylene vinyl-alcohol (EVOH) layer incorporate polyethylene as the water barrier and also have the potential to substantially reduce the diffusion of non-polar volatile organic compounds (VOCs). The permeability of a co-extruded EVOH GM via diffusion is significantly lower than linear low-density polyethylene (LLDPE), high-density polyethylene (HDPE), and polyvinyl chloride (PVC) GM

(McWatters and Rowe 2010, 2011; Armstrong 2011).

For the proper design and analysis of a barrier system containing a co-extruded GM, the transport parameters must be determined such that solute flux is correctly accounted for. Batch testing (sorption/immersion) of traditional, single-composition GMs have historically provided simple, quick, and accurate results (Park et al. 2012a). Furthermore, in comparison to more complex double-compartment apparatus tests (i.e., diffusion testing), batch testing of homogeneous GMs generally provides reasonable results because solute loss during testing is minimized (Park et al 2012a). However, with a co-extruded GM, a batch test is not appropriate for determining transport parameters because solute migration through the interior EVOH layer is not represented (McWatters and Rowe 2010, Eun et al. 2014b). Further, batch tests cannot simulate the layered configurations of GM and compacted clay liner (CCL) or geosynthetic clay liner (GCL) performing as composite liners. Thus, diffusion testing in columns with multi-layered configurations that incorporate co-extruded GMs is required to validate the transport of contaminants via diffusive flux.

Analytical modeling of composite liners has been verified with experimental results (Park et al. 2012b). However, few studies have systematically investigated the behavior of VOC transport through composite liners that use a co-extruded EVOH GM as a contaminant barrier in addition to a CCL or GCL. Therefore, a laboratory study to evaluate VOC transport and to identify the situational migration through GM enhanced with EVOH is warranted. This research effort evaluates the relative rates of transport of common VOCs

through composite landfill liners constructed with a co-extruded GM containing a layer of EVOH and compares these rates to those of conventional HDPE. The transport characteristics of composite liners employing GCL are investigated in comparison to CCL. Based on the results of diffusion testing with composite liners employing a co-extruded EVOH GM, transport parameters are evaluated and quantified as compared to those of HDPE GM. Further, by conducting numerical analysis (i.e., finite difference method) using obtained transport parameters, VOC transport is estimated in simulating practical condition of composite liners.

2.3 BACKGROUND

2.3.1 Overview of EVOH

Enhanced geomembranes that act as chemical barriers with higher durability are suitable for use in landfill covers and liner applications. For example, HDPE GMs with added fluorination limit VOC diffusion through liners (Sangam and Rowe 2005). Another technique is co-extrusion which is the process of extruding two or more materials through a single die with two or more orifices arranged so that the extrudates merge and weld together into a laminar structure before chilling. The first co-extruded, multi-layered GMs had HDPE outer layers and low-density polyethylene as the inner layer (Kolbasuk 1991). These multi-layered GMs have evolved to include co-extruded GMs with polyamide (nylon) as the inner layer. Polyamides have a lower permeability to organic solvents and gases than pure polyethylene resins (Yeh and Fan-Chiang

1996; Gonzalez-Nunez et al. 2001).

Co-extruded GMs with EVOH layers take advantage of the properties of polyethylene as a water barrier, while having the potential to substantially reduce the diffusion of VOCs. EVOH is a random copolymer of ethylene and vinyl alcohol including polar oxygen–hydrogen (-OH) groups. Because the monomer mainly exists as tautomer acetaldehyde, the copolymer is prepared by polymerization of ethylene and vinyl acetate to provide the ethylene vinyl acetate (EVA) copolymer followed by hydrolysis (Armstrong 2011). EVOH copolymer is defined by the mole % of ethylene content, thus lower ethylene content grades have higher barrier properties for non-polar organic contaminants; higher ethylene content grades have more flexible easy for extrusion. Eq. (1) represents the chemical formulation of EVOH.

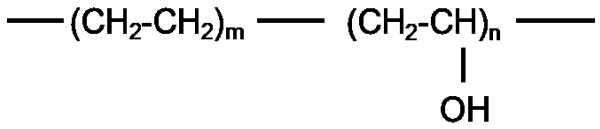

(1)

EVOH with polarity has outstanding barrier properties to non-polar gases such as oxygen, nitrogen, volatile compounds, and helium (Zhang et al. 1999, 2000; Byun et al. 2007; McWatters and Rowe 2011). Moreover, EVOH laminar is typically a combination of a highly ordered crystalline structure interspersed with disordered amorphous regions that combine for high resistance to diffusion of both gasses and solvents.

The manufacturing process of a co-extruded GM with EVOH is more

complicated relative to monomer-type GMs. First, an HDPE or LLDPE outer layer is extruded through a die with an orifice and then is dried. Next, an EVOH laminar is arranged such that the extruded layers merge and weld together onto the laminar. Each material is fed to the die from a separate extruder, but the orifices may be arranged so that each extruder supplies two or more plies of the same material. The ply of the EVOH GM is manufactured to produce the desired barrier properties (Kolbasuk 1991; Armstrong 2011).

2.3.2 Diffusive Transport through Composite Liner

In saturated soil, one-dimensional (1-D) mass transport of a non-decaying solute via diffusion can be expressed as (Hashimoto et al. 1964; Freeze and Cherry 1979):

$$\frac{\partial C_s}{\partial t} = \frac{D^*}{R}\frac{\partial^2 C_s}{\partial z^2}, \qquad z > 0 \tag{2}$$

where C_s is the concentration of the organic compound in the pore water of the soil liner [M/L^3], z is the distance along the direction of mass transport [L], t is elapsed time [T], R is the retardation factor, and D^* is the effective diffusion coefficient [L^2/T]. Partitioning of organic compounds between soil particles and solution can be quantified by the partition coefficient (K_d) as follows:

$$K_d = \frac{C_s}{C_w} \tag{3}$$

where C_w is the equilibrium concentration in solution [M/L^3] and C_s is the concentration adsorbed to the soil particle [M/M]. Similarly, the partition or distribution coefficient (K_g) between the GM and the solution can be defined as (Leo et al. 1971):

$$K_g = \frac{C_g}{C_w} \tag{4}$$

where C_g is the equilibrium concentration of organic compound with the GM [M/M] and K_g is the dimensionless GM-water partition coefficient of the organic compound.

The organic compound sorbed to the surface of a GM begins transport through the GM by molecular diffusion. Diffusion through a GM is typically described using Fick's second law. The governing equation for 1-D constant diffusion for organic compounds in the GM can be represented as (Park and Nibras 1993; Park et al. 1996; Sangam and Rowe 2001b; Joo et al. 2004, 2005; Park et al. 2012a, b):

$$\frac{\partial C_g}{\partial t} = D_g \frac{\partial^2 C_g}{\partial z^2}, \qquad -L_g < z < 0 \tag{5}$$

where t is elapsed time [T], D_g is the diffusion coefficient of the organic compound in the GM [L^2/T], z is the distance along the direction of diffusion [L], and L_g is thickness of the GM [L]. Eq. (4) is valid if the diffusion coefficient in the GM is temporally and spatially invariant (Foose et al. 2001; Foose et al. 2002).

Desorption of the organic compound is the last transport step from the GM to the outer solution or received medium (e.g., soil). This step is an inverted version of adsorption. Use of Eqs. (2) to (5) requires transport parameters (e.g., partition and diffusion coefficients) of composite liners that can be estimated by fitting experimental data from diffusion column tests.

2.4 MATERIALS

2.4.1 Organic Compounds

Five VOCs were used as organic contaminants: methylene chloride (MC), methyl tertiary butyl ether (MTBE), trichloroethylene (TCE), toluene (TOL), and chlorbenzene (CB). These VOCs are considered representative types of VOCs (i.e., alkanes, ethers, alkenes, aromatic hydrocarbones, and halogenated aromatic hydrocarbons) among the 31 VOCs that were reported in lysimeters from 34 landfill sites in Wisconsin (Klett et al. 2005). Toluene was detected in 49 of 54 cells, methylene chloride in 34 cells, TCE in 15 cells, MTBE in 17 cells, and chlorobenzene in 9 cells. Among the detected VOCs, MC had the largest percentage (85%) of samples exceeding Wisconsin ground water enforcement standards (ES). TCE had 41% of the samples exceeding the ES, TOL 5.2% and MTBE 3.6%. Despite frequent detection, chlorobenzene did not have any samples exceeding the ES (Klett et al. 2005). General properties of these VOCs are described in Table 2.1 (Schwarzenbach et al. 2003; Lake and Rowe 2005; Park et al. 2012b). For the testing program, the VOC solutions were prepared by filling a 1-L flask with distilled and deionized (DDI) water. Sodium azide (0.05%)

was added to prevent microbial activity.

2.4.2 Geomembrane

A co-extruded GM with a 0.05-mm-thick layer of EVOH was used to examine the diffusive transport of VOC contaminants. Two EVOH GMs of varying thickness (1.0 mm and 1.5 mm) and having different outer layers (LLDPE for 1.0 mm and HDPE for 1.5 mm) were evaluated (henceforth labeled as 1.0-mm-EVOH GM and 1.5-mm-EVOH GM, respectively) (Fig. 2.1). Due to polar oxygen–hydrogen (-OH) groups of EVOH, EVOH has outstanding barrier properties to non-polar gases such as oxygen, nitrogen, volatile compounds, and helium (Zhang et al. 1999; Zhang et al. 2000). EVOH laminar is typically a combination of a highly ordered crystalline structure interspersed with disordered amorphous regions that shows high resistance to diffusion of gas and solvent (Zhang et al. 1999; Zhang et al. 2000; McWatters and Rowe 2011). Hence, a co-extruded EVOH GM is expected to allow less migration of VOC through a composite liner employing the GM. Smooth, black, 1.5-mm-thick HDPE GM was used as a control to compare with co-extruded HDPE GM with EVOH film. Also, a column with a compacted clay liner (CCL) without GM was tested. The geomembranes were cut to high precision with a milling machine that allowed for a tight fit in the testing column.

2.4.3 Compacted Clay Liner

Kamm clay was used as the CCL for column testing because the clay has

been used for constructing liners at Dane County Landfill in Madison, Wisconsin, and has been extensively characterized (Park et al. 2012b, Eun et al. 2014b). The optimum water content of Kamm clay at reduced compaction effort is 21%. Reduced compactive effort was chosen to lower the hydraulic conductivity sufficiently to finish saturation and sampling in the desired time prior to the main diffusion test (Park et al. 2012b). For saturation, a 0.05% solution of sodium azide from DDI water was used to reduce microbe activity. Stabilization of hydraulic conductivity was achieved when the ratio of inflow and outflow approached unity (fluctuation < 10%). The saturated hydraulic conductivity of the compacted Kamm clay was approximately 3.5×10^{-8} cm/s.

2.4.4 Geosynthetic Clay Liner

Geosynthetic clay liners are widely used as a substitute or supplement to a CCL in a landfill. A reinforced GCL (Bentomat ST®, CETCO) consisting of a layer of sodium bentonite between a woven and a non-woven geotextile, which are needle-punched together, was installed beneath the GM in the column tests for this study. The GCL tested has been used at many field sites and its performance as a barrier has been confirmed (Malusis and Shackelford 2002). The properties of the GCL are shown in Table 2.2. Uniform Ottawa sand was used as an attenuation layer and placed beneath the GCL. The attenuation layer for the column test works to support the GCL underlying the geomembrane. The Ottawa sand was 99.3% silica (SiO_2) and 0.1% Fe_2O_3. The particles were rounded, medium-sized sand (< 2.0 and > 0.425 mm) and classify as a poorly

graded sand (SP) according to USCS classification (ASTM D 2487), with the particle distribution shown in Fig. 2.2.

For saturation of the GCL, bentonite paste was first applied around the circumference with a small spatula to prevent side-wall leakage as shown in Fig. 3. After sealing the interface with the side wall, a hydraulic gradient was applied to the column base (i.e., bottom-up saturation). After two days, the direction of water flow was changed to flow downward, thus beginning the saturation check of the GCL. Similar to the saturation procedure for the CCL, the ratio of inflow and outflow was targeted to range between 0.9 and 1.1 for confirmation of saturation. The hydraulic conductivity of the saturated GCL stabilized to 5.5×10^{-10} cm/s in 7 d.

2.5 METHODS

2.5.1 Diffusion Column Tests

Column-type diffusion experiments consisted of a CCL overlain by two types of GMs (a co-extruded EVOH GM and an HDPE GM). The test for EVOH GMs was replicated. The bench-scale composite liner column is shown in Fig. 2.3(a). The column (20-cm height, 15.5-cm diameter) was constructed with aluminum. The testing column is divided into upper and lower compartments such that the tested GM sits at the joint of the compartments. In the joints, two polytetrafluoroethylene (PTFE) rectangular gaskets were installed on the top and bottom of the GM to minimize the adsorption of VOC solute and/or loss of VOC solution through the joint as shown in Fig. 2.3(b). Three sampling ports were

installed in the column to allow for the identification of the breakthrough concentration from column top to bottom at 20-, 40-, and 80-mm depth. The sampling ports included a brass connector and cap with two septa to extract sample with minimal loss of VOC during sampling. The end of the port was filled with a packed glass-fiber filter (< 0.7 μm) to limit migration of soil particles into the sample. For good contact during the column diffusion test, stainless steel beads were placed on the GM (1.0-kPa-confining pressure). The PTFE rectangular gasket sealed the gap between the column and plates.

The concentration of the VOC solution in the upper chamber decreased with time because some solute adsorbed and migrated through the tested GM during testing. To maintain a constant VOC concentration in the upper chamber, a concentrated VOC solution was occasionally injected though the sampling port in the top plate. To mix the injected solution quickly and to keep the concentration of VOC consistent, two stirrers made of aluminum and magnetic discs were located on the top plate. The matrix of setups for diffusion column testing is described in Table 2.3.

2.5.2 Batch Tests

Equilibrium batch isotherm tests were conducted to determine the partition coefficients of the VOCs for Kamm clay, bentonite from a GCL, and attenuation sand, which were the materials used in the various composite liners evaluated in the diffusion column tests. The method described by Park et al. (2012b) and Kim et al. (2001) was used for the batch tests. The soils, including Kamm clay and

bentonite from a GCL, were crushed, ground, and passed through a number four sieve (mesh opening = 4.75 mm). The soils were then air dried and stored in a desiccator at room temperature before testing. The sand was also washed with DDI water and air dried. The soil (25 g) was then placed in a 40-mL amber glass vial and solution was added to fill the vial (soil-liquid ratio approximately 1 kg/L). The bentonite from the GCL was hydrated with DDI water before mixing with the VOC solution, but the hydration minimally influenced the sorption of VOC to the bentonite (Kim et al. 2003; Lake and Rowe 2005; Paumier et al. 2011). The vial was sealed using a screw cap with a Teflon-coated septum. The largest achievable soil-liquid ratio (1:1 g/L) was used for the batch tests to closely simulate conditions in the bench-scale liner (Kim et al. 2003).

Solutions having initial concentrations of 10, 40, 70, and 100 mg/L of each VOC were used for tests conducted with multi-solute mixtures of VOCs. Solutions were prepared using the methods described previously and transferred to each vial from 1-L flasks using a peristaltic pump. When VOC solution was moved into each vial from the flask, the Teflon tube of the pump was attached to the bottom of the vials to minimize loss of VOC (Parker and Britt 2012). The filled vials were tumbled in a rotator at 30 revolutions per minute, rpm, for 8 d at 23.5 °C, which is sufficient time to reach equilibrium according to previous research (Park et al. 2012a). After tumbling, the vials were centrifuged at 2,000 rpm (429 g) for 15 min to assure equivalent dispersion of VOC in the vial. The supernatant was transferred to auto sampler vials using a glass syringe without opening the cap of the vial and was then analyzed by GC.

Three replicates were conducted for each concentration and two controls without solids were also prepared to check for losses (< 5.0%). Concentrations were adjusted for losses using the loss data from the controls.

Similar to the soils, partition coefficients of VOCs for the EVOH and HDPE GM were measured independently using equilibrium batch tests. The general procedure to conduct the batch tests was similar to that used with the soils except in the preparation of the specimens. Specimens of geomembrane were cut into strips (17 × 80 mm) from a large HDPE geomembrane sheet, washed with DDI water, and placed in a desiccator for 48 h before use in the experiments. A strip of geomembrane (1.40 g – 1.93 g) was placed in an amber glass vial (40 mL), solution was added to fill the vial, and the vial was sealed with a screw cap with a Teflon-coated septum. Solutions having initial concentrations of 10, 40, 70, and 100 mg/L of each VOC were used for the tests, which was identical to concentrations used with the soils.

2.5.3 Measurement of Concentration

VOC concentrations were measured using a Shimadzu GC-2010 gas chromatograph (GC) equipped with an auto sampler, flame ionization detector (FID), and Restek RTX-624 column (length = 30 m, inner diameter = 0.32 mm, and film thickness = 1.80 μm). Temperatures of the injection port and the FID were 280 °C. The sample split ratio was 3.0, and the injection volume was 0.5 μL. The column had initial column temperature of 35 ºC and hold time of 5 min. The column was heated to 100 °C at a rate of 10 °C/min, held at 100 °C for 3

min, heated to 220 ºC at a rate of 40 °C/min, then held at 220 °C. The total run time for each injection was 20 min. The detection limits (DLs) were 0.82 mg/L for MC, 0.53 mg/L for TCE, 0.34 mg/L for TCE, 0.31 mg/L for TOL, and 0.22 mg/L for CB.

2.6 ANALYSIS OF DIFFUSION COLUMN TESTS

2.6.1 Comparison of VOC Concentration through Composite Liner with 1.5-mm EVOH GM over CCL

Measured concentrations of VOCs at the sampling ports in the testing column were extracted with increasing time and depth. Concentrations measured at the upper (20-mm depth), middle (40-mm depth), and lower (80-mm depth) sampling ports in the composite liner employing 1.5-mm-EVOH GM over CCL are shown in Fig. 2.4(a) through Fig. 2.4(c). At 150 d, significant concentrations of VOCs at the first sampling port (depth = 20 mm) were recorded [Fig. 4(a)] that were higher than detection limits (0.2~0.8 mg/L). After breakthrough, migration of MC, MTBE, and TCE was slightly greater than for TOL and CB. With increasing time, the migration of MC, TCE, and CB increased markedly, while the migration of TOL and MTBE increased gradually. TOL migrates less than similar non-polar VOCs (i.e., arenes) such as CB because TOL has the smallest negative charge (dielectric constant = 2.4) and higher hydrophobicity; hence, TOL tends to dissolve less into the EVOH layer of the GM, thus decreasing the amount of TOL solute available to migrate through the outer layer made of HDPE. Further, TOL has less Brownian motion due to its larger molecular diameter and lower diffusive

transport through the outer layer (i.e., HDPE) in comparison to similar aromatic hydrocarbons such as CB (Lake and Rowe 2005; Park et al. 2012b; Eun at al. 2014a, b). Therefore, TOL exhibited relatively lower flux.

MTBE and MC, which have relatively high polarity because of strong covalent bonds relative to other non-polar VOCs (e.g., TOL and CB), breakthrough earlier in the EVOH GM in the initial time of the column testing (< 150 d) (Schwarzenbach 2003). However, MTBE migrates less with increasing time because MTBE partitions minimally to the HDPE outer layer, which leads to less solute transport (Park et al. 2012b). MTBE has a partition coefficient that is two orders of magnitude smaller than the other non-polar VOCs tested. Because MTBE has the least amount of partitioning (K_g = 0.8) into HDPE among the VOCs tested, the migration of MTBE is less than other VOCs even though MTBE has high polarity. MC, which also has high polarity and a partition coefficient one order of magnitude higher than MTBE, showed the highest migration in testing. At 350 d, MC approached approximately 9.6% of input concentration (100 mg/L), while MTBE was the least and approached 2.5%. TCE (an alkene, which has a median strength of covalent bonding among the VOCs tested) showed relatively high migration through the EVOH GM because TCE can more readily migrate through both the EVOH layer and the HDPE outer layer.

At 40-mm depth, concentrations of VOCs above the DL were recorded in 175 d [Fig. 2.4 (b)]. At 300 d, MC approached approximately 5.1% of input concentration (100 mg/L), which was the highest, and MTBE approached 1.9%, which was the least. With increasing depth, the effect of transport parameters

might be diminished because the difference of concentration among VOCs is reduced (Park et al. 2012b). At 80-mm depth [Fig. 2.4 (c)], VOC concentrations were less than 2.5% of input concentration; however, the order of migration for the different VOCs was identical to those at 20-mm depth.

2.6.2 Comparison of VOC Concentration through Composite Liner with 1.0-mm EVOH GM over CCL

Measured concentrations of VOCs in the composite liner employing 1.0-mm-EVOH GM are shown in Fig. 2.5 (a) – (c). At 70 d, significant breakthrough of VOC concentrations at the first sampling port (depth = 20 mm) in the composite liner were detected (> DLs), which is much faster than those in the composite liner employing 1.5-mm-EVOH GM [Fig. 2.4 (a)]. The flux also increased faster than those in the 1.5-mm-EVOH GM composite liner. At 200 d, the concentration detected in the composite liner employing 1.0-mm-EVOH GM was approximately two times higher than those in the composite liner employing 1.5-mm-EVOH GM. For example, MC detected in 1.5-mm-EVOH GM was 4.2 mg/L, whereas MC detected in 1.0-mm-EVOH GM was 10.8 mg/L. The thickness and material type of the outer layer influenced the transport behavior of VOC through the co-extruded GM.

In the initial time of the test after breakthrough (< 150 d), TOL migrated markedly less than other non-polar compounds such as TCE and CB in the 1.0-mm-EVOH GM due to the higher hydrophobicity of TOL for EVOH. This trend is similar to the 1.5-mm-EVOH GM. However, MC showed significantly different

migration levels between the 1.0-mm-EVOH and 1.5-mm-EVOH GMs. During the early testing period (< 200 d), similar to the 1.5-mm-EVOH GM, MC showed the highest migration followed by TCE. However, after 200 d for the 1.0-mm-EVOH GM, the flux of MC gradually reduced and MC migrated lower than the other non-polar VOCs. This occurs because MC has a lower partition coefficient to the outer layer (non-polar polyethylene, PE) due to higher polarity (i.e., lower hydrophobicity). Hence, the effect of the EVOH layer in the 1.0-mm-EVOH GM was less than that in the 1.5-mm-EVOH GM. MTBE migrated at the lowest concentration due to having the lowest partitioning to PE, which was used as the outer layer of the co-extruded GM. TCE showed the highest migration through the 1.0-mm-EVOH GM (similar to the 1.5-mm-EVOH GM) because TCE diffuses more rapidly through both the EVOH layer and the HDPE outer layer. At the 40-mm depth, the VOC concentration in 1.0-mm-EVOH GM was detected lower than at the 20-mm depth [Fig. 2.5 (a) and (b)]; however, the order of migration was identical to those at the 20-mm depth with increasing time. This trend continued at the 80-mm depth [Fig. 2.5 (c)].

2.6.3 Comparison of VOC Concentration through Composite Liner with 1.5-mm EVOH GM over GCL

To investigate VOC transport through composite liners of varying configurations and layers, a series of column tests were conducted with GCL underlain by an attenuation layer (i.e., silica sand). Similar to composite liners that included a CCL, VOC concentrations were measured at the three sampling

ports placed at the same depths (i.e., 20-, 40-, and 80-mm) as shown in Fig. 2.6 (a) - (c). Measured concentrations of VOCs in the composite liner employing 1.5-mm-EVOH GM overlying a GCL in column-type diffusion experiments are shown in Fig. 2.6 (a). At 180 d, significant breakthrough of VOC concentrations at the first sampling port (depth = 20 mm, immediately below the GCL) were recorded (> DL). The breakthrough time for VOCs in the composite liner including the GCL was delayed around 30 d in comparison to the same configuration with a CCL [see Fig. 2.4 (a)]. The slower breakthrough time for the liner with the GCL was possibly due to a much lower diffusion coefficient in the GCL due to higher touristy of bentonite in comparison to clay (Shackelford and Daniel 1991). At breakthrough, the concentrations of MC and TCE were slightly greater than for TOL. The ordering of VOCs concentrations in the composite liner with GCL was similar to that in the CCL because the bentonite in GCL, which is composed of mostly inorganic compounds (e.g., montmorillonite), tends to minimally influence partitioning of VOC solute to the surface of bentonite particles (Headley et al. 2001; Paumier et al. 2011). However, with increasing time, the concentration of TCE increased markedly, while that for TOL increased gradually because TCE diffuses more rapidly through both the EVOH layer and the HDPE outer layer, however TOL diffuses slower through the EVOH layer due to its lower polarity. Overall, TOL and MTBE migrated less through the composite liners with GCL, similar to the cases with CCL.

After breakthrough through the GCL component of the composite liner containing 1.5-mm-EVOH GM, the concentration of VOCs in the attenuation layer

(i.e., sand) increased quickly compared to those through the CCL because VOC solutes can migrate more rapidly through layers with lower tortuosity (Shackelford and Daniel 1991). For instance, at 300 d, the concentration of TOL in the attenuation layer at 20-mm depth increased by around 39% (from 4.1 mg/L to 5.7 mg/L) compared to that in the CCL. Furthermore, the migration of VOC might be faster with increasing depth in the attenuation layer. The effect of the layer to reduce the migration of VOC might be languished in the attenuation layer in comparison to CCL. For example, at 300 d, the concentration of TOL decreased from 5.7 mg/L to 3.1 mg/L for depths of 20 mm to 80 mm, respectively, in the GCL with the underlying attenuation layer. In comparison, in the composite system with the CCL, the concentration of TOL decreased markedly (from 4.1 mg/L to 0.4 mg/L) between sampling depths of 20 mm and 80 mm.

At the 40-mm depth, VOC concentrations ranged from 3.1% to 11.9% of input concentration (100 mg/L) at 320 d [Fig. 2.6(b)]. Further, at the 80-mm depth, VOC concentrations ranged from 2.5% to 7.9% of input concentration at 350 d [Fig. 2.6(c)]. Because of minimizing sampling effect, the different sequence was selected for the sampling from the sampling port (Park et al. 2012b). The variance of VOCs in the GCL with the underlying attenuation layer is narrower than in the CCL at the 20-mm depth; however, the order of migration for the different VOCs was similar to those at the 20-mm depth.

2.6.4 Comparison of VOC Concentration through Composite Liner with 1.0 mm-EVOH GM over GCL

Measured concentrations of VOCs in the composite liner employing 1.0-mm-EVOH GM over GCL are shown in Fig. 2.7 (a) - (c). At 100 d, significant breakthrough of VOC concentrations at the first sampling port (depth = 20 mm) in the composite liner employing 1.0-mm-EVOH co-extruded GM were detected, which was approximately 30 d faster than those in the composite liner employing the 1.5-mm-EVOH GM. The difference of breakthrough time between the 1.0-mm- and 1.5-mm-EVOH GM with GCL is similar to those columns with the CCL. In addition, VOC flux also increased faster than those employing 1.5-mm-EVOH GM. At the same time period (i.e., at 300 d), the concentration detected in the composite liner employing 1.0-mm-EVOH GM was several times higher than those in the composite liner employing 1.5-mm-EVOH GM. For example, MC detected in the 1.5-mm-EVOH GM was 8.2 mg/L, whereas MC detected in the 1.0-mm-EVOH GM was 25.5 mg/L. For the co-extruded GMs evaluated in this study, the thickness and material type of the outer layer significantly influenced the overall rate of VOC transport.

Similar to the 1.5-mm-EVOH GM, TOL migrated less than the other non-polar VOCs in the 1.0-mm-EVOH GM due to its hydrophobicity for EVOH. In the 1.0-mm-EVOH GM, TCE had the highest levels of flux, followed by MC. However, similar to the columns with the CCL, MC showed various flux. In the early testing period (< 200 d), similar to 1.5-mm-EVOH GM, MC showed the highest concentrations followed by TCE in 1.0-mm-EVOH GM. However, after 200 d in

1.0-mm-EVOH GM, the increasing rate of concentration of MC gradually reduced and the concentration of MC is markedly lower compared with other VOCs except MTBE. In similar to CCL cases, this occurs because MC has a lower partition coefficient to the outer layer (non-polar polyethylene, PE) due to higher polarity (i.e., lower hydrophobicity). Hence, the effect of the EVOH layer in the 1.0-mm-EVOH GM was less than that in the 1.5-mm-EVOH GM. At the 40-mm depth, the migration of VOCs in 1.0-mm-EVOH GM was detected as lower than at the 20-mm depth. The 80-mm depth is lower than those of 40-mm depth; however, the order of migration is identical to those at the 20-mm depth [Fig. 2.7 (b) and (c)].

2.7 CHRACTERISITICS OF DIFFUSIVE TRANSPORT THROUGH COMPOSITE LINERS DEPENDING ON GEOMEMBRANE TYPE

2.7.1 Effect of HDPE GM

For control testing, concentrations of VOCs were measured in the column with CCL only and the composite liner employing an HDPE GM (see Fig. 2.8). Significant flux (> DLs) of VOCs occurred in the CCL within 2 d, while breakthrough of VOCs through the composite liner including the HDPE GM occurred at approximately 35 d. Because of lower partition and higher diffusion coefficients of clay liners (Kim et al. 2001; Park et al. 2012b) in comparison to HDPE GM, the concentration of VOCs increased much more rapidly in the CCL than in the composite liner with the HDPE GM. At 50 d, the concentration of VOCs at the first sampling port (depth = 20 mm) in the CCL approached nearly

40% of the 100 mg/L source concentration. The concentration of VOCs at the first sampling port (depth = 20 mm) in the composite liner employing HDPE GM approached almost 60 mg/L in 200 d. HDPE GMs have been observed to reduce the migration of VOC in comparison to CCLs without GM (Sangam and Rowe 2001a; Park et al. 2012b). For example, at 70 d, the concentration of MC at 20-mm depth was 54% lower in the composite liner than in the CCL.

2.7.2 Effect of EVOH GM

Figure 2.9 (a) shows migration of selected VOCs (i.e., MC and TCE) with time through the co-extruded EVOH GM in comparison to the HDPE GM overlying CCL. The HDPE GM had more rapid breakthrough and higher migration rates of VOC in comparison to the EVOH GM. For example, at 200 d, the concentration of MC at 20-mm depth was 4.3 times higher (4.4 times higher for TCE) in the composite liner employing HDPE GM in comparison to the column with the 1.0-mm-EVOH GM. The EVOH film in the co-extruded GM played an important role as a barrier with respect to VOC migration through these composite liners.

Further, diffusive behavior reflects the relative rates of transport of VOCs between EVOH GM and HDPE GM. The order of VOC flux in the composite liner with an HDPE GM was different from those with the 1.5-mm-EVOH GM. In contrast to the case of 1.5-mm-EVOH GM, the concentrations for the less hydrophobic MC are markedly lower compared to other VOCs in the composite liner employing HDPE GM [see Fig. 2.8 (a)]. In 1.0-mm-EVOH GM, MC migrated

similar to TCE; however the flux of MC was reduced at 220 d. MC showed higher migration in the 1.5-mm-EVOH GM rather than other GMs.

Figure 2.9 (b) showed the different migration of VOCs with time to compare the migration rate of VOC through co-extruded EVOH GM to the HDPE GM overlying GCL. Generally, the trend of migration of VOCs in GCL is similar to those in the CCL. However, at 20-mm depth, the HDPE GM in GCL allowed slower breakthrough time (i.e., 45 d) and higher migration rates of VOC because the bentonite in the GCL has smaller partition and diffusion coefficient than clay in the CCL. The effect of EVOH GM to prevent the migration of VOC is remarkably effective compared to HDPE GM in GCL. However, the difference of VOC migration between EVOH GM and HDPE GM is reduced when EVOH GM is employed with GCL and attenuation layer in comparison to CCL. The order of migration rate in the composite liner with an HDPE GM and EVOH GM overlying the GCL was similar to those overlying the CCL. Accordingly, the EVOH GM is an effective barrier to the migration of VOC when combined with either CCL or GCL.

2.8 MEASUREMENT OF TRANSPORT PARAMETERS

2.8.1 Transport Parameters of Soils and GCL

Sorption isotherms for Kamm clay, bentonite, and Ottawa sand are shown in Fig. 2.10. Partition coefficients were computed by fitting the linear isotherm [Eq. (3)] to the sorption data using least-square regression. The isotherms are approximately linear, which is consistent with previous studies on VOC sorption

to clay barrier soils (Edil et al. 1995; Kile et al. 1995; Headly et al. 2001; Lake and Rowe 2005). The Kamm clay had the highest partition coefficient among soils tested due to the higher organic carbon content. Similarly, the sand had the lowest partition coefficient because this sand was mostly composed of silicate (very low organic carbon content). Table 2.4 summarizes the measured partition coefficients. The partition coefficients for bentonite are lower than those reported in previous studies (Headly et al. 2001; Lake and Rowe 2005) because of the lower organic carbon content and higher soil-liquid ratio used in the batch test.

The measured partition coefficients from the batch tests were compared to estimated values based on organic carbon content. The soil-water partition coefficient, K_d, for an organic compound is often estimated using the organic compound/organic carbon partition coefficient, K_{oc}, of the organic compound (Kim et al. 2001; Lake and Rowe 2005). For soils with varying organic carbon content, f_{oc}, the soil-water partition coefficient for a given VOC can be obtained from

$$K_d = f_{oc} \cdot K_{oc} \tag{6}$$

K_{oc} is a reasonably constant value for a large number of soils with relatively low f_{oc} in the range of 0.1- 6% (Kile et al. 1995; Kim et al. 2001). To obtain K_{oc}, the measured soil-water partition coefficients for the soils were divided by the organic carbon mass fraction, f_{oc} of 1.06%.

$$\log K_{oc} = 0.92 + 0.36 \cdot \log K_{ow} \qquad (R^2 = 0.92) \qquad (7)$$

Since K_{ow} values of most organic compounds are readily available, K_d for soil is estimated by using Eqs. (6) and (7) with f_{oc} in the range of 0.1 – 6.0%. Fig. 11 shows the comparison between the measured K_d values for Kamm clay, bentonite, and sand from the batch tests and the K_d values estimated from Eqs. (6) and (7). Both values except in sand are statistically identical ($p > 0.05$) from a paired F-test because the equation was developed based on clay data (Kim et al. 2001). Thus, the measured partition coefficient is reliable.

Effective diffusion coefficients for the VOCs were measured using a series of single-reservoir diffusion tests following the method described by Park et al. (2012a) and Shackelford and Daniel (1991). The tests were conducted employing: (1) clay only, (2) sand only, and (3) GCL with sand. The test was set up and conducted in the same manner as the bench-scale composite liner test (Fig. 3) except no GM was installed. Diffusion coefficients were obtained by fitting the temporal concentration data simultaneously from three sampling ports equal to 20, 40, and 80 mm below the composite surface with the one-dimensional finite-difference model. Nonlinear least-squares regression was used to obtain the fit. Partition coefficients from equilibrium batch tests were used as input to the model (Kim et al. 2001a; Park et al. 2012). Effective diffusion coefficients and apparent tortuosity factor for the Kamm clay, Ottawa sand, and bentonite are summarized in Table 2.5 for each VOC. For the GCL, the geotextile surrounding the bentonite only slightly influenced the diffusion coefficient and thus could be

neglected for the estimation (Lake and Rowe 2005; Paumier et al. 2011). The effective diffusion coefficient of bentonite was smallest, ranging from 5.5×10^{-7} m^2/s to 5.9×10^{-7} m^2/s for the five VOCs because the apparent tortuosity factor (τ_a) of bentonite is smallest, ranging from 0.01 to 0.22. Sand had the highest diffusion coefficient, ranging from 5.7×10^{-6} m^2/s to 6.9×10^{-6} m^2/s, because sand has the highest τ_a ranging from 0.2 to 0.35, which means the lowest tortuosity (Shackelford and Daniel 1991; Park et al. 2012b; Lake and Rowe 2005).

2.8.2 Transport Parameters of Geomembrane

Sorption isotherms for the VOC are shown in Fig. 2.12. Partition coefficients were computed by fitting the linear isotherm [Eq. (4)] to the sorption data using least-square regression. The measured partition coefficients are summarized in Table 2.6. The isotherms are approximately linear, which is consistent with previous studies on VOC sorption to the geomembrane in given range of low concentrations (< 100 mg/L) (Edil et al. 1995; Park et al. 1996; Sangam and Rowe 2005). Because the EVOH film is thin enough to neglect in comparison to the surface area of HDPE, the sorptive behavior of VOC to the HDPE outer layer was similar between the co-extruded EVOH and HDPE GM during the batch test (McWatters and Rowe 2010, Eun et al. 2014a, b). The partition coefficient of 1.5-mm EVOH having an HDPE outer layer GM and HDPE GM is statistically identical based on analysis of paired F-tests. However, the EVOH GM having LLDPE outer layer showed significantly higher partition coefficient in comparison to other GMs.

Diffusion coefficients for 1.5-mm-EVOH GM, 1.0-mm-EVOH GM, and HDPE GM were estimated from experimental data obtained from diffusion column tests containing composite liners and Eqs. (2) to (5). Similar to the procedure used to determine the effective diffusion coefficient of soils, nonlinear least-squares regression was used to obtain the best-fit to the experimental data. Partition coefficients of the soils used were obtained from the equilibrium batch testing described previously, which were used as a fixed input parameter in the model to estimate diffusion coefficients of the co-extruded EVOH and HDPE GM. A control test was conducted using an aluminum sheet instead of a geomembrane to adjust corrections for losses.

The estimated diffusion coefficients of VOCs for the 1.5-mm-EVOH GM, 1.0-mm-EVOH GM, and HDPE GM are summarized in Table 2.7. To verify the estimations of the diffusion coefficients for the GMs, estimated diffusion coefficients of VOCs for HDPE GM were compared to literature, as shown in Fig. 2.13 (a). The values of the coefficients are statistically identical according to the paired F-test ($p > 0.05$). Hence, the method to estimate the diffusion coefficient is reliable.

The diffusion coefficients of 1.0-mm-EVOH GM are slightly lower than those of 1.5-mm-EVOH GM because the EVOH film (0.04 mm) in the 1.0-mm-EVOH GM occupies a larger portion of the entire thickness of the GM in comparison to the EVOH film in the 1.5-mm-EVOH GM. The film significantly influences the equivalent diffusion coefficient value in the co-extruded GM (Eun et al. 2014b). Thus, the equivalent diffusion coefficient for 1.0-mm-EVOH GM

should be smaller than that for 1.5-mm-EVOH GM. Typically, non-polar VOCs such as TOL and CB have smaller diffusion coefficient than polar VOCs such as MC and MTBE because migration of non-polar VOC would be buffered at EVOH film (Eun et al. 2014b).

The diffusion coefficients of co-extruded EVOH GM and HDPE GM are compared in Fig. 2.13 (b). Co-extruded EVOH GM had measured diffusion coefficients that were approximately more than 20 times smaller than the HDPE GM. In the co-extruded EVOH GM, the magnitude of diffusion coefficient estimated was in agreement with the VOC migration demonstrated in the diffusion column test (Fig. 2.4 – Fig. 2.7). With a higher diffusion coefficient, more rapid and higher migration of concentration occurs. Based on the comparison, the lower diffusion coefficients of co-extruded EVOH GMs shows that co-extruded EVOH GM would be an effective barrier for reducing VOC migration through composite liners.

2.9 IMPLICATION FOR LANDFILL DESIGN

2.9.1 Modeling of Composite Liners

To investigate the relative migration of VOCs with EVOH GM compared to HDPE GM under field conditions, analytical modeling employing the finite difference method (FDM) was conducted and the migration through the actual field thickness of a composite liner in a landfill predicted. A general configuration of a Wisconsin composite landfill liner was assumed for the modeling. According to Wisconsin Administrative Code NR 504 (Department of Natural Resources 2007), landfills that accept municipal solid waste require a composite liner.

Composite liners consist of two components. In Wisconsin, the upper component must consist of 1.5-mm thick or thicker GM (commonly HDPE), and the lower component must consist of ≥ 1.2-m-thick compacted clay liner with a saturated hydraulic conductivity of 1×10^{-7} cm/s or lower. In the model, a co-extruded EVOH GM was used instead of the typical HDPE GM. The separation distance between the top of the bedrock surface and the bottom of the composite liner must be at least 3.0 m, which does not influence the transport of solute. The subgrade soil located under the compacted clay liner must consist of fine-grained soil. The model established in this study has 4-m subgrade beneath 0.6-and 1.2-m CCL. Measured transport parameters from this study were used as input parameters to the model. Park et al. (2012a) shows that predictions should coincide closely with measurements from the landfill cells if carefully conducted experiments were run.

2.9.2 VOC Transport in Field Site

Contaminant transport was modeled by using analytical methods [from Eq. (2) to Eq. (5)] developed in EXCEL spreadsheets to create illustrative examples of the relative performance of HDPE and EVOH GM. Discretizing was conducted according to the Crank-Nicholson method for 1-D diffusion of the contaminant transport. A composite liner system with a 1.5-mm-thick coextruded EVOH GM and 1.5-mm-thick HDPE GM overlying a 1.2-m-thick clay liner (per WDNR Code NR 504) as well as a 0.6-m-thick clay liner (per RCRA Subtitle D). A 4.0-m-thick less permeable subgrade layer below the composite liner was also employed to

simulate the field conditions. The top boundary for the leachate was set as a constant concentration boundary, and the bottom boundary for the bedrock surface was set as a no flux boundary. In this case, no natural attenuation layer below the composite liner is assumed. Compacted clay properties and geomembrane parameters were based on results obtained from this study. Properties of the subgrade soil are from Foose et al. (2002). Transport parameters used in the modeling are summarized in Table 2.8. TOL was chosen as the simulation contaminant because TOL is most abundant and frequently found VOC in Wisconsin landfills (Klett et al. 2005). The initial contaminant concentrations are assumed to be 100 μg/L, which is higher than geometric mean of TOL found in Wisconsin landfills and thus conservative. Since the diffusion of VOC is a concern of this study, the geomembrane was assumed free of defects (holes) and, therefore, any contaminants collected in the aquifer would be exclusively from diffusion.

Fig. 2.14 presents an example of the predicted variation in TOL concentrations with time for different barrier systems. The WDNR system of (GM + 1.2-m CCL) and the RCRA Subtitle D system (GM + 0.6-m CCL) were examined for both HDPE and EVOH GMs. First, for the WDNR system, TOL concentrations are higher for the case where a conventional HDPE GM is used (see Fig. 2.14). For example, the highest concentration of TOL was approximately 9.7 μg/L for the 1.5-mm-EVOH GM, while the concentration was about 12.4 μg/L for the 1.5-mm-HDPE GM in the WDNR configuration (GM + 1.2-m CCL) in one hundred years. Similarly, for the RCRA Subtitle D configuration,

the predicted concentration of TOL was 63.8 μg/L for the HDPE GM compared to 53.9 μg/L for the EVOH GM. For the conditions examined, the EVOH GM helps reduce contaminant migration at 100 years to levels between 21.8% and 14.3% lower than the migration given by the HDPE GM. With a thicker clay liner (WDNR), the beneficial effect of EVOH GM in the WDNR system decreased by 7.5% in comparison to RCRA Subtitle D. Based on measured transport coefficients from this study and the model comparison, the EVOH showed better performance in mitigating the migration of VOC when accompanied by a thick CCL.

To examine the significance of use of an EVOH GM, additional analyses were performed to estimate the comparable thickness of CCL required with a conventional HDPE GM to provide a composite liner that would give the same protection as the EVOH GM over 0.6-m and 1.2-m of CCL (see Fig. 2.14). The results indicate that an additional 0.10 m and 0.27 m of compacted clay would be required for the RCRA Subtitle D and WDNR CCLs, respectively, to achieve the same level of protection as that provided by the EVOH GM for the contaminant examined.

The relative thinness (0.05 mm) of the EVOH layer has a notable effect and several important practical implications. First, the performance of the co-extruded GM could be further improved by adopting manufacturing procedures that increase the thickness of the EVOH layer. Moreover, further research is required to assess how well the EVOH GM stands up to field use (e.g., scratching during installation). Migrations of VOCs due to advection from water

flow were not considered in this model. A field trial using the EVOH GM would be worthwhile to examine the performance of the EVOH GM over both short- and long-term timeframes.

2.10 CONCLUSIONS

This research effort experimentally evaluated and compared the relative rates of transport of common VOCs through composite landfill liners constructed with co-extruded GMs that contain a layer of EVOH in comparison to conventional HDPE GM. Based on the results of diffusion testing with composite liners, VOC breakthrough in composite linear employing high-density polyethylene (HDPE) GMs (35 d) occurred more than two and four times faster than employing co-extruded EVOH GMs with LLDPE and HDPE outer layer, respectively (≈ 70 and 150 d) and with significantly higher VOC concentrations. Unlike the composite liner employing HDPE GM, the concentrations of MC are markedly higher compared to other VOCs in the composite liner employing EVOH GM due to its lower hydrophobicity. This behavior reflects the relative rates of transport of these VOCs between EVOH GM and HDPE GM. According to transport parameters obtained from diffusion testing, regardless of type of EVOH GM, co-extruded EVOH GM had measured diffusion coefficients that were more than 20 times smaller in comparison to HDPE GM. The diffusion coefficients of a 1.5-mm-EVOH GM were 0.56×10^{-13} m^2/s for MC, 0.58×10^{-13} m^2/s for MTBE, 0.18×10^{-13} m^2/s for TCE, 0.15×10^{-13} m^2/s for TOL, and 0.16×10^{-13} m^2/s for CB. The diffusion coefficients of a 1.0-mm-EVOH GM were 0.51 ×

10^{-13} m^2/s for MC, 0.54 × 10^{-13} m^2/s for MTBE, 0.17 × 10^{-13} m^2/s for TCE, 0.12 × 10^{-13} m^2/s for TOL, and 0.13 × 10^{-13} m^2/s for CB. In the co-extruded EVOH GM, the magnitudes of estimated diffusion coefficients were in good agreement with those of the VOC migration demonstrated in the diffusion column test. For the CCL and GCL composite liners, the concentration of VOCs was lower in the CCL compared to the GCL. Moreover, the concentration was more dependent on transport parameters in the GCL. However, this dependency becomes less significant as increasing depth. Modeling of VOC migration through a composite liner in a field site indicated that contaminant impact was approximately 14 and 22 percent lower when a co-extruded GM with 0.6-m and 1.2-m CCL was used. To achieve the same level of protection as provided by the co-extruded GM underlain by 0.6 m (RCRA Subtitle D) and 1.2 m (WDNR) of compacted clay, an additional 0.1 m and 0.27 m of compacted clay is needed, respectively, in conjunction with a conventional GM. Based on the comparison, the EVOH showed better performance in mitigating the migration of VOC when accompanied by a thick CCL. Thus, co-extruded EVOH GMs acted as an effective barrier to VOC migration in composite liners.

2.11 ACKNOWLEDGMENTS

The authors appreciate the support of Kuraray CO., Ltd. The opinion, findings and conclusions expressed herein do not represent the views of Kuraray CO., Ltd.

2.12 REFERENCES

Armstrong R. B. (2011). “Improving performance of geosynthetics for containment of volatile organic compounds through the use of ethylene vinyl alcohol (EVOH).” *Geo-Frontier 2011,* ASCE, Florida.

ASTM. (2011). “Standard Practice for Classification of Soils for Engineering Purposes (Unified Soil Classification System.” *D2487,* In Annual Book of ASTM Standards Vol. 04.08, ASTM International, West Conshohocken, PA.

Byun, Y. J., Hong, S. I., Kim, K. B., Jeon, D. H., Kim, J. M., Whiteside, W. S., and Park, H. J. (2007). “Physical and chemical properties of γ-irradiated EVOH film.” *Radiation Physics and Chemistry*, 76 (6), 974-981.

Edil, T. B., Wambold, W. S., and Park, J. K. (1995). “Partitioning of VOCs in clay liner materials.” *Geoenvironment 2000*, ASCE GSP 46, 775-790. 20.

Edil, T. B. (2007). “Is aqueous-phase VOC transport from modern landfills a potential environmental problem?” *Proceeding*, Sardinia 2007, *11th Int. Landfill Symposium*, Cagliari, Italy.

Eun, J., Tinjum, J. M., Benson, C. H., and Edil, T. B. (2014a). “Volatile organic compound (VOC) transport through composite liner with co-extruded geomembrane containing ethylene vinyl-alcohol (EVOH).” Accepted to *Geo-Congress 2014*, ASCE, Atlanta.

Eun, J., Tinjum, J. M., Benson, C. H., and Edil, T. B. (2014b). “Transport parameters of volatile organic compounds (VOCs) in co-extruded geomembrane containing ethylene vinyl-alcohol (EVOH).” Submitted to

Journal of Geotechnical and Geoenvironmental Engineering

Foose, G. J., Benson, C. H., and Edil, T. B. (2001). "Equivalent of composite geosynthetic clay liners as barrier to volatile organic compounds." *Geosynthetic '99 conferences.*

Foose, G. J. (2002). "Transit-time design for diffusion through composite liners." *Journal of Geotechnical and Geoenvironmental Engineering*, 128 (7), 590-601.

Foose, G. J., Benson, C. H., and Edil, T. B. (2002). "Comparison of solute transport in three composite liners." *Journal of Geotechnical and Geoenvironmental Engineering,* 128 (5), 1-13.

Freeze, R. A., and Cherry, J. A. (1979). Ground water. Prentice-Hall, Englewood Cliffs, New Jersey.

Gonzalez-Nunez, R., Padilla, H., De Kee, D., and Favis, B. D. (2001). "Barrier properties of polyamide-6/high density polyethylene blends." *Polymer Bulletin*, (Berlin), 46, 323-330.

Hashimoto, I., Deshpande, K. B., and Thomas, H. C. (1964). "Peclet numbers and retardation factors for ion exchange columns." *Industrial and Engineering Chemistry Fundamentals*, 3 (3), 213-218.

Headley, J. V., Boldt-Leppin, B. E. J., Haug, M. D., and Peng, J. (2001). "Determination of diffusion and adsorption coefficients for volatile organics in and organophillic clay – sand – bentonite liner." *Canadian Geotechnical Journal*, 38 (4), 809-817.

Huysmans, M. and Dassargues, A. (2007). "Equivalent diffusion coefficient and

equivalent diffusion accessible porosity of a stratified porous medium." *Transport Porous Medium*, 66, 421-438.

Joo, J. C., Kim, J. Y., and Nam, K. (2004). "Mass transfer of organic compounds in dilute aqueous solutions into high density polyethylene geomembranes." *Journal of Geotechnical and Geoenvironmental Engineering*, 130 (2), 175-183.

Joo, J. C., Nam, K., and Kim, J. Y. (2005). "Estimation of mass transport parameters of organic compounds through high density polyethylene geomembranes using a modified double-compartment apparatus." *Journal of Geotechnical and Geoenvironmental Engineering*, 131 (5), 790-799.

Kile, D. E., Chiou, C. T., Zhou, H., Li, H., and Xu, O. (1995). "Partitioning of nonpolar organic pollutants from water to soil and sediment organic matters." *Environmental Science and Technology*, 29 (5), 1401-1406.

Kim, J. Y., Edil, T. B., and Park, J. K. (2001). "Volatile organic compound (VOC) transport through compacted clay." *Journal of Geotechnical and Geoenvironmental Engineering*, 127 (2), 126-134.

Kim, J. Y., Shin, M., Park, J., and Nam, K. (2003). "Effect of soil solids concentration in batch tests on the partition coefficients of organic pollutants in landfill liner-soil materials." *Journal of Material Cycles and Waste Management*, 5 (1), 55-62.

Klett, N., Edil, T. B., Benson, C. H., and Connelly, J. (2005). "Evaluation of volatile organic compounds in Wisconsin landfill leachate and lysimeter

samples." *Final Report to the University of Wisconsin System Groundwater Research Program*, Department of Civil and Environmental Engineering, University of Wisconsin at Madison, Madison, WI.

Kolbasuk, G. (1991). "Co-extruded HDPE/VLDPE multilayer geomembrane." *Geotextiles and Geomembranes,* 10 (4), 601–612.

Lake, C. B., and Rowe, R. K. (2005). "A comparative assessment of volatile organic compound (VOC) sorption to various types of potential GCL bentonites." *Geotextiles and Geomembranes,* 23 (4), 323–347.

Leo, A., Hansch, C., and Elkins, D. (1971). "Partition coefficients and their uses." *Chemical Reviews,* 71 (6), 525–616.

Malusis, M. and Shackelford, C. (2002). "Chemico-Osmotic Efficiency of a Geosynthetic Clay Liner." *Journal of Geotechnical and Geoenvironmental Engineering*, 128 (2), 97-106.

McWatters, R. S. and Rowe, R. K. (2010). "Diffusive transport of VOCs through LLDPE and Two coextruded geomembrane." *Journal of Geotechnical and Geoenvironmental Engineering*, 136 (9), 1167-1177.

McWatters, R. S. and Rowe, R. K. (2011). "Sorption and diffusion of BTEX through thin-film EVOH." *Geo-Frontiers 2011* ASCE, 2073-2083.

Nefso, E. K. and Burns, S. E. (2007) "Comparison of the equilibrium sorption of five organic compounds to HDPE, PP, and PVC geomembranes." *Geotextiles and Geomembranes*, 25, 360-365.

Park, J. K., and Nibras, M. (1993). "Mass flux of organic chemicals through polyethylene geomembranes." *Water Environment Research*, 65 (3),

227-237.

Park, J. K., Sakti, J. P., and Hoopes, J. A. (1996). “Transport of organic compounds in thermoplastic geomembranes, I: Mathematical model.” *Journal of Environmental Engineering*, 122 (9), 800-806.

Park, M. G., Benson, C. H., and Edil T. B. (2012a). “Comparison of batch and double compartment tests for measuring VOC transport parameters in geomembranes.” *Geotextiles and Geomembranes*, 31 (1), 15–30.

Park, M. G., Edil T. B. and Benson, C. H. (2012b). “Modeling volatile organic compound transport in composite liners.” *Journal of Geotechnical and Geoenvironmental Engineering*, 138 (6), 641-657.

Parker, L. and Britt, S. (2012). “The Effect of bottle fill rate and pour technique on the recovery of volatile organics.” *Ground Water Monitoring and Remediation,* 32 (4), 78-86.

Paumier, S., Touze-Foltz, N., Mazeas, L., and Guenne, A. (2011). “Quantification of volatile organic compounds diffusion for virgin geosynthetic clay liners and for a GCL after contact with a synthetic leachate.” *Journal of Geotechnical and Geoenvironmental Engineering*, 137 (11), 1039-1046.

Sangam, H. P. and Rowe, R. K. (2001a). “Migration of dilute aqueous organic pollutants through HDPE geomembranes.” *Geotextiles and Geomembranes*, 19, 329-357.

Sangam, H. P. and Rowe, R. K. (2001b). “The role of HDPE geomembranes in retarding the diffusive migration of organic contaminants through composite liner systems.” *Proceeding*, Sardinia 2001, *8th Int. Landfill*

Symposium, Cagliari, Italy.

Sangam, H. and Rowe, R. (2005). ”Effect of surface fluorination on diffusion through a high density polyethylene geomembrane.” *Journal of Geotechnical and Geoenvironmental Engineering*, 131 (6), 694-704.

Schwarzenbach, R. P., Gschwend, P. M., and Imboden, D. M. (2003). Environmental organic chemistry. Second edition. Wiley-Interscience, NJ.

Shackelford, C. D. and Daniel, D. E. (1991). “Diffusion in saturated soil I: Background.” *Journal of Geotechnical Engineering*, 7 (3), 467-484.

Wisconsin Department of Natural Resources (2007). “LANDFILL LOCATION, PERFORMANCE, DESIGN AND CONSTRUCTION CRITERIA.” Chapter NR 504.

Yeh, J. and Fan-chiang, C. (1996). “Permeation mechanisms of xylene in blow-molded bottles of pure polyethylene, polyethylene/polyamide and polyethylene/ modified polyamide blends.” *Journal of Polymer Research,* 3 (4), 211-219.

Zhang, Z., Britt, I. J., and Tung, M. A. (1999). “Water absorption in EVOH films and its influence on glass transition temperature.” *Journal of Polymer Science, Part B. Polymer Physic*, 37, 691–699.

Zhang, Q., Lin, W., Chen, Q., and Yang, G. (2000). “Phase structure of EVOH copolymers as revealed by variable temperature solid state high resolution.” 13C NMR spectroscopy. *Macromolecules*. 33, 8904-8906.

2.13 TABLES

Table 2.1 Properties of VOCs used in experiments

Compound	MC	MTBE	TCE	TOL	CB
Chemical formula	CH_2Cl_2	CH_3-O-$C(CH_3)_3$	$CHCl=CCl_2$	C_6H_5-CH_3	C_6H_5Cl
Type of compound	Alkane	Ether	Alkene	Arene	Arene
Molecular weight (g/mol)	84.93	88.15	131.39	92.14	112.56
Density (g/mL)	1.33	0.740	1.46	0.867	1.11
log K_{ow}	1.31	0.94	2.42	2.69	2.78
Solubility (mg/L)	20000	48000	1100	515	500
Vapor pressure (kPa)	57.5	32.4	10.0	3.72	1.59
Dielectric constant	8.9	4.5	3.4	2.4	2.7
Melting point(C°)	-97.2	-108.6	-84.7	-94.95	-45.31
Boiling point(C°)	40	55	87.21	110.63	131.72

Note: MC: Methylene chloride, MTBE: Methyl Tertiary Butyl Ether, TCE: Trichloroethylene, TOL: Toluene, CB: Chlorobenzene.

K_{ow}: partition coefficient between octanol and water

Table 2.2 Engineering properties of GCL

Property	Method	Bentomat ST®
Bentonite Swell Index[1] (ml/2 g)	ASTM D 5890	> 24
Bentonite Fluid Loss[1](ml)	ASTM D 5891	< 18
Bentonite Mass[2] (g/ m^2)	ASTM D 5993	> 4600
Grab Strength[3] (N)	ASTM D 5993	> 600
Peel Strength[3] (N)	ASTM D 4632	> 65
Permeability[4](D = 100 mm) (m/sec)	ASTM D 5887	5 x 10^{-11}
Woven Geotextile Mass (g/m^2)	ASTM D 5261	> 105
Non-woven Geotextile Mass (g/m^2)	ASTM D 5261	> 200
Hydrated Internal Shear Strength[5] (kPa)	ASTM D 5321	> 24

Table 2.3 Experimental cases according to liner configurations

Liner Materials	Number of Experiment	Liner Configuration
1.5-mm HDPE GM + CCL	1	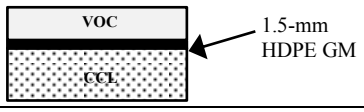
1.5-mm HDPE GM + GCL	1	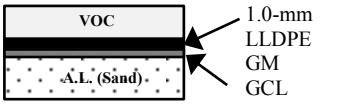
1.5-mm HDPE GM + CCL	2 (Duplicate)	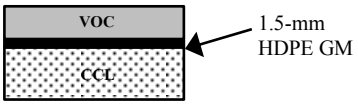
1.0-mm LLDPE GM + CCL	2 (Duplicate)	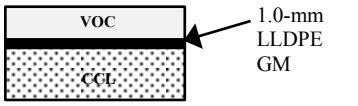
1.5-mm HDPE GM + GCL	2 (Duplicate)	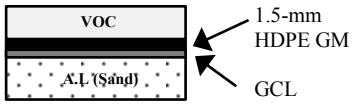
1.0-mm LLDPE GM + GCL	2 (Duplicate)	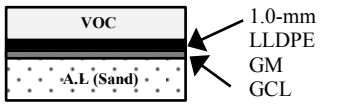
Aluminum plate + CCL	1	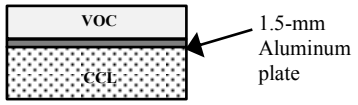
No GM + CCL	1	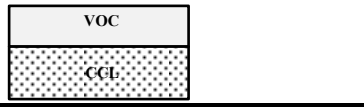

Table 2.4 Partition coefficients (K_d) of soils

Type	Unit	MC	R^2	MTBE	R^2	TCE	R^2	TOL	R^2	CB	R^2
Kamm clay	L/kg	0.097	0.93	0.092	0.86	0.178	0.96	0.192	0.96	0.217	0.95
Kamm clay (Park et al. 2012a)		0.079	0.62	0.059	0.72	0.165	0.91	0.141	0.94	0.207	0.89
Bentonite (Bentomat ST®)		0.040	0.87	0.045	0.79	0.108	0.94	0.120	0.92	0.117	0.93
Ottawa sand		0.015	0.87	0.017	0.91	0.026	0.97	0.026	0.95	0.027	0.92

Table 2.5. Diffusion coefficients (D_s) of soils

Type	Unit	MC	MTBE	TCE	TOL	CB	Apparent tortuosity factor (τ_a)
Kamm clay	$\times 10^{-5}$ m^2/s	0.140	0.138	0.147	0.146	0.139	0.12
Kamm clay (Park et al. 2012a)		0.153	0.118	0.139	0.117	0.129	0.13
Bentonite (Bentomat ST®)		0.059	0.056	0.054	0.052	0.053	0.01-0.22
Ottawa sand		0.56	0.69	0.58	0.57	0.55	0.2-0.35

Table 2.6. Partition coefficients (K_g) of geomembrane

Type	Unit	MC	R^2	MTBE	R^2	TCE	R^2	TOL	R^2	CB	R^2
1.0-mm EVOH GM	L/kg	5.8	0.96	1.9	0.92	157.9	0.93	195.8	0.95	171.1	0.96
1.5-mm HDPE GM		3.4	0.96	0.8	0.96	69.0	0.96	88.6	0.96	112.0	0.84
1.5-mm HDPE GM (Park et al. 2012a)		2.1	0.88	0.6	0.78	63.2	0.98	86.7	0.98	108.9	0.99
1.5-mm EVOH GM		3.1	0.97	0.7	0.91	62.1	0.87	84.3	0.94	107.1	0.95

Table 2.7 Diffusion coefficients (D_g) of geomembrane

Type	Unit	MC	MTBE	TCE	TOL	CB	p value
1.0-mm EVOH GM with CCL	$\times 10^{-13}$ m^2/s	0.49	0.51	0.15	0.11	0.12	0.45
1.0-mm EVOH GM with GCL		0.53	0.57	0.18	0.13	0.14	
1.5-mm HDPE GM with CCL		10.0	11.05	5.17	4.06	2.86	0.19
1.5-mm HDPE GM (Park et al. 2012a)		8.86	7.74	5.45	3.77	3.96	
1.5-mm EVOH GM with CCL		0.53	0.55	0.17	0.14	0.15	0.42
1.5-mm EVOH GM with GCL		0.58	0.61	0.19	0.15	0.16	

Table 2.8 Input transport parameters of TOL

Type	Partition coefficient (K_d, K_g) (L/kg)	Diffusion coefficient (D) ($\times 10^{-13}$ m^2/s)	Porosity (n)
Clay	0.19	1460*	0.375
Subgrade**	0.01	0.57*	0.30
1.5-mm HDPE GM	88.6	4.06	-
1.5-mm EVOH GM	84.3	0.14	-

* Effective diffusion coefficient
** Foose et al. (2001)

2.14 FIGURES

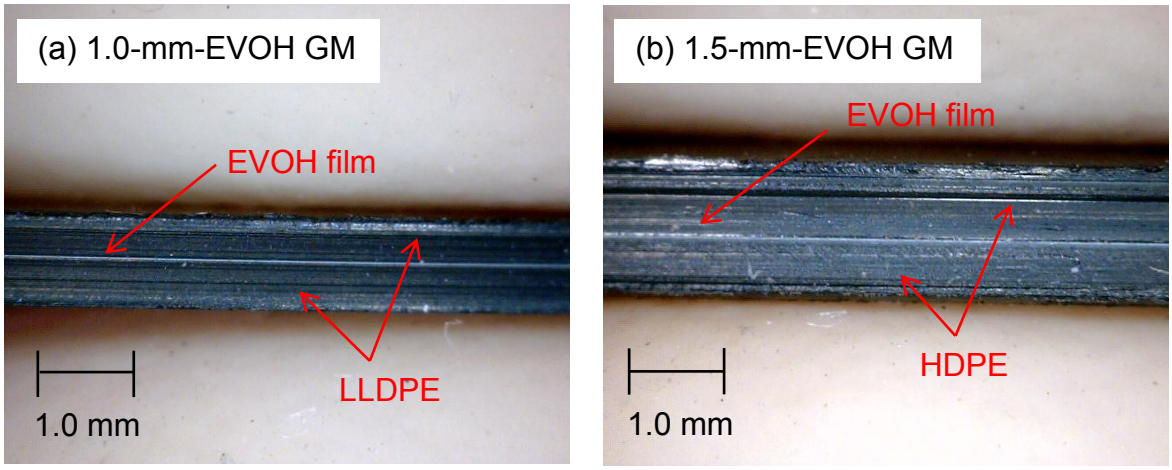

Figure 2.1 Co-extruded EVOH GMs used for composite liner.

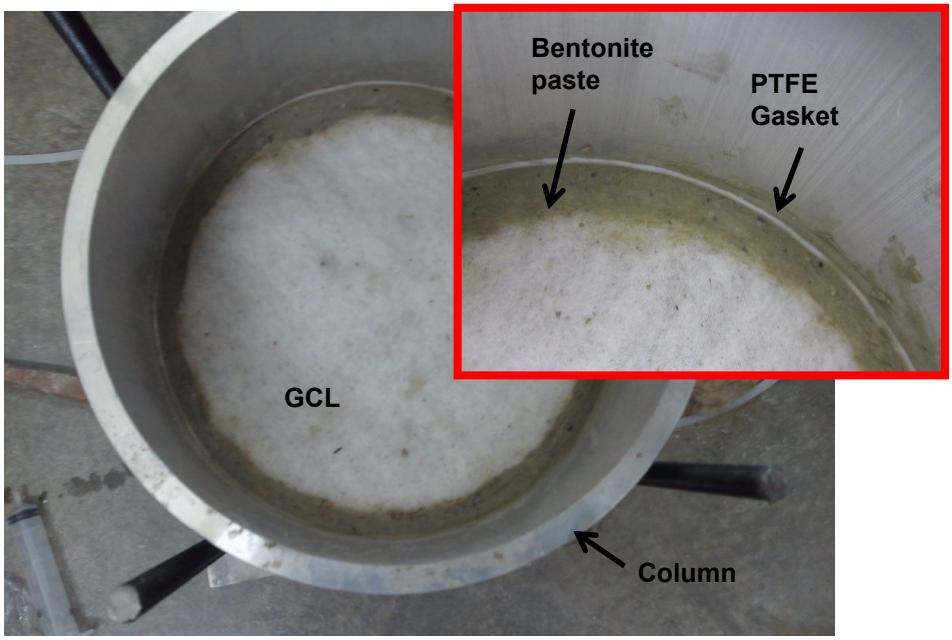

Figure 2.2 Bentonite paste coated the circumference of the GCL.

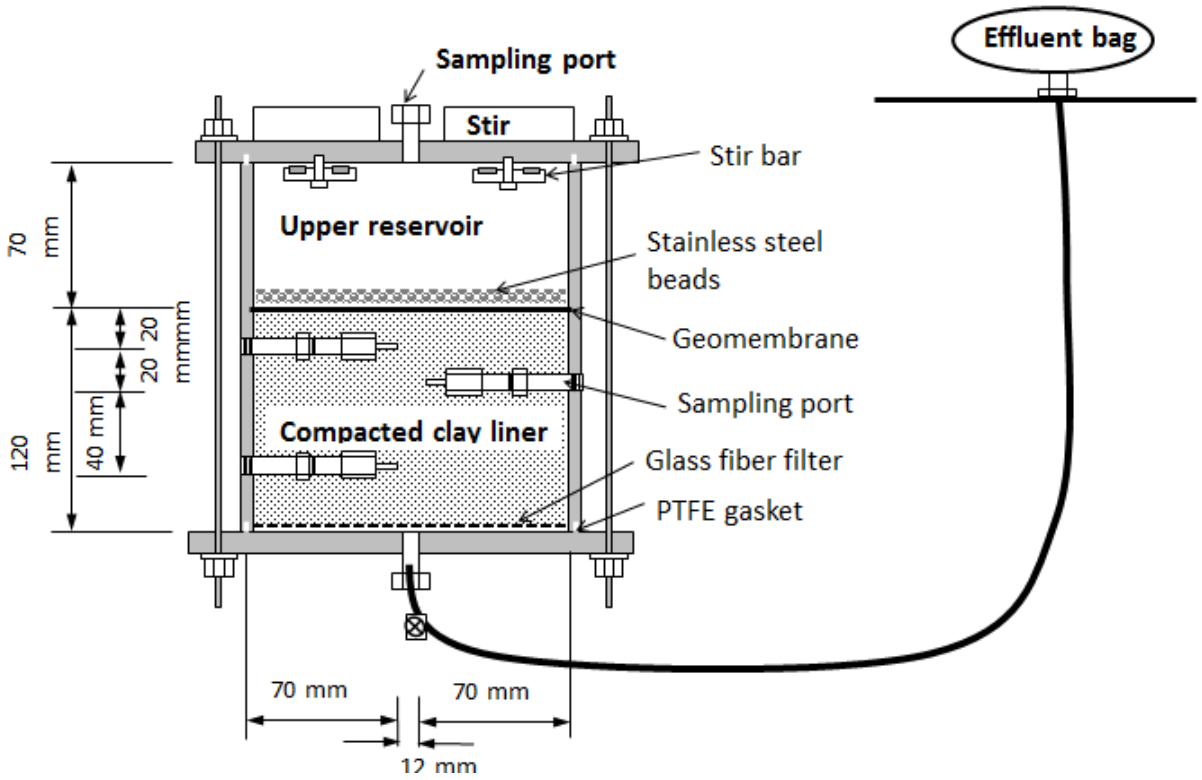

(a) Bench-scale experimental setup

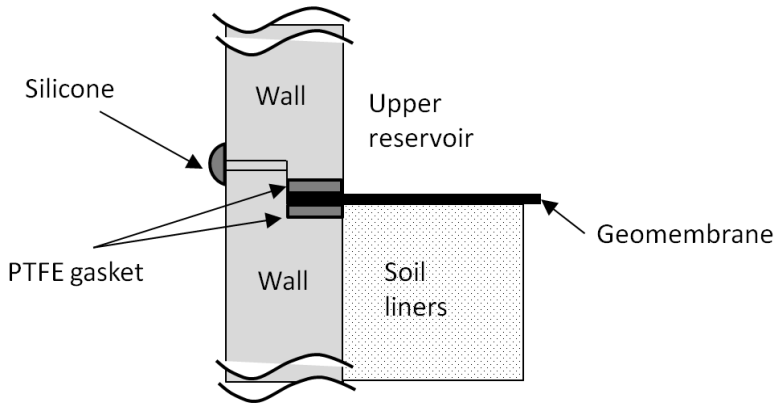

(b) Schematics of cross section of the joint area (no scale)

Figure 2.3 Diffusion column tests.

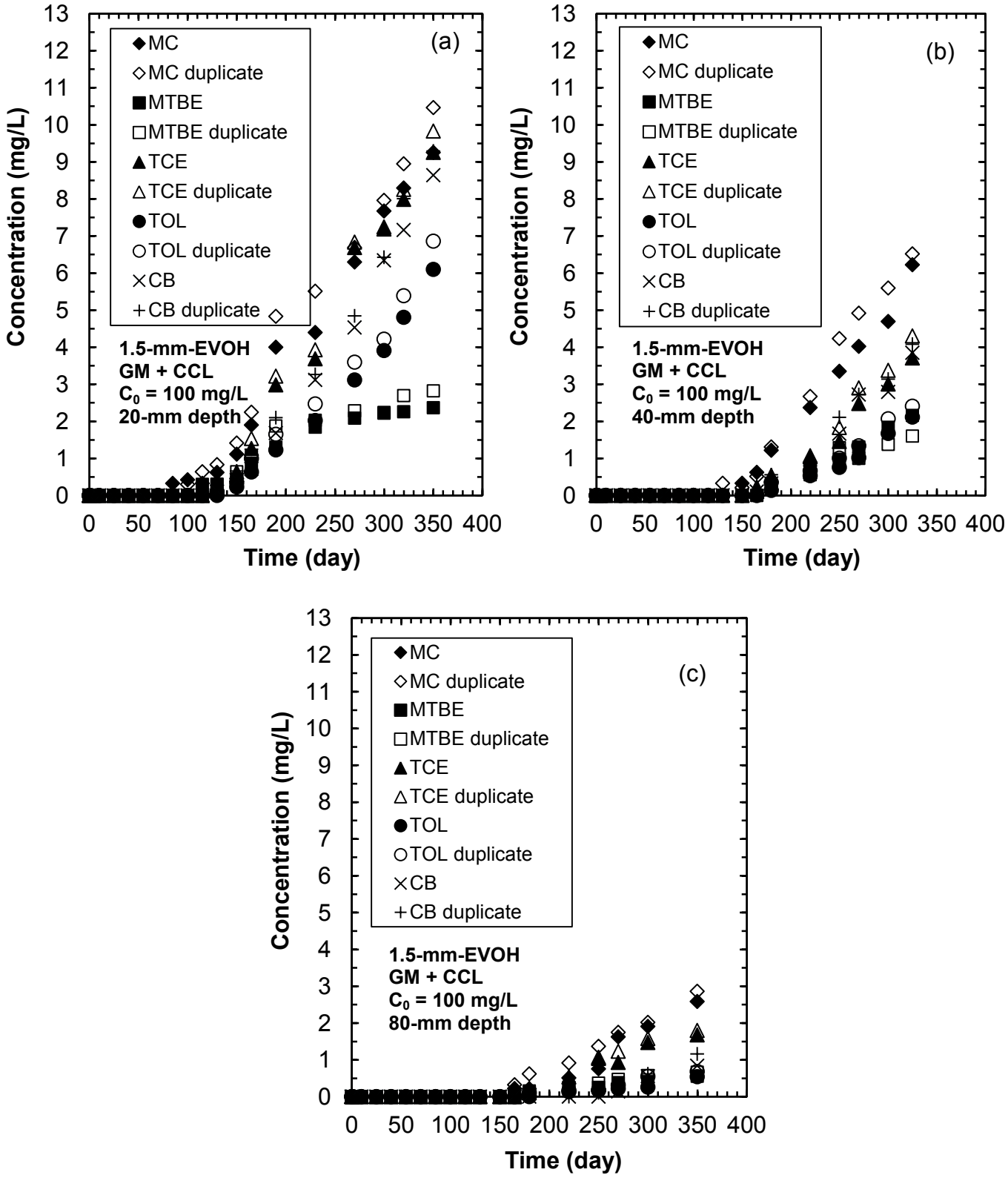

Figure 2.4 Concentration of VOCs through composite liners employing 1.5-mm-EVOH GM overlying CCL: (a) 20-mm depth; (b) 40-mm depth; and (c) 80-mm depth.

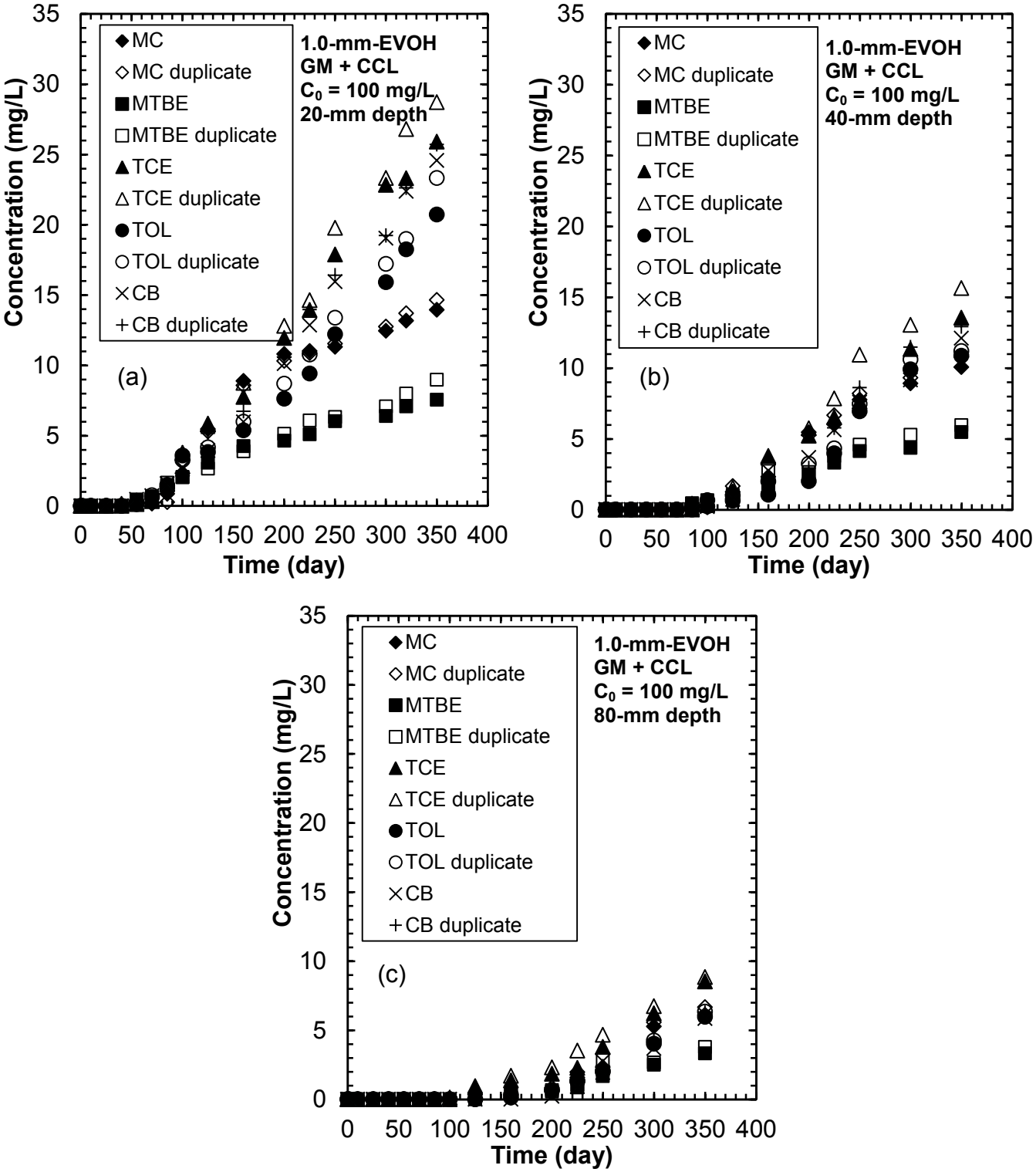

Figure 2.5. Concentration of VOCs through composite liners employing 1.0-mm-EVOH GM overlying CCL: (a) 20-mm depth; (b) 40-mm depth; and (c) 80-mm depth.

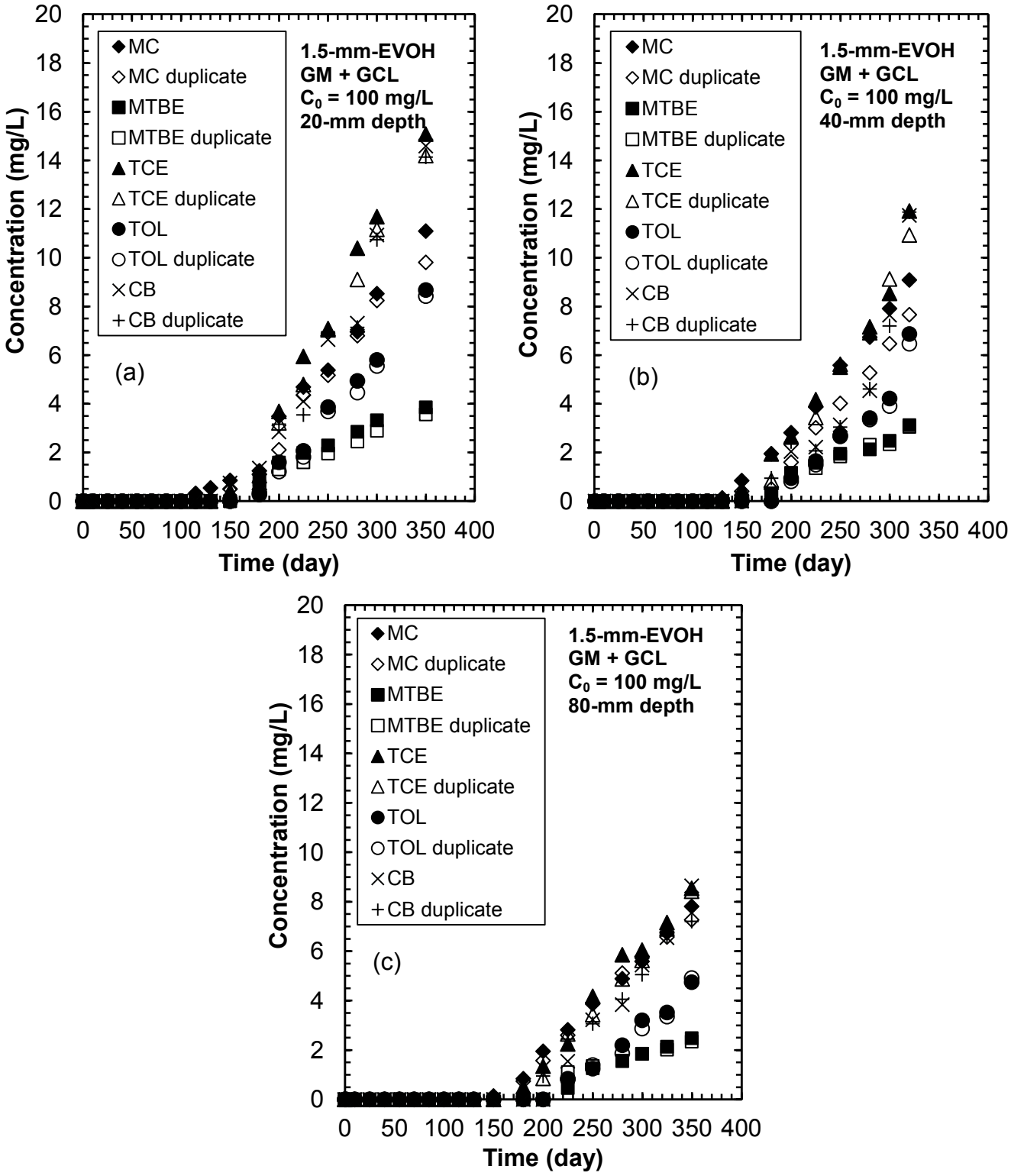

Figure 2.6. Concentration of VOCs through composite liners employing 1.5-mm EVOH GM overlying GCL: (a) 20-mm depth; (b) 40-mm depth; and (c) 80-mm depth.

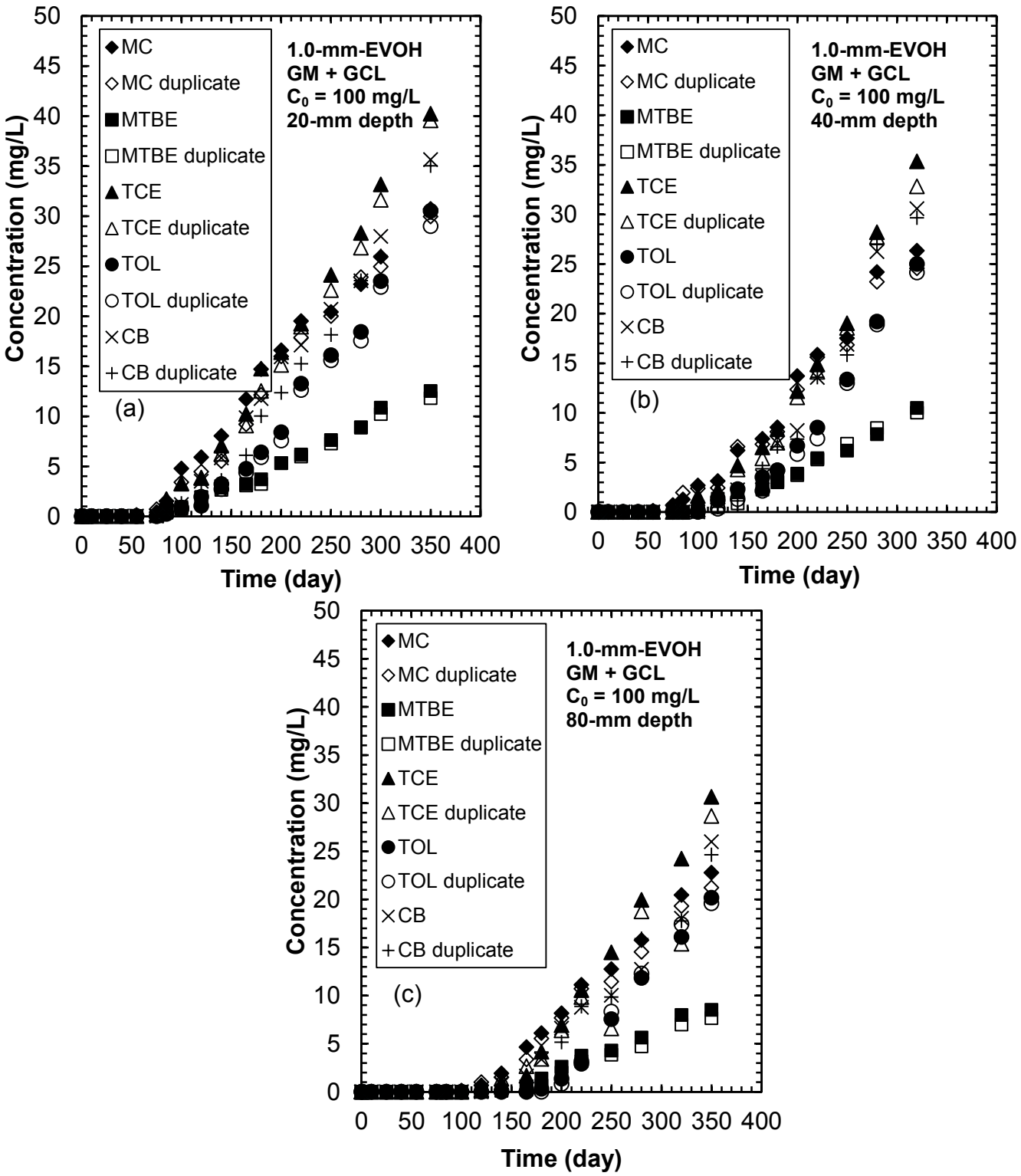

Figure 2.7 Concentration of VOCs through composite liners employing 1.0-mm-EVOH GM overlying GCL: (a) 20-mm depth; (b) 40-mm depth; and (c) 80-mm depth.

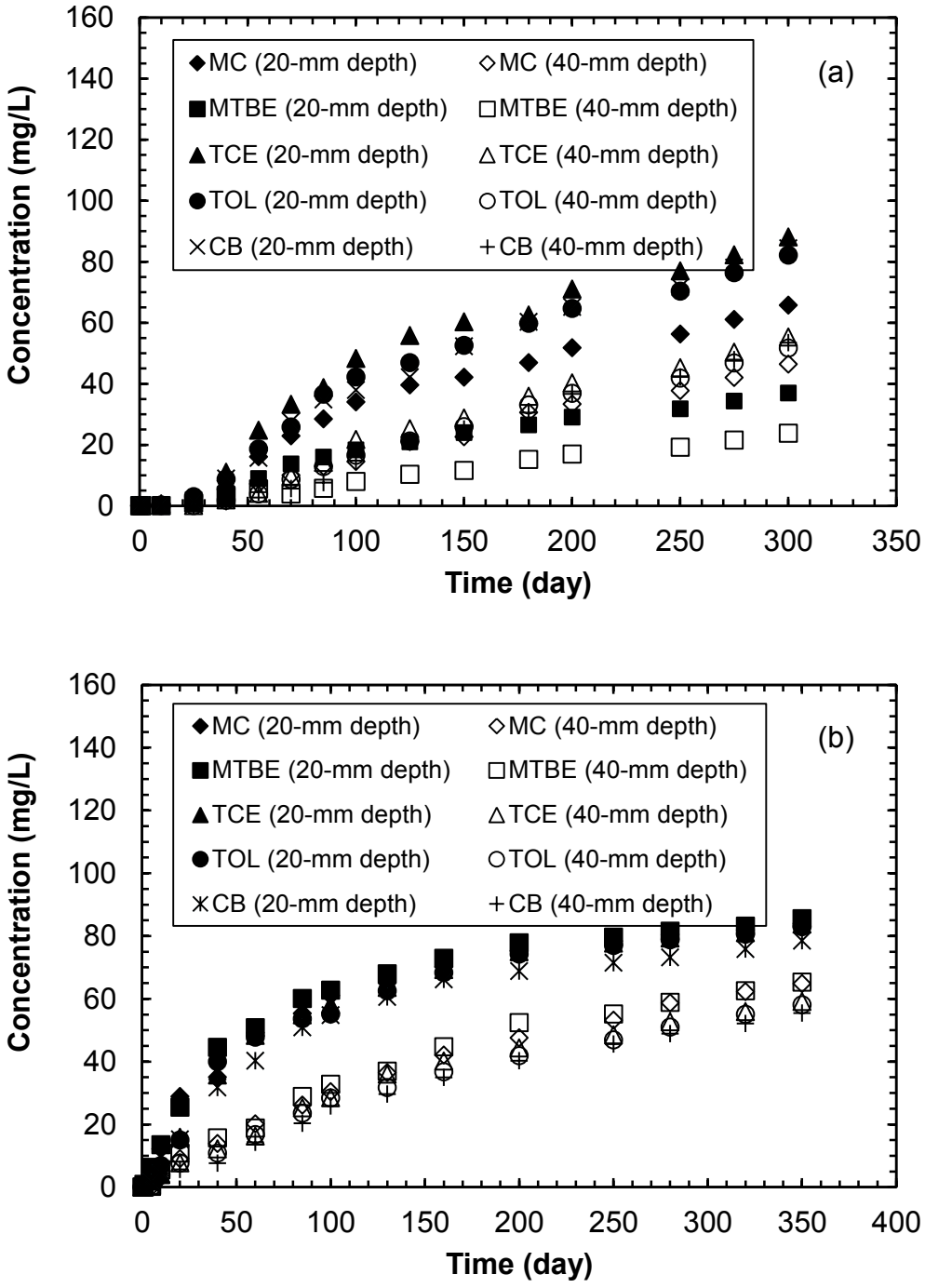

Figure 2.8 Concentration of VOCs through composite liners employing HDPE GM overlaying CCL and no GM overlying CCL: (a) HDPE GM overlaying CCL; (b) CCL only.

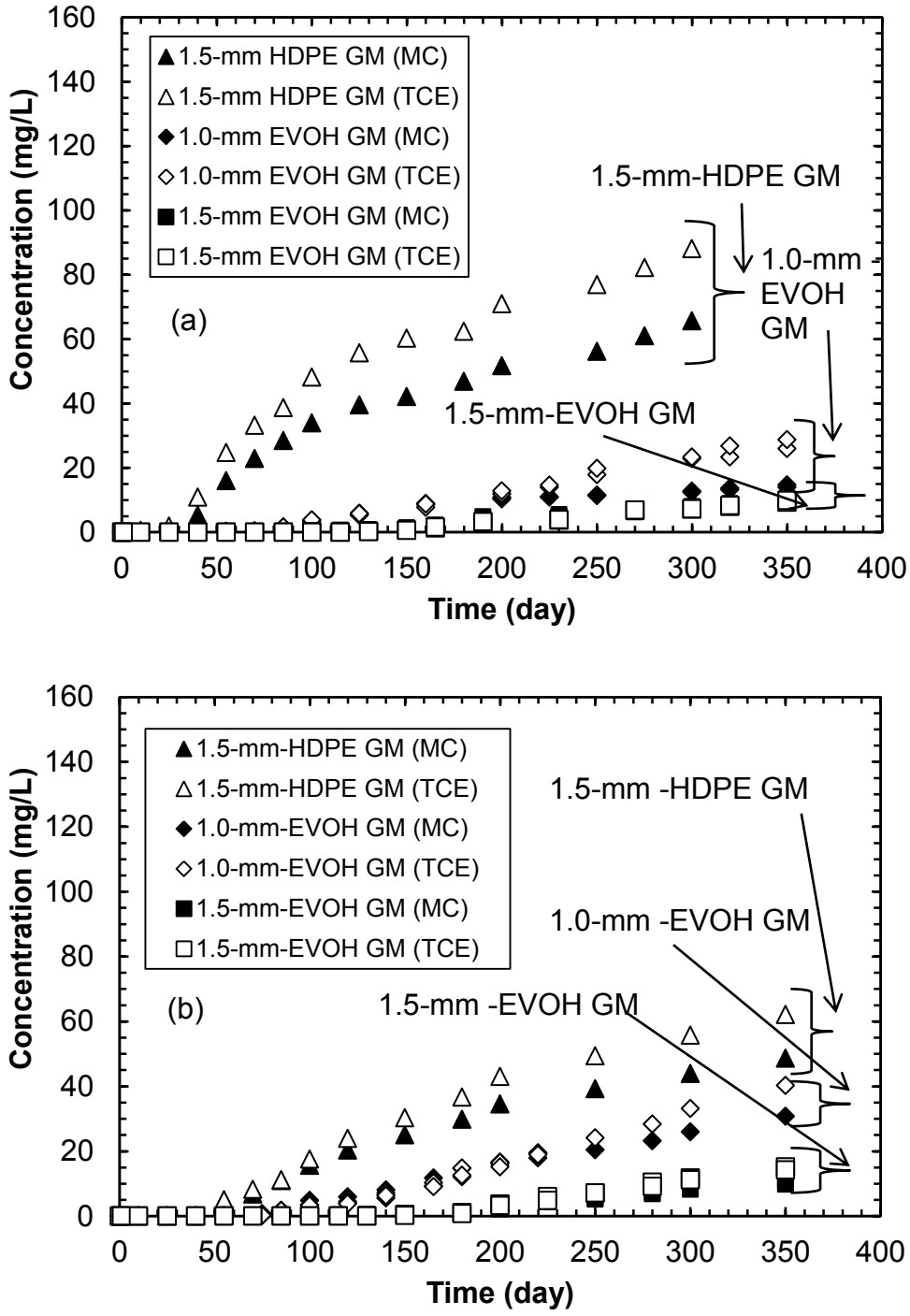

Figure 2.9 Comparison of VOC concentration through composite liners employing HDPE GM and EVOH GM overlying CCL and GCL: (a) EVOH and HDPE with CCL; (b) EVOH and HDPE with GCL.

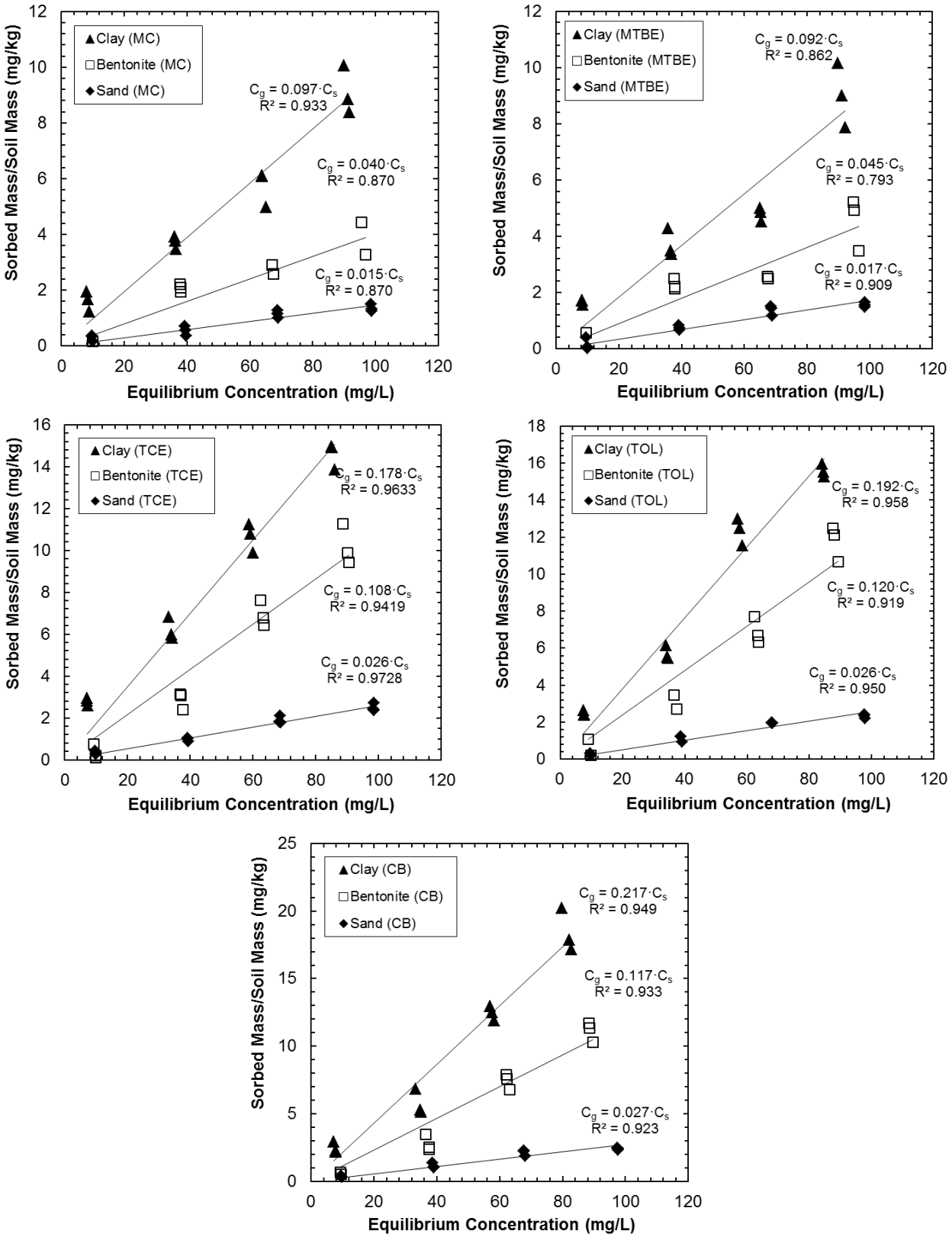

Figure 2.10 Sorption isotherms of VOCs for clay, bentonite and sand.

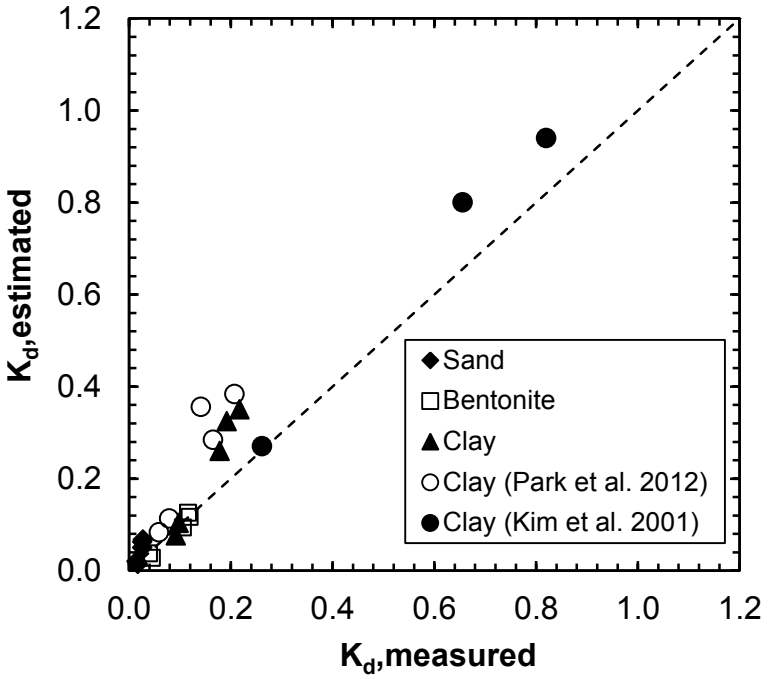

Figure 2.11 Comparison between estimated and measured partition coefficient of soils.

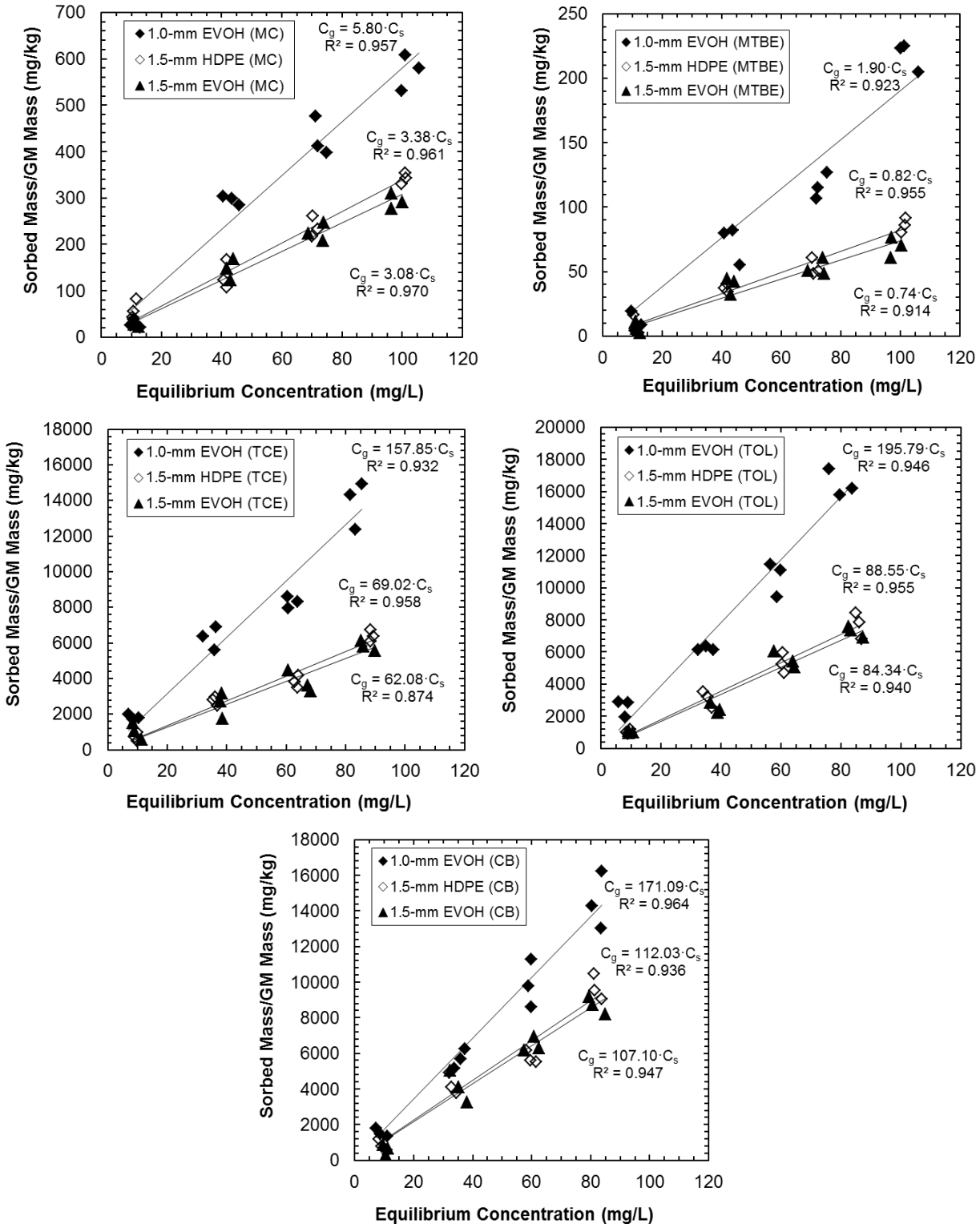

Figure 2.12 Sorption isotherms of VOCs for 1.0-mm EVOH GM, 1.5-mm-HDPE GM and 1.5-mm-EVOH GM.

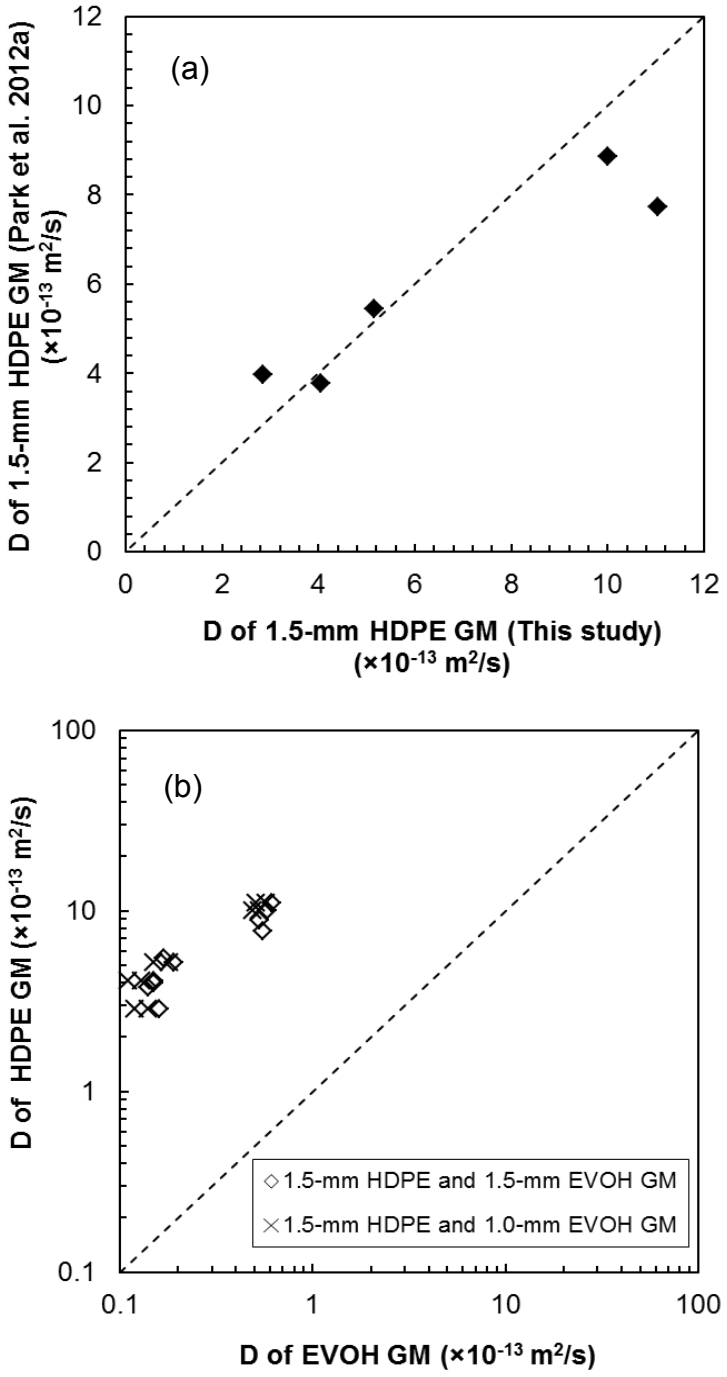

Figure 2.13 Comparison of diffusion coefficient (D) of GMs: (a) D of HDPE GM from this study and from Park et al.(2012a); (b) D of 1.5-mm HDPE GM and 1.5-mm EVOH GM, and D of 1.5-mm HDPE GM and 1.0-mm EVOH GM from this study.

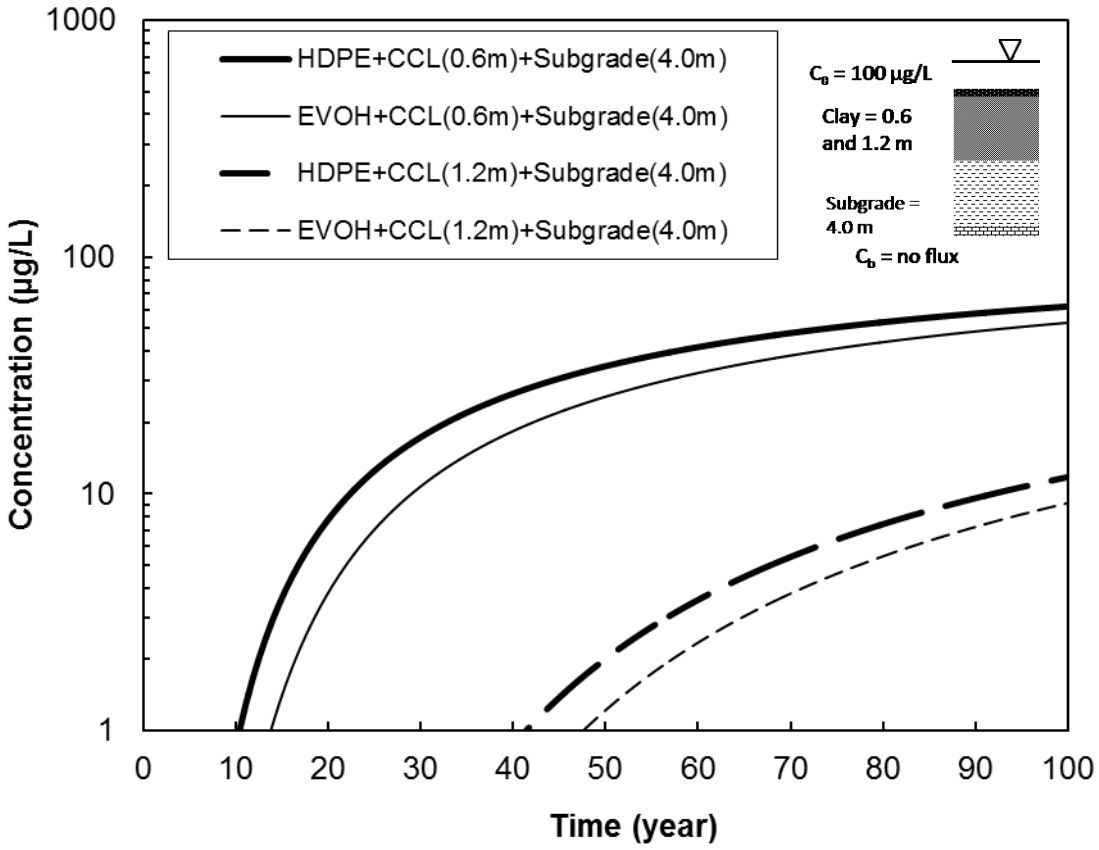

Figure 2.14 Migration of TOL through composite liner.

Chapter 3 Transport Parameters of Volatile Organic Compounds (VOCs) in Co-Extruded Geomembrane Containing Ethylene Vinyl-Alcohol (EVOH)

3.1 ABSTRACT

In this study, the transport behavior of non-polar organic contaminants (e.g., common VOCs found in landfill leachate) through a co-extruded geomembrane containing EVOH were evaluated with a series of batch tests. To evaluate the equivalency of transport behavior in co-extruded EVOH GM, the transport parameters (e.g., the partition and diffusion coefficients) of each layer in the EVOH GM were measured by separate batch tests. Equivalent diffusion coefficients were derived analytically based on the sorptive and diffusive behaviors of VOCs through the co-extruded GM. Overall, the linear low-density polyethylene (LLDPE) GM had the highest partition coefficient (1.9-195.8 L/kg) and the pure EVOH laminar had the lowest partition coefficient (0.69-0.94 L/kg). The diffusion coefficient of co-extruded GM (0.14 - 0.59 × 10^{-13} m^2/s) was approximately 16-29 times smaller than that of high-density polyethylene (HDPE) GM (2.86 – 11.05 × 10^{-13} m^2/s). The chemical characteristics of each material in a co-extruded EVOH GM show a strong linear relationship with the partition coefficient on a log-log scale. However, the relationships with HDPE, LLDPE, and maleic anhydride were reversed to those of EVOH, which is directly related to the polarity between the non-polar VOC and EVOH. For validation of the equivalent diffusion equation, the diffusion coefficients for the co-extruded GM

were compared to those obtained from modified double-compartment apparatus tests. The migration of VOCs through composite liners employing a co-extruded GM was modeled numerically with an equivalent diffusion coefficient, and compared to experimental data from diffusion column tests. For each VOC, the magnitude of the equivalent diffusion coefficient was in agreement with the VOC migration demonstrated in the diffusion column test.

Keywords: Co-extruded geomembrane; Diffusion coefficient; Partition coefficient; Diffusion; Equivalency; Volatile organic compounds; EVOH (ethylene vinyl-alcohol); Batch test; Modified double-compartment apparatus test.

3.2 INTRODUCTION

A co-extruded geomembrane (GM) is a type of GM that is being introduced by the geosynthetic industry to enhance the performance of GMs as barriers to contaminant flux (Sangam and Rowe 2005; Edil 2007; McWatters and Rowe 2010). Co-extruded GMs with an ethylene vinyl-alcohol (EVOH) layer incorporate polyethylene as the water barrier and also have the potential to substantially reduce the diffusion of non-polar volatile organic compounds (VOCs). The permeability of a co-extruded EVOH GM via diffusion is significantly lower than linear low-density polyethylene (LLDPE), high-density polyethylene (HDPE), and polyvinyl chloride (PVC) GM (McWatters and Rowe 2010, 2011).

For the proper design and analysis of a barrier system containing a co-extruded GM, the transport parameters (e.g., the partition and diffusion coefficients) for the composite barrier must be determined such that solute flux is

correctly accounted for (Foose et al. 2001, 2002; Chen et al. 2009). Batch testing (sorption/immersion) of traditional, single-composition GMs has historically provided simple, quick, and accurate results. Furthermore, in comparison to more complex double-compartment apparatus tests (i.e., diffusion testing), batch testing of homogeneous GMs generally provides reasonable results because solute loss during testing is minimized (Park et al. 2012a). However, with a co-extruded GM, a batch test is not appropriate for determining transport parameters because solute migration through the interior EVOH layer is not represented (McWatters and Rowe 2010; Eun et al. 2014a, b). The physical-chemical mechanisms (i.e., diffusion and sorption) responsible for solute transport through a co-extruded EVOH GM are not well understood.

The objective of this study is to investigate transport behavior of non-polar organic contaminants (e.g., common VOCs found in landfill leachate) through a co-extruded geomembrane containing EVOH with a series of batch tests. To evaluate the equivalency of transport behavior in co-extruded EVOH GM, the transport parameters of each layer in the EVOH GM were measured by separate batch tests. Sorptive and diffusive behaviors at the interfaces of co-extruded GMs (i.e., non-homogeneous layers in series) were accounted for with a derived equation that estimates an equivalent diffusion coefficient. For validation of the equation, the transport parameters for a co-extruded GM obtained using batch tests were compared to the transport parameters obtained from modified double-compartment apparatus (MDCA) tests. Furthermore, the relationship between the chemical characteristics (i.e., octanol-water partition coefficient, aqueous

solubility, and molecular diameter) and transport parameters of each material in a co-extruded EVOH GM was investigated to identify the transport behavior through the GM and to evaluate the migration of solute through a co-extruded EVOH GM. Finally, the migration of VOCs through composite liners employing the GM was modeled numerically with the equivalent diffusion coefficients, and compared to experimental data from diffusion column tests.

3.3 BACKGROUND

3.3.1 Co-extruded EVOH Geomembrane

EVOH is a random copolymer of ethylene and vinyl alcohol including polar oxygen–hydrogen (-OH) groups. Because the monomer mainly exists as tautomer acetaldehyde, the copolymer is prepared by polymerization of ethylene and vinyl acetate to provide the ethylene vinyl acetate (EVA) copolymer followed by hydrolysis (Armstrong 2011). EVOH copolymer is defined by the mole % of ethylene content, thus lower ethylene content grades have higher barrier properties for non-polar organic contaminants; higher ethylene content grades have more flexible easy for extrusion. Eq. (1) represents the chemical formulation of EVOH.

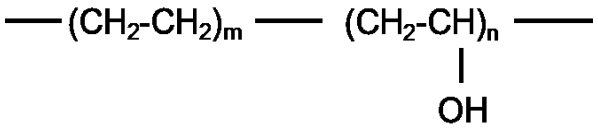

(1)

EVOH with polarity has outstanding barrier properties to non-polar gases

such as oxygen, nitrogen, volatile compounds, and helium (Zhang et al. 1999; Zhang et al. 2000; Byun et al. 2007; McWatters and Rowe 2011). EVOH laminar is typically a combination of highly ordered crystalline structures interspersed with disordered amorphous regions that shows high resistance to diffusion of gas and solvent (Zhang et al. 1999; McWatters and Rowe 2011). Accordingly, co-extruded GMs with EVOH layers are being manufactured to take advantage of the properties of polyethylene as a water barrier, while having the potential to substantially reduce the diffusion of organic compounds. For instance, composite liners employing the co-extruded EVOH GMs are expected to allow less migration of organic contaminants (i.e., VOCs).

The manufacturing process of a co-extruded GM with EVOH is more complicated relative to monomer-type GMs. First, an HDPE or LLDPE outer layer is extruded through a die with an orifice and then is dried. Next, an EVOH laminar is arranged such that the extruded layers merge and weld together onto the laminar. Each material is fed to the die from a separate extruder, but the orifices may be arranged so that each extruder supplies two or more plies of the same material. The ply of the EVOH GM is manufactured to produce the desired barrier properties (Kolbasuk 1991; Armstrong 2011).

3.3.2 Diffusive Transport through Composite Liner

The solute transport through multi-layered systems is described by combining the solute transport through the individual layers that compose the system. In a landfill system, solute transport through composite liners has been

investigated by combining transport of solute through the soil and geomembrane components (Foose et al. 2001, 2002; Sangam and Rowe 2001b; Chen et al. 2009). The physical mechanism of transport through composite liners includes three steps, as shown in Fig. 3.1: Step (1) absorption of the permeating species into the GM and equilibration in the GM surface, Step (2) diffusion through the GM in the direction of the lower chemical potential, and Step (3) desorption of the permeating species from the GM surface and removal into the ambient medium (Park and Nibras 1993; Park et al. 1996; Sangam and Rowe 2001b; Joo et al. 2004, 2005; Park et al. 2012b).

The solute first sorbs to the GM outer layer from the contaminant solution. The partition or distribution coefficient (K_g) between the GM and the solution is defined as (Leo et al. 1971)

$$K_g = \frac{C_g}{C_w} \tag{2}$$

where C_w is the equilibrium concentration in solution [M/L^3], C_g is the equilibrium concentration of the organic compound in the HDPE GM [M/M], and K_g is the dimensionless GM-water partition coefficient of the organic compound.

Next, the organic compound sorbed on the surface of a GM begins transport through the GM by molecular diffusion. Diffusion in a GM is typically described using Fick's second law. The governing equation for one-dimensional (1-D) constant diffusion for organic compounds in a GM can be represented as (Park and Nibras 1993; Park et al. 1996; Sangam and Rowe 2001b; Joo et al.

2004, 2005; Park et al. 2012a, b)

$$\frac{\partial C_g}{\partial t} = D_g \frac{\partial^2 C_g}{\partial z^2}, \qquad -L_g < z < 0 \tag{3}$$

where t is elapsed time [T], D_g is the diffusion coefficient of the organic compound in the GM [L^2/T], z is the distance along the direction of diffusion [L], and L_g is thickness of the GM [L]. Eq. (3) is valid if the diffusion coefficient in the GM is temporally and spatially invariant (Foose 2002; Foose et al. 2002). Desorption of the organic compound is the last transport step from the GM to the outer solution or received medium (e.g., soil). This step is an inverted version of adsorption.

For a saturated compacted clay liner (CCL), 1-D mass transport of a non-decaying solute via diffusion can be expressed as (Hashimoto et al. 1964; Freeze and Cherry 1979)

$$\frac{\partial C_s}{\partial t} = \frac{D^*}{R} \frac{\partial^2 C_s}{\partial z^2}, \qquad z > 0 \tag{4}$$

where C_s is the concentration of the organic compound in the pore water of the soil liner [M/L^3], z is the distance along the direction of mass transport [L], t is elapsed time [T], R is the retardation factor, and D^* is the effective diffusion coefficient [L^2/T]. Partitioning of organic compounds between soil particles and the solution can be quantified by the partition coefficient (K_d), which is defined as

$$K_d = \frac{C_s}{C_w} \quad (5)$$

where C_s is the concentration adsorbed to the soil particle [M/M]. Use of Eqs. (2) to (5) requires transport parameters (e.g., partition and diffusion coefficients) of composite liners that can be estimated by fitting experimental data from diffusion column tests (Park et al. 1996; Foose et al. 2001 Park et al. 2012b).

3.4 EQUIVALENT DIFFUSION THROUGH A CO-EXTRUDED GEOMEMBRANE

Solute transport through a multi-layered system has been extensively investigated (Foose et al. 2001; Huysmans and Dassargues 2007; Dingemans et al. 2008; McWatters and Rowe 2010; Li and Cleall 2010). For instance, in porous media such as soil, the harmonic mean of the diffusion coefficient can be derived based on the concept of mass conservation in a similar manner to the calculation of the equivalent hydraulic conductivity in the vertical direction (Foose et al. 2001; Huysmans and Dassargues 2007; Dingemans et al. 2008; Li and Cleall 2010).

The equivalent diffusion coefficient of solute through a co-extruded GM can be derived by the concept of mass conservation in a similar manner to other composite layers. For simplification, the equivalent diffusion coefficient for a three-layered system of co-extruded GM is derived at steady state. The transport of solute through a co-extruded GM is described in Fig. 3.2. The flux of solute is identical through all layers due to mass conservation:

$$J_{total} = J_1 = J_2 = J_3 \quad (6)$$

where J_{total} is solute flux through the entire co-extruded GM and J_1, J_2, and J_3 are the solute fluxes through each layer [$L^{-2}\,T^{-1}$]. According to Fick's first law, the flux of solute through all layers can be represented as

$$J_{total} = D_{eq}\frac{C_{1,inter}-C_{2,outer}}{L_{gt}} = D_{eq}\frac{K_{g1}\cdot C_{w,inter}-K_{g1}C_{w,outer}}{L_{gt}} \quad (7)$$

where D_{eq} is the equivalent diffusion coefficient, $C_{w,inter}$ and $C_{w,outer}$ are the concentrations [M/L^3] of the solution above the geomembrane and below the geomembrane, respectively. L_{gt} is the total thickness of the co-extruded geomembrane [L].

Similar to Step 1 in composite liners, the absorption of the solute from the solution into the GM and the equilibration in the GM surface is described by the partition (distribution) coefficient of the GM. According to the definition of the partition coefficient [Eq. (2)] between a solution and a geomembrane, $C_{1,inter}$ can be rewritten as follows and be applied to Eq. (7):

$$C_{1,inter} = K_{g1}\cdot C_{w,inter} \quad (8)$$

where $C_{w,inter}$ is the equilibrium concentration of solution in the upper reservoir, $C_{1,inter}$ is the concentration of solution in the first layer of the geomembrane, K_{g1} is the partition coefficient between the solution and the geomembrane (outer layer of co-extruded GM). In a series of layers, similar to the case of an entire GM, the

flux can be defined according to Fick's first law. Flux through layers 1 to 3 can be described by using Fick's first law and the partition coefficient between GMs and the following equation can be written by using Eqs. (7) and (8):

$$J_1 = D_{g1}\frac{\Delta C_1}{L_{g1}} = D_{g1}\frac{C_{1,inter}-C_{1,outer}}{L_{g1}} = D_{g1}\frac{k_{g1}\cdot C_{1,inter}-C_{1,outer}}{L_{g1}} \quad (9)$$

$$J_2 = D_{g2}\frac{\Delta C_2}{L_{g2}} = D_{g2}\frac{C_{2,inter}-C_{2,outer}}{L_{g2}} \quad (10)$$

$$J_3 = D_{g3}\frac{\Delta C_3}{L_{g3}} = D_{g3}\frac{C_{3,inter}-C_{3,outer}}{L_{g3}} = D_{g3}\frac{C_{3,inter}-K_{g1}\cdot C_{w,outer}}{L_{g3}} \quad (11)$$

where D_{g1}, D_{g2}, and D_{g3} are the diffusion coefficients of layer 1, 2, and 3, respectively [L^2/T]. C_{g1}, C_{g2}, and C_{g3} are the concentrations of layers 1, 2 and 3, respectively [M/L^3]. $L_{g1,}$ L_{g2} and L_{g3} are the thicknesses of layers 1, 2 and 3, respectively [L]. ΔC_1, ΔC_2, and ΔC_3 are the differences in concentration between the inner and outer sides of each layer [M/L^3]. The total degradation of concentration through the membrane is a summation of the degrading concentration in each layer.

$$\Delta C_{total} = \Delta C_1 + \Delta C_2 + \Delta C_3 \quad (12)$$

In using Eqs. (6) and (12), the equivalent diffusion coefficient is derived for the case involving three layers as

$$D_{eq} = \frac{L_{gt}}{\frac{L_{g1}}{D_{g1}} + \frac{L_{g2}}{D_{g2}} + \frac{L_{g3}}{D_{g3}}} \quad (13)$$

If Eq. (13) is generalized, the following equation describes the equivalent diffusion coefficient through a co-extruded GM consisting of n layers.

$$D_{eq} = \frac{L_{gt}}{\sum_1^n \frac{L_{gn}}{D_{gn}}} \quad (14)$$

3.5 MATERIALS AND METHODS

3.5.1 Volatile Organic Compounds

Five VOCs were used as organic contaminants: methylene chloride (MC), methyl tertiary butyl ether (MTBE), trichloroethylene (TCE), toluene (TOL), and chlorobenzene (CB). These VOCs are considered representative types of VOCs (i.e., alkanes, ethers, alkenes, aromatic hydrocarbones, and halogenated aromatic hydrocarbons) among the 31 VOCs that were reported in lysimeters from 34 landfill sites in Wisconsin (Klett et al. 2005). Furthermore, the VOCs were used extensively in previous studies (Park et al. 2012a, b; Eun et al. 2014a, b). General properties of these VOCs are described in Table 3.1 (Schwarzenbach et al. 2003; Lake and Rowe 2005). For the testing program, the VOC solutions were prepared by filling a 1-L flask with distilled and deionized (DDI) water and sodium azide (0.05%) was added to prevent microbial activity.

VOC concentrations were measured using a Shimadzu GC-2010 gas chromatograph (GC) equipped with an auto sampler, flame ionization detector

(FID), and Restek RTX-624 column (length = 30 m, inner diameter = 0.32 mm, and film thickness = 1.80 μm). The detection limit was 0.82 mg/L for MC, 0.53 mg/L for MTBE, 0.34 mg/L for TCE, 0.31 mg/L for TOL, and 0.22 mg/L for CB.

3.5.2 Geomembrane

Two co-extruded GMs with EVOH were used to examine the diffusive transport of VOC contaminants, which have 1.0-mm and 1.5-mm thicknesses, respectively. The co-extruded GM was produced by RAVEN Co. (South Dakoda, USA) using EVOH with 3.5% $CaCO_3$ inert filler supplied by EVAL-Kuraray Ltd. (Texas, USA). The geomembrane is composed of a five layer structure (see Fig. 3.3). The first and outer layer is composed of LLDPE or HDPE, and surrounds the inner layers. The second layer, which was approximately 0.05-mm thick, was comprised of an adhesive polymer used to bond the outer PE to the EVOH. The adhesive polymer or “Tie” was a maleic anhydride grafted PE, which is used extensively in the automotive industry for plastic fuel tanks (Armstrong 2011). Maleic anhydride ($C_4H_2O_3$) used for the tie adhesive is a type of organic compound involving oxidation. The barrier core layer in all cases was approximately 0.04 to 0.05-mm thick and was composed of 32 mol% of ethylene copolymer EVOH. The fourth and fifth layers were adhesive tie and PE again. For controls, conventional HDPE GM was also tested as supplied by RAVEN Co. The selected properties of each layer were described in Table 3.2. Smooth, black, 1.5-mm-thick HDPE GM was used as a control to compare with co-extruded HDPE GM with EVOH film.

Moreover, batch tests were conducted on 0.5-mm thick layers of pure EVOH and maleic anhydride to identify the transport parameters (i.e., partition and diffusion coefficients) of the materials. The parameters obtained for pure EVOH and maleic anhydride were used to estimate the equivalent diffusion coefficient.

3.5.3 Equilibrium Batch Test

Equilibrium batch tests were conducted to obtain partition coefficients of the VOCs to the co-extruded GM, conventional HDPE GM, pure EVOH laminar, and tie adhesive (i.e., maleic anhydride) sheet. The test procedure follows that of Park et al. (2012a). Membrane samples were cut into strips (17 mm × 80 mm), approximately 3.1 g to 6.2 g of geomembrane (3-5 strips) was placed in an amber glass vial (40 mL), and solution was added to fill the vial (solid-liquid ratio = 0.15). The vial was sealed with a screw cap and Teflon-coated septum. The partition coefficient was unaffected by a low solid-liquid ratio (0.04-0.16) (Park et al. 2012a). Control tests were also conducted without geomembrane samples. Data from the control tests were used to make corrections for losses, although the corrections were very small to negligible (Park et al. 2012a). Solutions having initial concentrations of 10, 40, 70, and 100 mg/L of each VOC were used for tests conducted with multi-solute mixtures of VOCs. Solutions were prepared using the methods described previously and transferred to each vial from 1-L flasks using a peristaltic pump. When VOC solution was moved into each vial from the flask, the Teflon tube of the pump was attached to the bottom of the

vials to minimize loss of VOC (Parker and Britt 2012). After adding the solution, the filled vials were tumbled in a rotator at 30 revolutions per min (rpm) for 8 d at 23.5 °C, which is sufficient time to reach equilibrium according to previous research (Park et al. 2012a). After tumbling, the vials were centrifuged at 2,000 rpm (429 g) for 15 min to assure equivalent dispersion of VOCs in the vial. The supernatant was transferred to auto sampler vials using a glass syringe without opening the cap of the vial and was then analyzed by GC using the methods described previously. Three replicates were conducted for each concentration and two controls without solids were also prepared to check for losses (< 5.0%). Concentrations were adjusted for losses using the loss data from the controls. Partition coefficients were computed by fitting the linear isotherm [Eq. (3)] to the sorption data using least-square regression. The isotherms are approximately linear, which is consistent with previous studies on VOC sorption to GMs (Nefso and Burn 2007; McWatters and Rowe 2010; Park et al. 2012a).

3.5.4 Kinetic Batch Tests

Kinetic batch tests were performed for the co-extruded GM and homogeneous, single polymer layers including HDPE GM, pure EVOH, and the tie adhesive to obtain the diffusion coefficient of each material. Based on the results from the test, the equivalent diffusion coefficient can be estimated. The testing method was adopted from Sangam and Rowe (2001a), Joo et al. (2004), and Park et al. (2012a). Geomembrane samples were cut into strips (17 mm × 80 mm), similar to the equilibrium batch test, approximately 3.1 g to 6.2 g of

geomembrane (3-5 strips) was placed in an amber glass vial (40 mL), and solution was added to fill the vial (solid-liquid ratio = 0.05 to 0.15). The initial concentration for all five VOCs was 100 mg/L. The vial was then sealed with a screw cap and PTFE-coated septum. The GM was cut to the largest size that would fit in the glass vial as a single strip to achieve a solid-liquid ratio comparable to the ratio used in the equilibrium batch test (Park et al. 2012a). Control tests were also conducted without GM specimens. Vials were prepared and handled using the same method employed for the batch tests. Two replicate vials were prepared (including controls) for periodic decommissioning during the experiment. Samples where decommissioned and sampled after 1, 2, 3, 5, 7, and 9 days from the start of the test. Similar to equilibrium batch testing, when VOC solution was moved into each vial from the flask, the Teflon tube of the pump was attached to the bottom of the vials to minimize the loss of VOC (Parker and Britt 2012). The supernatant was transferred to auto sampler vials using a glass syringe without opening the cap of the vial and was then analyzed by GC using the methods described previously. Concentrations were adjusted for losses using the loss data from the controls similar to the equilibrium batch test. The VOC concentration data were analyzed assuming a planar sheet of geomembrane suspended in a well-stirred solution of limited volume. The analytical solution for this system is given by Crank (1975):

$$\frac{C_t}{C_0} = \exp\left(\frac{D_g t (K_g)^2}{A^2}\right) erfc\left(\frac{D_g t (K_g)^2}{A^2}\right)^{0.5} \quad (15)$$

where C_t is the concentration of the VOC in the solution at time t [M/L^3], C_0 is the initial concentration of the organic compound in the solution [M/L^3], D_g is the diffusion coefficient [L^2/T], t is the elapsed time [T], K_g is the partition coefficient (dimensionless), and A is the half thickness of the solution in contact with both sides of the geomembrane [L], which is calculated by dividing the volume of the solution by the area of the geomembrane. Eq. (15) was fit to the data using nonlinear least-squares regression.

3.5.5 Modified Double-Compartment Apparatus Test

The modified double-compartment apparatus (MDCA) test was conducted to obtain partition and diffusion coefficients for the co-extruded GM as shown in Fig. 3.4. The general concept of the test followed previous studies (Park et al. 1996; Joo et al. 2005; Park et al. 2012a). The testing column (20-cm height, 15.5-cm diameter) constructed with brass was divided into upper and lower compartments and the tested GM was placed at the joint of the compartments. In the joint, two polytetrafluoroethylene (PTFE) rectangular gaskets were installed on the top and bottom of the GM to minimize the adsorption of VOC solute and/or loss of VOC solution through the joint as shown in Fig. 3.4. In the previous apparatus (Park et al. 1996; Park et al. 2012a), a significant loss of VOC during testing occurred at the flange of the compartments. However, in this study, the double sealing joint was adapted to install a specimen of the membrane in between the compartments. This modification minimized the loss of VOC and achieved reliable results to estimate accurate transport parameters. The PTFE

rectangular gasket was also used to seal the slit between the column and the top and bottom plates effectively. In addition, a control employing a stainless steel plate was conducted simultaneously. No VOCs were detected in the effluent (lower) reservoir during the control test and the change in concentration in the upper reservoir was less than 3% over a 40-d monitoring period. Data from the control tests were used to make corrections for losses.

The influent (upper) compartment was filled with VOC solution having an initial concentration of 100 mg/L for all five VOCs. To mix the solution in the influent reservoir equivalently during the test, a stirrer made of aluminum and magnetic discs were located on the top plate. The effluent (lower) compartment was initially filled with DDI water spiked with 0.05% sodium azide. During the test, the solution in the effluent reservoir was also stirred continuously with a magnetic stirrer to obtain a well-mixed solution. Samples were collected periodically from the sampling ports to monitor concentrations in the influent and effluent reservoirs. The sampling ports included a brass connector and cap with two septa to extract samples with minimal loss of VOC during sampling. The concentration of the VOC solution in the upper chamber decreased with time because some solute was adsorbed and migrated through the GM during testing.

Partition and diffusion coefficients for each VOC were determined by inversion using the 1-D finite-difference model from Park et al. (2012a) and least-squares regression. This model solves Eq. (3) for $0 < z < L_g$, where L_g is the thickness of the geomembrane [L]. Eq. (2) is used to define the relationship between C_g at the upper and lower surfaces of the geomembrane in Eq. (3) and

the aqueous phase concentrations measured in the reservoirs. The finite-difference model was verified by Park et al. (2012b) by using POLLUTE (Rowe et al. 2004). The difference between concentrations predicted by both models was less than 1%, on average.

3.6 EXPERIMENTAL RESULTS

3.6.1 Analysis of Equilibrium Batch Test

Sorption isotherms for the VOC are shown in Fig. 3.5 and 3.6. Partition coefficients were computed by fitting the linear isotherm [Eq. (2)] to the sorption data using least-square regression. The measured partition coefficients for each material consisting co-extruded GM are summarized in Table 3.3. The isotherms are approximately linear, which is consistent with previous studies on VOC sorption to the geomembrane in a given range of low concentrations (less than 100 mg/L) (Edil et al. 1995; Park et al. 1996; Sangam and Rowe 2005; Park et al. 2012a). Because the EVOH film is thin enough to neglect in comparison to the surface area of HDPE in a co-extruded GM, the sorptive behavior of VOC to the HDPE outer layer was similar between the 1.5-mm-thick co-extruded EVOH and the HDPE GM during the batch test (see Fig. 3.5) (McWatters and Rowe 2010, Eun et al. 2014a, b). The partition coefficients of 1.5-mm-EVOH GM having an HDPE outer layer and the HDEP GM were statistically identical based on analysis of paired F-tests ($p > 0.05$). However, the 1.0-mm-EVOH GM having an LLDPE outer layer showed a remarkably higher partition coefficient (1.9–195.8 L/kg) in comparison to other GMs because of lower crystallinity of LLDPE (Park

et al. 1996). For example, the partition coefficients of MC, TOL for LLDPE GM are 1.7 and 2.2 times higher than those for HDPE GM, respectively.

The slope of the sorption isotherm is dependent upon the interactions between VOC and the sheet material, as shown in Fig. 3.6. The slope of the sorption isotherm for VOCs was higher for the non-polar sheets including HDPE GM, which means the non-polar GM sheets have higher partition coefficients. Generally, LLDPE GM had the highest partition coefficient (1.9–195.8 L/kg) and pure EVOH laminar had the lowest partition coefficient (0.69-0.94 L/kg). However, depending on the polarity of the VOC, the slope of the sorption isotherm can be markedly different. For instance, the slopes of non-polar VOCs including TOL and CB (aromatic hydrocarbons) for the HDPE GM were higher and the partition coefficients were much higher than those of maleic anhydride and pure EVOH. However, MC (alkane) and MTBE (ether), which have relatively high polarity among the VOCs tested, showed lower slopes for HDPE GM in comparison to the maleic anhydride. This trend was reversed in the EVOH film. For example, the partition coefficient of MC was higher in the EVOH sheet than that for the TOL. However, the partition coefficients of polar VOCs in the EVOH laminar are still lower than those in other non-polar sheets. The sorptive behavior of VOCs to EVOH shows lower affinity based on the results of this study. Hence, EVOH can be an effective material as a barrier to diffusive VOC flux.

3.6.2 Analysis of Kinetic Batch Test

Decreasing concentrations of the selected VOCs (i.e., MC and MTBE) in

the solution over time obtained from kinetic batch tests are shown in Fig. 3.7. Fits of Eq. (15) are shown as the smooth lines in Fig. 3.7. To estimate the diffusion coefficients, the partition coefficients obtained from the equilibrium batch tests were input to Eq. (15), and the equation was fit to the kinetic batch test data by adjusting only the diffusion coefficient (D_g). This method yields more accurate results compared to a method that adjusts the partition and diffusion coefficients simultaneously (Park et al. 2012a). The parameters were fitted using non-linear least-squares regression with Microsoft Excel Solver using the generalized reduced gradient algorithm (Park et al. 2012a).

To verify the method, the diffusion coefficients of HDPE GM for VOCs were compared to Park et al. (2012a). For all five compounds, the diffusion coefficients found in this study were within (2-12)% of those obtained from the literature except MTBE (= 29%). Paired F-tests returned $p = 0.18$ for the diffusion coefficients, indicating no statistically significant difference ($p > 0.05$) between the diffusion coefficients obtained using the two methods. Diffusion coefficients obtained for the comparisons are summarized in Table 3.4.

The inclination of plotting data of VOC concentration was the lowest in EVOH sheet among tested materials including maleic anhydride sheet, and HDPE GM. Diffusion coefficients of each material, obtained from the kinetic batch tests, are summarized in Table 3.5. Overall, HDPE GM had the highest diffusion coefficient (2.86-11.05 × 10^{-13} m^2/s) and pure EVOH sheet had the lowest diffusion coefficient (0.0046-0.0262 × 10^{-13} m^2/s). The diffusion coefficient for the EVOH sheet was several orders of magnitude smaller than conventional HDPE

and LLDPE GM. As anticipated, non-polar VOCs (aromatic hydrocarbons) including TOL and CB showed steeper declination of the concentration in HDPE GM; however the VOCs showed a more gentle declination in pure EVOH sheet. This trend was exactly opposite for polar VOCs such as MC and MTBE. The VOCs showed a more gentle declination of the concentration for HDPE GM; however, the VOCs show steeper inclination in pure EVOH sheet. This trend represents the characteristics of affinity between polarity of the VOC and non-polar sheet of polyethylene-type GM and polar sheet of EVOH GM.

3.6.3 Analysis of Modified Double Compartment Apparatus (MDCA) Test

In the MDCA tests, the initial concentration for all five VOCs in the upper reservoir was 100 mg/L. Typical relative concentrations in the influent (upper) and effluent (lower) reservoirs over time are shown in Fig. 3.8 for MC and CB. Similar data were obtained for the other compounds. Generally, VOCs with lower affinity for HDPE (MC and MTBE) did not migrate as much during the test period [e.g., Fig. 3.8 (a)], whereas VOCs with higher affinity for HDPE (CB, TOL, and TCE) sorbed to the surface of the co-extruded GM and thus reduced the concentration in the influent [e.g. Fig. 3.8 (b)]. Even though some amount of the VOCs with high affinity for HDPE sorbed to the outer layer of the co-extruded GM, minimal diffusion through the co-extruded GM occurred since the solute minimally diffused through the EVOH film in the GM. Therefore, almost no concentration was detected in the effluent reservoir during the given time. The smooth lines in Fig. 3.8 correspond to fits with the finite difference model (Joo et

al. 2005; Park et al. 2012a). To fit the diffusion coefficient, the partition coefficient obtained from the equilibrium batch test was used as input. Similar to the kinetic batch test, parameters were fitted using least-squares regression with Microsoft Excel Solver. The partition coefficients used as input and the diffusion coefficients obtained from the model are summarized in Table 3.6.

To validate the enhanced performance of the MDCA test apparatus, the partition and diffusion coefficients were fitted to the experimental data simultaneously. The partition coefficients for the conventional HDPE GM obtained from the MDCA test and the equilibrium batch tests are compared in Fig. 3.9. Additionally, the partition coefficients obtained from previous DC tests are compared to the coefficients from the MDCA test. All of the data fell above the 1:1 line, indicating that the MDCA test yields a slightly higher partition coefficient than the equilibrium batch test. A paired F-test returned $p = 0.41$ (> 0.05), indicating that the two sets of partition coefficients are statistically identical. However, the partition coefficient for MC from the previous DC test apparatus (Park et al. 2012a) was a factor of 52% higher than that from the equilibrium batch test. Partition coefficients for the other VOCs from the DC test were higher (20-30% >). A paired F-test returned $p = 0.32$ (> 0.05), indicating that the two sets of partition coefficients from the DC and equilibrium batch tests are also considered to be identical, but had a significantly higher p value than the MDCA. Therefore, the MDCA testing apparatus can provide reliable data compared to the DC test apparatus.

Diffusion coefficients of co-extruded GM obtained from the MDCA test are

compared to those of HDPE GM obtained from kinetic batch tests in Fig. 3.10. Co-extruded EVOH GM had measured diffusion coefficients that were approximately 25 times smaller than the HDPE GM. This comparison of the diffusion coefficients for the different materials shows that co-extruded EVOH GM can be an effective barrier for reducing VOC migration through composite liners.

3.7 CHEMICAL CHARACTERIZATION OF VOLATILE ORGANIC COMPOUNDS WITH TRANSPORT PARAMETERS

3.7.1 Relationship with Partition Coefficient

Chemical properties related to the polarity of VOCs including the octanol-water partition coefficient (K_{ow}), aqueous solubility (A.S.), and molecular diameter (d_m) were investigated to determine how the chemical properties of each material composing the co-extruded GM impacted the sorptive behavior of VOC to the materials. Figure 3.10 shows the relationship between the chemical properties and the partition coefficient. An empirical relationship between the partition coefficient and K_{ow} for HDPE GM has been reported by many researchers (Park and Nibras 1993; Sangam and Rowe 2001b; Joo et al. 2004; Nefso and Burns 2007; Park et al. 2012a). Most relationships are linearly proportional with log-log axes (Fig. 3.11). In most polymer-penetrant systems, partition coefficients generally increase with an increase in similarity between the components, according to “like dissolves like” (August and Taztky 1984; Sangam and Rowe 2001). In general, the permeation affinity has the following order: alcohols < acids < nitro derivatives < aldehydes < ketones < esters < ethers < aromatic

hydrocarbons < halogenated aromatic hydrocarbons (August and Taztky 1984; Sangam and Rowe 2001a).

With increasing log K_{ow}-related polarity, chemical hydrophobia increases and the partitioning of VOC shows higher affinity to the HDPE GM [Fig. 3.11 (a)]. In the GM, the log K_{ow} and log K_g represented this affinity and followed the order: CB > TOL > TCE > MTBE > MC. For the EVOH film, the relationship between the partition coefficient and K_{ow} was linear but slightly negative. The negative slope is statistically significant (F value = 126.13 >> 1.0, correlation coefficient = 0.988). Because of the alcohol group (-OH) in EVOH, the chemical hydrophobia decreases and the partition of VOC shows lower affinity to the EVOH film with increasing log K_{ow}. Maleic anhydride, which is the acid anhydride of maleic acid, showed a higher slope than EVOH but much lower than HDPE and LLDPE. With high affinity for the GM and sheet, the slope is steeper. Table 3.7 summarizes the variable of the empirical relationship for each material.

Similar to log $K_{ow,}$ a strong relationship between log A.S. and log K_g exists [Fig. 3.11 (b)]. The increasing affinity for HDPE and LLDPE with decreasing A.S. reflects the increasing hydrophobicity of the VOCs. The trend of A.S. and K_g is reversed with A.S. and K_{ow}. However, in the EVOH sheet, the relationship between the partition coefficient and A.S. is still linear but slightly positive. The positive slope is statistically significant (F value = 170.23 >> 1.0, correlation coefficient = 0.991). Further, maleic anhydride showed a higher slope than EVOH, but a much lower slope than HDPE and LLDPE.

Similar to trends with previous properties, log K_g generally increased with

increasing d_m in HDPE and LLDPE GM [Fig. 3.11 (c)]. However, the large MTBE molecule is an exception to the trend. Larger VOC molecules tend to be more hydrophobic (higher K_{ow}) due to the lower electronegativity of larger molecules (Meylan and Howard, 1995; Sangam and Rowe, 2001a). However, MTBE is oxygenated, which permits hydrogen bonding with water molecules, and MTBE therefore has lower hydrophobicity compared to the other VOCs with similar d_m (Park et al. 2012a). Other than MTBE, a stronger relationship between d_m and K_g was obtained. In the EVOH laminar, the relationship between the partition coefficient and d_m is still linear but slightly negative. The negative slope is statistically significant (F value = 21.25 >> 1.0, correlation coefficient = 0.956). Maleic anhydride shows a higher slope than EVOH but much lower than HDPE and LLDPE.

3.7.2 Relationship with Diffusion Coefficient

Similar to the partition coefficient, chemical properties related to the polarity of the compound including the octanol-water partition coefficient (K_{ow}), aqueous solubility (A.S.), and molecular diameter (d_m) were investigated. In particular, how the properties among different materials impacted the diffusive behavior of the VOCs. Figure 3.12 shows the relationship between the chemical properties and diffusion coefficient. The empirical relationship between the properties and the diffusion coefficient is relatively weak in comparison to the partition coefficient. This trend was also found in other studies (Sangam and Rowe 2001a; Joo et al. 2005; Park et al. 2012a). In most correlations between

the chemical properties and the diffusion coefficient, the R-squared value is less than 0.5. The diffusive behavior is dependent upon not only molecular affinity, but also crystallinity and molecular weight related to Brownian motion. If the molecular weight increases, the electronegativity among molecular compounds increases and the affinity increases. Hence, diffusion would be active. However, beyond a certain molecular weight, molecular Brownian motion would be reduced and the diffusion would also be reduced (Shackelford and Daniel 1991). This mechanism is similar to antagonism where the involvement of multiple agents induces and reduces their overall effect. Crystallinity can greatly influence the diffusive transport. As crystallinity increases, diffusion is reduced (Armstrong 2011).

According to previous research (Sangam and Rowe 2001a; Joo et al. 2005; Park et al. 2012a), the diffusion coefficient is less correlated to chemical properties due to the complexity and inter-relationships of these properties. Empirical relationships between D_g vs K_{ow} and D_g vs d_m reflect weakly negative linear or convex polynomial equation, as shown in Fig. 3.12. However, the empirical relationship between D_g and A.S. is linear and slightly positive.

3.8 VALIDATION OF EQUIVALENT DIFFUSON COEFFICIENT OF A CO-EXTRUDED GEOMEMBRANE

3.8.1 Comparison between Estimated and Measured Diffusion Coefficients

To validate the approach that uses an equivalent diffusion coefficient for VOC transport through a co-extruded GM, the equivalent diffusion coefficients

estimated by Eq. (14) were compared to measured diffusion coefficients obtained from MDCA test. Table 3.8 shows the measured and estimated values of diffusion coefficient for both methods. A paired F-test returned $p = 0.39$ (< 0.05), indicating that the two sets of partition coefficients are identical. Therefore, the proposed equation [Eq. (14)] for an equivalent diffusion coefficient can provide a reliable value. If the Eq. (14) is used, the equivalent diffusion coefficient can be estimated readily and quickly by using results from kinetic batch testing. Diffusion coefficients for TCE, TOL, and CB obtained from the two tests differed by less than 4%, whereas diffusion coefficients for MC and MTBE from the two tests differed by approximately 11%, on average. Relative larger differences were obtained for MC and MTBE because the MDCA test did not reach equilibrium for these VOCs.

3.8.2 Comparison between Measured and Predicted VOC Transport through Composite Liner

To further validate the equivalent diffusion coefficient for co-extruded GM, VOC transport through a composite liner with numerical modeling [i.e., finite difference method (FDM)] was compared to data from laboratory diffusion column testing. Two sets of diffusion column tests, including a duplicate, were conducted (Eun et al. 2014b). In the diffusion column test, a composite liner employing 1.5-mm co-extruded GM with a compacted clay liner (CCL) was used. The initial concentration of VOCs was 100 mg/L. The concentration in the influent reservoir was kept constant. The upper component consisted of 1.5-mm co-

extruded GM, and the lower component consisted of a 0.12 m of CCL with a saturated hydraulic conductivity of 1×10^{-9} m/s or lower. Eq. (2) to Eq. (5) was used to simulate VOC transport in the FDM (Foose et al. 2001; Park et al. 2012b). The numerical modeling (i.e., finite difference method) for VOC transport through composite liner was validated by the accurate results of diffusion column tests of composite liner with HDPE GM overlaying CCL (Park et al. 2012b). More details of the diffusion column test are described in Eun et al. (2014b). Parameters for each layer of the composite liner that were used as input to the FDM are represented in Table. 3.9.

Figure 3.13 shows the predicted and measured concentration of VOCs at 20-mm depth below the GM in the diffusion column test. Generally, the migration of VOCs predicted by numerical modeling was in good agreement with those measured by the column test. Further, for each VOC, the magnitude of the diffusion coefficient estimated was in agreement with the VOC migration demonstrated in the diffusion column test (Eun et al. 2014b). With a higher diffusion coefficient, more rapid and higher contaminant flux levels occur. Larger differences were obtained for MC and MTBE because the transport parameters estimated by Eq. (14) did not coincide with those of the batch test.

3.9 CONCLUSIONS

The purpose of this study was to evaluate equivalent diffusion coefficients of five VOCs through a co-extruded GM containing EVOH via a series of batch tests. An equivalent diffusion coefficient was derived analytically based on the

sorptive and diffusive behaviors through co-extruded GM (i.e., non-homogeneous layers in series). First, the transport parameters of each material composing the co-extruded GM and the GM were measured from batch tests. Overall, LLDPE GM had the highest partition coefficient (1.9–195.8 L/kg) and pure EVOH laminar had the lowest partition coefficient (0.69-0.94 L/kg). However, depending on the polarity of the related VOC, the coefficient can be influenced markedly. The diffusion coefficient of co-extruded GM (0.14-0.59 × 10^{-13} m^2/s) is approximately 16-29 times smaller than that of HDPE GM (2.86–11.05 × 10^{-13} m^2/s). Furthermore, the diffusion coefficient of pure EVOH sheet is several orders of magnitude smaller than that of HDPE GM. The incorporation of co-extruded GM in landfill cover/liner systems may substantially decrease the diffusive transport of non-polar organic compounds such as methane and VOCs.

The chemical characteristics of each material in a co-extruded EVOH GM (i.e., octanol-water partition coefficient, aqueous solubility and molecular diameter) show a strong linear relationship with the partition coefficient on a log-log scale. The relationship of the characteristics (i.e., octanol-water partition coefficient, aqueous solubility and molecular diameter) with HDPE, LLDPE, and maleic anhydride was reversed to those of EVOH due to the polarity of the material. However, the empirical relationship between the properties and the diffusion coefficient is relatively weak in comparison to the partition coefficient.

For validation of the proposed equation, the transport parameters for a co-extruded GM obtained using batch tests were compared to the transport parameters obtained from a modified double-compartment apparatus (MDCA)

test. The MDCA testing apparatus provides reliable data compared to the previous DC test apparatus due to minimizing the loss of VOCs. The equation to estimate the equivalent diffusion coefficient can provide reliable values because the measured and estimated diffusion coefficients are statistically identical. For another validation of the equivalent diffusion coefficient, the migration of VOCs predicted by numerical modeling using the coefficient were compared to those measured in diffusion column tests. The predicted and measured concentrations of VOCs were in good agreement. Further, for each VOC, the magnitude of the estimated diffusion coefficient was in agreement with the VOC migration demonstrated in the diffusion column test.

3.10 ACKNOWLEDGMENTS

The authors appreciate the support of Kuraray CO., Ltd. The opinion, findings and conclusions expressed herein do not represent the views of Kuraray CO., Ltd.

3.11 REFERENCES

Armstrong R. B. (2011). “Improving performance of geosynthetics for containment of volatile organic compounds through the use of ethylene vinyl alcohol (EVOH).” *Geo-Frontier 2011* ASCE, Florida.

August, H., and Taztky, R. (1984). “Permeability of commercial available polymeric liners for hazardous landfill leachate organic constituents.” *International Conference on Geomembrane*, Denver, USA, 151-156.

Byun, Y. J., Hong, S. I., Kim, K. B., Jeon, D. H., Kim, J. M., Whiteside, W. S., and Park H. J. (2007). “Physical and chemical properties of γ-irradiated EVOH film.” *Radiation Physics and Chemistry*, 76 (6), 974-981.

Chen, Y., Xie, H., Ke H., and Chen, R. (2009). “An analytical solution for one-dimensional contaminant diffusion through multi-layered system and its applications.” *Environmental Geology*, 58, 1083-1094.

Crank, J. (1975). The mathematics of diffusion, 2nd Ed., Clarendon, Oxford, United Kingdom, 11-24.

Dingemans, M., Dewulf, J., Braeckman, L., van Langenhove, H., Friess, K., Hynek, V., and Sipek, M., (2008). “Mass transfer characteristics for VOC permeation through flat sheet porous and composite membrane: The impact of the different membrane layers on the overall membrane resistance.” *Journal of Membrane Science*, 322, 234-242.

Edil, T. B., Wambold, W. S., and Park, J. K. (1995). “Partitioning of VOCs in clay liner materials.” *Geoenvironment 2000*, ASCE GSP 46, 775-790. 20.

Edil, T. B. (2007). “Is aqueous-phase VOC transport from modern landfills a

potential environmental problem?" *Proceeding*, Sardinia 2007, *11th Int. Landfill Symposium*, Cagliari, Italy.

Eun, J., Tinjum, J. M., Benson, C. H., and Edil, T. B. (2014a). "Volatile organic compound (VOC) transport through composite liner with co-extruded geomembrane containing ethylene vinyl-alcohol (EVOH)." Accepted to *Geo-Congress 2014* ASCE, Atlanta.

Eun, J., Tinjum, J. M., Benson, C. H., and Edil, T. B. (2014b). "Volatile organic compound (VOC) transport through composite liner with co-extruded geomembrane containing ethylene vinyl-alcohol (EVOH)." Submitted to *Journal of Geotechnical and Geoenvironmental Engineering.*

Foose, G. J., Benson, C. H., and Edil, T. B. (2001). "Equivalent of composite geosynthetic clay liners as barrier to volatile organic compounds." *Geosynthetic '99 conferences.*

Foose, G. J. (2002). "Transit-time design for diffusion through composite liners." *Journal of Geotechnical and Geoenvironmental Engineering*, 128 (7), 590-601.

Foose, G. J., Benson, C. H., and Edil, T. B. (2002). "Comparison of Solute Transport in three composite liners." *Journal of Geotechnical and Geoenvironmental Engineering,* 128 (5), 1-13.

Freeze, R. A., and Cherry, J. A. (1979). Ground water. Prentice-Hall, Englewood Cliffs, New Jersey.

Hashimoto, I., Deshpande, K. B., and Thomas, H. C. (1964). "Peclet numbers and retardation factors for ion exchange columns." *Industrial and*

Engineering Chemistry Fundamentals, 3 (3), 213-218.

Huysmans, M. and Dassargues, A. (2007). “Equivalent diffusion coefficient and equivalent diffusion accessible porosity of a stratified porous medium.” *Transport Porous Medium*, 66, 421-438.

Joo, J. C., Kim, J. Y., and Nam, K. (2004). “Mass transfer of organic compounds in dilute aqueous solutions into high density polyethylene geomembranes.” *Journal of Geotechnical and Geoenvironmental Engineering*, 130 (2), 175-183.

Joo, J. C., Nam, K., and Kim, J. Y. (2005). “Estimation of mass transport parameters of organic compounds through high density polyethylene geomembranes using a modified double-compartment apparatus.” *Journal of Geotechnical and Geoenvironmental Engineering*, 131 (5), 790-799.

Klett, N., Edil, T. B., Benson, C. H., and Connelly, J. (2005). “Evaluation of volatile organic compounds in Wisconsin landfill leachate and lysimeter samples.” *Final Report to the University of Wisconsin System Groundwater Research Program*, Department of Civil and Environmental Engineering, University of Wisconsin at Madison, Madison, WI.

Kolbasuk, G. (1991). “Co-extruded HDPE/VLDPE multilayer geomembrane.” *Geotextiles and Geomembranes,* 10 (4), 601–612.

Lake, C. B., and Rowe, R. K. (2005). “A comparative assessment of volatile organic compound (VOC) sorption to various types of potential GCL bentonites.” *Geotextiles and Geomembranes,* 23 (4), 323–347.

Leo, A., Hansch, C., and Elkins, D. (1971). “Partition coefficients and their uses.” *Chemical Reviews*, 71 (6), 525–616.

Li, Y. and Cleall, P. J. (2010). “Analytical solutions for contaminant diffusion in double-layered porous media.” *Journal of Geotechnical and Geoenvironmental Engineering*, 136 (11), 641-657.

McWatters, R. S. and Rowe, R. K. (2010). “Diffusive transport of VOCs through LLDPE and Two coextruded geomembrane.” *Journal of Geotechnical and Geoenvironmental Engineering*, 136 (9), 1167-1177.

McWatters, R. S. and Rowe, R. K. (2011). “Sorption and diffusion of BTEX through thin-film EVOH.” *Geo-Frontiers 2011* ASCE, 2073-2083.

Meylan, W. M. and Howard, P. H. (1995). “Atom/fragment contribution method for estimating octanol-water partition coefficients.” *Journal of Pharmacy Science*, 84 (1), 83-92.

Nefso, E. K. and Burns, S. E. (2007). “Comparison of the equilibrium sorption of five organic compounds to HDPE, PP, and PVC geomembranes.” *Geotextiles and Geomembranes*, 25, 360-365.

Park, J. K., and Nibras, M. (1993). “Mass flux of organic chemicals through polyethylene geomembranes.” *Water Environment Research*, 65 (3), 227-237.

Park, J. K., Sakti, J. P., and Hoopes, J. A. (1996). “Transport of organic compounds in thermoplastic geomembranes, I: Mathematical model.” *Journal of Environmental Engineering*, 122 (9), 800-806.

Park, M. G., Benson, C. H., and Edil, T. B. (2012a). “Comparison of batch and

double compartment tests for measuring VOC transport parameters in geomembranes." *Geotextiles and Geomembranes*, 31 (1), 15–30.

Park, M. G., Edil, T. B. and Benson, C. H. (2012b). "Modeling volatile organic compound transport in composite liners." *Journal of Geotechnical and Geoenvironmental Engineering*, 138 (6), 641-657.

Parker, L. and Britt, S. (2012). "The Effect of bottle fill rate and pour technique on the recovery of volatile organics." *Ground Water Monitoring and Remediation*, 32 (4) 78-86.

Rowe, R. K., Quigley, R. M., Brachman, R. W., and Booker, J. R. (2004). Barrier systems for waste disposal facilities. Taylor and Francis Group, New York.

Sangam, H. P. and Rowe, R. K. (2001a). "Migration of dilute aqueous organic pollutants through HDPE geomembranes." *Geotextiles and Geomembranes*, 19, 329-357.

Sangam, H. P. and Rowe, R. K. (2001b). "The role of HDPE geomembranes in retarding the diffusive migration of organic contaminants through composite liner systems." *Proceeding*, Sardinia 2001, *8th Int. Landfill Symposium*, Cagliari, Italy.

Sangam, H. and Rowe, R. (2005). "Effect of surface fluorination on diffusion through a high density polyethylene geomembrane." *Journal of Geotechnical and Geoenvironmental Engineering*, 131 (6), 694-704.

Schwarzenbach, R. P., Gschwend, P. M., and Imboden, D. M. (2003). Environmental organic chemistry. Second edition. Wiley-Interscience, NJ.

Shackelford, C. D. and Daniel, D. E. (1991). “Diffusion in saturated soil I: Background.” *Journal of Geotechnical Engineering*, 7 (3), 467-484.

Zhang, Z., Britt, I. J., and Tung, M. A. (1999). “Water absorption in EVOH films and its influence on glass transition temperature.” *Journal of Polymer Science, Part B. Polymer Physics*, 37, 691–699.

Zhang, Q., Lin, W., Chen, Q., and Yang, G. (2000). “Phase structure of EVOH copolymers as revealed by variable temperature solid state high resolution.” 13C NMR spectroscopy. *Macromolecules*. 33, 8904-8906.

3.12 TABLES

Table 3.1 Properties of VOCs used in experiments

Compound	MC	MTBE	TCE	TOL	CB
Chemical formula	CH_2Cl_2	CH_3-O-$C(CH_3)_3$	$CHCl=CCl_2$	C_6H_5-CH_3	C_6H_5Cl
Type of compound	Alkane	Ether	Alkene	Arene	Arene
Molecular weight (g/mol)	84.93	88.15	131.39	92.14	112.56
Density (g/mL)	1.33	0.740	1.46	0.867	1.11
log K_{ow}	1.31	0.94	2.42	2.69	2.78
Solubility (mg/L)	20000	48000	1100	515	500
Vapor pressure (kPa)	57.5	32.4	10.0	3.72	1.59
Dielectric constant	8.9	4.5	3.4	2.4	2.7
Melting point (C°)	-97.2	-108.6	-84.7	-94.95	-45.31
Boiling point (C°)	40	55	87.21	110.63	131.72

Note: MC: Methylene chloride, MTBE: Methyl Tertiary Butyl Ether, TCE: Trichloroethylene, TOL: Toluene, CB: Chlorobenzene.

K_{ow}: partition coefficient between octanol and water

Table 3.2 Engineering properties of co-extruded GM

Property	Method	Unit	HDPE	LLDPE	Maleic anhydride	EVOH
Thickness	ASTM D 5944	mm	1.5	1.0	0.5	0.5
Puncture resistance	ASTM D 4833	N	520	380	280	100
Tear resistance	ASTM D 1004	N	100 × 100	70 × 70	40 × 40	45 × 50
Load at break	ASTM D 6693	N	15000	10300	8300	6500
Elongation at break	ASTM D 6693	%	10000	600	500	180
Tensile strength	ASTM D 6693	kN/m	18.7	14.5	10.5	8.3

Table 3.3 Partition Coefficient (K_g) from equilibrium batch test

Type	K_g (L/kg)				
	MC	MTBE	TCE	TOL	CB
Pure EVOH	0.885	0.938	0.701	0.690	0.704
Maleic anhydride (Tie)	5.61	3.80	19.90	29.20	24.84
HDPE	3.38	0.82	69.02	88.56	112.03
LLDPE	5.80	1.90	157.85	195.79	171.09

Table 3.4 Diffusion coefficient (D_g) of HDPE GM from kinetic batch test

Type	D_g ($\times 10^{-13}$ m^2/s)					
	MC	MTBE	TCE	TOL	CB	Paired F-test
HDPE	10.1	11.05	5.17	4.06	2.86	p = 0.18 > 0.05
HDPE (Park et al. 2012)	8.86	7.74	5.45	3.77	3.96	

Table 3.5 Diffusion coefficient (D_g) from kinetic batch test

Type	D_g ($\times 10^{-13}$ m^2/s)				
	MC	MTBE	TCE	TOL	CB
Pure EVOH	0.0214	0.0262	0.0061	0.0046	0.0054
Maleic anhydride (Tie)	1.5	2.18	1.16	0.92	1.27
HDPE (outer layer)	9.67	10.24	5.15	3.24	3.63
LLDPE	4.4	3.1	9.1	7.1	8.1

Table 3.6 Partition used and diffusion coefficient (D_g) obtained from MDCA test

Type	Unit	MC	MTBE	TCE	TOL	CB
K_g of co-extruded GM	L/kg	9.67	10.24	5.15	3.24	3.63
D_g of co-extruded GM	$\times 10^{-13}$ m^2/s	0.587	0.697	0.182	0.140	0.161

Table 3.7 Variables of linear equation for each material of the co-extruded GM

	K_g vs K_{ow}			K_g vs A.S.			K_g vs d_m		
	$\log K_g = a \cdot \log K_{ow} + b$			$\log K_g = a \cdot \log$ A.S. $+ b$			$\log K_g = a \cdot \log d_m + b$		
	a	b	R^2	a	b	R^2	a	b	R^2
LLDPE (Outer layer)	1.155	-0.8	0.985	-1.044	5.185	0.989	19.02	-8.206	0.931
HDPE (Outer layer)	1.142	-0.961	0.980	-1.030	4.948	0.978	16.91	-7.254	0.923
Maleic anhydride (Tie)	0.450	0.156	0.984	-0.408	2.490	0.991	7.648	-2.856	0.969
Pure EVOH	-0.076	0.041	0.977	0.068	-0.350	0.983	-1.277	0.543	0.914

Table 3.8 Comparison of diffusion Coefficient (D_g) measured from MDCA test and that estimated from Eq. (14)

Compounds	Unit	1.5-mm-EVOH GM (HDPE outer layer)		Paired F-test	1.5-mm HDPE GM
		Estimated	Measured		Measured
MC	$\times 10^{-13}$ m^2/s	0.628	0.587	p = 0.39 > 0.05	10.1
MTBE		0.802	0.697		11.05
TCE		0.181	0.182		5.17
TOL		0.137	0.140		4.06
CB		0.162	0.161		2.86

Table 3.9 Input transport parameters for simulation of diffusion column testing with a composite liner containing co-extruded GM

Compound	Compacted clay (Eun et al. 2014b)		1.5-mm co-extruded GM	
	Partition coefficient (K_d) (L/kg)	Diffusion coefficient (D*) ($\times 10^{-5}$ m^2/s)	Partition coefficient (K_g) (L/kg)	Diffusion coefficient (D_g) ($\times 10^{-13}$ m^2/s)
MC	0.097	0.14	9.67	0.587
MTBE	0.092	0.138	10.24	0.697
TCE	0.178	0.147	5.15	0.182
TOL	0.192	0.146	3.24	0.140
CB	0.217	0.139	3.63	0.161

3.13 FIGURES

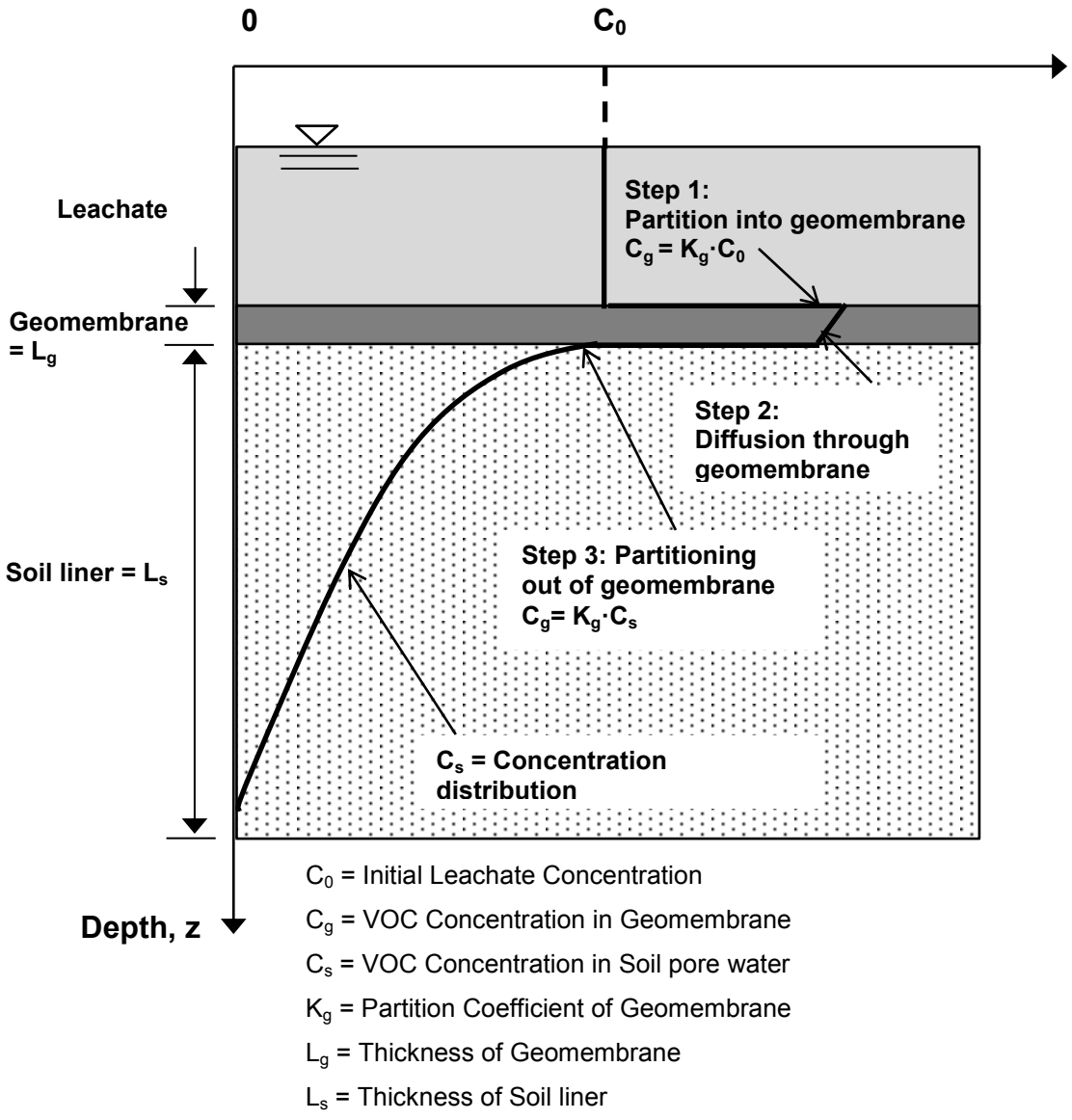

Figure 3.1 Schematic of mechanisms involved in one-dimensional VOC transport through composite liners with intact geomembrane (modified from Park et al. 2012b).

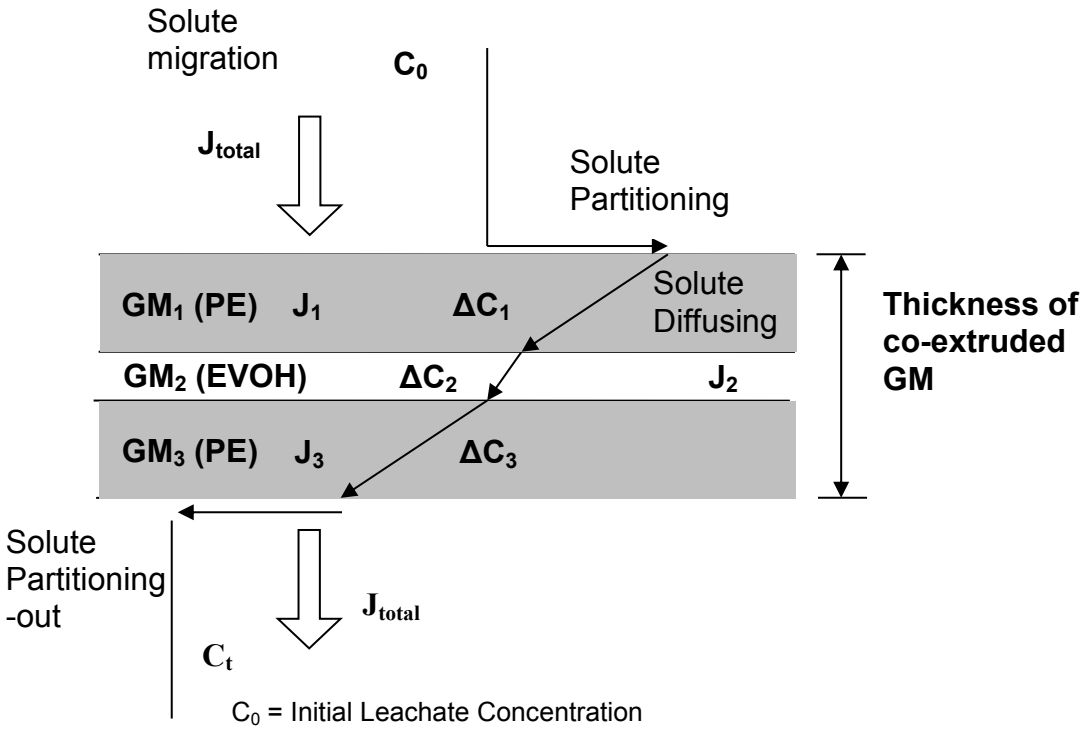

C_0 = Initial Leachate Concentration

ΔC_1, ΔC_2, ΔC_3= Difference of VOC concentration in each layer

J_1, J_2, J_3 = VOC flux in each layer

J_{total} = VOC flux in entire GM

Figure 3.2 A conceptual schematic of solute transport through co-extruded EVOH GM.

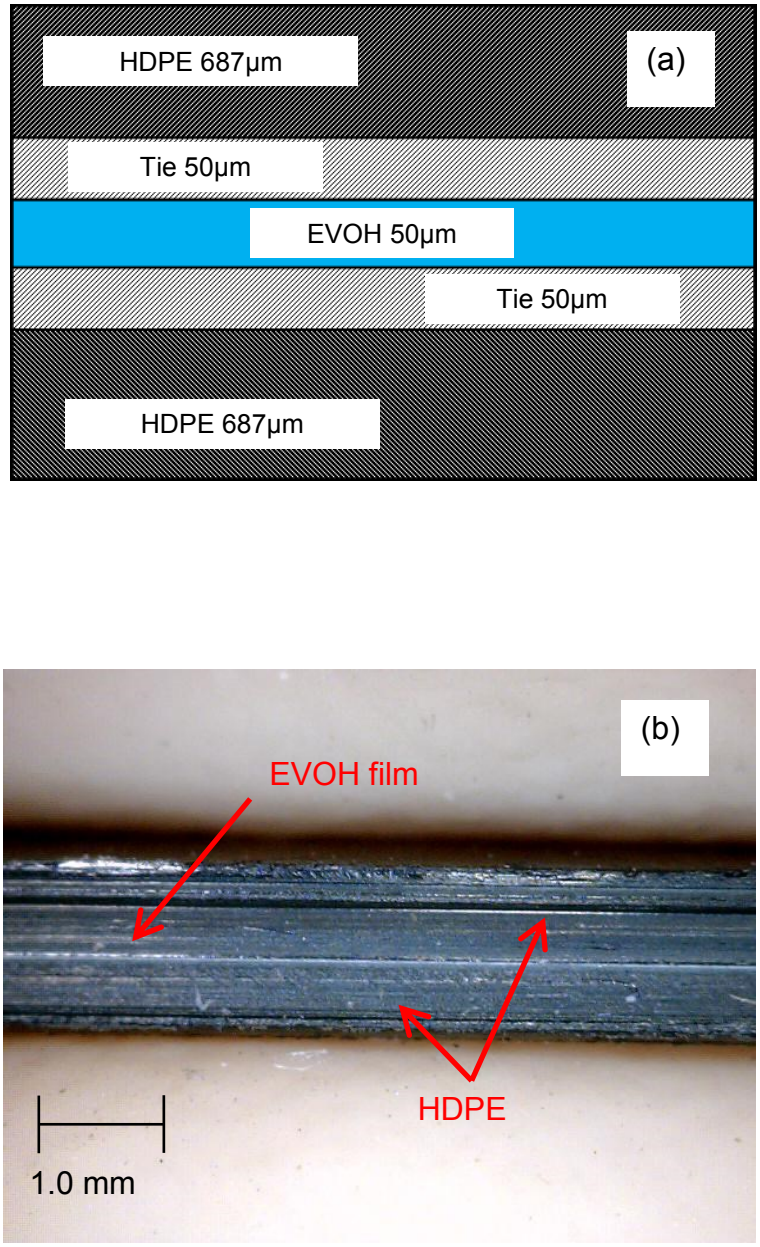

Figure 3.3 Layer of the co-extruded EVOH GM: (a) Cross section schematic of 1.5-mm co-extruded EVOH GM (No scale); and (b) Micro photo of 1.5-mm co-extruded EVOH GM.

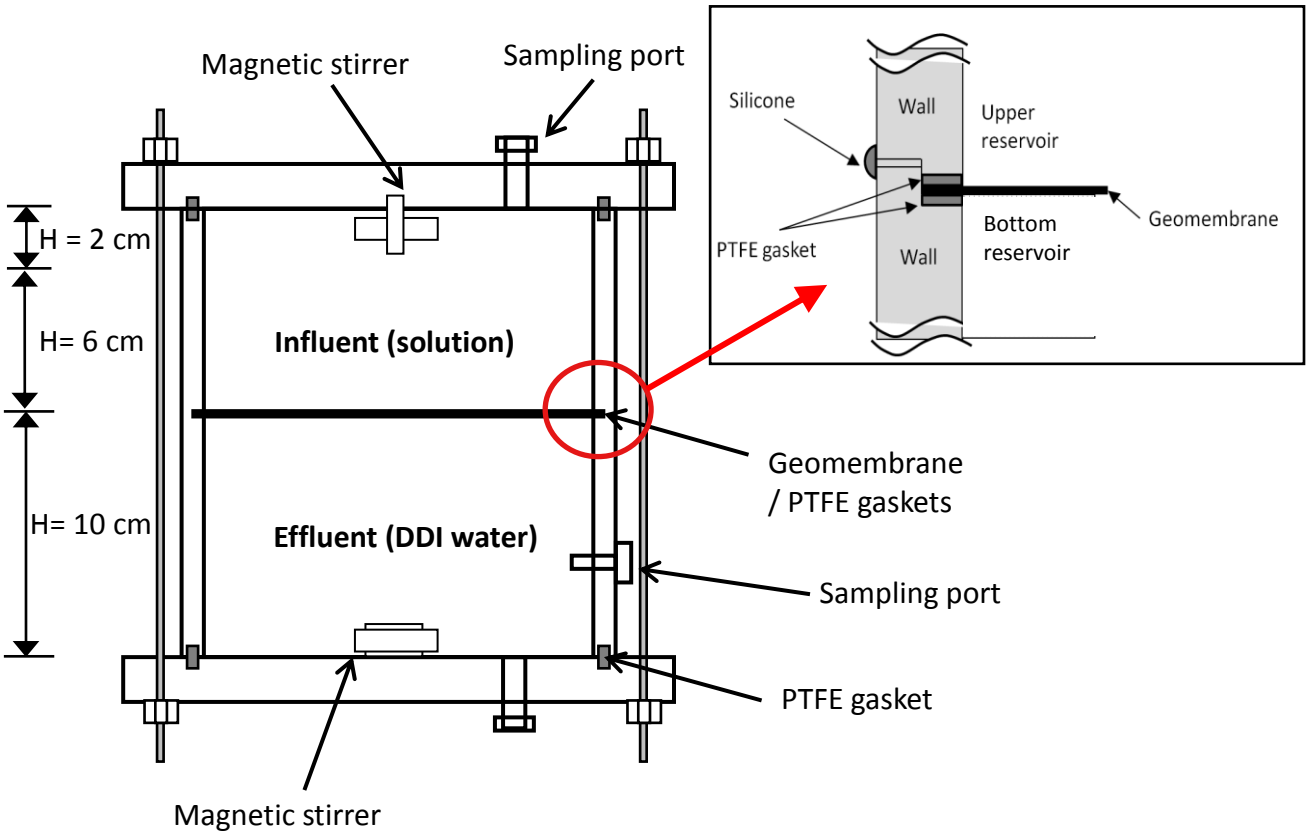

Figure 3.4 Modified double-compartment apparatus (MDCA).

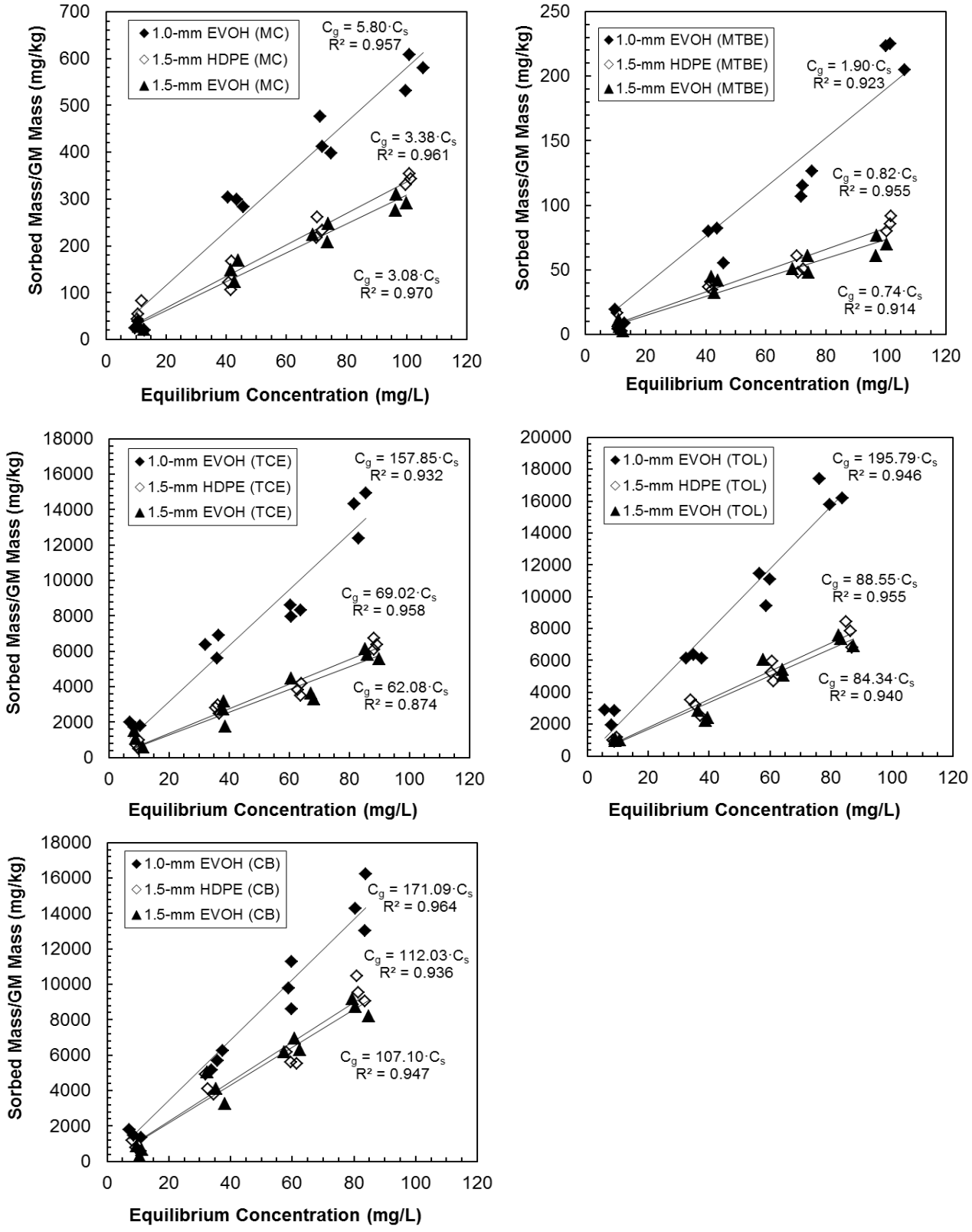

Figure 3.5 Sorption isotherm of VOC for two co-extruded EVOH GMs and HDPE GM.

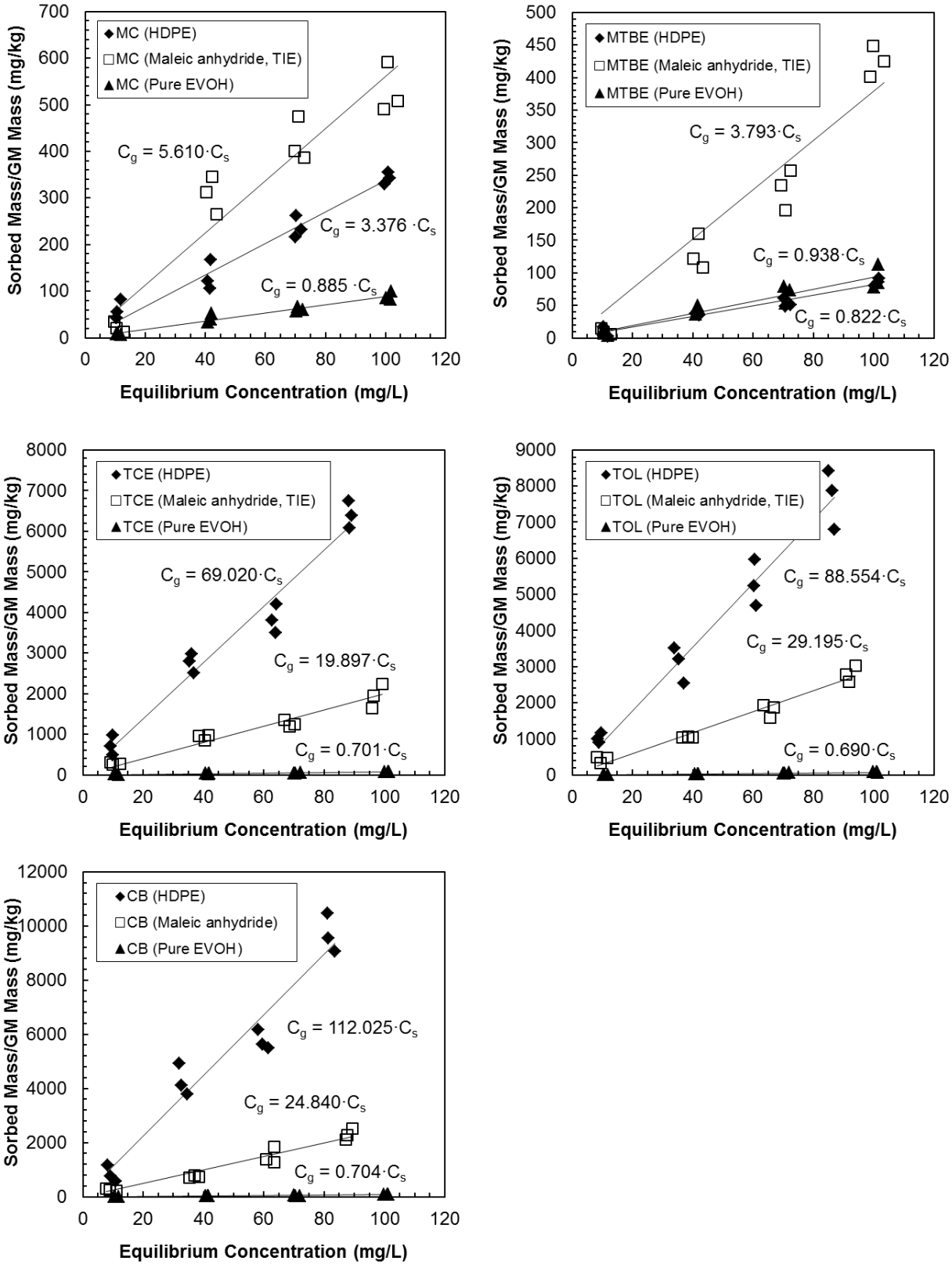

Figure 3.6 Sorption isotherm of VOC for materials used in co-extruded GM.

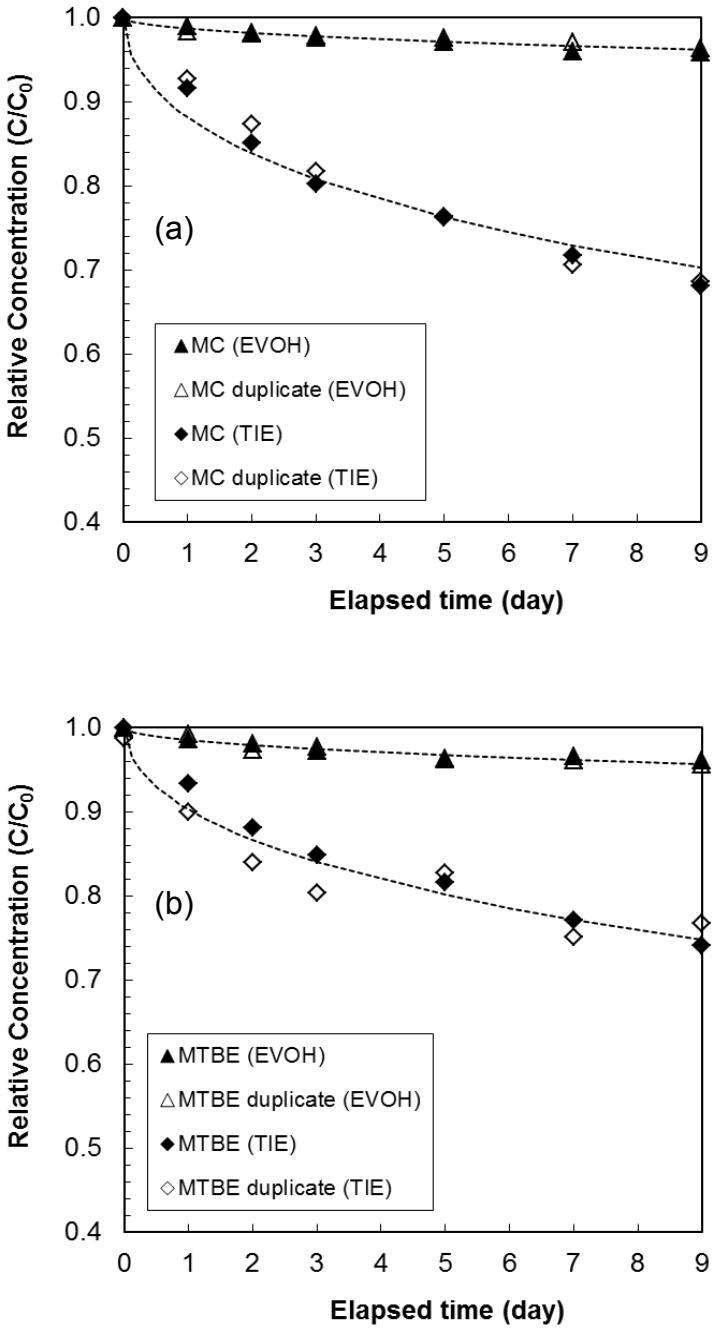

Figure 3.7 Decreasing concentrations with time recorded from kinetic batch test: (a) MC; and (b) MTBE.

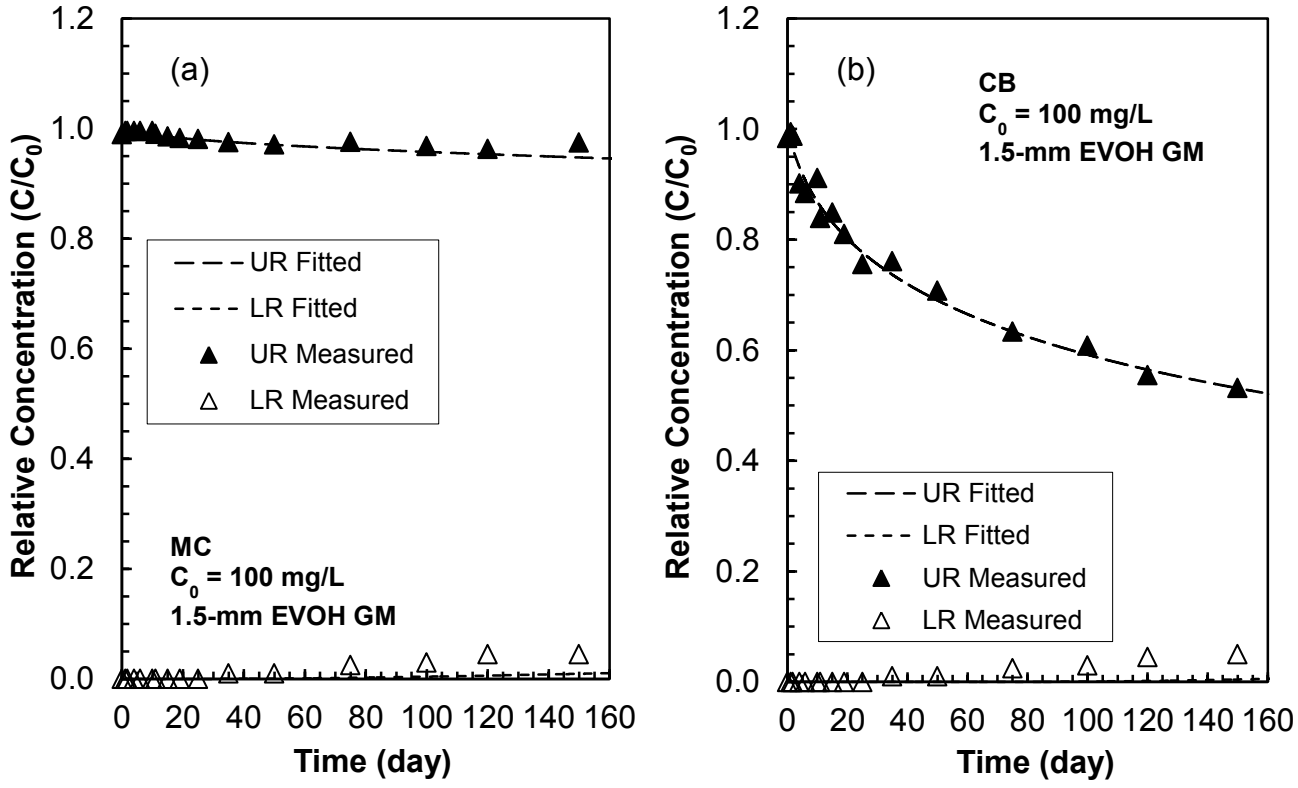

Figure 3.8 Relative concentrations in the influent (upper) and effluent (lower) reservoirs in MDCA test: (a) MC; and (b) CB.

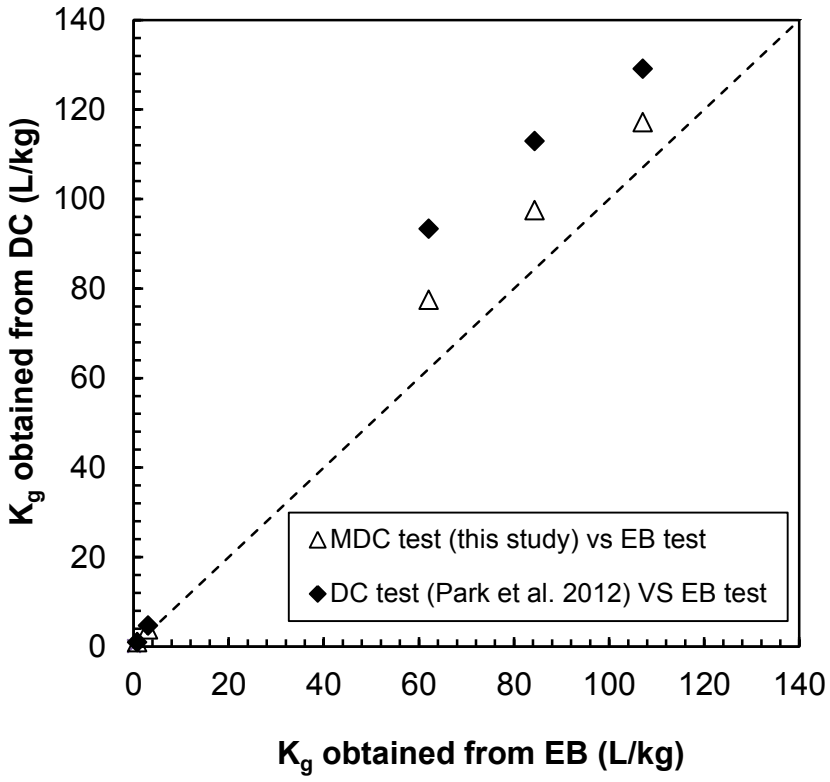

Figure 3.9 Comparison of partition coefficient between co-extruded GM obtained from MDCA test and HDPE GM obtained from equilibrium batch (EB) test.

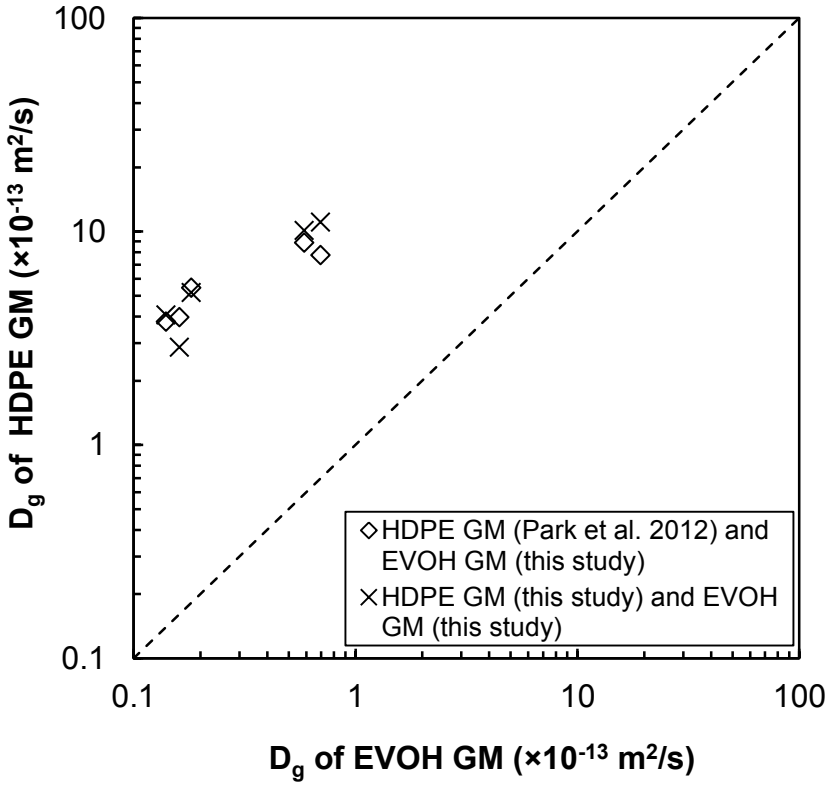

Figure 3.10 Comparison of diffusion coefficient between co-extruded GM (HDPE outer layer) obtained from MDCA test and HDPE GM obtained from kinetic batch (KB) test.

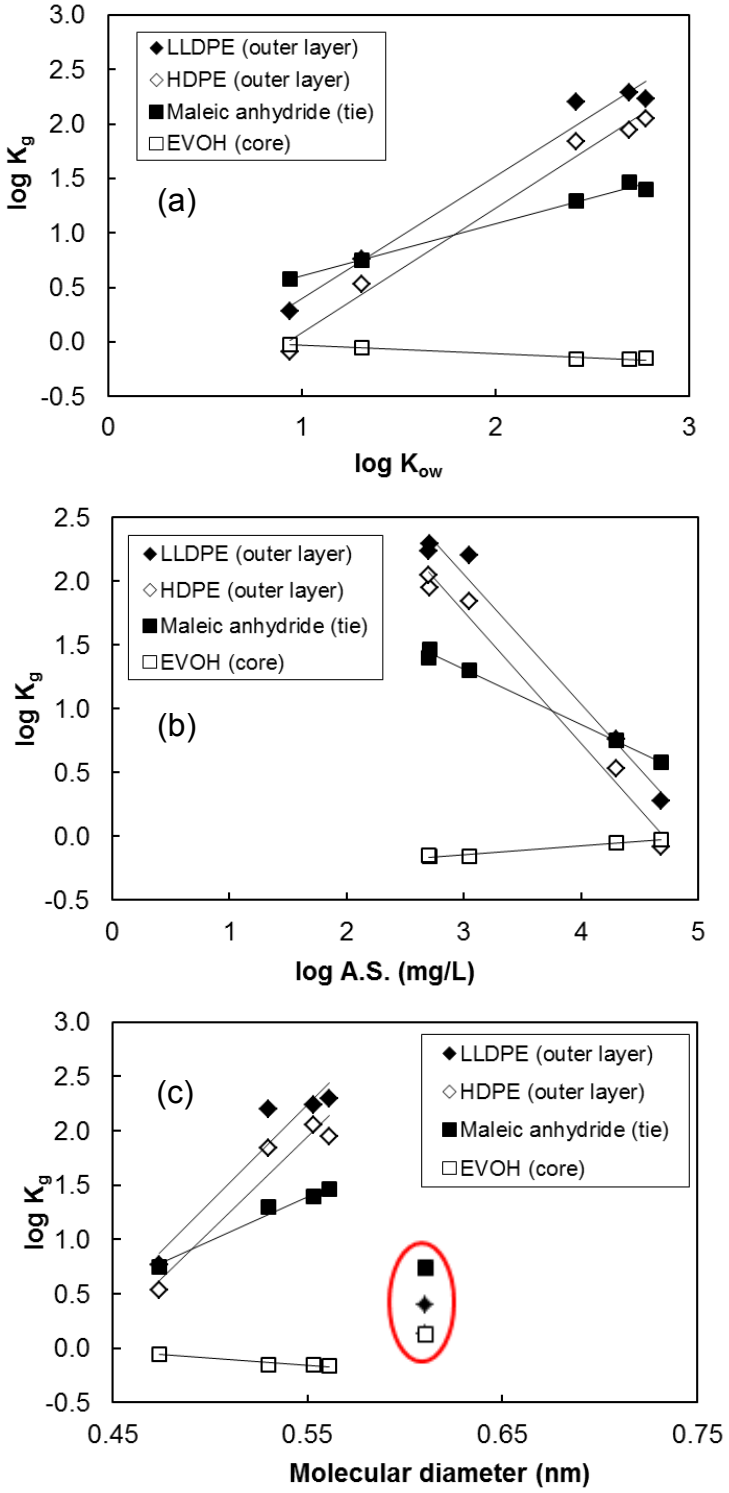

Figure 3.11 Relationship between chemical properties of VOCs and partition coefficient: (a) octanol-water partition coefficient (log·K_{ow}) vs partition coefficient (K_g); (b) aqueous solubility (A.S.) vs partition coefficient (K_g); and (c) molecular diameter (d_m) vs partition coefficient (K_g).

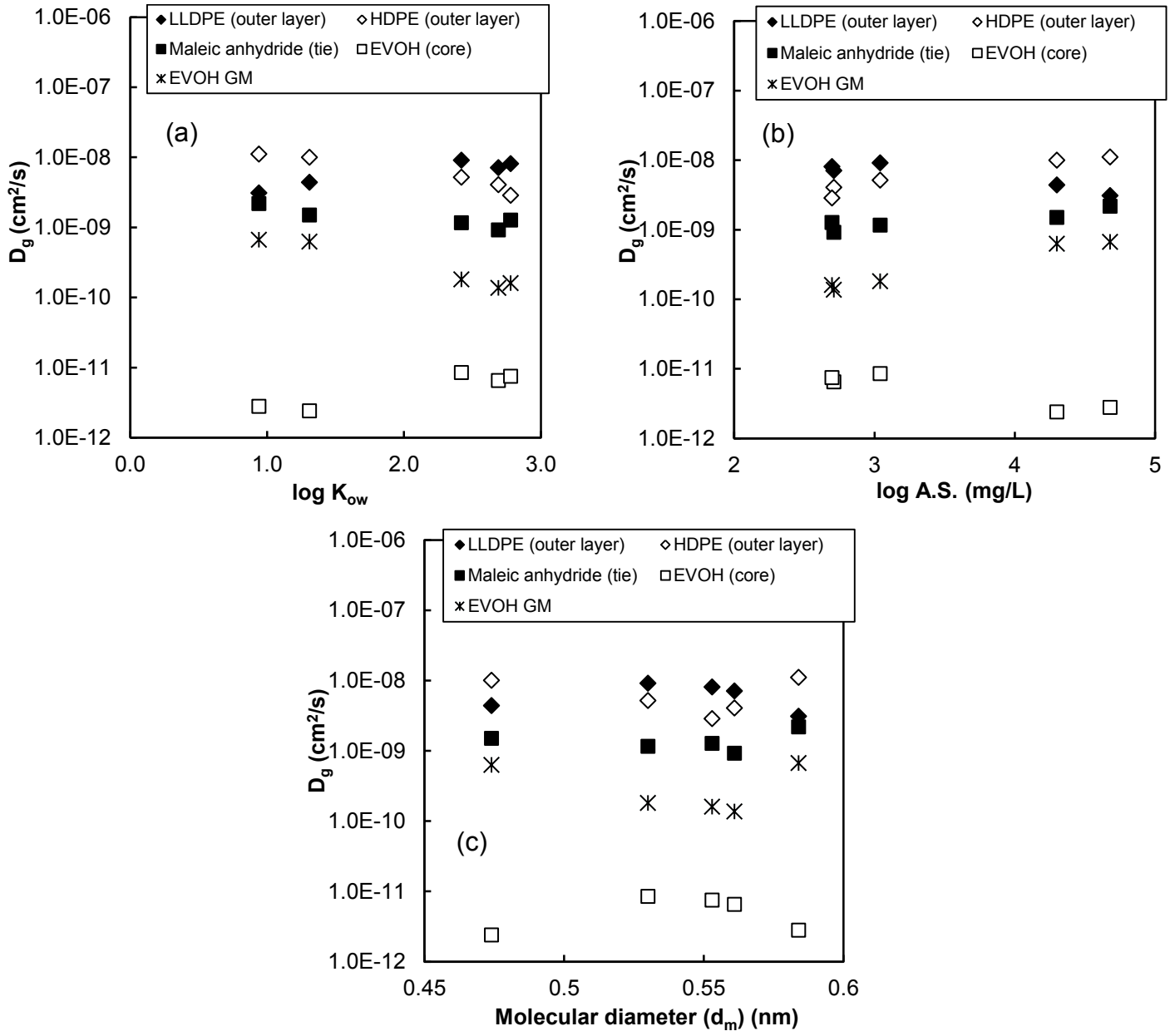

Figure 3.12 Relationship between chemical properties of VOCs and diffusion coefficient: (a) octanol-water partition coefficient (log·K_{ow}) vs diffusion coefficient (D_g); (b) aqueous solubility (A.S.) vs diffusion coefficient (D_g); and (c) molecular diameter (d_m) vs diffusion coefficient (D_g).

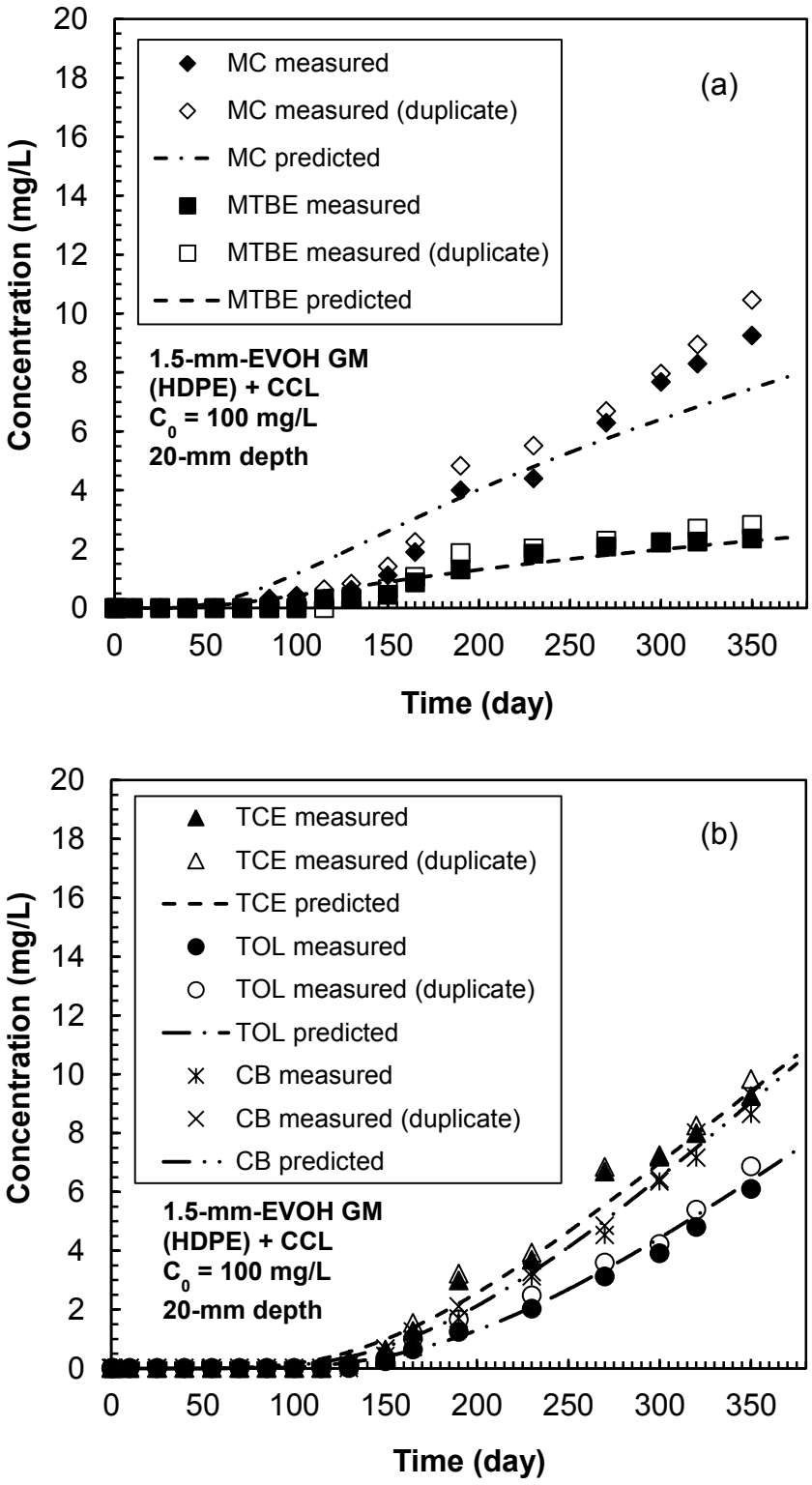

Figure 3.13 Predicted and measured concentration of VOCs: (a) MC and MTBE (polar VOCs); (b) TCE, TOL, CB (Non-polar VOCs).

Chapter 4 Methane Transport through Interim Cover with Co-Extruded Geomembrane Containing Ethylene Vinyl-Alcohol (EVOH)

4.1 ABSTRACT

During the operation of a landfill site, methane gas, which contributes to greenhouse gas emissions that may induce global warming, has been typically managed by incorporating geomembranes (GM) that are impermeable to the gas generated within the interim cover layer. This research evaluates the relative rates of transport of methane through composite interim covers that include a geosynthetic layer constructed with a co-extruded GM with a laminate of ethylene vinyl-alcohol (EVOH) in comparison to conventional, single material GMs. The co-extruded GM takes advantage of the potential of EVOH to substantially reduce the diffusion of non-polar organic compounds such as methane. A series of column tests constructed with EVOH GM, thin polyethylene (PE) GM, linear low-density polyethylene (LLDPE) GM, and polyvinyl chloride (PVC) GM in composite with different soil types such as clay, silt, and sand were conducted. Based on the experimental results, soil type minimally influenced diffusive behavior of methane through the interim cover in comparison to GM type. The LLDPE and PVC GMs produced five times more rapid breakthrough (≈ 20 d) of methane and higher flux in comparison to the EVOH GM (≈ 100 d). The order of the concentration in terms of highest flux was PE > LLDPE > PVC > EVOH. Further, the co-extruded EVOH GM had measured diffusion coefficients that were more than 170-250 times smaller compared to conventional GMs. The

diffusion coefficients for were 0.012 × 10^{-11} m^2/s for 0.76-mm co-extruded EVOH GM, 3.43 × 10^{-11} m^2/s for 0.1-mm PE GM, 2.55 × 10^{-11} m^2/s for 0.76-mm LLDPE GM, and 2.01 × 10^{-11} m^2/s for 0.76-mm PVC GM. Analytical modeling of methane migration through a composite cover indicated that the EVOH GM helps reduce the flux of methane [approximately 0.96 mL(STP) m^{-2} d^{-1}] to levels two orders of magnitude lower than the migration for the conventional GMs. Thus, co-extruded EVOH GMs acted as an effective barrier to methane migration in interim covers.

Keywords: Geomembrane; Interim cover; Diffusion; Methane; EVOH (Ethylene-vinyl alcohol); PE; LLDPE; PVC.

4.2 INTRODUCTION

In landfills, interim covers are placed over inactive sections of the landfill (i.e., areas not currently being filled) while other parts of the landfill are still in operation. Interim covers provide odor, vermin, and bird control, and also improve the appearance such that it is similar to the surrounding area when work is stopped temporarily. The most important role of the cover, however, is to control landfill gas (LFG) emissions, particularly methane and hydrogen sulfide (H_2S). A considerable amount of gas (19-40 Tg/year) is generated in global MSW landfills as organic waste decomposes (Bogner and Matthews 2003). A major portion of LFG is methane (≈ 50%), which is produced by the anaerobic degradation of organic waste and can occur for more than thirty years (Bogner and Matthews 2003; Mor et al. 2006). Methane is 20 to 30 times more potent than carbon dioxide (CO_2) as a GHG, and methane emissions substantially

contribute to global warming (Boeckx et al. 1996; Didier et al. 2000; Mackie and Cooper 2009).

There are two primary methods for managing the emission of methane from landfill sites (Aitchison 1993; Boeckx et al. 1996). One method is to recover the LFG and use it for energy production, which is generally regarded as the optimal approach. Another is to encourage methane-oxidation in the soil covering the landfill. This can be an economical and more effective option for reducing emissions in smaller and older landfills with lower amounts of methane generation compared to gas extraction, which becomes inefficient at low methane contents (Aitchison 1993; Boeckx et al. 1996). However, compacted soil in daily, intermediate, or final covers can become desiccated by the high temperatures typical of a landfill environment and thus may not provide an effective barrier to the transport of methane gas (Gebert et al. 2010).

An alternative method to handle methane emission is to incorporate a geomembrane (GM) within the interim cover layer that is impermeable to the gas generated during the performance life of the interim cover. A GM is intended to minimize gas emission through the cover; however, a cover still allows some gas emission via diffusion through the GM. Several researchers (Haxo et al. 1984; Haxo 1990; Haxo and Pierson 1991; Pierson and Barroso 2002; Stark and Choi 2005) have reported the diffusive gas permeability for GMs. Haxo et al. (1984) showed that the gas permeability of polymeric materials differs for a given generic polymer type and structure. In general, the greater the polymer crystallinity, the lower the gas permeability. Polymer crystallinity represents the

degree of structural order of a material and is specified in GMs as the percentage of the bulk volume of the material that is crystalline. Haxo et al. (1984) also showed that gas permeability varies with type of gas and temperature. Mark and Gaylord (1964) showed that the gas permeability coefficient is independent of GM thickness, assuming no pinholes in the GM, because the gas permeability coefficient is a material property for non-porous media that reflects the permeability of the GM compound. Stark and Choi (2005) investigated the methane gas transmission rate, permeance, and permeability coefficient of polyvinyl chloride (PVC), linear low-density polyethylene (LLDPE), and high-density polyethylene (HDPE) GMs by performing the standard gas transport test (ASTM D1434). The measured permeability of methane through a PVC GM was slightly less than the gas permeability through an LLDPE GM, but slightly higher than the gas permeability through an HDPE GM as in same thickness.

The study of gas transport through composite covers is limited although gas diffusion in soil and other porous media has been extensively investigated (e.g., Jellick and Schnabel 1986; Collin and Rasmuson 1987, 1988; Mackay et al. 1997). The gas transport process through a composite liner combines step-wise sequences through the GM and soil. Kim and Benson (2004) conducted numerical analyses for gas-phase advective transport, gas-phase diffusive transport, and liquid-phase advective transport in multi-layer composite (MLC) caps placed over oxygen-consuming mine waste. Results of the analyses showed that the main mechanism for oxygen transport through MLC caps is gas-phase diffusion because only diffusive flux of oxygen is allowed through a small

fraction of MLC in a steady-state condition. Gas-phase diffusive flux typically comprised at least 99% of the total oxygen flux. Based on these results, diffusive gas transport in intact composite covers can be assumed to dominate. Aubertin et al. (2000) reviewed the basic theory used to calculate diffusive gas flux and introduced an experimental procedure to evaluate the effective diffusion coefficient, D_e, which controls this flux. The experimental results obtained from a nonwoven needle-punched GCL were compared to values from the predictive model that relates D_e to porosity and degree of saturation. The results obtained from Bentofix® samples correlated well with values measured on other porous media and to those obtained from a predictive model developed for soils. The degree of saturation in the soil pores was important for the diffusive flux of gas. Based on the work by Aubertin et al. (2000), the degree of saturation is a significant factor in considering gas diffusion through a variably saturated soil medium.

An ethylene vinyl-alcohol (EVOH) film, which has the potential to substantially reduce the diffusion of methane, is proposed as a laminate inside conventional GMs to enhance cover performance. However, there are few studies that have investigated the performance of co-extruded GMs with EVOH layers as a contaminant barrier for methane. Moreover, the composite action of the cover, including soil layers, has not been considered in detail.

This study experimentally evaluates relative methane flux through various configurations of interim covers and identifies the performance of an interim cover that includes EVOH as part of the co-extruded GM. Based on the results of

diffusion testing with composite layers including a co-extruded EVOH GM, diffusion coefficients were evaluated and quantified as compared to those of PE, LLDPE, and PVC GM. Further, a numerical analysis was conducted to extend the laboratory work to various configurations of composite covers to support the feasibility of incorporating EVOH GM as a cover material.

4.3 BACKGROUND

4.3.1 Co-extruded EVOH Geomembrane

Co-extruded GMs with EVOH layers take advantage of the properties of polyethylene as a water barrier, while having the potential to substantially reduce the diffusion of organic compounds. EVOH is a random copolymer of ethylene and vinyl alcohol involving in polar oxygen–hydrogen (-OH) groups. Because the monomer mainly exists as its tautomer acetaldehyde, the copolymer is prepared by polymerization of ethylene and vinyl acetate to provide the ethylene vinyl acetate (EVA) copolymer. This is followed by hydrolysis (Armstrong 2011). EVOH copolymer is defined by the mole percentage of ethylene—lower ethylene content grades have higher barrier properties; higher ethylene content grades require lower temperatures for extrusion. Eq. (1) describes the chemical formula of EVOH:

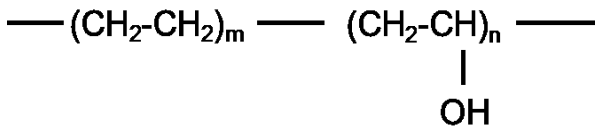

(1)

Polar EVOH has outstanding barrier properties to non-polar gases such as oxygen, nitrogen, volatile compounds, and helium (Zhang et al. 1999; Zhang et al. 2000; Byun et al. 2007; McWatters and Rowe 2010, 2011). Moreover, EVOH laminar is typically a combination of a highly ordered crystalline structure interspersed with disordered amorphous regions that show high resistance to diffusion of gas and solvent. Hence, co-extruded EVOH GM is expected to allow less migration of methane through composite covers employing the GM.

4.3.2 Mechanism of Diffusive Transport of Gas

The transport of small molecules through a non-porous GM occurs due to random molecular motion of individual molecules. The physical mechanism of gas transport includes three steps: (1) absorption of the permeating species into the GM and equilibration in the GM surface, (2) diffusion through the GM in the direction of the lower chemical potential, and (3) desorption of the permeating species from the GM surface and displacement into the ambient medium (Mark and Gaylord 1964; Pierson and Barroso 2002; Stark and Chio 2005). Molecular diffusion of a gas or vapor is similar to diffusion contaminant transport through aqueous solution. If the boundary conditions on both sides of the GM are constant, steady-state flux of a permeant can be expressed by Fick's first law as

$$J = -D_g \frac{\partial C_g}{\partial z} \tag{2}$$

where J is the diffusive flux [M/L^3], D_g is the diffusion coefficient in the GM [L^2/T],

C_g is the concentration of the diffusing substance in the GM [M/L^3], and z is the distance through the GM normal to the section [L]. Therefore, the mass flux is proportional to the concentration gradient, dc/dx, through the GM.

After a certain permeation time, steady-state is reached, which implies that concentrations remain constant at all points within the GM. Under these conditions and by introducing boundary conditions for a planar sheet, the flux may be described as (Crank 1975)

$$J = D_g \frac{(C_{g0} - C_{g1})}{L} \quad (3)$$

where C_{g0} and C_{g1} are the permeant concentrations on the upstream and the downstream side of the membrane [M/L^3], respectively, and L is the GM thickness [L]. When the ambient concentration in contact with the GM surface is known, the solute is sorbed to the GM surface according to the distribution coefficient between the penetrant and the GM surface as described by the Nernst distribution law (Park and Nibras 1993; Sangam and Rowe 2001, 2005):

$$C_g = K \cdot C_s \quad (4)$$

where C_g is the sorbed concentration to the GM at equilibrium [M/M], C_s is the ambient concentration in contact with the GM surface [M/L^3], and K is the dimensionless GM-water distribution coefficient of the solute. In a rubbery polymer, which has elastic properties, the molecular sorption of gases at low

concentration is typically described by Henry's law. In the case of transport of gases, vapor pressure p is used instead of surface concentration:

$$C_g = S \cdot p \tag{5}$$

where S is the solubility coefficient. When the solubility coefficient of a gas in a polymer is extremely low, the diffusion coefficient of that gas is considered constant (Pierson and Barroso 2002). If the diffusion coefficient is constant over the pressure range, the permeability coefficient ($P = D_g \cdot S$) can be used instead of the diffusion coefficient because the concentration of the gas within the GM is difficult to measure:

$$J = D_g \cdot S \frac{(p_0 - p_1)}{l} = P \frac{(p_0 - p_1)}{l} = P \frac{\Delta p}{l} \tag{6}$$

where P is the permeability coefficient [L^2/T], p_0 and p_1 are the gas pressures on either side of the GM [F/L^2], and Δp is an increment of pressure [F/L^2].

In the non-steady state, the gas sorbed to the GM begins transport through the GM by molecular diffusion, which represents that the variation of gas flux over a certain position is the concentration of gas in time. The diffusion in a GM is typically described using Fick's second law. The governing equation for one-dimensional (1-D) constant diffusion for gases in the GM can be represented as (Mark and Gaylord 1964; George and Thomas 2001; Pierson and Barroso 2002)

$$\frac{\partial C_g}{\partial t} = D_g \frac{\partial^2 C_g}{\partial z^2}, \qquad -L_g < z < 0 \tag{7}$$

where t is elapsed time [T], D_g is the diffusion coefficient of the gases in the GM [L^2/T], z is the distance along the direction of diffusion [L], and L_g is thickness of the GM [L]. Similar to Eq. (2), Eq. (7) is valid if the diffusion coefficient in the GM is temporally and spatially invariant (Stark and Choi 2005, Pierson and Barroso 2002).

Similar to Eq. (7), 1-D mass transport of a non-decaying solute via diffusion through a porous medium (e.g., soil) can be expressed as (Hashimoto et al. 1964; Freeze and Cherry 1979)

$$\frac{\partial C_s}{\partial t} = D_e \frac{\partial^2 C_s}{\partial z^2}, \qquad z > 0 \tag{8}$$

where C_s is the concentration of the gases in the soil liner [M/L^3], z is the distance along the direction of mass transport [L], t is elapsed time [T], and D_e is the effective diffusion coefficient [L^2/T], which can be estimated by the free diffusion coefficient (D_0) as follows (Currie 1961; Gradwell 1961; Grable and Siemer 1968):

$$D_e = D_0 \cdot \alpha \cdot (\mathrm{n_a})^{\beta} \tag{9}$$

where D_0 is the diffusion coefficient in free air [L^2/T] and η_a is the air filled porosity, which are valid for n_a ranging from 0 to 0.6 [L^3/L^3]. α and β are material properties depending on density, unit weight, and angularity of material particles (Kim and

Benson, 2004). The effective gas diffusion coefficient in soil is typically smaller than the diffusion coefficient in free air because of the tortuosity caused by soil solids and the presence of pore water. Figure 4.1 shows the relationship between diffusion coefficient ratio (D_e/D_0) and air-filled porosity from selected models. With increasing particle size, the effective diffusion coefficient increases by 25% of air-filled porosity. However, these models are generally applicable only within a narrow range of water saturation (generally for dry conditions) because the model does not consider diffusive transport through water.

4.4 MATERIALS AND METHODS

4.4.1 Methane Gas

Methane gas (CH_4) was used as the non-polar organic contaminant for a diffusion column test. Chemical and physical properties of methane are described in Table 4.1 (Schwarzenbach et al. 2003). Methane is a simple alkane and exists as a gas at standard temperature and pressure (STP). The methane tested was supplied from Air Gas Inc. and had high purity (> 99.9%). Methane concentrations were measured using a Shimadzu GC-2014 gas chromatograph (GC) equipped with an auto sampler, injector (methanizer), flame ionization detector (FID), and Restek MTX-502 stainless steel column (packed, length = 15 m, and inner diameter = 0.32 mm). To eliminate oxygen inside the fuel cell, which could damage the methanizer, the fuel cell was warmed for at least 2 h at 25 °C. Argon gas was used as a carrier gas. For the measurement of methane, temperatures of the injection port and the FID were set at 380 °C and 200 °C,

respectively. The detection limit was 1.2%.

4.4.2 Geomembranes

Four types of GMs were used for the cover material including a co-extruded EVOH GM (0.76 mm) and homogeneous polymer PE (0.1 mm), PVC (0.76 mm), and LLDPE (0.76 mm) GMs. A co-extruded GM with a 0.04-mm laminar of EVOH was used to examine the diffusive transport of methane. The co-extruded GM was produced by RAVEN Co. (South Dakoda, USA) using EVOH with 3.5% $CaCO_3$ of inert filler supplied by EVAL-Kuraray Ltd. (Texas, USA) as shown in Fig. 4.2. The 0.76-mm-thick PVC and LLDPE GMs were supplied by GSE Inc. and the 0.1-mm-thick PE sheet was supplied by Husker. General engineering properties of the GMs tested are provided in Table 4.2. In most polymer-penetrant systems, partition coefficients generally increase with an increase in similarity between the components, according to “likes dissolves likes” (August and Taztky 1984; Sangam and Rowe 2001). The GMs tested were custom cut with a milling machine for installation into the testing column.

4.4.3 Cover Soils

Three types of soils (clay, silt, and sand) were used as cover material for the column testing because these soils have been commonly used for constructing liners at Dane County Landfill in Madison, Wisconsin. The effect of soil type on methane transport was investigated. The clay, silt, and sand have been extensively characterized (Bareither et al. 2008, Park et al. 2012). The

water content in the soil was air dry (less than 3% w/w) to simulate typical worst-case field conditions for a soil cover. The properties of the soils are presented in Table 4.3.

4.4.4 Diffusion Column Tests

The column-type diffusion experiments consisted of soil underlain by three types of GMs (a co-extruded EVOH GM and LDPE, LLDPE and PVC GMs). The column for EVOH GMs was replicated. The experimental setup of bench-scale composite liner column is shown in Fig. 4.3(a). The column (20-cm height, 15.5-cm diameter) was constructed with aluminum. The testing column was divided into upper and lower compartments, and the tested GM was placed at the joint of the compartments. In the joints [Fig. 4.3(b)], two polytetrafluoroethylene (PTFE) rectangular gaskets were installed on the top and bottom of the GM to minimize the adsorption of methane solute and/or loss of methane through the joint. Methane gas was allowed to migrate from the bottom to the top of the column. The methane, which was controlled by a pressure regulator, stayed in the bottom chamber of the column and was the contaminant source. Methane gas in the bottom chamber was supplied at 10 kPa to simulate conditions existing within a waste mass prior to installation of an active gas management system (Czepiela et al. 2003; Benson et al. 2012). Sampling ports were installed in the influent and effluent reservoirs. These ports were designed to collect gas, and two septa were used to eliminate leakage during sampling. To maintain a constant concentration of methane in the bottom reservoir, the concentration was checked periodically

from the bottom sampling port. In the top plate, there were two sampling ports—one for extraction of samples from the upper chamber and the other for injecting gas to keep the pressure balance equal during extraction of samples. Methane concentrations were monitored at regular intervals in the lower and upper reservoirs to evaluate the methane concentration through the cover profile.

Methane that passed through the cover in the diffusion column test was mixed in the upper reservoir of the column to keep measured concentrations constant regardless of the sampling placement. Two stirrers made of aluminum and magnetic discs were located on the top plate to mix the methane gas in the upper chamber. Testing columns were set up in an air-circulated hood, where the temperature is consistent at 23 °C ± 0.5 °C. The varying arrangements of the diffusion column tests are described in Table 4.4.

4.5 ANALYSIS OF DIFFUSION COLUMN TEST

4.5.1 Comparison of Methane Concentration through Soil Cover

Transported methane was extracted with time via the upper sampling ports in the testing column. Concentrations measured in the upper reservoir in the cover experiments are shown in Figure 4.4. Within approximately 1 h, significant breakthrough of methane concentration (> 1.2%, the detection limit) was found in the columns that included soil-only covers. With increasing time, the concentration of methane in the top reservoir for the silica sand cap increased more rapidly compared to those with clay or silt. For example, the concentration for sand approached more than 80% (C/C_0) at about 8 h, while the concentration

for silt and clay approached the same concentration in 18 h. Due to varied tortuosity of the soils, the migration rates were different. The migration rate for sand was faster than those for clay and silt because the tortuosities of clay and silt are higher than that of sand. Typically, the apparent tortuosity factor (τ_a) of clay ranging from 0.05 to 0.20 is smaller than uniform sand ranging from 0.2 to 0.35, which means higher tortuosity. The tortuosity can vary depending upon water content (Shackelford and Daniel 1991; Park et al. 2012; Lake and Rowe 2005). The difference of tortuosity associated with soil type might be a significant factor that influences the rate of diffusive transport of methane through soil covers. To reach an effluent concentration of methane in the upper reservoir identical to the supplied concentration in the bottom chamber of the test column, it will take more than twice the amount of time as it took to reach 80% of the source concentration. This is the reason to choose 80% (C/C_0) for comparison of the relative concentration. Regardless of soil type, the migration of methane through soil-only covers broke through within a couple of hours.

4.5.2 Comparison of Methane Concentration through Composite Cover with EVOH, PE, LLDPE and PVC GM over Soils

Similar to measurement of methane through soil cover, measured concentrations of methane through composite covers employing soil with GM at the upper sampling ports in the testing column were extracted with increasing time periodically. Concentrations measured at the upper reservoir in the cover experiment are shown in Figure 4.3 (a).

As discussed previously, the breakthrough point of soil-only covers occurred in a couple of hours. However, in composite covers, the breakthrough points were delayed at least 50 times further. Within approximately 4 d, significant concentrations of methane (> detection limits, normally 1.2%) were found in the column tests employing soils with the PE GM. The breakthrough point for the LLDPE and PVC GMs occurred at approximately 18 d. Starkly contrasting, the breakthrough of methane for the EVOH GM occurred at approximately 100 d, regardless of underlying soil type. Therefore, the effect of the soil layer can be neglected because the time to breakthrough in this composite cover employing EVOH GM was significantly longer than in the soil-only covers. For example, regardless of soil type, the migration of methane through soil cover only broke through within hours (< 2 h) and reached the supplying concentration within days (< 3 d), which was relatively faster than covers employing soil with GM, as shown in Fig. 4.5.

With increasing time, the concentration of methane transported through the composite cover with the 0.1-mm-thick PE increased more rapidly as compared to all other composite GMs. For example, the concentration of methane in the upper chamber of the column with the PE GM approached 80% C/C_o around 40 d, while the concentration transported through the cover employing the EVOH GM was still lower than detection limits at this time. The order of the concentration in terms of highest flux was PE > LLDPE > PVC > EVOH. The methane flux through the PVC composite was slightly smaller than that of the LLDPE composite. The PVC should have higher transport of methane

than LLDPE due to lower crystallinity of the PVC than LLDPE, but the actual difference of the concentration between PVC and LLDPE was not significantly different. This is due to chloride group of PVC imposing polarity (Wypych 2008). The polarity of the chloride group in PVC might impede the transport of methane through PVC GM. Methane flux and breakthrough time for the EVOH GM was the least among all composite GMs tested. Therefore, based on diffusion column testing, EVOH GM acted as an effective barrier to methane migration in interim covers.

4.6 MODLEING OF METHANE TRANSPORT THROUGH COMPOSITE COVER

4.6.1 Analytical Modeling of Methane Transport

To evaluate experimental data from diffusion column testing, analytical modeling employing the finite difference method (FDM) was conducted with transport parameters from the literature. Contaminant transport was modeled by using analytical methods [Eq. (7) to Eq. (9)] developed in EXCEL spreadsheets. Discretization was conducted according to the Crank-Nicholson method for 1-D contaminant transport via diffusion (Foose et al. 2001; Foose et al. 2002; Eun et al. 2014). The continuity of concentration and conservation of mass equation was applied at the interface between the GM and the soil as (Foose et al. 2002; Park et al. 2012)

$$J = D_g \frac{\partial C_g}{\partial z} = D_e \frac{\partial C_s}{\partial z}, \qquad z = 0 \qquad (12)$$

where D_e is the effective diffusion coefficient and C_s is the concentration of methane in the soil.

A 6-cm-thick soil layer (variably clay, silt, or sand) in the diffusion column test was modeled. The bottom boundary for the methane source was set as a constant concentration (= 32%) boundary. The top reservoir is briefly opened to attain atmospheric conditions and then is closed as a free diffusion boundary. In this case, no natural attenuation of methane in the soil layer is assumed. Figure 4.1 shows the dependency of effective diffusion coefficient on air-filled porosity according to various types of soils. For each soil layer, various effective diffusion coefficients for the methane were used based on the assumption of different air-filled porosity associated with soil type (Currie 1961; Gradwell 1961; Grable and Siemer 1968). The ratio of effective diffusion coefficient over the free diffusion coefficient for sand ranged from 0.04 to 0.18 in the dry condition.

4.6.2 Modeling Verification

The migration of methane through soil-only covers as measured from the diffusion column tests was compared to analytical predictions using effective diffusion coefficients obtained from literature (Currie 1961; Gradwell 1961; Grable and Siemer 1968). The input parameters for the modeling effort are shown in Table 4.5 and model results are shown in Figure 4.6. Good agreement between measured and predicted methane concentrations for different soils types was achieved. For instance, the upper-chamber concentrations of methane for the sand-only column increased more rapidly in comparison to those for the clay-only

column and with the analytical prediction. Therefore, the model was deemed reliable for simulating methane transport through soil-only covers.

4.6.3 Comparison of Diffusion Coefficient for GMs

Diffusion coefficients for various types of GMs including co-extruded EVOH, PE, LLDPE, and PVC were independently estimated from experimental data obtained from the diffusion column tests containing composite covers. The coefficients were estimated by back-calculating and fitting the temporal concentration data simultaneously with the 1-D FDM model. Nonlinear least-squares regression was used to obtain the best-fit for Eqs. (7) to (9) (Eun et al. 2014; Park et al. 2012). For the co-extruded EVOH GM, the GM with sand was used to estimate the diffusion coefficient because the effect of soils can be neglected based on the comparison of methane migration between only soil layer and composite cover. The time to breakthrough or reach steady-state of methane concentration for soil cover is significantly faster by more than a couple of order magnitude to be compared to composite cover with GM. The diffusion coefficients were estimated as 0.012×10^{-11} m^2/s for the co-extruded EVOH GM, 3.43×10^{-11} m^2/s for the 0.1-mm PE GM, 2.55×10^{-11} m^2/s for the 0.76-mm LLDPE GM, and 2.01×10^{-11} m^2/s for the 0.76-mm PVC GM.

In the composite GM covers, use of the estimated diffusion coefficients in the analytical modeling resulted in good agreement with the measured methane flux from the diffusion column tests (see Fig. 4.7). Also, the orders of magnitude for the diffusion coefficients for GMs were identical to those for methane flux measured by (Stark and Choi 2005). With a higher diffusion coefficient, a more

rapid, higher flux occurs. Estimated diffusion coefficients of methane for the four types of GMs are compared to experimental results in Fig. 4.8. Co-extruded EVOH GM had a measured diffusion coefficient that was two orders of magnitude smaller compared to the other GMs. Based on the permeability coefficients, a co-extruded EVOH GM would be an effective barrier for significant reduction of methane migration through composite covers.

Diffusion coefficients for selected GMs including PE, LLDPE and PVC obtained from the diffusion column test were compared to existing data from the literature (Michaels and Bixler 1961; USEPA 1998; Lin and Freeman 2004; Tremblay et al. 2006). In the GMs, the estimated diffusion coefficients are in agreement with the methane migration demonstrated in the diffusion column tests. The estimated coefficients for the three soils are summarized in Table 4.6. Based on a paired F-test, the values are not statistically different from those in literature (correlation F value = 1.25 > 1 and p = 0.47 > 0.05). Therefore, the modeling provided reliable results for investigating methane transport.

4.7 METHANE FLUX THROUGH COMPOSITE COVERS

To investigate the relative reduction in flux of methane that can be achieved with EVOH GM under field conditions, analytical modeling employing the FDM was conducted via Eqs. (2) to (6), and the flux through a representative thickness of an interim cover in a landfill were predicted at steady state. Figure 4.9 presents an example of the predicted variation of the flux with time for different cover systems. The four configurations for the interim composite covers

were 0.3 m of silty soil, 0.3 m of silty soil with 0.76-mm-LLDPE GM, 0.3 m of silty soil with 0.76-mm-PVC GM, and 0.3 m of silty soil with 0.76-mm-EVOH GM. Additionally, the flux obtained by Stark and Choi (2005) was compared to the prediction from this study. The flux through conventional GMs including PE, LLDPE, and PVC predicted by this study and that measured by Stark and Choi (2005) was similar and ranged between 200 and 400 [mL(STP) m^{-2} d^{-1}] regardless of GM. The transient period to reach steady-state of the flux lasted for approximately one month for the conventional GMs. However, the transient period of the flux lasted for approximately four months for the EVOH GM. The interim cover with the conventional GM layer allowed more than two orders of magnitude higher fluxes through the cover than for the cases where EVOH GMs were used. For example, the flux of methane through the PE GM ranged from approximately 305 [mL(STP) m^{-2} d^{-1}]. However, the flux of methane through the EVOH GM ranged from approximately 0.96 [mL(STP) m^{-2} d^{-1}]. Based on this comparison, the cover employing the EVOH GM showed much better performance in mitigating the migration of methane.

The fact that the EVOH layer has a notable effect while being so thin (0.05 mm) has several important practical implications. First, the performance of the co-extruded GM could be further improved by adopting procedures that increased the thickness of the EVOH layer. Second, care is needed if specifying the permeation characteristics required or the thickness of the EVOH layer (since a thickness less than that of the GM tested herein could result in properties that do not meet the design requirements). Third, further research is required to

assess how well the EVOH GM stands up to field use (e.g., scratching during installation). The effect of temperature on migration of methane also needs to be considered. A field trial using the EVOH GM is recommended for evaluation of short- and long-term performance.

4.8 CONCLUSIONS

This research effort experimentally evaluated and compared the relative rates of transport of methane through interim covers constructed with co-extruded GMs that contain a layer of EVOH in comparison to conventional GM including PE, LLDPE, and PVC. Based on the experimental results from these diffusion column tests employing composite covers, soil type minimally influenced the diffusive behavior of methane through the interim soil cover in comparison to the GM component. Conventional GMs (PE, LLDPE, and PVC) allowed more rapid and higher fluxes of methane through composite covers than that containing a co-extruded GM with EVOH. According to the diffusion coefficient estimated from the column test, LLDPE and PVC GM produced five times more rapid breakthrough and a couple of magnitude higher VOC flux in comparison to the EVOH GM, even though they are of identical thicknesses (0.76 mm). Further, the co-extruded EVOH GM had measured diffusion coefficients that were more than 170-250 times smaller in comparison to conventional GMs. The diffusion coefficients were estimated as 0.012×10^{-11} m^2/s for the co-extruded EVOH GM, 3.43×10^{-11} m^2/s for the 0.1-mm PE GM, 2.55×10^{-11} m^2/s for the 0.76-mm LLDPE GM, and 2.01×10^{-11} m^2/s for the 0.76-

mm PVC GM. In the conventional GMs, the magnitude of the estimated diffusion coefficient was in good agreement with those from methane migration experiments detailed in the literature. Modeling of methane migration through a composite cover at field scale indicated that the EVOH GM helps reduce the flux of methane [approximately 0.96 mL(STP) m^{-2} d^{-1}] to levels that are two orders of magnitude lower than the migration given by the conventional GMs. Thus, co-extruded EVOH GMs acted as an effective barrier to methane migration in the configurations evaluated.

4.9 ACKNOWLEDGMENTS

The authors appreciate the support of Kuraray CO., Ltd. The opinion, findings and conclusions expressed herein do not represent the views of Kuraray CO., Ltd.

4.10 REFERENCES

Aitchison, E. (1993). “Options for reducing-methane emission from landfill sites.” In Methane and Nitrous Oxide: Methods in National Emissions Inventories and Options for Control (A. R. van Amstel, Ed.), pp. Z-230. *International IPCC Workshop, 1993*. Amersfoort, the Netherlands.

Armstrong R. B. (2011). “Improving performance of geosynthetics for containment of volatile organic compounds through the use of ethylene vinyl alcohol (EVOH).” *Geo-Frontier 2011,* ASCE, Florida.

ASTM (2003). “Standard test method for determining gas permeability characteristics of plastic film and sheeting.” *D1434*. West Conshohocken, PA: American Society for Testing and Materials.

Aubertin, M., Aachib, M., and Authier, K. (2000). “Evaluation of diffusive gas flux through covers with a GCL.” *Geotextiles and Geomembranes*, 18 (2-4), 215-233.

August, H., and Taztky, R. (1984). “Permeability of commercial available polymeric liners for hazardous landfill leachate organic constituents.” *International Conference on Geomembrane*, Denver, USA, 151-156.

Bareither, C. Edil, T. B., Benson, C. H., and Mickelson, D. M. (2008). “Geological and physical factors affecting the friction angle of compacted sands.” *Journal of Geotechnical and Geoenvironmental Engineering*, 134(10), 1476-1489.

Benson, C. H., Edil, T. B., and Wang, X. (2012). “Evaluation of a final cover slide at a landfill with recirculating leachate.” *Geotextiles and Geomembranes*,

35 (11-12), 100-106.

Boeckx P., Van Cleemput O., and Villaralvo I. (1996). “Methane emission from a landfill and the methane oxidation capacity of its covering soil.” *Soil Biology and Biochemistry*, 28 (10-11), 1397-1405.

Bogner, J. and Matthews, E. (2003) “Global methane emissions from landfills: new methodology and annual estimates 1980–1996.” *Global Biogeochemistry Cycles*, 17, 1065-1078.

Byun, Y. J., Hong, S. I., Kim, K. B., Jeon, D. H., Kim, J. M., Whiteside, W.S., and Park H. J. (2007). “Physical and chemical properties of γ-irradiated EVOH film.” *Radiation Physics and Chemistry*, 76 (6), 974-981.

Collin, M. (1987). “Mathematical modeling of water and oxygen transport in layered soil covers for deposits of pyritic mine tailings.” Licenciate Treatise. Royal Institute of Technology. Department of Chemical Engineering. S-100 44 Stockholm, Sweden.

Collin, M., and Rasmuson, A. (1988). “Gas diffusivity models for unsaturated porous media.” *Soil Science Society of America Journal*, 52, 1559-1565.

Crank, J. (1975). The mathematics of diffusion, 2nd Ed., Clarendon, Oxford, United Kingdom, 11-24.

Currie, J. A. (1961). “Gaseous diffusion in porous media: part 3. wet granular materials.” *British Journal of Applied Physics*, 12, 275-281.

Czepiela, P. M., Shorter, J. H., Moshera, B., Allwine, E., McManus, J. B., Harriss, R. C., Kolb, C. E., and Lamb, B. K. (2003). “The influence of atmospheric pressure on landfill methane emissions.” *Water Management*, 23 (7),

593-598.

Didier, G., Bouazza, A., and Cazaus, D. (2000). “Gas permeability of geosynthetic clay liner.” *Geotextiles and Geomembranes*, 18 (2-4), 235-250.

Eun, J., Tinjum, J. M., Benson, C. H., and Edil, T. B. (2014). “Transport parameters of volatile organic compounds through co-extruded geomembrane containing ethylene vinyl-alcohol.” Submitted to *Journal of Geotechnical and Geoenvironmental Engineering.*

Foose, G. J., Benson, C. H., and Edil, T. B. (2001). “Analytical equations for predicting concentration and mass flux from composite liners.” *Geosynthetics International*, 8 (6), 551-575.

Foose, G. J., Benson, C. H., and Edil, T. B. (2002). “Comparison of Solute Transport in three composite liners.” *Journal of Geotechnical and Geoenvironmental Engineering,* 128 (5), 1-13.

Freeze, R. A., and Cherry, J. A. (1979). Ground water. Prentice-Hall, Englewood Cliffs, New Jersey.

Gebert, J., Groengroeft, A., and Pfeiffer, E. (2010). “Relevance of soil physical properties for the microbial oxidation of methane in landfill covers.” *Soil Biology and Biochemistry,* 43 (9), 1759-1767.

George, S.C. and Thomas, S. (2001). “Transport phenomena through polymeric systems.” *Progress in Polymer Science,* 26, 985-1017.

Grabel, A. R. and Siemer, E. G. (1968). “Effects of bluk density, aggregate size, and soil water suction on oxygen diffusion, redox potentials, and

elongation of corn roots." *Soil Science Society of America, Proceeding*, 32, 180- 186.

Gradwell, M. W. (1961). "A laboratory study of the diffusion of oxygen through pasture topsoils." *New Zealand Journal of Science*, 4, 250-270.

Hashimoto, I., Deshpande, K. B., and Thomas, H. C. (1964). "Peclet numbers and retardation factors for ion exchange columns." *Industrial and Engineering Chemistry Fundamentals*, 3 (3), 213-218.

Haxo, H. E. and Lahey, T. P. (1988). "Transport of dissolved organics from dilute aqueous solutions through flexible membrane liners." *Hazardous Waste and Hazardous Materials*, 5 (4), 275-294. 21.

Haxo, H. E. (1990). "Determining the transport through geomembranes of various permeants in different applications." *In Geosynthetic Testing for Waste Containment Applications* (ed. R. M. Koerner), *STP 1081*, 75–94. West Conshohocken, PA: American Society for Testing and Materials.

Haxo, H. E. and Pierson, P. (1991). "Permeability testing." In Geomembranes Identification and Performance Testing (eds A. Rolling and J-M. Rigo), RILEM Report 4, 219-240. RILEM.

Haxo, H. E., Miedema, J. A., and Nelson, N. A. (1984). "Permeability of polymeric membrane lining materials." *Proceedings of the International Conference on Geomembrane*, Denver, CO, 151-156.

Jellick, G. J., and Schnabel, R. R. (1986). "Evaluation of a field method for determining the gas diffusion coefficient in soils." *Soil Science Society of America Journal*, 50, 18-23.

Kim, H. and Benson, C. H. (2004). “Contribution of advective and diffusive oxygen transport through multilayer composite caps over mine waste.” *Journal of Contaminant Hydrology*, 71, 193-218.

Lake, C. B., and Rowe, R. K. (2005). “A comparative assessment of volatile organic compound (VOC) sorption to various types of potential GCL bentonites.” *Geotextiles and Geomembranes,* 23 (4), 323–347.

Lin, H. and Freeman, B.D. (2004). “Gas solubility, diffusivity and permeability in poly (ethylene oxide)” *Journal of Membrane Science*, 239,105-117.

Machaels, A. S. and Bixler, H. J. (1961). “Flow of gases through polyethylene.” *Journal of Polymer Science*, 50, 413-439.

Mackay, P. L., Yanful, E. K., and Rowe, R. K. (1997). “Diffusion coefficients of oxygen through unsaturated soils.” Preprint. 50th *Canadian Geotechnical Conference*. Ottawa 2, 649-656.

Mackie, K. R. and Cooper, C. D. (2009). “Landfill gas emission prediction using Voronoi diagrams and importance sampling.” *Environmental Modeling and Software*, 24, 1223-1232.

Mark, H. F. and Gaylord, N. G. (1964). “Encyclopedia of polymer and technology: Plastics, Resins, Rubbers, Fibers.” New York: Interscience Publishers.

McWatters, R. S. and Rowe, R. K. (2010). “Diffusive transport of VOCs through LLDPE and Two coextruded geomembrane” *Journal of Geotechnical and Geoenvironmental Engineering*, 136 (9), 1167-1177.

McWatters, R. S. and Rowe, R. K. (2011). “Sorption and diffusion of BTEX through thin-film EVOH.” *Geo-Frontiers 2011* ASCE, 2073-2083.

Mor, S., Ravindra, K., De Visscher, A., Dahiya, R. P., and Chandra, A. (2006). "Municipal solid waste characterization and its assessment for potential methane generation: A case study." *Science of the Total Environment*, 371 (1–3), 11–10.

Park, J. K. and Nibras, M. (1993). "Mass flux of organic chemicals through polyethylene geomembranes." *Water Environmental Research*, 65 (3), 227-237.

Park, M. G., Edil T. B., and Benson, C. H. (2012). "Modeling volatile organic compound transport in composite liners." *Journal of Geotechnical and Geoenvironmental Engineering*, 138(6), 641-657.

Pierson, P. and Barroso, M. (2002). "A pouch test for characterizing gas permeability of geomembranes." *Geosynthetics International*, 9 (4), 345-372.

Sangam, H. P. and Rowe, R. K. (2001). "Migration of dilute aqueous organic pollutants through HDPE geomembranes." *Geotextiles and Geomembranes*, 19, 329-357.

Sangam, H. and Rowe, R. (2005). "Effect of surface fluorination on diffusion through a high density polyethylene geomembrane." *Journal of Geotechnical and Geoenvironmental Engineering*, 131 (6), 694-704.

Schwarzenbach, R. P., Gschwend, P.M., and Imboden, D.M. (2003). Environmental organic chemistry. Second edition. Wiley-Interscience, NJ.

Shackelford, C. D. and Daniel, D. E. (1991). "Diffusion in saturated soil I: Background." *Journal of Geotechnical Engineering*, 7 (3), 467-484.

Stark, T. D. and Choi, H. (2005). “Methane gas migration through geomembranes.” *Geosynthetics International*, 12 (1), 1-6.

Trembaly, P., Savard M.M., Vermette, J., and Paquin R. (2006). “Gas permeability, diffusivity and solubility of nitrogen, helium, methane, carbon dioxide and formaldehyde in dense polymeric membranes using a new on-line permeation apparatus.” *Journal of Membrane Science*, 282, 245-256.

US EPA. (1998). “Greenhouse gas emissions from the management of selected materials. (EPA publication no. EPA530-R-98-013.) Washington, DC: U.S. Environmental Protection Agency.

Wypych, G. (2008) “PVC degradation and stabilization.” ChemTec; First edition.

Zhang, Z., Britt, I. J., and Tung, M. A. (1999). “Water absorption in EVOH films and its influence on glass transition temperature.” *Journal of Polymer Science, Part B. Polymer Physics*, 37, 691–699.

Zhang, Q., Lin, W., Chen, Q., and Yang, G. (2000). “Phase structure of EVOH copolymers as revealed by variable temperature solid state high resolution.” 13C NMR spectroscopy. *Macromolecules*. 33, 8904-8906.

4.11 TABLES

Table 4.1 Properties of methane

Compound	Methane
Chemical formula	CH_4
Type of compound	Alkane
Molecular weight (g/mol)	16.04
Specific volume (kg/m^3)	1.51
Specific gravity (m^3/kg)	0.554
Density of liquid (1 atm) (kg/m^3)	421
Gas constant R (J/kg°C)	518
Melting point (1 atm) (°C)	-182.6
Boiling point (760 mm Hg) (°C)	-161.7

Table 4.2 General engineering properties of the GMs tested

Property	Method	unit	PE	LLDPE	PVC	Co-extruded EVOH
Thickness	ASTM D 5944	mm	0.1	0.76	0.76	0.76
Puncture resistance	ASTM D 4833	N	40	280	270	280
Tear resistance	ASTM D 1004	N	11 × 11	50 × 50	28 × 28	56 × 68
Load at break	ASTM D 6693	N	600	8300	7800	8500
Elongation at break	ASTM D 6693	%	145	500	450	550
Tensile strength	ASTM D 6693	kN/m	0.38	14.5	13.1	15.2

Table 4.3 Properties of cover soils

Transport parameter	Unit	Sand	Silt	Clay
G_s	-	2.65	2.72	2.7
γ_{dmax}	kN/m^3	18.2	19.4	17.8
ω_{opt}	%	3	10.5	18.3
LL (%)	%	-	18	48
PL (%)	%	-	-	27
USCS Symbol	-	SP	ML	CL
D_{50}	mm	0.55	0.01	-
C_u	-	2.2	15.0	-
C_c	-	0.9	6.7	-

Table 4.4 Experimental cases of diffusion column test

Liner Materials	Number of Experiment	Cover Configuration
EVOH (0.76 mm) + Sand	2 (Duplicate)	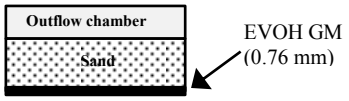
PE (0.10 mm) + Sand	1	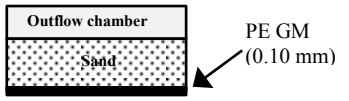
LLDPE (0.76 mm) + Sand	1	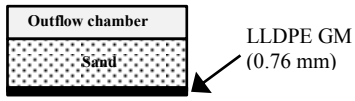
PVC (0.76 mm) + Sand	1	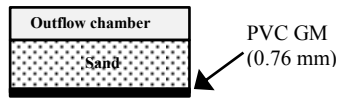
EVOH (0.76 mm) + Silt	1	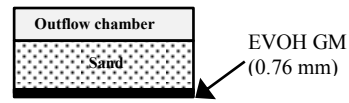
EVOH (0.76 mm) + Clay	1	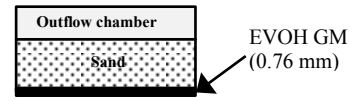
No GM + Sand	2 (Duplicate)	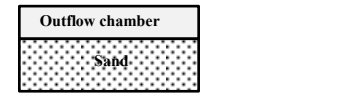
No GM + Silt	1	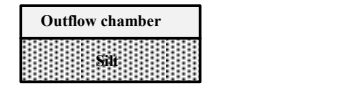
No GM + Clay	1	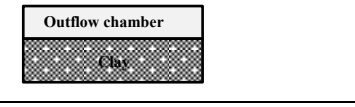
Aluminum plate + Sand	1	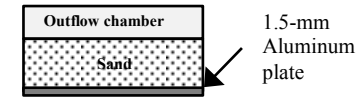

Table 4.5 Input parameters to model diffusion column test

Type	Free diffusion coefficient (D_0) ($\times 10^{-4}$ m^2/s) (Stark and Choi 2005)	Air-filled porosity (η_a)	Effective diffusion coefficient (D_e) ($\times 10^{-4}$ m^2/s)
Clay	0.2	0.16	0.0146
Silt		0.18	0.0063
Sand		0.22	0.0033

Table 4.6 Diffusion coefficients between estimated and measured for the GMs

Type	Effective diffusion coefficient (D_e) from analytical solution ($\times 10^{-11}$ m^2/s)	Diffusion coefficient (D_e) from literature ($\times 10^{-11}$ m^2/s)	Literature	Paired F-test
PE	3.43	3.20	Lin and Freeman (2004)	F = 1.26; p = 0.47 > 0.05
LLDPE	2.55	1.93 - 2.52	Michaels and Bixler (1961); Tremblay et al. (2006)	
PVC	2.01	2.70	US EPA (1998)	

4.12 FIGURES

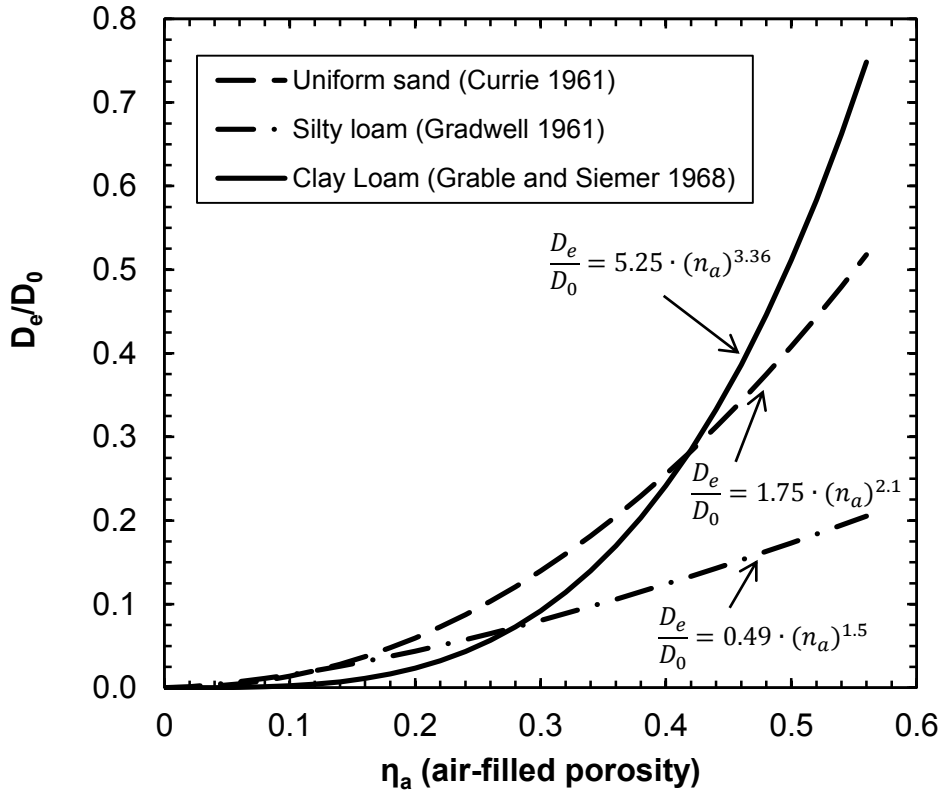

Figure 4.1 Relationship between ratio of effective diffusion coefficient over free diffusion coefficient and air-filled porosity.

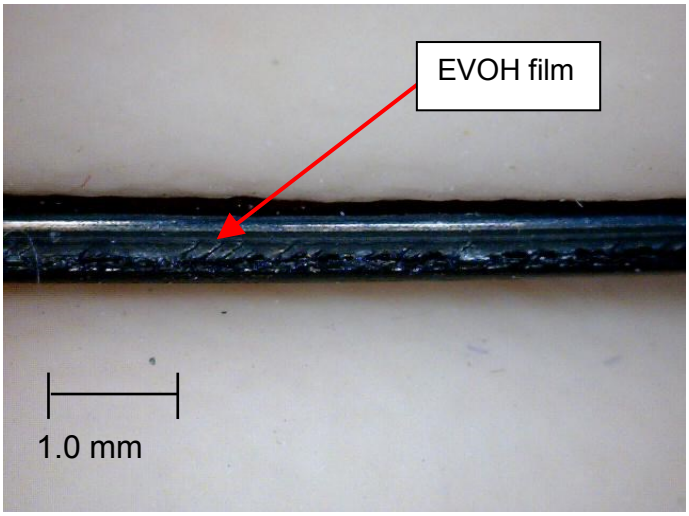

Figure 4.2 Co-extruded EVOH GM (0.76 mm).

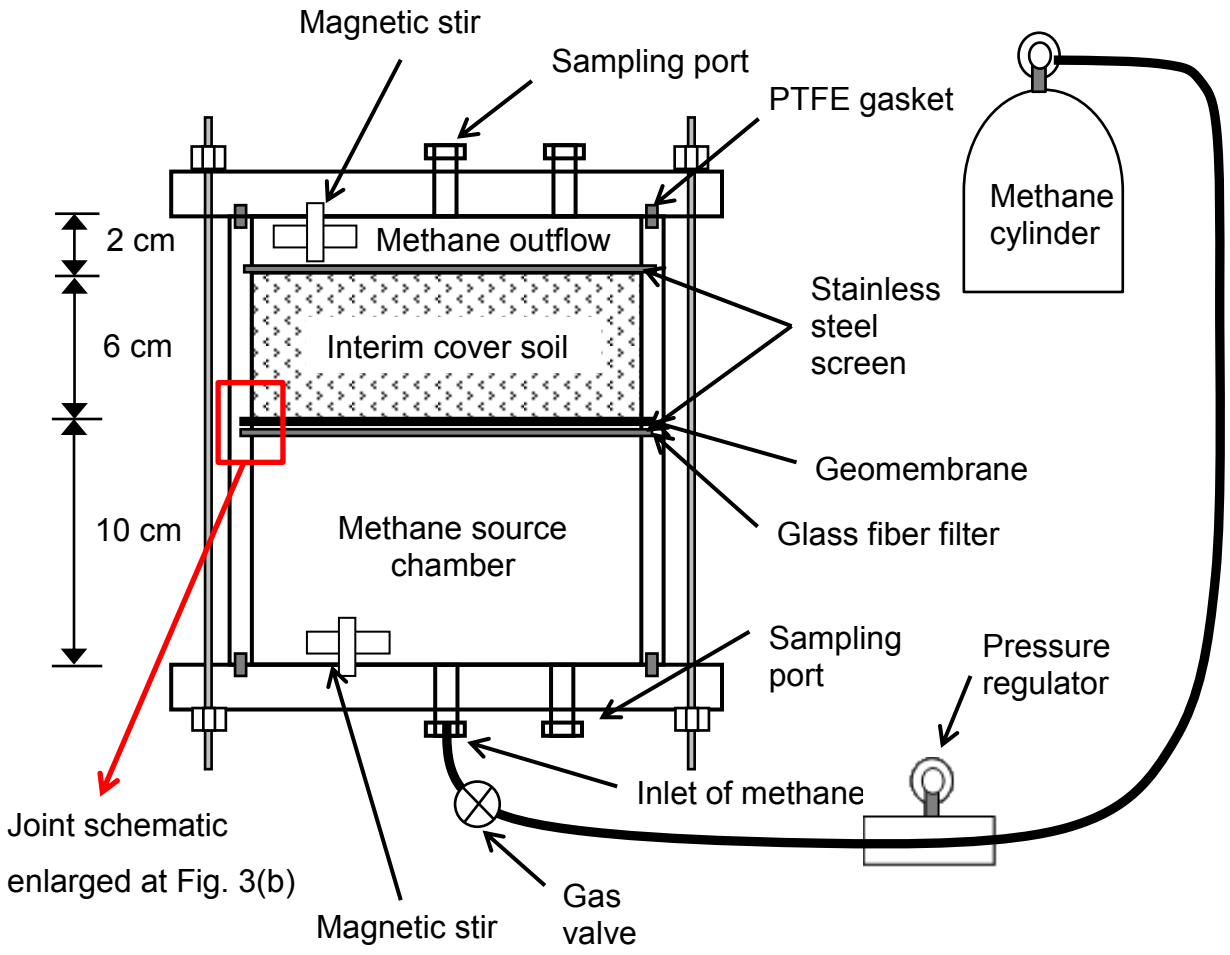

(a) column apparatus

Figure 4.3 Bench-scale experimental setup for methane diffusion testing: (a) column apparatus; (b) joint of upper and bottom compartment (continued)

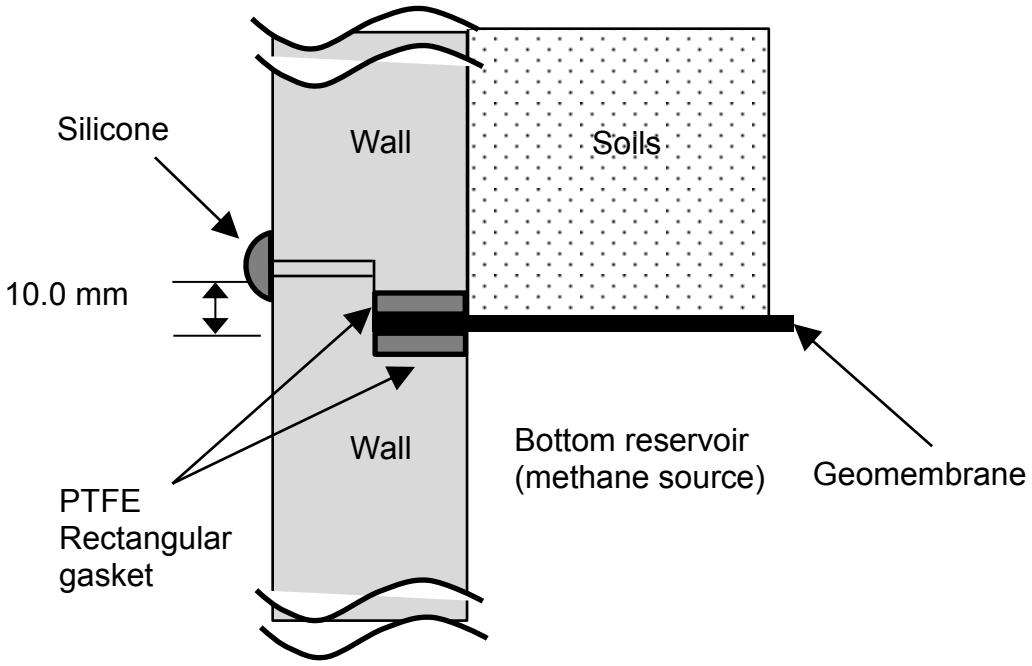

(b) Joint of upper and bottom compartment.

Figure 4.3 Bench-scale experimental setup for methane diffusion testing: (a) column apparatus; (b) joint of upper and bottom compartment.

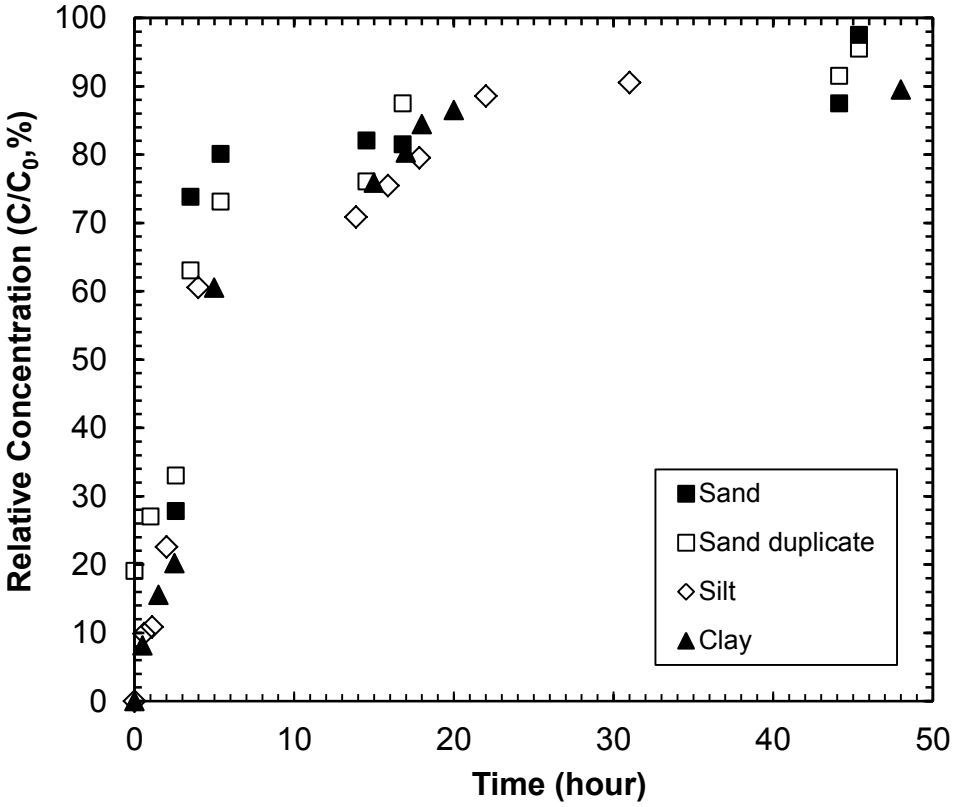

Figure 4.4 Concentration of methane in upper chamber for soil covers without GM.

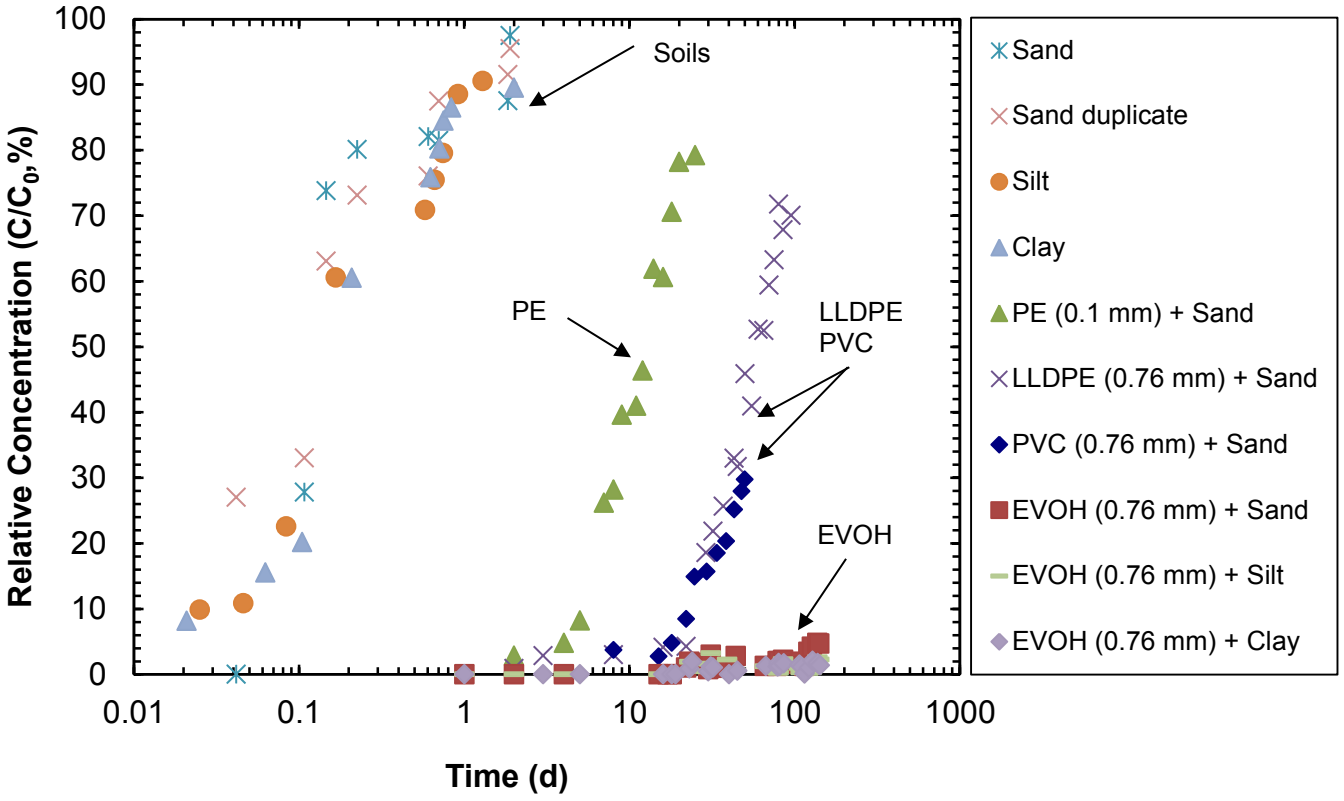

Figure 4.5 Concentration of methane in upper chamber for cover with soil only and composite covers with a GM.

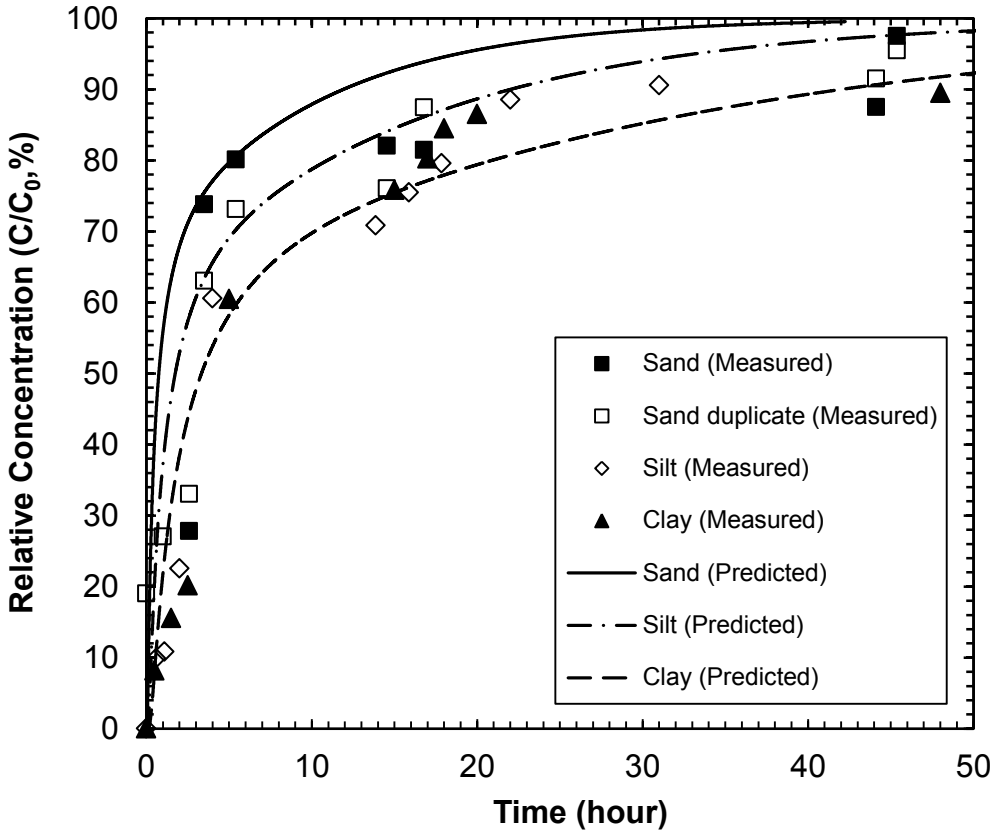

Figure 4.6 Methane transport through soil-only cover.

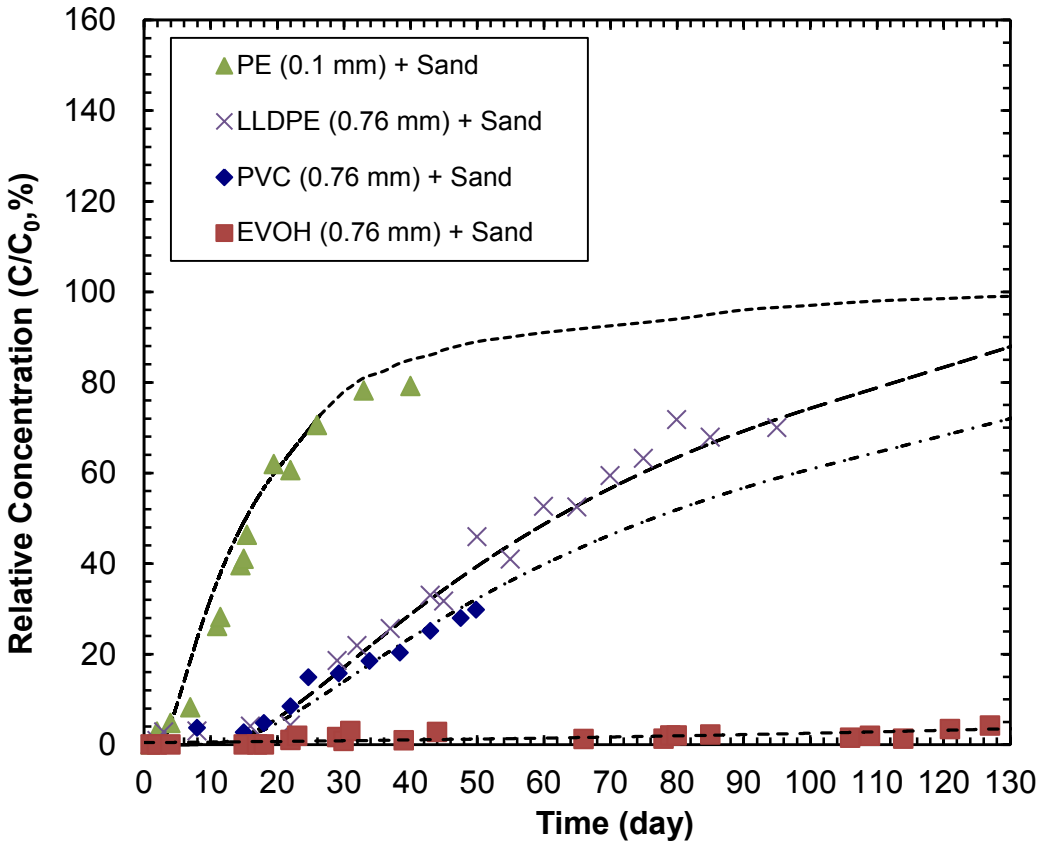

Figure 4.7 Predicted migration of methane through composite covers.

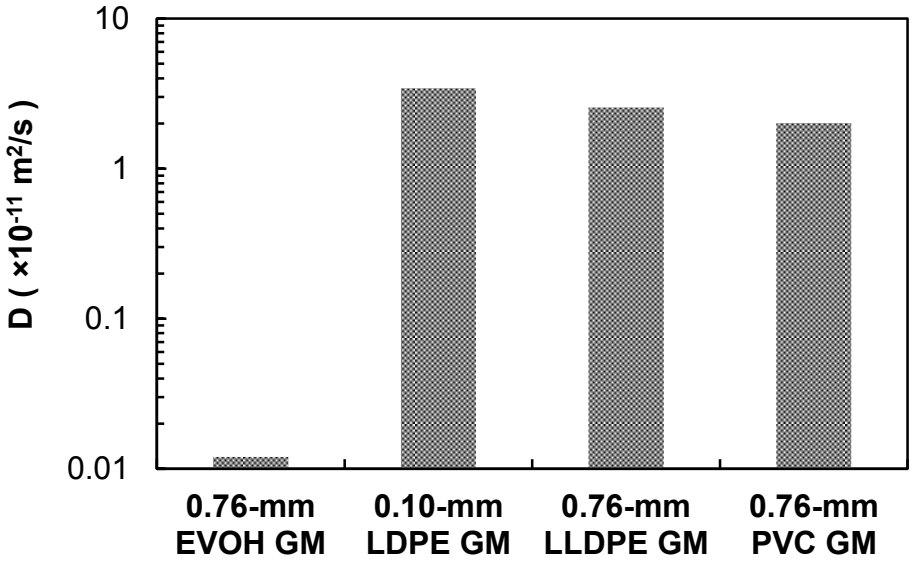

Figure 4.8 Comparison of diffusion coefficients for various GMs.

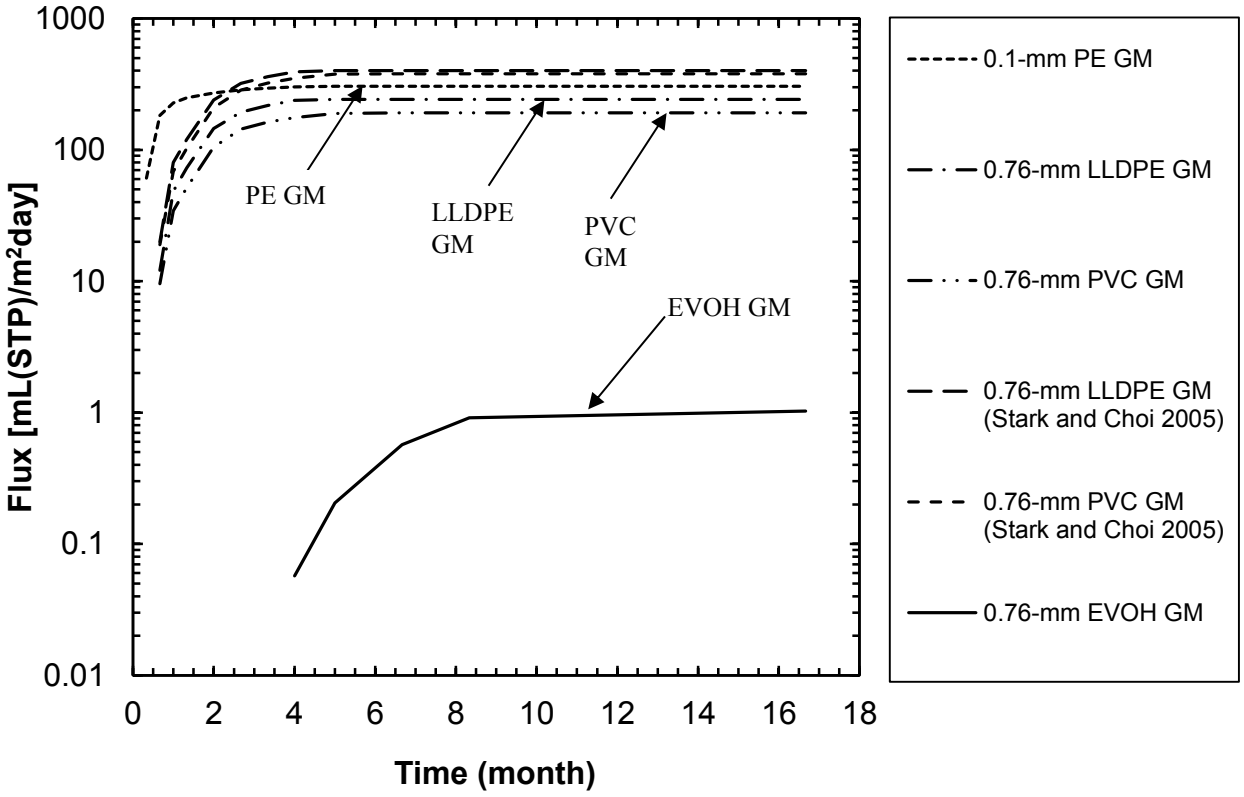

Figure 4.9 Comparison of flux for PE, LLDPE, EVOH GM with an underlying silty soil.

Chapter 5 Conclusions

5.1 SUMMARY AND CONCLUSIONS

A co-extruded geomembrane (GM) with a layer of ethylene vinyl-alcohol (EVOH) is being introduced in environmental containment applications to take advantage of the hydrophobic properties of polyethylene as a barrier to contaminant flux; specifically, the potential to substantially reduce the diffusion of non-polar volatile organic compounds [e.g., volatile organic compounds (VOCs) and methane]. This dissertation presented a comprehensive study on the migration of VOC and methane through composite barriers constructed with co-extruded EVOH GM. The specific methods, results, and findings drawn from this study are summarized below.

This research experimentally measured the relative migration of five common VOCs through composite landfill liners constructed with two types of co-extruded GM containing EVOH. To simulate *in situ* configurations of composite liners, a series of column tests with different types of GMs overlying either a compacted clay liner (CCL) or a geosynthetic clay liner (GCL) were conducted. VOC breakthrough in composite liners employing high-density polyethylene (HDPE) GMs occurred (≈ 35 d) more than two and four times faster than composite liners with co-extruded EVOH GMs with linear low-density polyethylene (LLDPE) and HDPE outer layers, respectively (≈ 70 to 150 d) and with significantly higher VOC concentrations. Co-extruded EVOH GMs with LLDPE and HDPE as an outer layer had measured diffusion coefficients (0.11-

0.57 × 10^{-13} m^2/s and 0.14-0.58 × 10^{-13} m^2/s, respectively) more than 20 times smaller in comparison to conventional HDPE GM (2.86-11.05 × 10^{-13} m^2/s). For the CCL and GCL composite liners, the concentration of VOCs at 80-mm depth was much lower in the CCL compared to the GCL. Numerical modeling (finite difference method) of VOC migration through a composite liner with 0.6-m-thick and 1.2-m-thick CCL with a co-extruded EVOH GM indicated that contaminant transport was approximately 14% and 22% lower, respectively in one hundred years. To achieve the same level of protection as provided by the co-extruded GM underlain by 0.6 m (RCRA Subtitle D) and 1.2 m (WDNR) of compacted clay, one would need an additional 0.1 m and 0.27 m of compacted clay, respectively, in conjunction with a conventional GM. Based on the comparison, the EVOH showed better performance in mitigating the migration of VOC compared to HDPE GM when accompanied by a thick CCL. Thus, co-extruded EVOH GMs acted as an effective barrier to VOC migration in composite liners.

The diffusive transport of organic contaminant (i.e., VOCs) was investigated through a co-extruded GM containing EVOH with a series of batch tests. To evaluate the equivalency of transport behavior in a co-extruded EVOH GM, the transport parameters of each layer for the EVOH GM consisting of the GM were measured by the batch tests separately. An equivalent diffusion coefficient was derived analytically based on the sorptive and diffusive behaviors through co-extruded GM (i.e., non-homogeneous layers in series). Overall, the LLDPE GM had the highest partition coefficient (1.9-195.8 L/kg) and the pure EVOH laminar had the lowest partition coefficient (0.69-0.94 L/kg). However,

depending on the polarity of the related VOC, the coefficient can be influenced markedly. The diffusion coefficient of co-extruded GM (0.14-0.59 × 10^{-13} m^2/s) was approximately 16-29 times smaller than that of HDPE GM (2.86–11.05 × 10^{-13} m^2/s). Furthermore, the diffusion coefficient of pure EVOH sheet is several orders of magnitude smaller than that of HDPE GM. The incorporation of co-extruded GM in landfill cover/liner systems may substantially decrease the diffusive transport of non-polar organic compounds such as methane and VOCs. The chemical characteristics of each material in a co-extruded EVOH GM (i.e., octanol-water partition coefficient, aqueous solubility and molecular diameter) show a strong linear relationship with the partition coefficient on a log-log scale. The relationship of the characteristics (i.e., octanol-water partition coefficient, aqueous solubility and molecular diameter) with HDPE, LLDPE and maleic anhydride was reversed with EVOH due to the polarity of the material. However, the empirical relationship between the properties and the diffusion coefficient is relatively weak in comparison to the partition coefficient. For validation of the proposed equation to estimated equivalent diffusion coefficient, the transport parameters for a co-extruded GM obtained using batch tests were compared to the transport parameters obtained from a modified double-compartment apparatus (MDCA) test. The MDCA testing apparatus provides reliable data compared to the previous double-compartment apparatus test due to minimizing the loss of VOCs. The measured and estimated diffusion coefficients were statistically identical, thus the equation to estimate the equivalent diffusion coefficient can provide reliable values. For another validation of the equivalent

diffusion coefficient, the migrations of VOCs predicted by numerical modeling using the coefficient were compared to those measured in diffusion column tests. The predicted and measured concentrations of VOCs were in good agreement. Further, for each VOC, the magnitude of the estimated diffusion coefficient agreed with the VOC migration demonstrated in the diffusion column test.

The relative rates of transport of methane through interim cover constructed with co-extruded GMs that contain a layer of EVOH were evaluated and compared in comparison to conventional GM including polyethylene (PE), LLDPE, and polyvinyl chloride (PVC). Based on the experimental results from these diffusion column tests employing composite covers, soil type minimally influenced diffusive behavior of methane through the interim cover in comparison to GM type. The LLDPE and PVC GMs produced five times more rapid breakthrough (≈ 20 d) of methane and higher flux in comparison to the EVOH GM (≈ 100 d). Further, the co-extruded EVOH GM had measured diffusion coefficients that were more than 170-250 times smaller compared to conventional GMs. The diffusion coefficients for were 0.012×10^{-11} m^2/s for co-extruded EVOH GM, 3.43×10^{-11} m^2/s for 0.1-mm PE GM, 2.55×10^{-11} m^2/s for 0.76-mm LLDPE GM, and 2.01×10^{-11} m^2/s for 0.76-mm PVC GM. Analytical modeling of methane migration through a composite cover indicated that the EVOH GM helps reduce the flux of methane [approximately 0.96 mL(STP) m^{-2} d^{-1}] to levels two orders of magnitude lower than the migration for the conventional GMs. Thus, co-extruded EVOH GMs acted as an effective barrier to methane migration in interim covers.

5.2 FUTURE RESEARCH

According to comprehensive laboratory work of this study, co-extruded EVOH GM is reliably effective in reducing transport of non-polar organic contaminant (i.e., VOC and methane) through barrier system where it is used. However, there is a lack of information on how best to apply the material in the field and how to identify the relative migration rates of organic contaminants between EVOH GM and conventional PE GM under *in-situ* conditions. The hypothesis of future study can be that a co-extruded EVOH GM, employed in in composite liner and interim cover, is expected to allow less transport of organic contaminant (e.g., VOC and methane) than conventional PE GM and this was confirmed in lab-scale tests.

APPENDIX 1

Saturation of Clay

1 kg of stainless steel beads and a 2-kg dead weight (overlaying the glass fiber filter) were placed on top of the compacted clay to prevent heaving and swelling of the clay during saturation (at 1.8 kPa confining pressure). For saturation, a 0.05% solution of sodium azide from DDI water was used to reduce microbe activity. The column setup with the compacted clay can is similar to the experimental setup of a rigid wall permeameter test. A sodium azide solution was used to fill the upper chamber and permeate the clay layer under an applied hydraulic gradient (Fig. A1.1). To reduce time to saturation, the hydraulic gradient was gradually increased from 20, as recommended by ASTM D5856, to 80. A hydraulic gradient > 80 was not applied because leakage occurs from the sampling port at this gradient. The hydraulic conductivity stabilized after 10 d from starting saturation. To confirm saturation, the ratio of inflow and outflow was checked periodically. When the saturation of the specimen was started, the ratio was less than 0.2 but gradually increased. After stabilization of hydraulic conductivity, the ratio of inflow and outflow approached unity (fluctuation < 10%). Total time to confirmation of saturation was around 3 weeks. Figure A1.2 shows the variation of hydraulic conductivity for seven testing setups and the ratios of inflow and outflow with time. The saturated hydraulic conductivity of the specimen was around 3.5×10^{-8} cm/s.

Figure A1.1 Saturation of CCL with applied hydraulic gradient from a pressure board

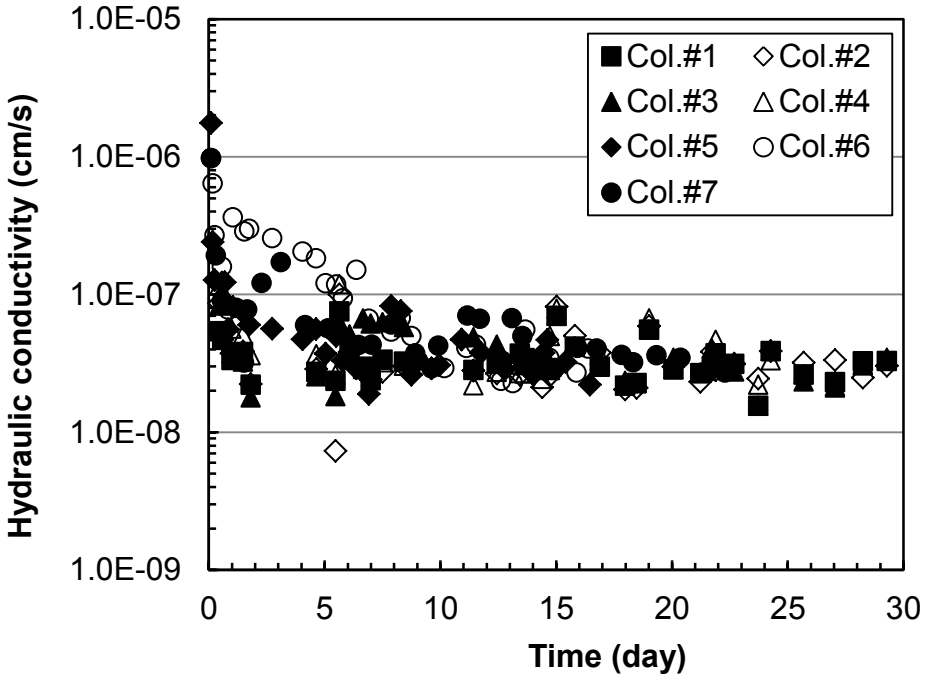

(a) Variation of hydraulic conductivity with time

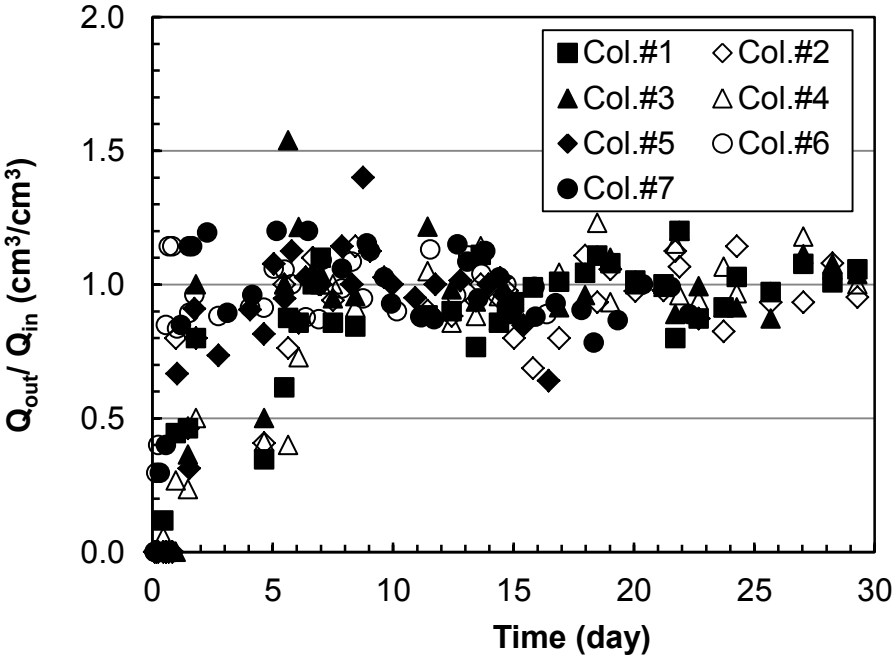

(b) Ratio of inflow (Q_{in}) and outflow (Q_{out})with time

Figure A1.2 Variation of hydraulic conductivity and the ratio of inflow and outflow in the clay columns

Saturation of GCL

For saturation of the GCL, several stages of the installation of the GCL into a testing column are needed to eliminate potential air at the interface between the GCL and the attenuation layer effectively. First, an attenuation layer consisting of silica sand was saturated. Then, the GCL was placed on the top of the sand surface and spread to make good contact with the sand layer. After the placement of GCL, bentonite paste was used to coat the entire circumference by spreading the paste with a small spatula to prevent side wall leakage as shown in Figure A1.3. Bentonite paste can seal the slits between the interfaces effectively. After sealing the slit with bentonite paste, the hydraulic gradient was applied to the column base (i.e., bottom-up saturation). When applying water from bottom-up, potential air bubbles existing at the interface between the GCL and sand can be removed during saturation. After two days, the direction of water flow was changed to flow downward, thus beginning the saturation check of the GCL. The height of outflow in the column was higher than that of sand layer in order that the water did not come out from the saturated sand layer during saturation (Fig. A1.3). Similar to the with saturation procedure of clay liner, the ratio of inflow and outflow should range between 0.9 and 1.1. Figure A1.4 shows the variation of hydraulic conductivity and the ratio of inflow and outflow with time for the GCL columns. The hydraulic conductivity of the saturated GCL stabilized around 5.5×10^{-10} cm/s in 7 d. Also, the ratio approached unity at the time.

Figure A1.3 Saturation of GCL occurs by applying a hydraulic gradient from a pressure board

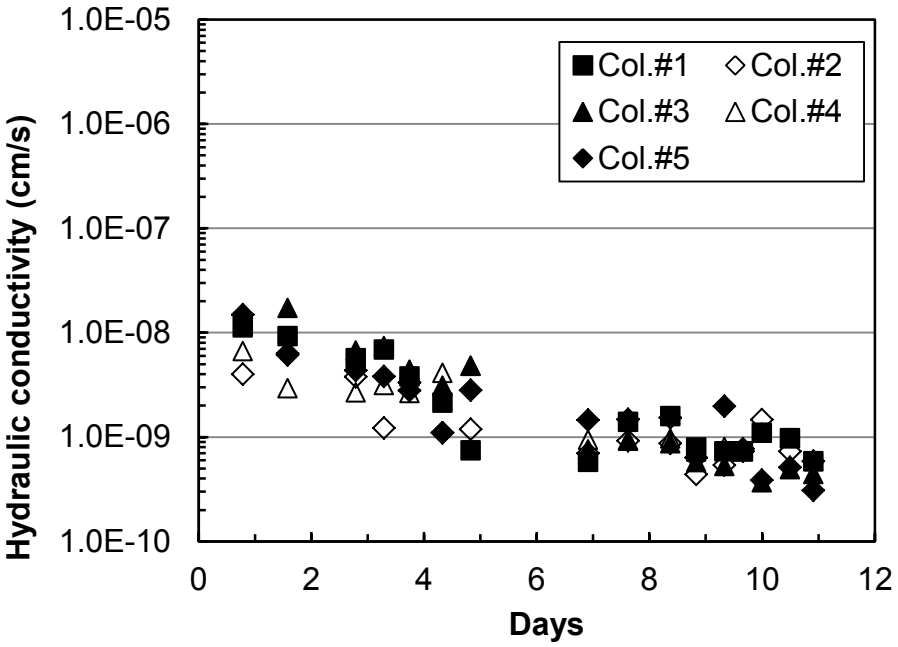

(a) Variation of hydraulic conductivity with time

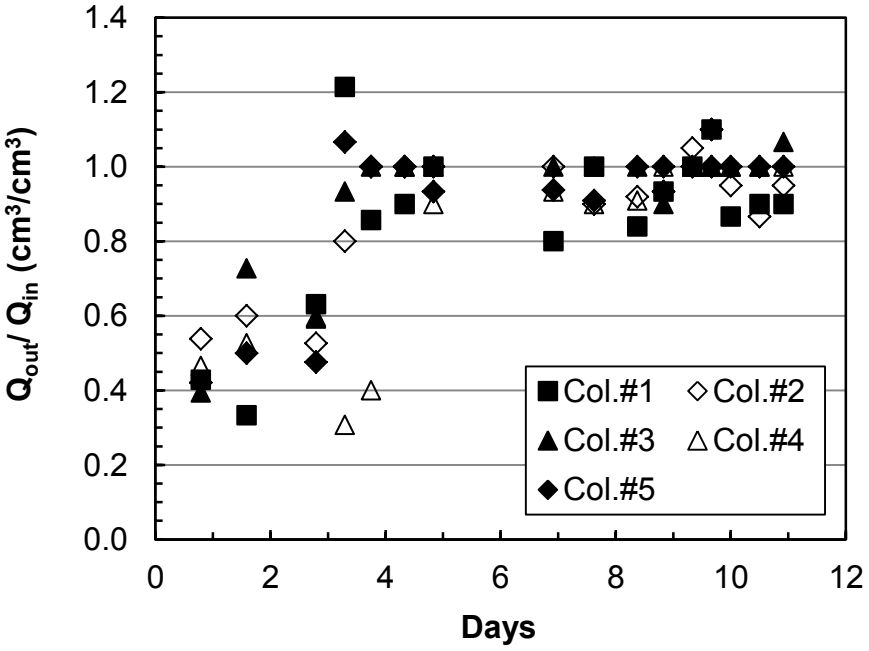

(a) Ratio of inflow (Q_{in}) and outflow (Q_{out})with time

Figure A1.4 Variation of hydraulic conductivity and the ratio of inflow and outflow in the GCL column

APPENDIX 2

Design of magnetic stir and stirrers

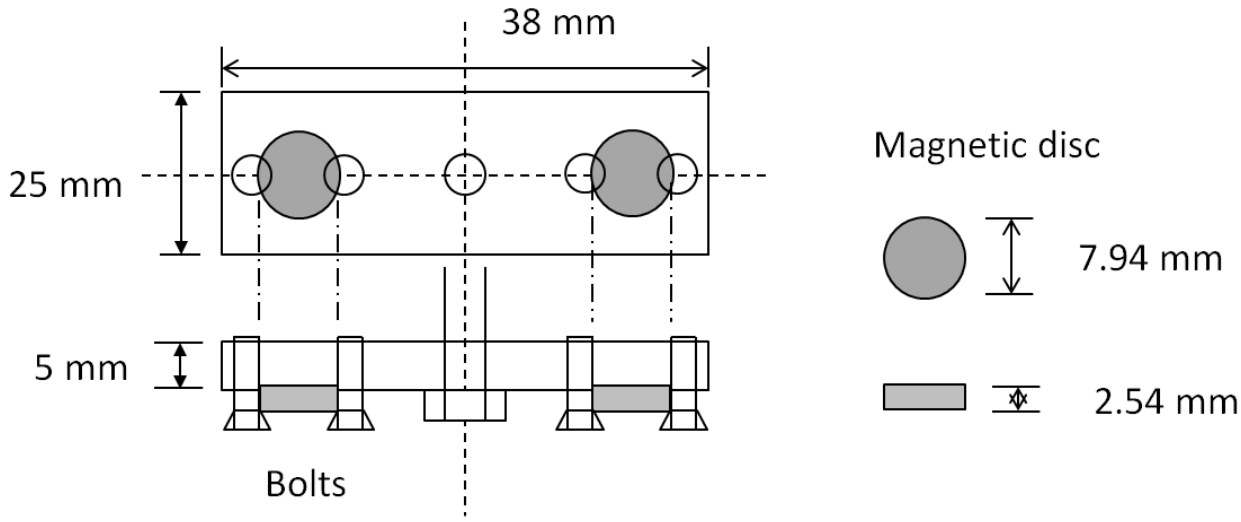

(a) Aluminum stirrer with magnetic discs

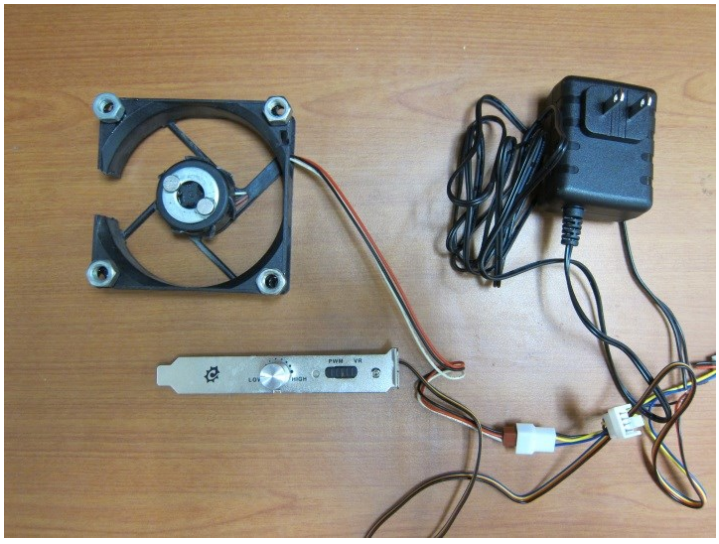

(b) Magnetic stirrer with switch and electrical adaptor and setting up on top plate of testing column

APPENDIX 3

Maintenance of VOC Concentration

The concentration of the VOC solution decreases with time because some solute is consequently adsorbed and migrated through the tested geomembrane during the test. For numerical modeling purposes, the concentration of VOC in the upper reservoir is proper to be consistent (Park et al. 2012). To maintain VOC concentration in the upper reservoir, a concentrated VOC solution was occasionally injected though the sampling port in the top plate. To mix the injected solution quickly and to keep the concentration of VOC consistent, two stirrers made of aluminum and magnetic discs were hung on the top plate. Magnetic stirrers were temporarily placed on the top plate when the solution was mixed and worked by rotating the stirrers inside the column. Chlorobenzene was chosen to check mix ability in the upper reservoir because the solubility of chlorobenzene is the lowest among five VOC tested. When a high concentration of VOC (e.g., chlorobenzene) is released in the upper reservoir (volume = 1.35 L), the concentration was stabilized within 20 min with the rotating stirrers. However, the concentration without stirrers does not stabilize in 70 min, as shown in Figure A3.1. The stainless steel beads in the column can impede the VOC solute in the high concentration of VOC solution to attach the specimen directly.

References

Park, M. G., Edil T.B. and Benson, C. H. (2012). “Modeling volatile organic compound transport in composite liners.” *Journal of Geotechnical and Geoenvirotal Engineering*, 138 (6), 641-657.

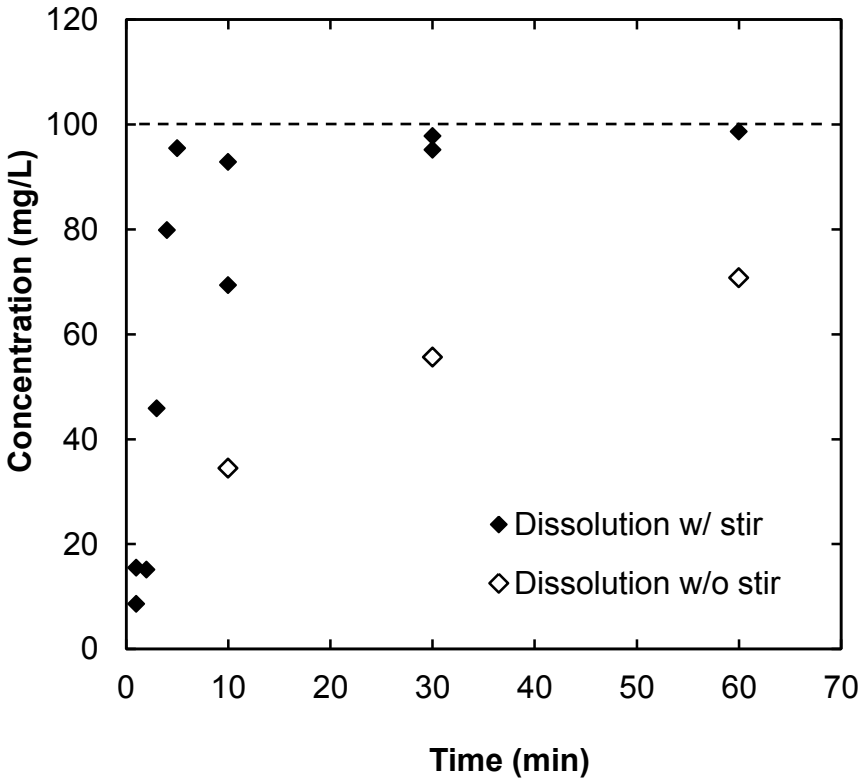

Figure A3.1 Dissolution of chlorobenzene in upper reservoir.

APPENDIX 4

Decreasing concentrations of TCE, TOL and CB with time recorded from kinetic batch test

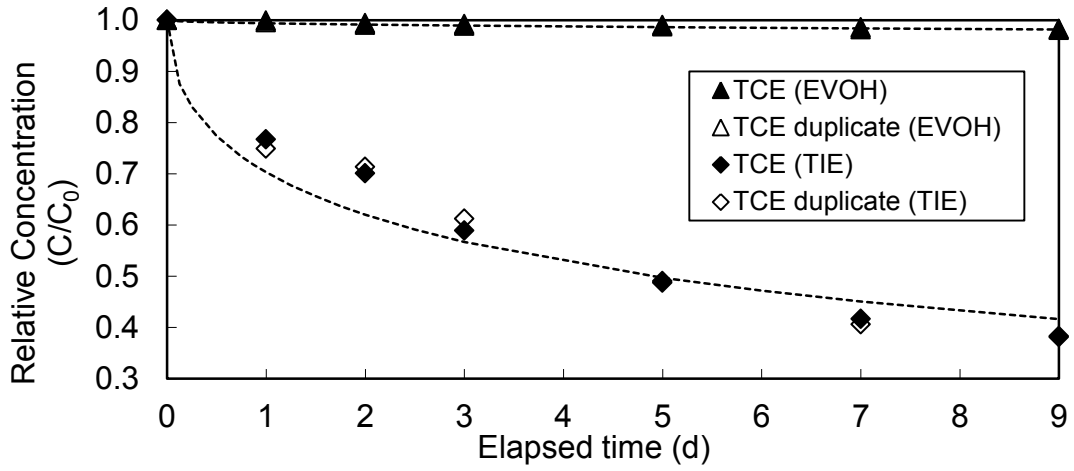

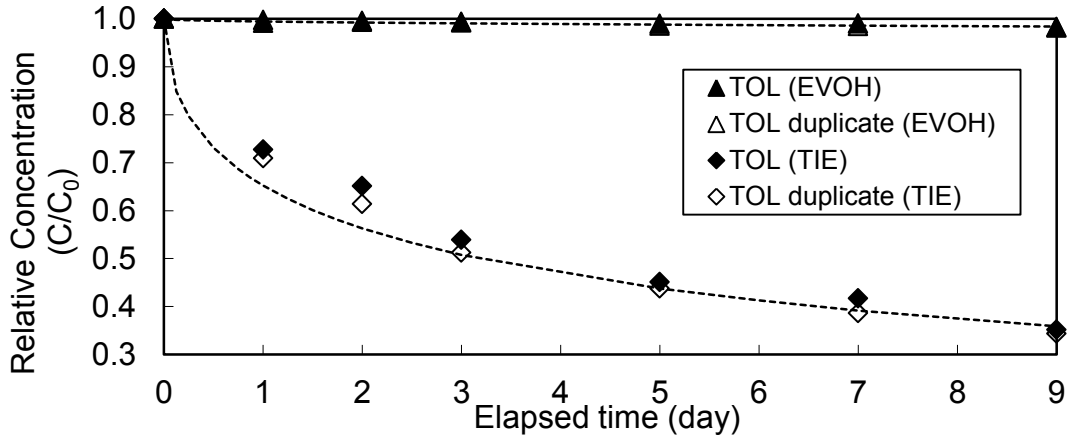

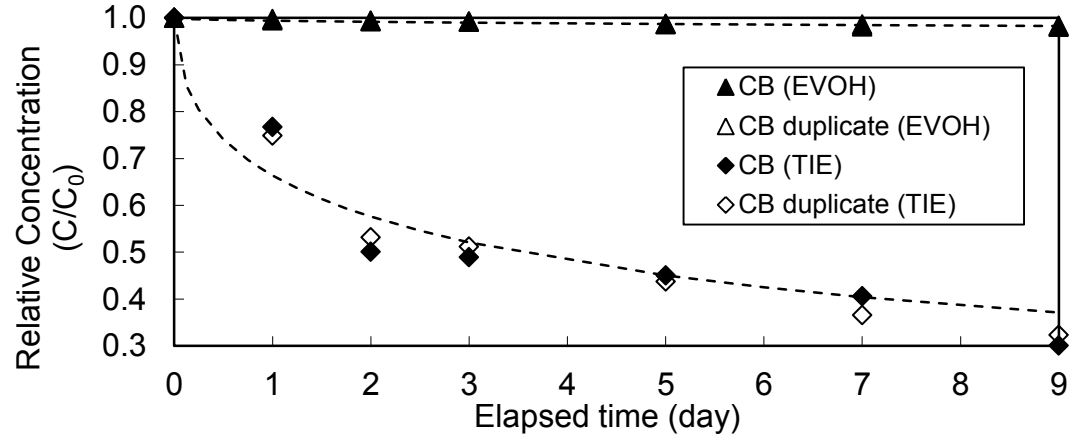

APPENDIX 5

Relative concentrations of MTBE, TCE, and TOL in the influent (upper) and effluent (lower) reservoirs in MDCA test

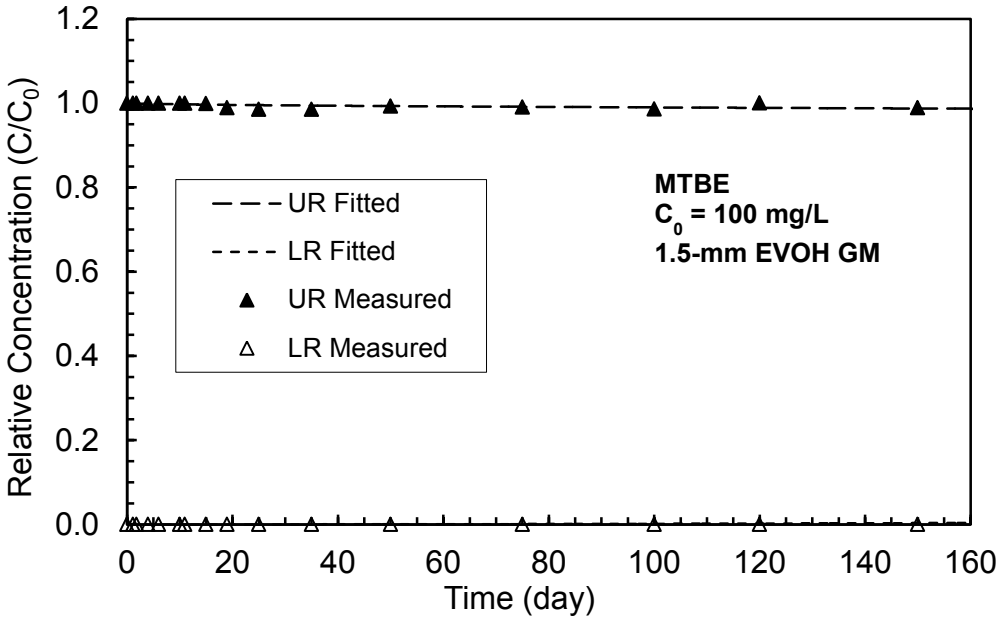

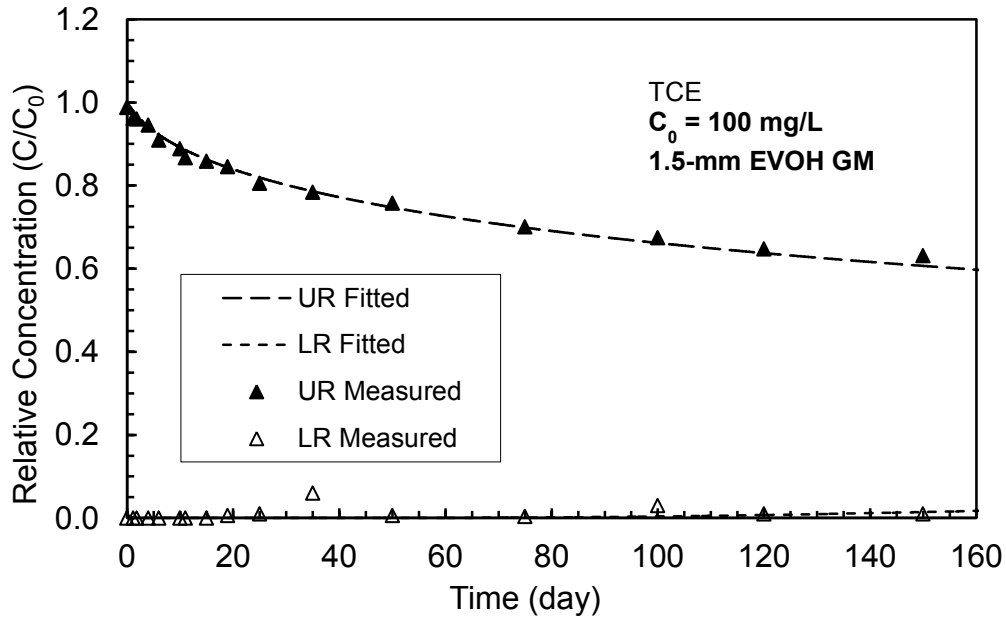

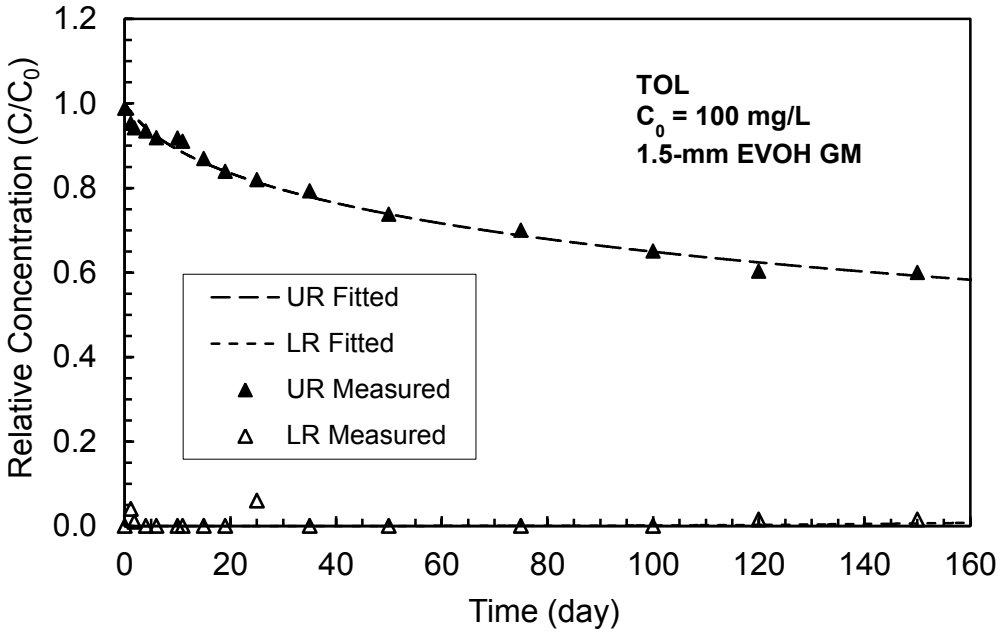
TOL
C0 = 100 mg/L
1.5-mm EVOH GM
UR Fitted
LR Fitted
UR Measured
LR Measured
Relative Concentration (C/C0)
Time (day)
0.0
0.2
0.4
0.6
0.8
1.0
1.2
0
20
40
60
80
100
120
140
160

APPENDIX 6

Unsaturated Transport of Gas Ebullition through Geotextile Sediment Cap

ABSTRACT

Gas ebullition from soft, organic sediments lying below sediment caps containing geotextiles may result in trap and retention of these gases due to the unsaturated hydraulic behavior of the geotextile. These gases may build up below the geotextile until the accumulating pressure either overcomes the confining pressure of the cap or the gas pressure exceeds the air-entry pressure (ψ_a) of the geotextile and is transmitted through the geotextile. A geotextile in a sediment capping system is generally designed as, and assumed to be, a permeable layer; however, a geotextile can become relatively impermeable if gases are trapped beneath and within the layer. This study examined how the failure mechanism of sediment capping geotextiles is functionally related to the unsaturated hydraulic behavior of the geotextiles. Series of laboratory tests including the hanging column test, water column apparatus test, and bubble point test were conducted to characterize the water retention properties and pore-size-distribution curves of common nonwoven geotextiles and a composite mat. The ψ_a obtained from the geotextile water characteristic curve (GWCC) varied from 0.4 kPa to 1.2 kPa and depended on the pore distribution of the capping geotextile. The ψ_a of the geotextiles increased with increasing normal stress due to decreasing pore size. An empirical correlation between ψ_a and *in situ* normal

pressure (σ'_n) is proposed as a normalized linear equation. The unsaturated hydraulic conductivity estimated from the GWCC was decreased from 1.8×10^{-3} m/s to 7.0×10^{-7} m/s with increasing suction. Composite layers did not significantly increase ψ_a, but organo clay used within a geotextile mat core had a remarkable influence. Gas retention and build up beneath a geotextile component in a sediment cap can be described mechanistically and modeled using the fundamental unsaturated properties of the geotextile. Failure of a sediment cap is initiated by increasing the ψ_a or reducing the hydraulic conductivity due to gas migration through the caps. Design recommendations to avoid failure of a sediment capping system from gas ebullition are suggested.

KEYWORDS: geotextile; sediment capping; geotextile water characteristic curve; pore size distribution curve; air entry pressure; gas ebullition; unsaturated flow; hydraulic conductivity.

INTRODUCTION

Sediment capping has been used for decades as a remediation technology for contaminated sediment by restraining contaminated material, and thus reducing the transfer of contaminants to the water column. In a sediment cap, submerged contaminants are contained by an engineered cap that typically contains sand, gravel, geotextiles, or combinations of these materials (Jacobs and Forstner 1999; Kavcar and Wright 2009; Starr and Braun 2010; Chattopadhyay et al. 2010). In comparison to gravel and sand layers, the use of

geotextiles in sediment capping systems reduces the total volume of capping material needed and the corresponding cost (U.S. EPA 2005). Geotextiles act as a separation layer in addition to providing a bioturbation barrier which stabilizes the cap, reduces contaminant flux, prevents mixing of cap material with underlying sediments, promotes uniform consolidation, and reduces erosion of the capping material (Jacobs and Forstner 1999; U.S. EPA 2005; Kavcar and Wright 2009; Starr and Braun 2010; Chattopadhyay et al. 2010).

A geotextile in a sediment capping system is generally designed as, and assumed to be, a permeable layer; however, a geotextile can become relatively impermeable if gases are trapped beneath and within the layer (Reible et al. 2006; Kellems et al. 2008; Kavcar and Wright 2009; Starr and Braun 2010; Chattopadhyay et al. 2010). A layer of gas beneath a geotextile and/or earthen capping material effectively blocks upward migration of pore water flow in a previously water permeable cap. Gas ebullition is an event to allow a sudden release of gas through a layer that result from a buildup of gas pressure below or within that layer. This phenomenon induces a functional failure of the cap due to either focused flow through a portion of the cap, which decreases the design life, or a complete rerouting of flow around the cap.

Many studies have investigated chemical principal to demonstrate flux concentration and resuspension through sediment capping systems (Dailer and Gentry 2004; Reible et al. 2006; Viana et al. 2007; Kellems et al. 2008; Kavcar and Wright 2009; Chattopadhyay et al. 2010; Starr and Braun 2010). Moreover, Mohan et al. (2000) investigated a design criteria of sediment capping in terms of

hydraulic and geotechnical principals. However, there is very limited information in practice or literature that identifies a functional mechanism for failure from gas ebullition of sediment capping systems including geotextiles. Further, the gas ebullition is strongly related to the water retention performance of geotextiles used in sediment caps. Accordingly, to understand the gas ebullition, the unsaturated hydraulic properties in terms of water retention characteristics of geotextiles should be investigated. However, the water retention characteristics of geotextiles have not been identified either and are possible to be dependent upon field and material conditions (Stormont et al. 1997; Iryo and Rowe 2003; Bouazza et al. 2006; Eun and Tinjum 2011b). The variables include material composition and the normal pressure on the capping system (i.e., overburden pressure).

The main objective of this study was to investigate how the failure mechanism of sediment capping geotextiles is functionally related to the unsaturated hydraulic properties of the geotextiles. A series of laboratory tests including the hanging column test, water column apparatus test, and bubble point test were conducted to characterize the water retention properties and pore-size-distribution curves of common capping geotextiles and geotextile composite with organo clay, Reactive Core Mat®. Variables that influence the water retention characteristics of the geotextiles were investigated. A functional failure mechanism is developed with a case study presented that exemplifies and supports this failure sequence.

BACKGROUND

Sediment cap function and role

The function of subaqueous sediment capping in lakes, rivers and coastal waters is a promising approach in developing a low-cost and low-technology alternative to conventional methods in remediation of contaminant sediment. The concept of capping sediments in-situ involves to place a cover over the submerged contaminated sediments with gravel, rock, and/or geosynthetic materials (i.e., geotextile) to seal it off, and thus to minimize contaminant release into the water column (Jacobs and Forstner 1999; Mohan et al. 2000; Yun et al. 2007; Kavcar and Wright 2009; Starr and Braun 2010; Chattopadhyay et al. 2010) (Fig. 1). Conventional off-site technologies, which names dredging, are complex and thus much costly where large areas of sediments are concerned as removing pollutants from the sediment by chemical or physical means. Furthermore, the sediment disposal through dredging needs to be secondary processing for not only the excavation of contaminant sediment but also the movement of the contaminated byproduct from the site generating the contaminant sediment and the cleanness as storing on a controlled area. During the procedure, excessive time and cost will be generated. Even where contaminated sediments must be excavated, underwater capping may still be preferable to above ground disposal. In this case, sediments may be deposited in either a natural depression or a space formed by dredging clean sediment before capping. In certain conditions, the cap reduces contaminant mobility and subsequent interaction between aquatic organisms and the contaminants.

Advantages and disadvantages of sediment capping and dredge are summarized in Table 1.

An international review of the application of sediment-capping techniques is given by Azcue et al. (1998). There have been several laboratory and field scale investigations into the capping of sediments with sand or gravel layers (Wang et al., 1991; Zeman 1994; Jacobs and Forstner 1999). Recently nonwoven geotextiles with additives (e.g., organo clay, bentonite) have been used as alternative of gravel and sand layers to cover contaminant sediment in capping system. In comparison to conventional materials, the use of geotextiles in sediment capping systems can save the total volume of capping material and the corresponding cost. However, the geotextile used in sediment covers has not been investigated in comparison to conventional materials. Further, there is no established specification to use the geotextile. Therefore, it is important to develop the capping design to find adequate low-cost sorbents because enormous amounts of material are necessary to cover large areas of sediment.

The capping system must be composed of materials showing physical and chemical stability. The design of capping system involves the proper application of hydraulic (armor and filter equations), chemical (diffusive and advective/dispersive transport equations), and geotechnical (settlement and stability equations) engineering principles (Mohan et al. 2000). The requirements to potential active barrier materials, accordingly, can be summarized as follows:

- Physical stability as isolating contaminated sediment.

- Chemical stability as reducing chemical contaminant flux to benthic organisms and water column.
- Sufficient hydraulic conductivity under hydrologic conditions in a site.
- Availability at low cost.

With capping, contaminants remain in place at the site, requiring long-term monitoring and maintenance to ensure that contaminants are not migrating in a long-term view to minimize running costs of the barriers.

Unsaturated properties of geotextile

The water retention curve of a geotextile, termed the geotextile water characteristic curve (GWCC), represents hydraulic performance via the capacity and tenacity of the geotextile to retain water in the pores. This capacity for water retention provides valuable information to relate and model air infiltration into and through geotextile. The ψ_a is defined as the pressure required to introduce air into and through the pores of a saturated porous media (ASTM D6836). The ψ_a value for a geotextile can be determined graphically by using techniques shown in Fig. 2. The point describes the ψ_a to intersect two straight lines, which are one drew from flat part of GWCC and the other drew from linearly decreasing part of GWCC. Once ψ_a is reached, water content decreases with increasing ψ from the saturated volumetric water contents, $\square_s$ to residual volumetric water content state, θ_r, where further removal of water from the geotextile would require vapor migration (Stormont et al. 1997). The shape of the GWCC is likely a function of geotextile type.

The GWCC can be quantified by fitting the suction and water content to a model. Van Genuchten's model (1980) was used to simulate the GWCCs in this study [Eq. (1)]:

$$\theta = \theta_r + (\theta_s - \theta_r)\left[\frac{1}{1+(\alpha\psi)^n}\right]^m \quad (1)$$

where ψ is matric suction, α is a parameter related to ψ_a, and m and n are area model parameters related to pore size distribution.

Unsaturated hydraulic conductivity (k_{uw}) for a geotextile in a cap can be predicted by using the GWCC (McCartney and Zornberg 2010). The function to predict k_{uw} for porous media has been presented as (Mualem et al. 1976; Nahlawi et al. 2007; McCartney and Zornberg 2010). Using Mualem's model, a relative hydraulic conductivity (k_r) in terms of saturation, which is a unitless ratio of k_{uw} over saturated hydraulic conductivity (k_0), can be represented:

$$k_r(S_e) = \frac{k_{uw}(S_e)}{k_0} = S_e^{\tau}\left[\int_0^{S_e}\frac{1}{h(S_e)}dS_e \Big/ \int_0^1 \frac{1}{h(S_e)}dS_e\right]^2 \quad (2)$$

where S_e is a degree of saturation in a geotextile, k_0 is the hydraulic conductivity measured at $\square_s$, h is a function of hydraulic head with varying S_e, and τ is a parameter which accounts for the dependence of the tortuosity and the correlation factors on the water content. Mualem et al. (1976) reported an optimum average for τ of about 0.5 for generally disturbed soil samples. Assuming m = 1-1/n, van Genuchten (1980) obtained a closed-form analytical solution to equation (2) to predict k_r at scaled volumetric water content. The k_{uw} can be calculated from k_r:

$$k_{uw}(S_e) = k_0 \cdot k_r(S_e) \ = k_0 \cdot \ S_e^{\tau}\left[1-(1-S_e^{\frac{1}{m}})^m\right]^2 \quad (3)$$

Eq. (3) allows an estimation of the hydraulic conductivity function to be obtained, when saturated hydraulic conductivity (k_0) is known, through the parameters of van Genuchten's Model, by applying a nonlinear least square procedure to fit the measured retention data to the model. According to McCartney and Zornberg (2010), the k_{uw} of nonwovern geotextile was ranged from 9.0 $\times 10^{-1}$ to 7.0 $\times 10^{-10}$ m/s depending on the variation of suction ranged from 0.1 to 2.5 kPa.

The functional failure of a capping system can be induced from either increasing the ψ_a due to in-service conditions or from trapped gas that lowers the impermeability. Given that gas build up in a geotextile/sand capping system creates an unsaturated flow regime, the water retention characteristics of the geotextile are necessary to model the unsaturated hydraulic behavior of the system. In particular, the ψ_a of a geotextile is an important parameter that describes the unsaturated hydraulic behavior of the geotextile. Furthermore, based on the water retention characteristics of the capping materials, the k_{uw} can be evaluated.

FAILULRE MECHANISM OF SEDIMENT GEOTEXTILE CAPS

A geotextile in a sediment capping system is designed as and nominally expected to perform as a permeable layer under normal conditions. When the sediment cap is permeable, gas migration through a sand/geotextile cap occurs as a series of ψ_a events (Kavcar and Wright 2009; Eun and Tinjum 2011a). A

geotextile is a highly compressible material composed of fiber filaments. The ψ_a can increases in situ through a reduction in pore sizes from overburden pressure as well as clogging (Palmeira and Gardoni 2002; Palmeira et al. 2005; Palmeira et al. 2008). Under low ψ_a, a geotextile can become impermeable if gases are trapped beneath and within the layer (Kellems et al. 2008; McCartney and Zornberg 2010). Depending on the magnitude of the effective overburden pressure applied to a geotextile cap, the stability of the capping system can be divided into the following scenarios:

- Stable condition

Scenario 1: $P_g < \psi_a < P'_{fm}$ and $P_{sw} < P'_{fm}$

Scenario 2: $\psi_a \leq P_g < P'_{fm}$ and $P_{sw} < P'_{fm}$

- Unstable condition

Scenario 3: $P_g \geq \psi_a > P'_{fm}$ and $P_{sw} < P'_{fm}$

Scenario 4: $\psi_a < P_g < P'_{fm}$ and $P_{sw} \geq P'_{fm}$

where P_g is the underlying gas pressure, P_{fm} is the overburden pressure from the fixing materials (e.g., armors or sands), and P_{bf} is the buoyant force of the fixing material under water. Because of P_{bf}, geotextile caps are subjected to an effective pressure equal to the difference between P_{fm} and P_{bf}. P'_{fm} ($=P_{fm} – P_{bf}$) is the effective overburden pressure, and P_{sw} is the water pressure due to seepage force from river bottom, which can generate the head difference between the level of ground water and the river bottom.

Gas generated from the decomposition of organic contaminants initially tends to be retained beneath geotextile caps because the gas pressure (P_g) does not exceed the ψ_a of the geotextile. In this case as described in Scenario 1, the geotextile cap is stable if the effective overburden pressure (i.e., P'_{fm}) applied on the surface of the caps is higher than the ψ_a. As P_g increases due to further decomposition of organic content, the gas pressure exceeds ultimately ψ_a and pass through the cap. The cap is still stable because the ψ_a is smaller than the P'_{fm} applied on the surface of the caps as described in Scenario 2. For Scenario 1 and 2, some amount of gas can be retained beneath or within the geotextile layer; however, P_g does not push the caps upward and cause damage because P_g is smaller than the P'_{fm}. For these scenarios, the seepage pressure (P_{sw}) from the bottom river is assumed to be less than the P'_{fm}. Under this condition, the generated gas does not displace the caps, which remain stable [Fig. 3(a)].

However, if the ψ_a of the cap is higher than the P'_{fm}, the gas may be retained beneath the geotextile caps and will accumulate until a pressure threshold is reached to be equal to the P'_{fm}. When the P_g is higher than the P'_{fm}, the overlying cap becomes buoyant, and the cap is displaced as described in Fig. 3(b). Some gas starts to migrate through the geotextile caps. This is an unstable condition due to gas ebullition that occurs when the P_g is greater than the ψ_a as described in Scenario 3.

Another unstable condition, which damages the capping system, is the reduction of water permeability due to gas trapped in the layer. As the gas fills the voids of the geotextile, the hydraulic conductivity (k_{uw}) of the unsaturated

geotextile caps significantly decreases and the caps become impermeable (McCartney et al. 2005; McCartney and Zornberg 2010). If the seepage pressure (P_{sw}) equal to or greater than the P'_{fm}, the geotextile caps can heave up against the pressure [Fig. 3(c)]. This is an unstable condition due to the reduction of the k_{uw} as described in Scenario 4. However, the magnitude of water flux is uncertain because flux is dependent on the difference in hydraulic head between the capping geotextile and the ground water table.

EXPERIMENTAL PROGRAM

Materials

Nonwoven geotextile is widely used for the layer to cover sediment contaminant (McDonough et al. 2007). Each geotextile made of polypropylene fibers was tested to compare the GWCCs obtained from a HCT and to investigate the factors influencing the ψ_a, such as composition type and applied normal pressure. Reactive Core Mat® (RCM) produced by CETCO® Inc. is evaluated in this study, which is a new type of sediment remediation material including a reactive layer containing one or more neutralizing or otherwise reactive materials (e.g., organoclay), which is proprietary adsorption medias highly effective in removing oils, greases and other high molecular weight/low solubility organics. The RCM is composed of three layers, including two nonwoven geotextiles (i.e., GT1 and GT2) around a core of organic clay. The separate layers and the combined layers of the RCM were tested to investigate the effect of composition. Four geotextiles (GT5, GT6, GT7 and GT8) were

tested additionally, which are all nonwoven geotextiles. Physical properties for the geotextiles used in this study are summarized in Table 2, including mass per unit area, thickness, and apparent opening size (AOS) (ASTM D5261, D5199). Organo clay included in the RCM was evaluated. The average unit weight of the clay was 9.52 kN/m^3 at 20% relative density. The D_{50} of the poorly graded clay is 1.1 mm and the particle size is close to sand overall [see Fig. 4 (a)]. Organo clay does not hydrate upon introduction to water as shown in Fig. 4(b).

Hanging column test (ASTM D6836)

Hanging column test (HCT) techniques can be used to measure the GWCC because the suction to approach residual volumetric water contents is typically small (i.e., < 10 kPa) in comparison to fine sand or clay (Iryo and Rowe 2003; Buazza et al. 2006). Fig. 5 shows the HCT apparatus. The geotextile specimen either absorbs or expels water to equilibrate with the suction in the porous stone. Deaired water was used for all tests. To achieve 100% saturation, the specimen was submerged in deaired water for at least 24 h while applying suction pressure. To reliably measure the ψ_a of the RCM's geotextile components, the HCTs were conducted at estimated *in situ* conditions (i.e., fully saturated with applied confining pressure of 2.0 kPa, when fixing material is approximately the 0.3 m of thickness). The confining pressure also ensured hydraulic continuity between the geotextile and the porous ceramic. To investigate the effect of normal pressure on the GWCC, pressures of 1.0, 2.0, 4.0 and 5.0 kPa were applied to selected geotextiles. Between the geotextile

specimen and the dead weight, a geogrid was placed to equally distribute the load over the whole surface of the geotextile specimen.

Saturation in a GWCC

To obtain a GWCC for a geotextile specimen, the volumetric water content (θ) is calculated as follows:

$$\theta = S_e \, n \tag{4}$$

where S_e is the degree of saturation and n is the porosity of the specimen. To express the measured gravimetric water content as a saturation value (i.e., volume of water per volume of voids in the specimen), the porosity of the specimen is required. Porosity is calculated as follows (Koerner 1998):

$$n = 1 - \frac{M_A}{\rho_f \, t} \tag{5}$$

where M_A is mass per unit area, ρ_f is fiber density (assumed to be 1.30 g/cm^3 for polypropylene); and t is specimen thickness measured while the specimen is subjected to the same vertical pressure used during the HCT. Saturation is obtained from the gravimetric water content, w, using the following relationship:

$$S_e = \frac{w \, M_A}{\rho_f \, t \, n} \tag{6}$$

Water column apparatus

A simple apparatus was constructed to measure the permeability of the samples of geotextile (see Fig. 6). A Plexiglas® column was cut in half, and a sample of selected geotextiles (i.e., GT1, GT6, and GT7) was placed between the two halves and held in place with long screw clamps. In a typical test, there was water above and below the geotextile. A tube entering the bottom of the column was used to introduce gas, simulating ebullition from sediments. For convenience, the water below the geotextile was dyed to make observation of penetration through the geotextile easily distinguishable.

Bubble point test (ASTM D6767)

The bubble point test (BPT) is a common method to obtain the pore size distribution (PSD) of geotextiles. In a geotextile, a wetting liquid is held in continuous pore channels by capillary attraction and surface tension (Elton et al. 2006, Eun and Tinjum 2011b). In bubble point testing (see Fig. 7), air is directed through a dry and wet geotextile specimen at various air flow rates, and the pressure difference expels water according to pore size. Pore size can be estimated by the Washburn (1921) equation. The Washburn equation describes the equilibrium of a fluid under a pressure gradient in a porous medium with circular openings; in this case, the geotextile pore openings of diameter, d. As represented in Eq. (7), pore size is related to the fluid and the pressure difference across the sample, thus:

$$d = \frac{4\sigma\cos\theta}{P} \tag{7}$$

where d is diameter at pressure (mm), σ is surface tension of the wetting fluid (N/m), θ is the equilibrium contact angle; and P is the pressure difference across the specimen (Pa).

As air flow rate increases through a geotextile in the wet condition, retained fluid exists in the pores because of capillarity. The PSD is obtained by comparing the flow rate through both wet and dry samples with the same pore size. The flow rate versus pore size is plotted on a semi-log scale as follows:

$$\%f = \left(1 - \frac{Q_w}{Q_D}\right) \cdot 100 \quad (8)$$

where %f is percent finer of pores, Q_w is true airflow from the wet run (L/min), and Q_D is true airflow from the dry run (L/min). A GWCC should be directly relatable to its PSD in terms of pore characteristics in the geotextile because the PSD of a geotextile is associated with water retention across the geotextile (Elton et al. 2006).

WATER RETENTION CHARACTERISTICS OF CAPPING GEOTEXTILE

Hydraulic properties of geotextile caps from GWCC

The hydraulic properties related to water retention characteristics in the geotextile were obtained from measured GWCCs. Figure 8 shows the GWCCs of seven geotextiles except GT4 and includes experimental data points measured from HCT and also predicted data, which is represented by dotted lines. The fitted retention curve is obtained from the least square residual optimization and using van Genuchten's model [Eq. (1)]. The GWCCs are described by near

constant θ up to ψ_a. Water held in the larger pores of the geotextile drain at a small ψ and a rapid decrease in θ occurs beyond ψ_a. All ψ_a values of GTs ranged from 0.40 to 1.2 kPa, which is congruent with the literature (Stormont et al. 1997; Iryo and Rowe 2003; Bouazza et al. 2006).

In the GWCC, hydraulic properties such as ψ_a and curve shape are affected by a number of internal factors, including the polymer type, fiber shape, fiber surface roughness, and any surfactants (Stormont et al. 1997). The hydraulic performance can vary significantly, depending on these physical characteristics. For instance, thickness and fiber density would be expected to affect the hydraulic behavior (e.g., saturation). Furthermore, outside factors affecting geotextiles can influence the hydraulic behavior. If the pore size of a geotextile decreases due to overburden pressure applied on the geotextile caps, the ψ_a increases with increasing capillarity in the geotextile. The saturated volumetric water contents (θ_s) was placed around 0.65 to 0.83 and the residual volumetric water contents (θ_r) was subjected to around 7.0 to 15.0 kPa. The θ_r is closer to zero with lower suction due to relatively large pores in the geotextile compared to clay or silt (Tinjum et al. 1997). The shape of the GWCC is closer to the SWCC of sand rather than those of silt and clay.

Results of water column apparatus

From the results of the water column apparatus tests, with increasing water pressure from bottom, air voids start to generate beneath the geotextile because of the capillarity of the geotextile caps. Approximately 10.7 cm of air

built up beneath a saturated piece of geotextile (GT7) before breakthrough. The layer of air did not collapse after breakthrough. Rather, gas bubbles were transmitted through the geotextile only when the gas layer beneath the geotextile exceeded 10.7 cm and the gas layer maintained a 10.7 cm bubble after the excess pressure was released.

Testing showed that gas bubbles did not readily penetrate the water-saturated geotextile. The resistance to that passage of gas through water-saturated pores describes the ψ_a. The height of water is a head equal to the ψ_a according to Bernoulli's equation:

$$\Delta h = \frac{\rho_w g}{\psi_a} \tag{9}$$

The height of the water column was around 10.7 cm, which is similar to approximating 1.0 kPa of the ψ_a. Compared to water column apparatus testing, the elevation head by water height build up in the column test is similar to the head of the ψ_a of selected geotextiles (GT1, GT6 and GT7) obtained from the HCT as shown in Fig. 9. The ψ_a is statistically related (i.e., correlation coefficient > 0.98) and linearly proportional to the head of water column. However, due to dead weight in HCT, the head of water column tests is smaller than that of HCT. In a saturated condition, water will flow through a saturated pore more easily than a gas bubble. This is due to surface tension at the interface between the gas and the water. (In cases where the pore material is hydrophilic, there can be added resistance from capillary action).

Relationship between PSD and GWCC

Figure 10 shows a comparison of the PSD curve of each geotextile obtained from the BPT. The ψ_a is related to the PSD analysis obtained from the BPT. The difference of the ψ_a values is due to pore size and porosity in the geotextile. For instance, GT2, GT5 and GT8, which have lower ψ_a values, have larger pores than GT1, GT6 and GT7, and have higher apparent opening size (AOS) [1.0 mm for GT2, GT5 and GT8 versus 0.35mm for GT1 and GT6, 0.25 mm for GT7) in the PSD. Therefore, a lower ψ_a initiates the de-watering process. Moreover, the shape of the GWCC is inter-related to the PSD. Typically, if the pore is poorly graded, the GWCC sharply decreases. For instance, the comparison of the PSD for GT1 with constant pore size and the PSD for GT2 which has distributed pores sizes demonstrates dramatically the difference in the reduction of water contents in the GWCC.

A composite layer shows the average pore distribution of each layer. For instance, the slope of the PSD for GT3 composed of GT1 and GT2 is more gradual than that of GT1, and steeper than that of GT2. θ_s tends to vary regardless of the PSD because the water retention characteristic of the geotextile varies depending on the characteristics of the geotextile such as the mass per area as well as the material type such as the polymer type, fiber shape, and fiber surface roughness. Therefore, GT2 and GT6 showed remarkably different ψ_a values with similar θ_s values, which is consistent with the different PSD curves. The low θ_r measured (< 0.1) indicates that the geotextiles have a very low water content when suction is high. (i.e., > 10 kPa).

Parameters of van Genuchten's model

Table 3 shows the model parameters obtained from fitting the experimental data from the GWCC to van Genuchten' model [Eq. (1)]. The parameters α, m, and n represent the characteristics of the GWCC. For the geotextile tested, the m ranged from 0.6 to 0.87, and the α ranged from 0.69 to 1.67. As shown in Fig. 9, the α is related to the initial curvature of the GWCC to represent ψ_a beginning diminishing water contents, and the n is related to the steep degree of the GWCC. As described in the PSD, the GT1 has consistent pore size. The GWCC of GT7 is the highest ψ_a among tested GTs, which has the lowest α. In opposite, GT5 has largest α (i.e., 1.67 kPa^{-1}) and smallest ψ_a (i.e., 0.4 kPa) among tested geotextiles. For instance, the GWCC decreased more rapidly for GT1 compared to GT2 because the n of GT1 is significantly higher (i.e., approximately 3 times) than that of GT2. Therefore, the θ_r decreased with increasing n or m, and the ψ_a increased with decreasing α. This is a similar trend to the model parameters of the soil water characteristic curve (SWCC) with granular materials found by using Eq. (1). For granular material, the n should typically range from 3.5 to 18 and m can be assumed to be 1-1/n. The α ranged from 0.1 to 3.5 (Clayton 1996).

VARIABLES OF CAPPING GEOTEXTILE AFFECTING ON WATER RETENTION CHARACTERISTICS

Effect of composite layers of geotextile products used in sediment caps

To identify the effect of composite layers on water retention behavior, the GWCC for GT3 was compared to those of singular layers. The θ_s of the composite layer was about 0.69, which is between the GT1 value of 0.78 and the GT2 value of 0.65 in terms of the volume as shown (see Fig. 11).

However, only a single value of ψ_a exists even though the composite layer was tested. The ψ_a of GT3 is approximately 0.85 kPa as shown in Fig. 11. The ψ_a of GT3 is similar to that of the GT1, which was the top layer in the composite. When the suction is fully applied on the top layer of the composite during dewatering, the suction approached the ψ_a of the top layer, and the water inside the largest pores was extracted from the upper layer. Because there was no significant difference between the ψ_a of the GT1 and the GT2 (even the GT2 has the lower ψ_a than the GT1), the suction already passed the ψ_a of the bottom layer before dewatering the top layer. Hence, the ψ_a of the bottom layer (GT2) is not represented clearly during dewatering in the composite layers (GT3). Associated with this phenomenon, the composite layer composed of singular layers with similar ψ_a shows a single value of ψ_a. However, the composite layer composed of larger pores (i.e., sand) and smaller pores (i.e., clay) has two ψ_a which can be distinguished significantly.

Effect of clay core

To investigate the effect of the clay layer on the water retention behavior of the RCM, the composite layers without clay core (GT3) and with clay core of 1.0-cm thickness (GT4) were compared in Fig. 12. As a control, a water retention curve of the organo clay was also measured. Because the unsaturated hydraulics of sediment caps act as a system, it is valuable to compare the ψ_a of composite layers including the clay layer as well as those not including the clay in the capping geotextile. Similar to the double-packed geotextile, the capping materials evaluated with clay core had a relatively lower initial or saturated θ (approximately 0.55) due to the lower initial θ of the clay core. The ψ_a of GT4 was equal to 1.2 kPa which was 41% higher than that of GT3 which was equal to 0.85 kPa. This occurs because the particles of the organo clay can migrate into the compressible geotextile (GT1), which might reduce pore voids existing on the surface layer of GT4. However, the shape of the GWCC for GT3 is noticeably similar to the SWCC of organo clay. The organo clay is like a granular material before the hydration with organic compounds. Total volume of pores in GT4 are similar to organo clay because most of the volume of GT4 is composed of clay particles. Hence, the SWCC of organo clay is fairly similar to the GWCC of GT4.

Variation of k_{uw} with gas migration

By using Eq. (2) and (3), the unsaturated hydraulic conductivity (k_{uw}) can be estimated as shown in Fig. 13. The variation of k_{uw} was evaluated to consider the effect of gas trapped in the layer of geotextiles with increasing suction. The

k_{uw} is several orders smaller in this range than saturated hydraulic conductivity (k_w) if the gas is supplied consistently to the geotextile caps. The k_w is given in Table 1. In Fig. 13, the k_{uw} for each geotextile ranged from 5.5×10^{-4} m/s to 7.0×10^{-7} m/s at 1.0 kPa of the suction.

Based on the results, the reduced k_{uw} can prevent pore water flow through the geotextile caps. The pore water pressure would build up on the bottom of the capping layer because of gas entrapped in the capping layer. The pressure can push the layer upward and damage the capping geotextile as a seepage force (see Fig. 15).

The water flux pressure from the bottom is a critical factor in causing damage to the capping geotextile. The water pressure can be generated by the difference in hydraulic head between the capping geotextile and the ground water table. The seepage pressure of spring water from the river bottom can be calculated by using Bernoulli's equation as follows:

$$P_{sw} = \rho_w g \Delta h - \frac{1}{2}\rho_w {v_s}^2 \tag{10}$$

where ρ_w is the density of water, g is the acceleration of gravity, and Δh is the difference of head between the capping geotextile and the level of ground water. According to Darcy's law, the flow velocity through geotextile caps can be described as follows:

$$v_s = k_{uw} \frac{\Delta h}{L} \tag{11}$$

where k_{uw} is the unsaturated hydraulic conductivity through the capping geotextile obtained from Fig. 13, and L is the thickness of the geotextile cap. The Δh can fluctuate highly depending on the seasonal and geographical condition (e.g., percolation and temperature). If the P_{sw} is higher than P_{fm}' as described in Scenario 4, the geotextile caps can be damaged from buoyance and displacement.

Effect of normal pressure applied on capping geotextiles

Geotextiles with smaller effective pores should have higher ψ_a values, and geotextiles with a wider range of pore sizes should exhibit greater changes in ψ with changes in water content (Eun and Tinjum 2012b). Effective normal pressure, σ'_n, in sediment capping is a function of the overburden material acting on the geotextile. Figure 14(a) shows GWCCs of the GT3 measured at variable effective normal pressure (σ'_n = 1.0, 2.0, 4.0 and 5.0 kPa) applied during the HCT. As σ'_n increases, the ψ_a of the GWCC increases. The ψ_a subjected to σ'_n of 1.0, 2.0, 4.0 and 5.0 kPa is 0.45, 0.85, 2.1 and 2.5 kPa, respectively. The θ_s of the geotextile decreases with increasing σ'_n. The reason for this change is because the pore size structure of a geotextile under increasing σ'_n is compressed and the fiber filaments occupy more volume in the geotextile. Geotextiles are compressive; thus, their volume readily changes with applied loading (Palmeira and Gardoni 2002). Because the hydraulic properties of geotextiles, such as θ_s and ψ_a, change with applied load, the *in situ* σ'_n applied to the geotextile at expected field conditions should be used in the experimental program used to

determine these hydraulic properties. Figure 14(b) represents the relationship between normalized ψ_a logarithmically and *in situ* σ'_n. The linear equation obtained from regression analysis quantifies the effect of *in situ* σ'_n on ψ_a:

$$ln\frac{\psi_a}{\psi_{a0}} = a \cdot \frac{\sigma'_n}{P_a} + b \quad (12)$$

where a and b are material parameters; in this case, 0.376 and -0.759, respectively; ψ_{a0} is the reference ψ_a at 2.0 kPa, and P_a is the reference stress equal to 1.0 kPa. Eq. (12) allows for a method to correlate *in situ* σ'_n and the ψ_a of the geotextile by an empirical normalization. The parameter a, which is less than zero, represents the increasing magnitude of ψ_a, the rate of which slows with increasing *in situ* σ'_n. According to Eq. (12), the effect of *in situ* σ'_n on the ψ_a amplified with increasing *in situ* σ'_n slightly under a given condition. However, in the high pressure range (i.e., >10 kPa), *in situ* σ'_n would influence the effect of ψ_a less because the compressibility of geotextile is limited.

PRACTICAL IMPLICATION

Case history of geotextile cap failure

In an oxbow lake adjacent to a river in northern Wisconsin, capped sediment contained high concentrations of lead. A sand cap (nominal 0.305 m-thick) was placed on the sediment to effectuate a physical barrier, thus preventing direct contact with and resuspension of the contaminated sediment. The sediments were soft, fine-grained, and organic-rich because the site is a low

energy environment surrounded by swamp and wooded area. To avoid the possibility of capping sand mixing with the underlying sediments, a non-woven needle-punched geotextile was placed between the sand and the sediment.

Inspections of the cap were performed irregularly, so the actual timing of a subsequent observed failure is not known with certainty. However, some years later, a 1.52 m × 2.54 m hole in the sediment cap was discovered. Scouring was ruled out as a cause due to the low energy environment. During a summer investigation portions of the geotextile caps, which had formerly been covered with sand, were observed protruding across the air-water interface in a whaleback position (see Fig. 15). When penetrated with a sharp object, gas escaped.

Design chart to prevent a failure of capping geotextiles

Based on the hydraulic properties obtained from the GWCC for the considered failure scenarios, the criteria to determine the possible damaged area of the capping geotextile can be developed depending on the gas pressure (P_g) versus effective overburden pressure ($P'_{fm} = P_{fm} – P_{bf}$) as shown in Fig. 16. The ψ_a is also a critical condition to determine the stability. The design procedure to evaluate stability of sediment capping including geotextiles is as follows:

Step 1) Evaluate the P'_{fm} applied on the capping system to set the lower bound of the criteria.

Step 2) Measure or estimate the ψ_a of geotextile cap from GWCC to set the upper bound of the criteria.

Step 3) Depending on P'_{fm}, the ψ_a needs to be increased according to Eq. (12).

Step 4) Surveys the P_g generated in the site and represent the range in the x-axis.

Step 5) Check value of Δh and k_{uw} to given condition.

Step 6) Calculate the P_{sw} to push up the capping system by using Eq. (10) and (11).

Step 7) From procedure 1) to 6), draw enveloped area in the plot to represent stable capping system.

When the P_{sw} is not considered, upper part of the pressure equilibrium between the P_g and the P'_{fm} (1:1 line) is stable because the P_g cannot over the P'_{fm}. The upper area beyond 1:1 line is always safe without considering $P_{sw.}$ If the P_g is placed the left of the ψ_a in the x-axis and the ψ_a is smaller than the P'_{fm}, the condition is satisfied to Scenario 1, which is stable. If the P_g is placed the right of the $\psi_{a,}$ but the ψ_a is smaller than the P'_{fm}, the condition is satisfied to be stable in Scenario 2. The P_g can dissipate as gas pass through geotextile caps. However, when the ψ_a is higher than the $P'_{fm,}$ the P_g can be accumulated to reach the $P'_{fm.}$ When the P_g is higher than the $P'_{fm,}$ the P_g begins to push the geotextile upward as described in Scenario 3. In Scenario 4, the area below the plot of spring water is unstable because the P_{sw} displace the geotextile caps higher than P'_{fm}. Therefore, the stable condition is accomplished to meet Scenario 1 and 2. The envelop of the stable zone is highly varied depending on various variables such as the ψ_a, P'_{fm}, P_{sw}, k_{uw}, and Δh. For instance, if the ψ_a increases, the unstable area should be increased (e.g., clogging).

Example application

Fig. 17 shows the example appication presented in this paper are illustrated using a case study of a confidential contaminated harbor in the US Great Lakes region (Mohan et al. 2000). Historical dredging of the harbor over the years created a unequilibrium between the river and natural bed, favoring continued long term deposition of sediments. The 0.305 m of nominal graded armor stone and 0.508 m of sand were layered over geotextile capping in the site. Based on the thickness of fixing material, the P'_{fm} can be estimated as 8.2 kPa. The GT4 including organoclay as a geotextile capping material was assumed to be installed between contaminant sediment and sands. The increased ψ_a was calculated by using Eq. (12), which is 11.4 kPa.

The gas fluxes from these observations vary largely from 0.3 to 2640 mL/m^2-day due to the different local conditions. Himmelheber and Hughes (2005) reported that the methane generation at sediment-water interfacial area highly vary depending on the temperature. The P_g can be estimated by measuring the gas bubble flux and assuming equilibrium between the gas bubble and water at specific temperature. For this example, the P_g varies depending on field conditions as described in Fig. 17. No head difference between geotextile capping and ground water was assumed for the example condition (i.e., $P_{sw} = 0$). Given conditions for example were described in Table 4. According to Fig. 17, the safe zone to install geotextile caps is ranged from 8.2 to 11.4 kPa of the P_g. To design sediment capping, it would be better to eliminate the gas before approaching lower bound of the criteria (i.e, $P_g = 8.2$ kPa).

Alternative enhancement for sediment capping system

Considering the scenarios discussed in the previous sections, several alternatives can be considered to mitigate the damage to the geotextile caps. One method is to place a heavy sediment cap beneath the layer. However, considering gas (e.g., methane) generated from sediments, this method is not enough to prevent the damage. Another logical design factor to address gas buildup beneath a geotextile layer of a sediment cap is venting. The system depicted shows a pipe set below a permeable section of a horizontal sediment cap. The pipe extends above the water line and could be used to inject material, or to exhaust gas. In any circumstance where a geotextile layer in a sediment cap is constructed with a horizontal or an undulating or concave surface, gas will accumulate in pockets beneath the cap. This leads to the idea of a sloped underside to cause gas to move. Another corollary issue to consider with the gas flow restrictions imposed by fine-grained sediments is a gas transmission layer. This layer could be constructed of coarse-grained material directly below the geotextile, and allow for the free movement of gas.

A combination of the alternative design factors could be used successfully to maintain a substantially gas-free geotextile layer so that a sediment cap can remain hydraulically permeable. In particular, when geotextile layers are used in an active cap, whose functional success relies on spatially and temporally continuous hydraulic permeability, this set of design features is necessary.

CONCLUSIONS

In this study, the failure mechanism of sediment capping geotextiles functionally related to the unsaturated hydraulic properties of the geotextiles was investigated. The failure scenario was comprehensively reviewed with a practical case. A series of laboratory tests including the HCT, water column apparatus test, and BPT were conducted to characterize the water retention properties and pore size distribution curves of the nonwoven geotextiles and Reactive Core Mat (RCM). The θ_s of the composite layer which combines singular layers is in the range between those values of the singular layers. The air entry pressure (ψ_a) varied from 0.45 to 1.2 kPa depending on the pore distribution of the capping material. The ψ_a of geotextiles increased with increasing normal stress due to decreasing pore size. The empirical correlation between ψ_a and *in situ* σ'_n was proposed as a normalized linear equation to quantify the relationship. From the geotextile water characteristic curve (GWCC), the unsaturated hydraulic conductivity (k_{uw}) was found to range from 7.0×10^{-7} m/s to 5.5×10^{-4} m/s at 1.0 kPa of the suction. Composite layers used as a capping layer do not influence the ψ_a significantly, but organo clay might increase the ψ_a. Gas ebullition is associated with the effects of the normal pressure and the gas migration on the ψ_a and the k_{uw} in the geotextiles, respectively. Hence, the failure is governed by increasing the ψ_a and reducing hydraulic conductivity due to gas migration through the caps. A design chart to estimate the failure of the sediment capping system from gas ebullition was proposed. The design chart needs to be

considered with alternative methods such as gas transmission layer, heavy fixing material, or a venting slope.

REFERENCES

ASTM D5199 Measuring the Nominal Thickness of Geosynthetics, American Society for Testing and materials, West Conshohocken, Pennsylvania, USA.

ASTM D6767 Pore Size Characteristics of Geotextiles by Capillary Flow Test, American Society for Testing and materials, West Conshohocken, Pennsylvania, USA.

ASTM D6836 Determination of the Soil Water Characteristic Curve for Desorption Using Hanging Column, Pressure Extractor, Chilled Mirror Hygrometer, or Centrifuge, West Conshohocken, Pennsylvania, USA.

Brooks, R. and Corey A. 1964. Hydraulic Properties of Porous Media. *Hydrology Paper*, Vol. 3, Colorado State University, Fort Collins, Co.

Benson, C.H. and Wang, X. 2004. Leak Free Pressure Plate Extractor for the Measuring Soil Water Characteristic Curve. *Geotechnical Testing Journal.* Vol. 27, No. 2:1-10.

Dailer, D.M., and Gentry, J.L. 2004. Design, Construction and Monitoring of a Contaminated Sediment Cap in the Columbia river, *Ports 2004*, ASCE.

Elton, D. J., Hayes, D.W. and Adanur S. 2006. Bubble Point Testing of Geotextiles: Apparatus and Operation. *Geotechnical Testing Journal*, Vol. 30, No. 1:1-8.

Eun, J., and Tinjum, J. 2011a. Unsaturated Transport of Ebullition Gas through Sediment Capping Geotextiles and Sand. *Proceedings of the 5th Asia-Pacific Conference on unsaturated soil*, ISSMGE, Nov. 14-16, 2011, Pattaya, Thailand.

Eun, J., and Tinjum, J. 2011b. Variation in Air Entry Suction of Nonwoven Geotextiles with Pore Size Distribution. *Proceedings of the 5th Asia-Pacific Conference on unsaturated soil*, ISSMGE, Nov. 14-16, 2011, Pattaya, Thailand.

Iryo, T, and Rowe, R.K. 2003. Hydraulic Behavior of Unsaturated Nonwoven Geotestiles. *Geotextiles and Geomembranes*, Vol. 23, No. 6:381-404.

Kavcar, P. C., and Wright, S.J. 2009. Effects of Gas Ebullition on Cohesive Sediment Resuspension and Cap Stability. *World environmental and water resource congress 2009: great rivers,* ASCE.

Klute, A., 1986, Water Retention: Laboratory Methods, Methods of Soil Analysis, Part 1, Agronomy Monograph No. 9, American Society of Agronomy-Soil Science of America, Second Edition, Madison, Wisconsin, USA, pp. 635-662.

Nahlawi, H., Bouazza, A. and Kodikara, J. K. 2007. Characterisation of geotextiles water retention using a modified capillary pressure cell. Geotextiles and Geomembranes, 25, No. 3, 186–193.

Palmeira, E.M. and Gardoni, M. G. 2002. Drainage and Filtration Properties of Non-woven Geotextiels under Confinement Using Different Experimental Techniques. *Geotextiles and Geomembranes,* Vol. 20, No. 2:97-115.

Stormont, J.C., Henry, K.S., and Evans, T.M. 1997. Water Retention Function of Four Nonwoven Polypropylene Geotextiles. *Geosynthetic International*, Vol. 4, No. 6:661-672.

Tinjum, J.M., Benson, C.H., and Blotz, L.R. 1997. Soil Water Characteristic Curves for Compacted Clays. ASCE *J. Geotech. & Geoenviron. Engrg.,* Vol. 123, No. 11:1060–1069.

US Environmental Protection Agency (EPA) 2007. Demonstration of the AquaBlock Sediment Capping Technology, *Innovative technology evaluation report.* EPA/540/R-07/008.

Van Genuchten, M. T.1980. A Closed Form Equation Predicting the Hydraulic Conductivity of Unsaturated Soils. *Soil Science Society of America Journal*, Vol. 44: 892-898.

Viana, P. Yin, Ke, Zhao, X. and Rockne, K. 2007. Active Sediment Capping for Pollutant Mixtures: Control of Biogenic Gas Production under Highly Intermittent Flows. *Land contamination & Reclamation*, Vol. 15, No. 4:413-425.

Table 1. Advantage and disadvantage of dredge and sediment capping

Method	Advantage	Disadvantage
Dredge	• Elimination of contaminant from in-situ • Less influence by hydrologic condition	• Generation of bioturbation • Strong damage on ecosystem • Complicate procedure • Need secondary procedure for contaminated byproduct • Expensive and slow
Sediment capping	• Fast and simple • Cost effective • Minimized bioturbation • Less impact on ecosystem	• No clear specification • Inappropriate in fast flow condition • Need long-term monitoring • Dependency of capping material

Table 2. Physical properties of geotextiles

Type	Material	Color	Weigh t, M_A (g/m^2)	Thickness, t (mm)	AOS (mm)	Hydraulic conductivity, k_w ($\times 10^{-3}$ m/s)
			D5261	D5199	D6767	D4491
GT1	Composite geotextile	White (top layer)	298	3.9	0.42	1.35
GT2		Black (Bottom layer)	319	2.2	1.1	1.1
GT3		Composite w/o clay core	617	6.1	0.40	1.2
GT4		Composite w/ clay core	3044	10.2	-	0.35
GT5	Nonwoven geotextile	Gray	256	2.5	0.95	1.8
GT6		Black	306	4.0	0.38	0.65
GT7		White gray	325	2.8	0.27	0.65
GT8		Black	275	2.8	0.92	1.2

Table 3. Parameters of van Genuchten's model

Property	unit	GT1	GT2	GT3	GT4	GT5	GT6	GT7	GT8
Residual volumetric water content, θ_r	m^3/m^3	0.03	0.00	0.02	0.04	0.07	0.02	0.07	0.07
Saturation volumetric water content, θ_s	m^3/m^3	0.78	0.65	0.69	0.55	0.71	0.65	0.68	0.83
Mode parameter, α	kPa^{-1}	0.96	1.35	0.82	0.49	1.67	0.69	0.54	1.10
Mode parameter, n	-	7.73	2.50	6.18	2.56	4.66	3.51	5.11	2.87
Mode parameter, m	-	0.87	0.60	0.84	0.61	0.79	0.72	0.80	0.65
Air entry pressure, ψ_a	kPa	0.75	0.45	0.85	1.20	0.4	0.85	1.20	0.55

Table 4. Given condition for example

Condition	unit	P'_{fm}	P_g	ψ_a	ψ'_a	P_{sw}
Value	kPa	8.2	varying	1.2	11.4	0

ψ'_a : increased ψ_a considering the effect of overburden pressure.

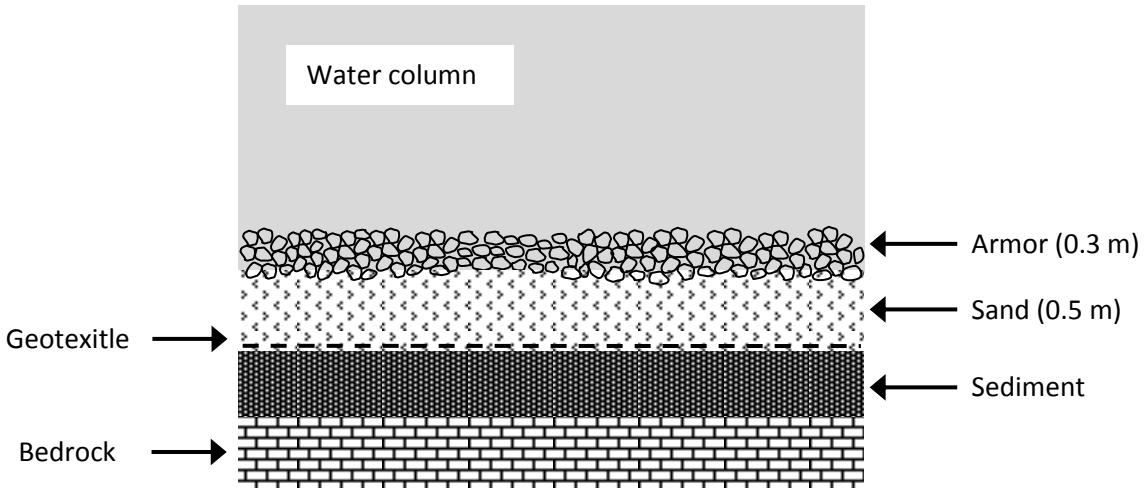

Figure 1. Schematic of sediment capping.

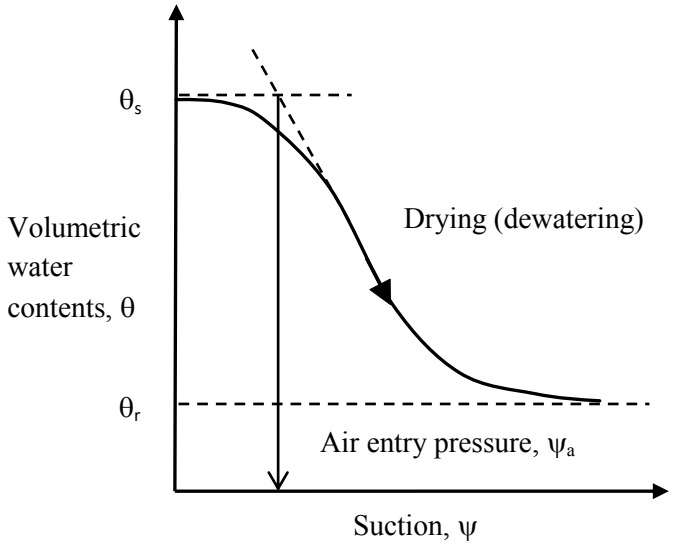

Figure 2. Typical water retention curve (GWCC).

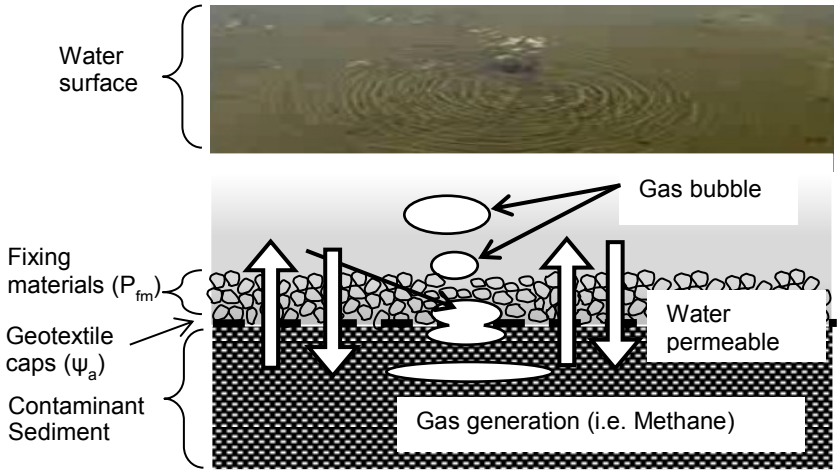

(a) Stable condition: Scenario 1: $P_g < \psi_a < P'_{fm}$ and $P_{sw} < P'_{fm}$ and Scenario 2: $\psi_a \leq P_g < P'_{fm}$ and $P_{sw} < P'_{fm}$

Figure 3. Functional failure mechanism of sediment capping system (continued).

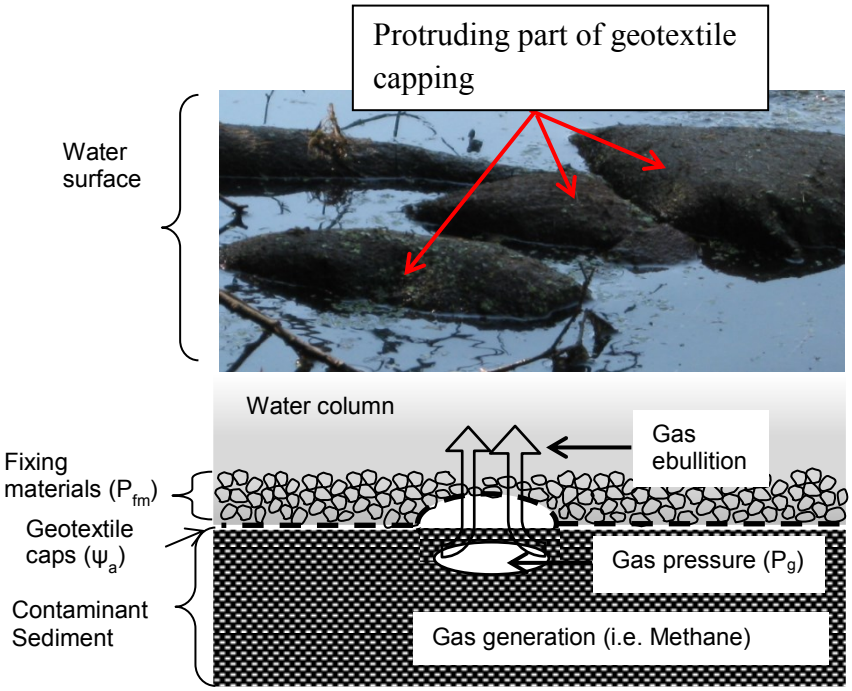

(b) Unstable condition, Scenario 3: $P_g \geq \psi_a > P'_{fm}$ and $P_{sw} < P'_{fm}$

Figure 3. Functional failure mechanism of sediment capping system (continued).

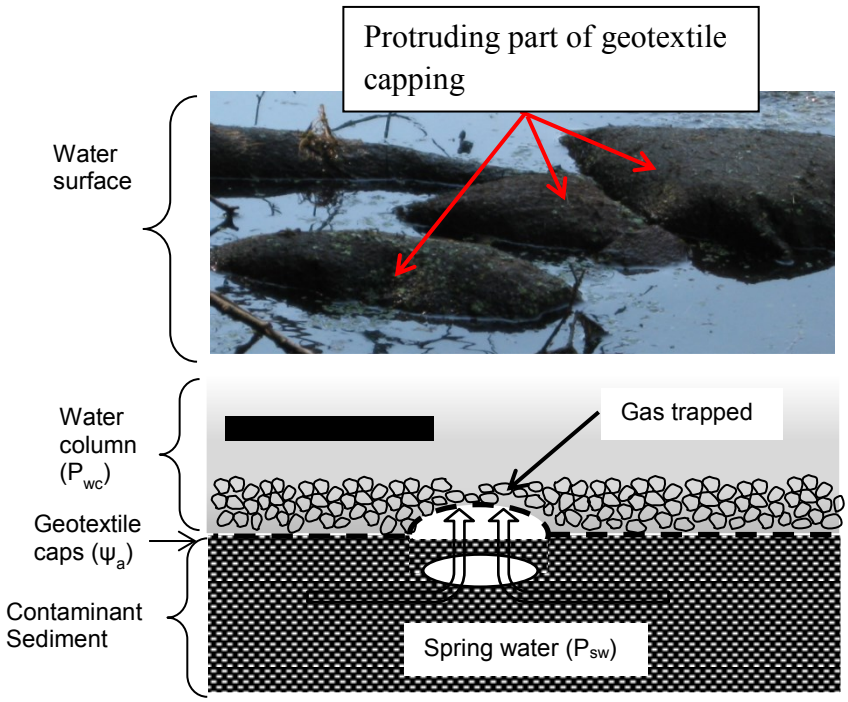

(c) Unstable condition, Scenario 4: $\psi_a < P_g < P'_{fm}$ and $P_{sw} > P'_{fm}$

Figure 3. Functional failure mechanism of sediment capping system.

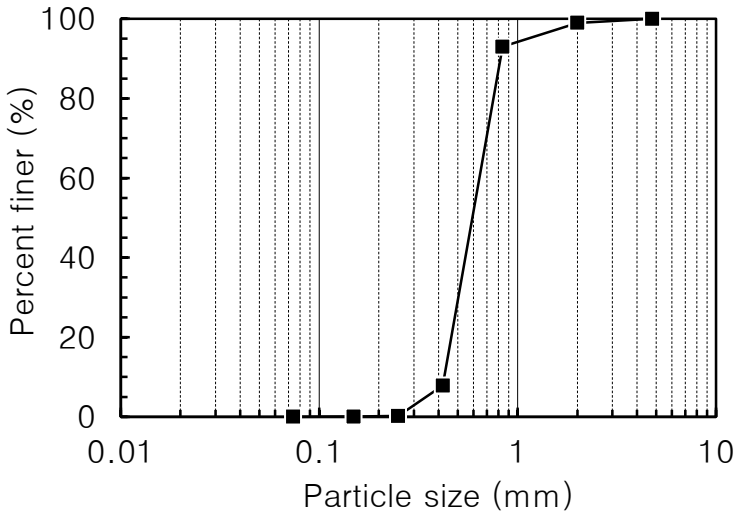

(a) Grain size distribution of organo clay

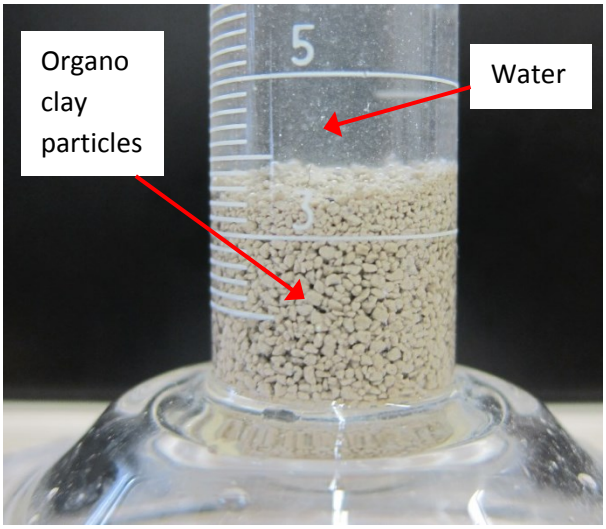

(b) No hydration of orano clay with water

Figure 4. Organo clay tested

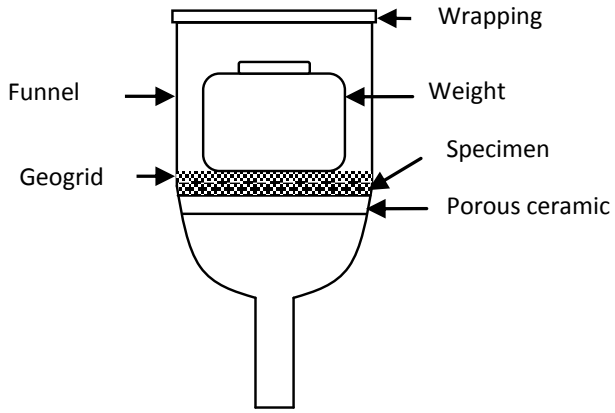

(a) Installation of geotextile specimen in funnel

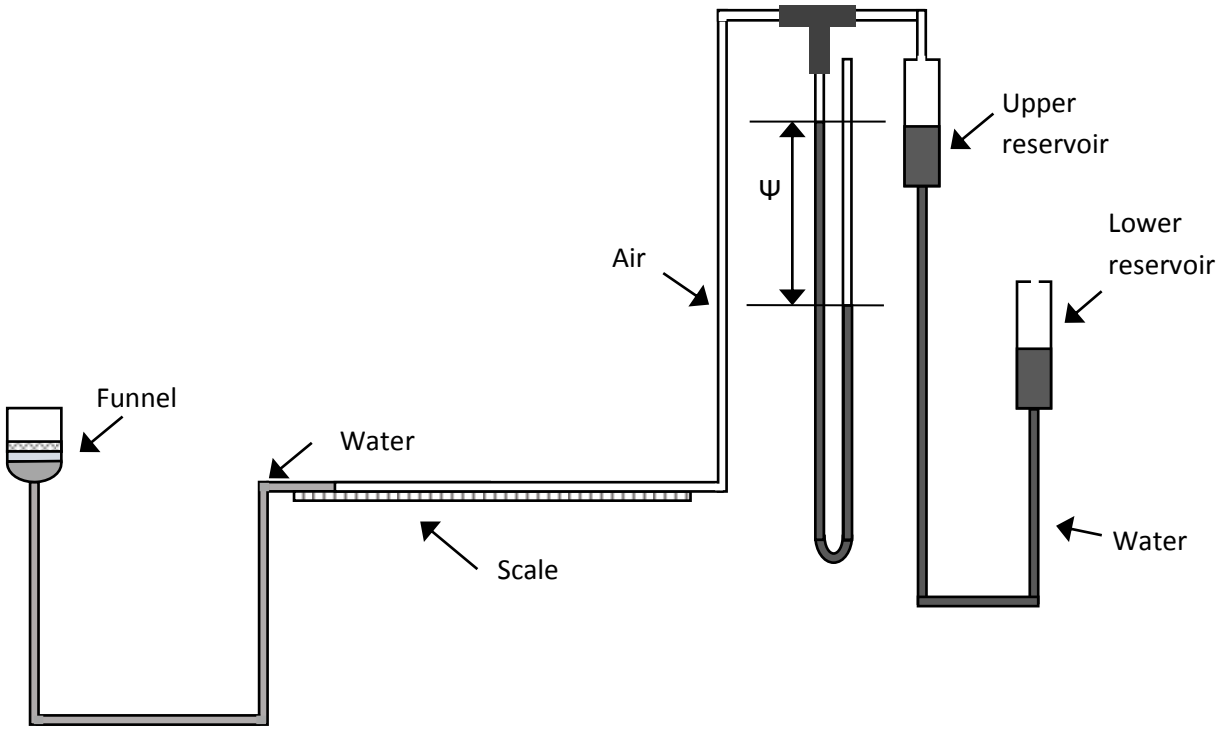

(b) Schematic of hanging column test apparatus.

Figure 5. Hanging column test apparatus.

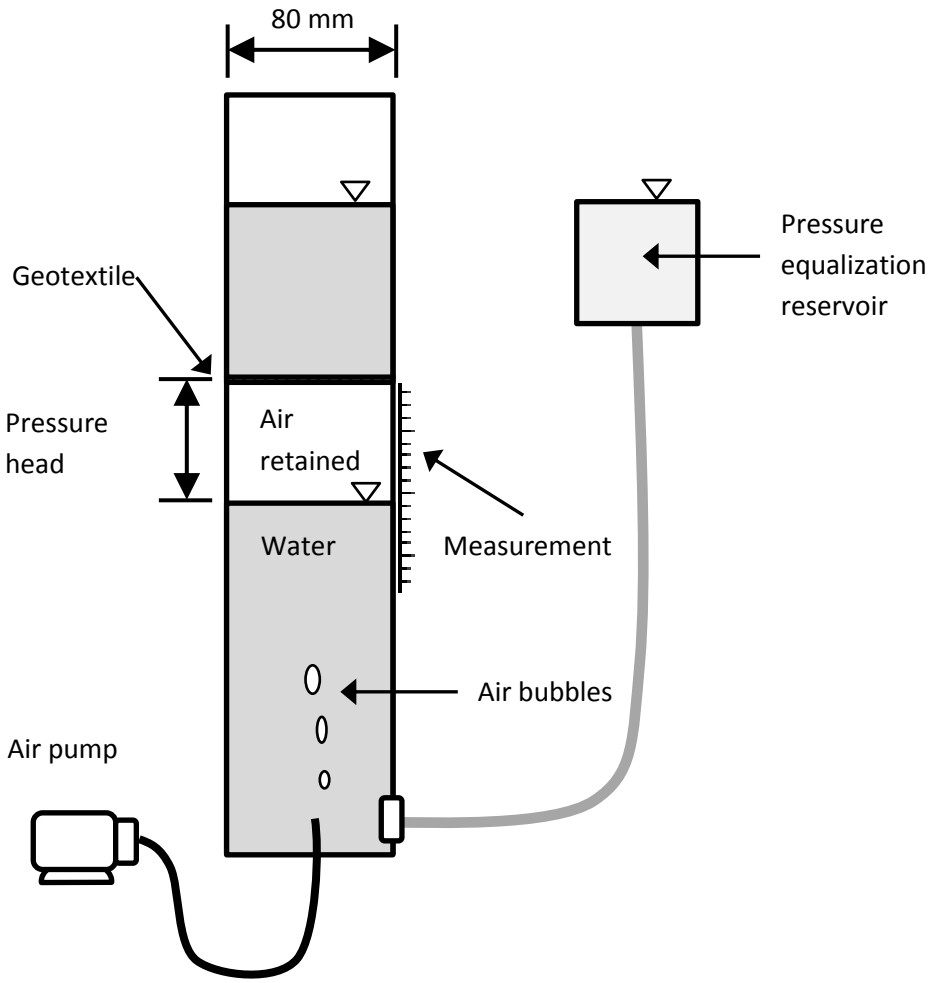

Figure 6. Experimental setup of water column test.

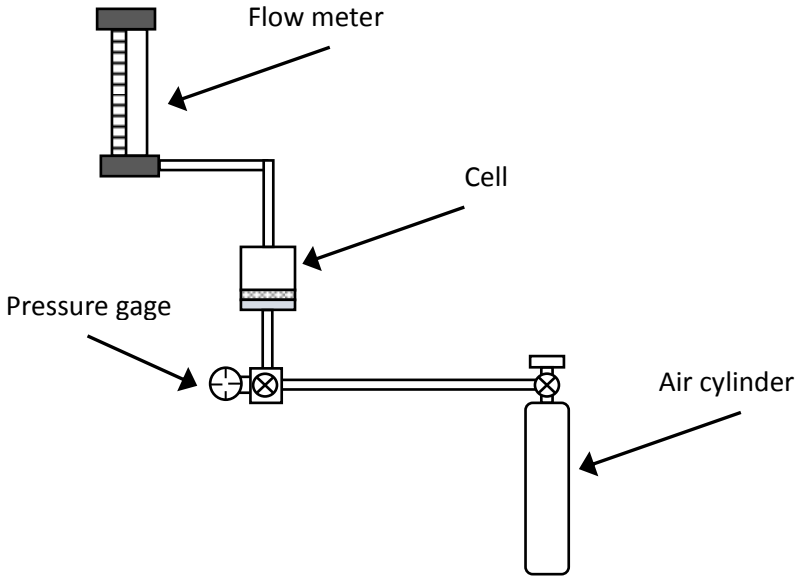

Figure 7. Bubble point test apparatus

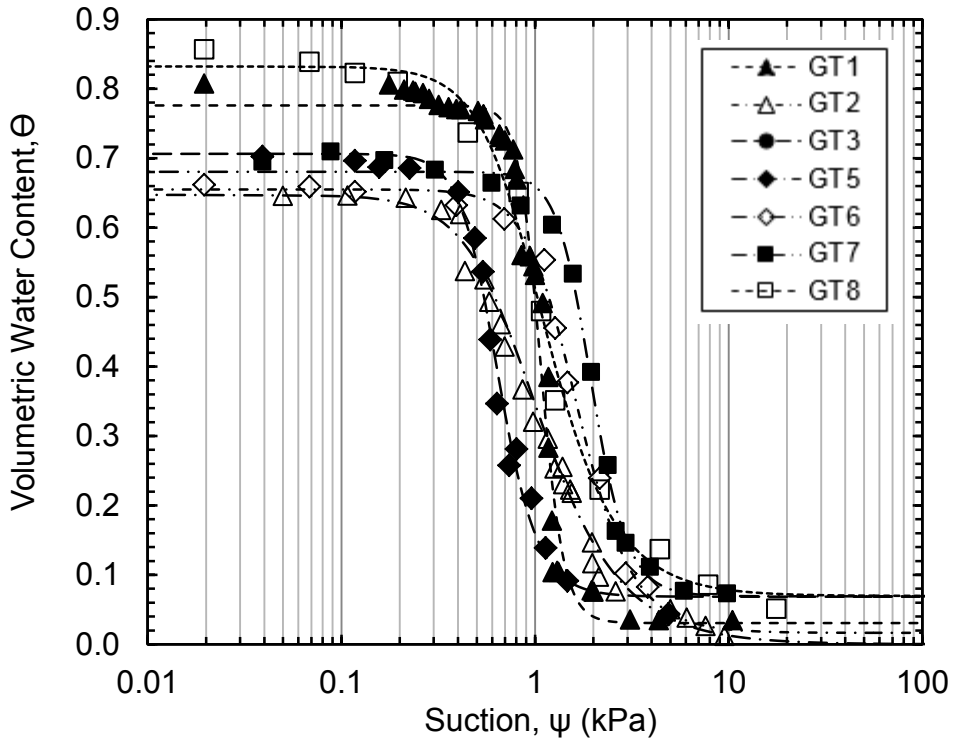

Figure 8. Geotextile water characteristic curves (GWCCs) of tested geotextiles.

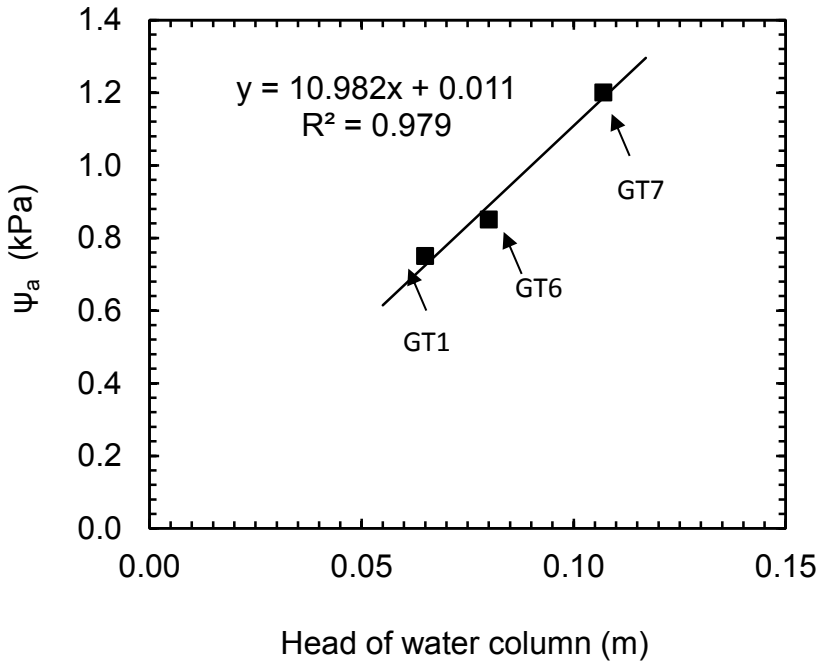

Figure 9. Relationship between air entry pressure and head of water column.

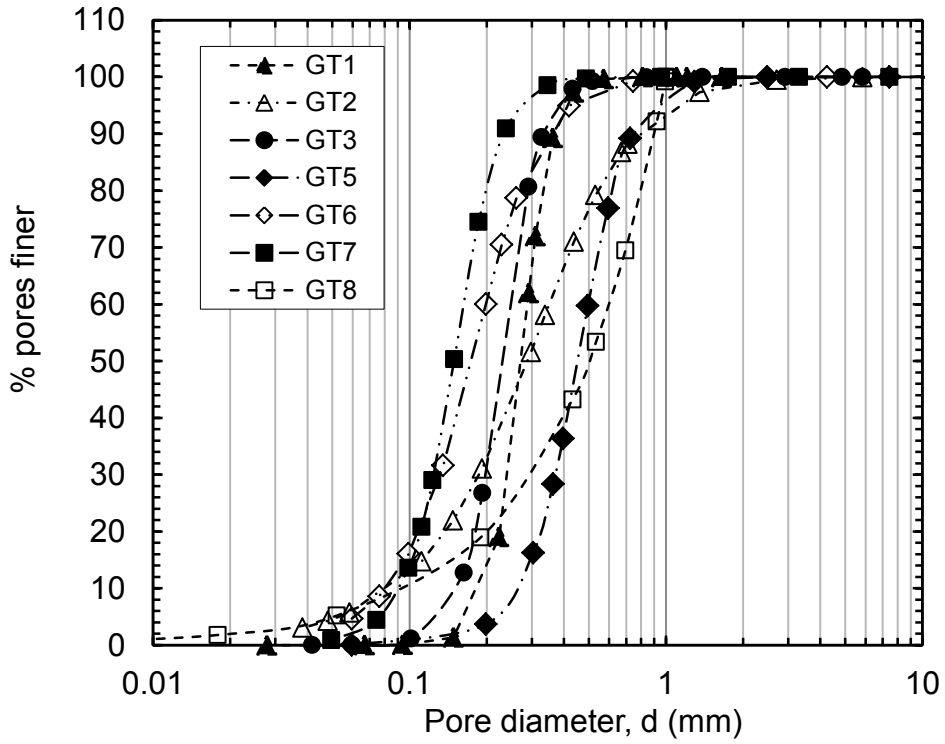

Figure 10. Pore size distribution curves of geotextiles.

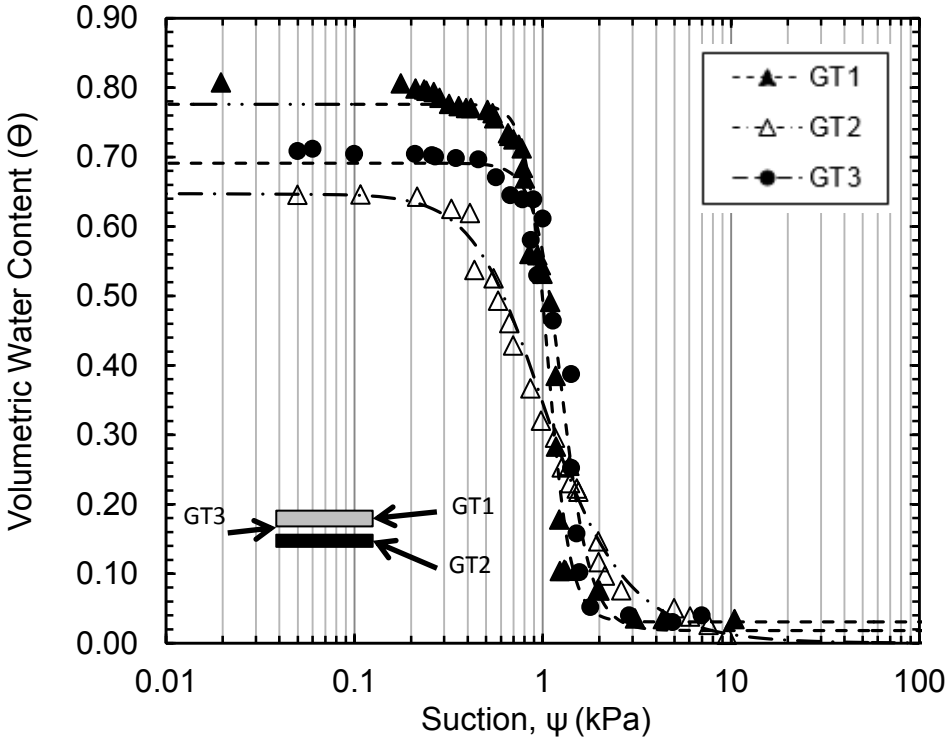

Figure 11. Comparison of geotextile water characteristic curves between composite layer w/o clay core and singular layer.

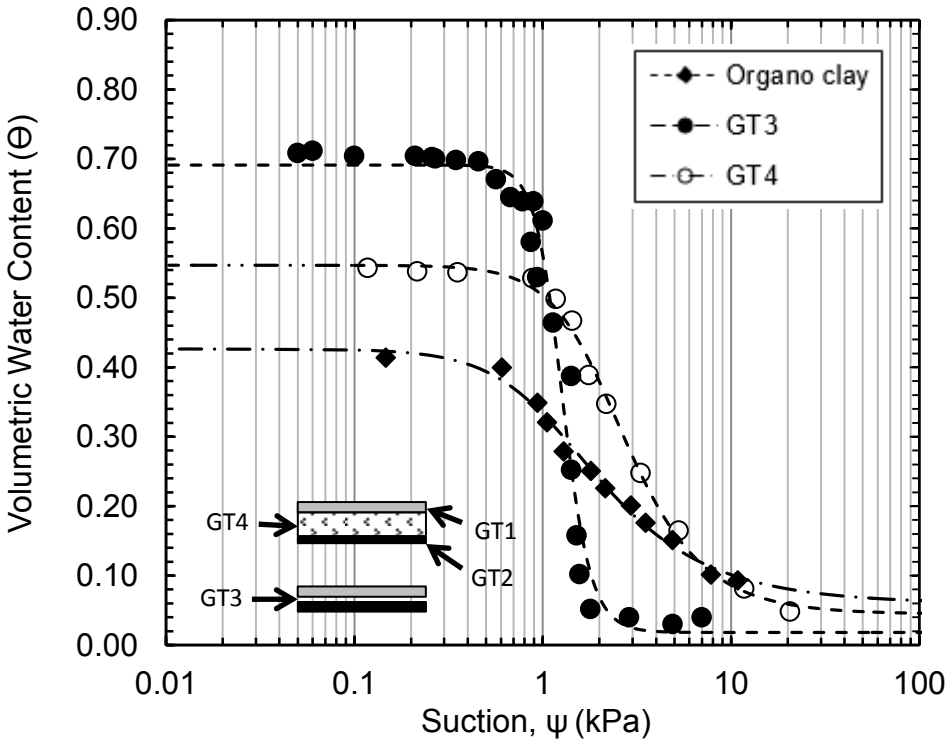

Figure 12. Comparison of geotextile water characteristic curves for composite layer between w/o clay core (GT3) and w/ clay core (GT4).

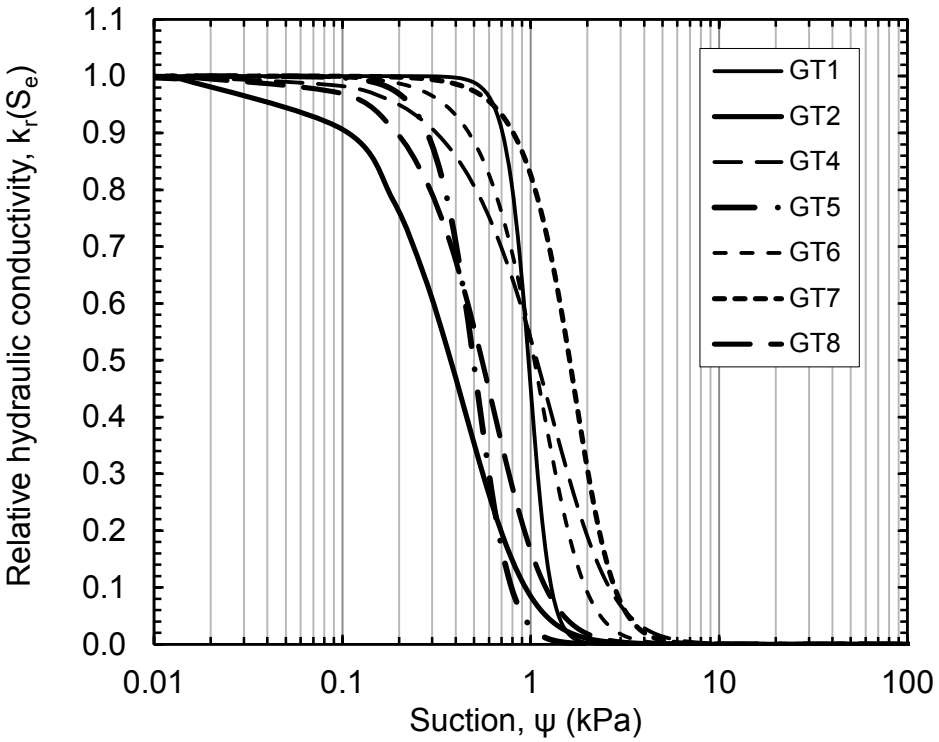

Figure 13. Relative hydraulic conductivity (k_r) estimated.

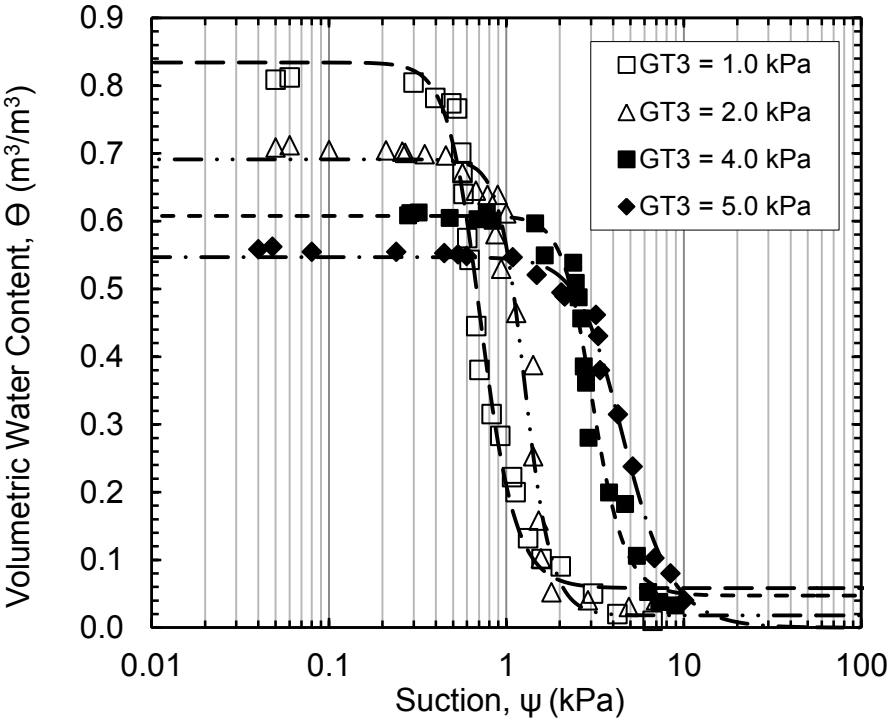

(a) Effect of σ'_n on ψ_a

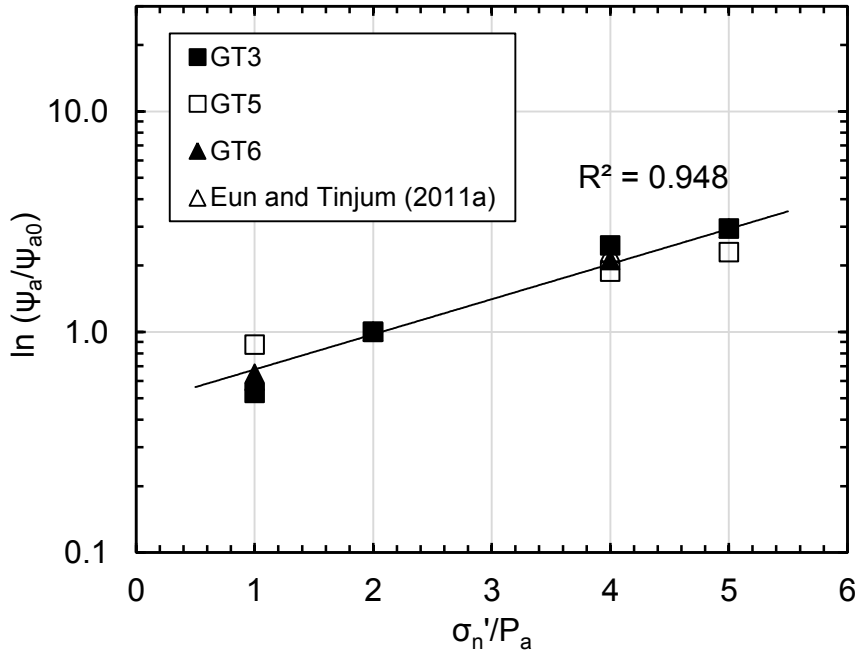

(b) Empirical correlation between ψ_a and *in situ* σ'_n

Figure 14. Relationship between the ψ_a and *in situ* σ'_n

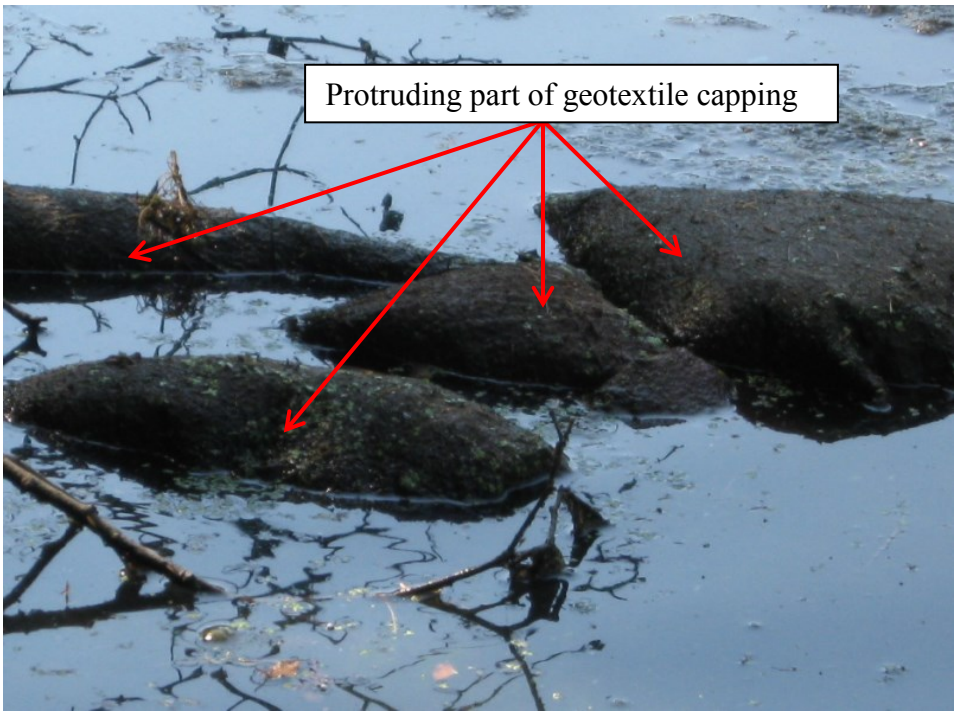

Figure 15. A failure of sediment capping system including geotextiles.

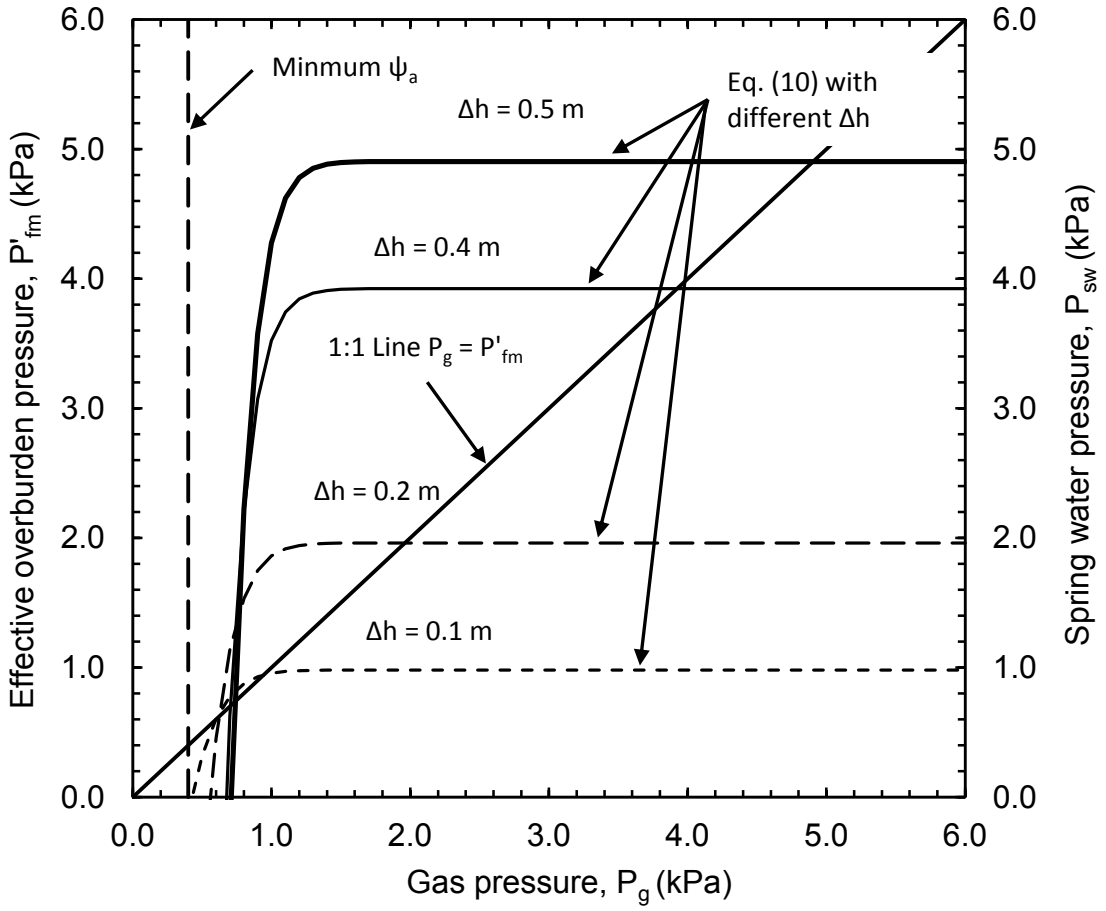

Figure 16. Design criteria of geotextile caps for stable condition.

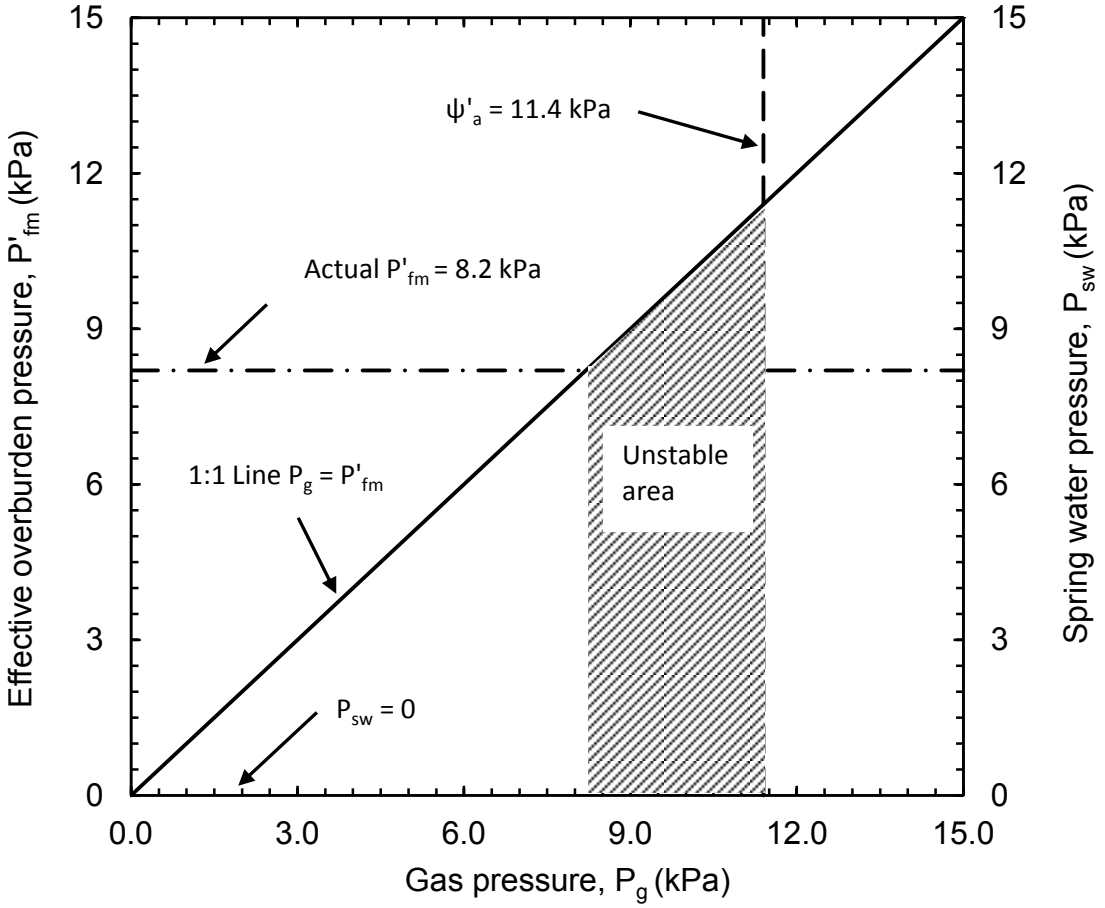

Figure 17. Example of design criteria.